Springer Theses
Recognizing Outstanding Ph.D. Research

Bernhard V. K. J. Schmidt

Novel Macromolecular Architectures via a Combination of Cyclodextrin Host/Guest Complexation and RAFT Polymerization

Springer

Springer Theses

Recognizing Outstanding Ph.D. Research

For further volumes:
http://www.springer.com/series/8790

Aims and Scope

The series "Springer Theses" brings together a selection of the very best Ph.D. theses from around the world and across the physical sciences. Nominated and endorsed by two recognized specialists, each published volume has been selected for its scientific excellence and the high impact of its contents for the pertinent field of research. For greater accessibility to non-specialists, the published versions include an extended introduction, as well as a foreword by the student's supervisor explaining the special relevance of the work for the field. As a whole, the series will provide a valuable resource both for newcomers to the research fields described, and for other scientists seeking detailed background information on special questions. Finally, it provides an accredited documentation of the valuable contributions made by today's younger generation of scientists.

Theses are accepted into the series by invited nomination only and must fulfill all of the following criteria

- They must be written in good English.
- The topic should fall within the confines of Chemistry, Physics, Earth Sciences, Engineering and related interdisciplinary fields such as Materials, Nanoscience, Chemical Engineering, Complex Systems and Biophysics.
- The work reported in the thesis must represent a significant scientific advance.
- If the thesis includes previously published material, permission to reproduce this must be gained from the respective copyright holder.
- They must have been examined and passed during the 12 months prior to nomination.
- Each thesis should include a foreword by the supervisor outlining the significance of its content.
- The theses should have a clearly defined structure including an introduction accessible to scientists not expert in that particular field.

Bernhard V. K. J. Schmidt

Novel Macromolecular Architectures via a Combination of Cyclodextrin Host/Guest Complexation and RAFT Polymerization

Doctoral Thesis accepted by
Karlsruhe Institute of Technology, Germany

Springer

Author
Dr. Bernhard V. K. J. Schmidt
Materials Research Laboratory
University of California
Santa Barbara, CA
USA

Supervisor
Prof. Christopher Barner-Kowollik
Department of Preparative
Macromolecular Chemistry
Institute for Technical Chemistry
and Polymer Chemistry
Karlsruhe Institute of Technology (KIT)
Karlsruhe
Germany

ISSN 2190-5053 ISSN 2190-5061 (electronic)
ISBN 978-3-319-06076-7 ISBN 978-3-319-06077-4 (eBook)
DOI 10.1007/978-3-319-06077-4
Springer Cham Heidelberg New York Dordrecht London

Library of Congress Control Number: 2014936427

Printed on acid-free paper

Springer is part of Springer Science+Business Media (www.springer.com)

Parts of this thesis have been published in the following journal articles:

1. Cyclodextrin-Complexed RAFT Agents for the Ambient Temperature Aqueous Living/Controlled Radical Polymerization of Acrylamido-Monomers
   Schmidt, B. V. K. J.; Hetzer, M.; Ritter, H.; Barner-Kowollik, C. *Macromolecules* **2011**, *44* (18), 7220–7232.

2. Miktoarm Star Polymers via Cyclodextrin-Driven Supramolecular Self-Assembly
   Schmidt, B. V. K. J.; Hetzer, M.; Ritter, H.; Barner-Kowollik, C. *Polym. Chem.* **2012**, *3*, 3064–3067.

3. Supramolecular Three-Armed Star Polymers via Cyclodextrin Host/Guest Self-Assembly
   Schmidt, B. V. K. J.; Rudolph, T.; Hetzer, M.; Ritter, H.; Schacher, F. H.; Barner-Kowollik, C. *Polym. Chem*. **2012**, *3*, 3139–3154.

4. UV-Light and Temperature Supramolecular ABA Triblock Copolymers via Reversible Cyclodextrin Complexation
   Schmidt, B. V. K. J.; Hetzer, M.; Ritter, H.; Barner-Kowollik, C. *Macromolecules* **2013**, *46* (3), 1054–1065.

5. Modulation of the Thermoresponsive Behavior of Poly(N,N-diethylacrylamide) via Cyclodextrin Host/Guest Interactions
   Schmidt, B. V. K. J.; Hetzer, M.; Ritter, H.; Barner-Kowollik, C. *Macromol. Rapid Commun*. **2013**, *34* (16), 1306–1311.

6. Complex Macromolecular Architecture Design via Cyclodextrin Host/Guest Complexes
   Schmidt, B. V. K. J.; Hetzer, M.; Ritter, H.; Barner-Kowollik, C. *Prog. Polym. Sci* **2014**, *39*, 235–249.

The true measure of a man is how he treats someone who can do him absolutely no good.

Samuel Johnson

I don't mind your thinking slowly; I mind your publishing faster than you think.

Wolfgang Ernst Pauli

Supervisor's Foreword

Since its introduction in the 1970s, supramolecular chemistry has had a significant impact on the chemical sciences. With nature as inspiration, opportunities to generate new materials employing supramolecular concepts appear to be infinite. Cyclodextrins belong to a group of compounds that are capable of engaging in strong supramolecular interactions—host/guest complexes with hydrophobic molecules. In a parallel development, the advent of living/controlled radical polymerization technologies, specifically the discovery of the RAFT/MADIX process in the late 1990s, had a significant impact on polymer chemistry and our ability to generate complex macromolecular architectures in a facile fashion. A myriad of new polymeric materials were suddenly accessible.

In the present thesis, the formation of novel macromolecular architectures via a combination of cyclodextrin-based host/guest chemistry and RAFT polymerizations is pioneered, which was a rather unexplored area at the start of the project. A systematic approach is taken: Commencing with the synthesis of guest end-functionalized polymers and the complexation of chain ends with cyclodextrins, the study progresses to establish the combination of cyclodextrin and guest containing macromolecular building blocks for the formation of complex dynamic macromolecular architectures. The key features of RAFT polymerization were utilized to achieve the research goal, i.e., its ability to provide macromolecules of predefined length and narrow size distribution. In addition, these key features include the ability to control the polymerization of functional monomers, e.g., water-soluble monomers, with fine control over polymer functionality, specifically the chain termini.

Initially, a method was developed to dissolve water-insoluble chain transfer agents in aqueous solution via host/guest complexation in order to synthesize water soluble polymers in a controlled fashion (Chap. 3). This method affords water-soluble polymers with hydrophobic end groups in one step at ambient temperature. These structures were subsequently utilized to modulate the self-assembly of a well-known thermoresponsive polymer via cyclodextrin host/guest interactions (Chap. 7). The supramolecular nature of the observed effect made it possible to reverse the thermoresponsive modulation via the addition of competing supramolecular guest molecules or by enzymatic degradation of the cyclodextrins. For the first time, a supramolecular ABA triblock copolymer formation via cyclodextrin-based interactions is described (Chap. 4). The pioneered

system has the outstanding feature of switchable connections between the different building blocks, which can be addressed by light or temperature. Thus, the block copolymers can be reversibly disassembled via external stimuli, a key requirement for their use as drug release systems. Furthermore, advanced and novel supramolecular star (Chap. 5) and miktoarm star (Chap. 6) polymers are described that can be disassembled via external stimuli or form nanoscopic aggregates upon heating. In summary, the present thesis demonstrates that cyclodextrin-based host/guest chemistry and RAFT polymerization are a perfect combination for the formation of complex and stimuli-responsive polymer architectures.

The thesis—combining two disciplines of chemistry—is of substantial value for chemists in the areas of polymer chemistry, supramolecular chemistry, materials science, colloidal science, and biomedical sciences. Several original research publications are based on it as well as a detailed review covering the field of cyclodextrin-mediated macromolecular architecture design. In addition, the thesis results have inspired further work by our group, e.g., the formation of X- and H-shaped star block copolymers, single-chain self-folding in water or the formation of supramolecular brushes.

On the basis of the results presented in this thesis, the formation of even more complex architectures is certainly possible. Furthermore, the combination of variable stimuli-responsive polymers will open new opportunities for advanced material design, while the utilization of supramolecular chemistry and cyclodextrin host/guest interactions appears to be an ideal tool for release system design. Importantly, cyclodextrin host/guest chemistry enables the implementation of self-assembly processes in aqueous environments.

Karlsruhe, February 2014 Prof. Christopher Barner-Kowollik

Abstract

The design of complex macromolecular architectures constitutes an important field in modern polymer chemistry and provides the opportunity to generate a broad range of materials with tuneable properties. The introduction of supramolecular chemistry had a significant impact on the synthesis of macromolecular architectures with a wide range of useful material properties ranging from self-healing to stimuli response. In particular, cyclodextrins (CDs) have proven to be versatile building blocks due to their ability to act as hosts in supramolecular inclusion complexes with hydrophobic molecules. In the course of the current thesis, the possibilities of the combination of CD-based supramolecular chemistry and reversible addition-fragmentation chain transfer (RAFT) polymerization with regard to the preparation of new macromolecular architectures were investigated. With the synthesis of variable macromolecular building blocks, a broad range of macromolecular architectures are accessible via CD host/guest chemistry.

A new method was developed to solubilize hydrophobic RAFT reagents in water and to utilize them in aqueous RAFT polymerizations of several acrylamides, i.e., *N,N*-dimethylacrylamide (DMAAm), *N,N*-diethylacrylamide (DEAAm), and *N*-isopropylacrylamide (NIPAAm). The polymerization kinetics were investigated showing control similar to fully water-soluble systems. Furthermore, high end-group fidelities were found and efficient chain extensions were performed. Thus, for the first time, water-soluble polymers with hydrophobic end groups were prepared in aqueous solution in one step with good control over molecular weight and molar mass dispersity ($Đ_m$).

After the preparation of end-functionalized polymers, the complexity of the architectures was increased via the utilization of several building blocks. Supramolecular three-arm star polymers were accessible via a threefold CD-functional core molecule and guest-functionalized polymers. The formation of supramolecular three-armed star polymers was shown to be temperature responsive leading to the disassembly of the star polymers after heating. This process proceeds in a reversible fashion as the supramolecular star polymers re-form after cooling to ambient temperature.

A further increase in complexity was achieved in the synthesis of AB_2 miktoarm star polymers. In this case, a mid-chain guest functionalized PDMAAm was synthesized as well as a β-CD-end functionalized PDEAAm. Complexation in water leads to the formation of the desired miktoarm star polymers. The PDEAAm

block was utilized to investigate the temperature-induced aggregation behavior. Significant differences between supramolecular miktoarm stars and nonstar-shaped polymers were found that can be attributed to different architectures in solution.

Furthermore, supramolecular-bound ABA block copolymers were prepared via the combination of CD end-functionalized poly(hydroxypropyl methacrylamide) (PHPMA) and doubly guest-functionalized PDMAAm or PDEAAm. Adamantyl- and azobenzene-guests were utilized allowing the disassembly of the block copolymers at elevated temperature (in the case of adamantyl- and azobenzene-guests) or via irradiation of UV-light (in the case of azobenzene-guests). The utilization of thermoresponsive PDEAAm, which loses water solubility at elevated temperatures, and PHPMA, which is water soluble in the complete temperature range, enables the study of temperature-induced aggregation of the system.

In addition, the thermoresponsive behavior of PDEAAm was modulated via the formation of supramolecular host/guest complexes with hydrophobic polymer end groups and CD. This effect could be reversed via the addition of competing guest molecules or via enzymatic degradation of the CD moieties.

Acknowledgments

First, and foremost, I am indebted to Prof. Christopher Barner-Kowollik for offering me the opportunity to undergo my doctoral studies under his supervision. I am thankful for his trust in my abilities, his enthusiasm for my project, the discussions that pushed the projects forward, and his support throughout my doctoral studies.

Furthermore, I would like to thank Prof. Helmut Ritter and Dipl. WiChem. Martin Hetzer for the support and fruitful discussions in our collaborative project.

I am thankful for the great cooperation with Prof. Felix Schacher and Dipl. Chem. Tobias Rudolph. It was a pleasure to work with you. Furthermore, I thank Prof. Mathias Rehahn and Dr. Markus Gallei for a great collaboration as well. Especially Markus has to be mentioned, as he had a significant impact on my lab-skills and on my development as a scientist.

Thanks go to Dr. Eva Blasco and Dr. Cesar Rodriguez-Emmenegger for fruitful collaborations during their stay in our group as visitor. I would also like to thank Dipl. Chem. Tanja Claus, Dipl. Chem. Doris Abt, and B.Sc. Janin Offenloch whom I supervised in their advanced lab course, diploma thesis, or bachelor thesis, respectively. It was a pleasure to work with you, to teach you, and to follow how you develop into good scientists.

Many thanks go to all present and former members of the *macroarc* research team. It was a pleasure to work and laugh with you. Furthermore, I thank the AC crew for the nice atmosphere and company, especially Dr. Anna-Marie Zorn, Dr. Dominik Voll, Dipl. Chem. Johannes Willenbacher, and Peter Gerstel. Additional thanks go to Dipl. Chem. Christiane Lang, Dr. Dominik Voll, Dipl. Chem. Johannes Willenbacher, and Dipl. Chem. Michael Kaupp for proof reading of this thesis.

Many thanks to Gabriele Herrmann and Evelyn Stüring for the support in administrative matters, as well as Dr. Maria Schneider and Peter Gerstel for ordering every item that was used in the course of this thesis. Furthermore, I would like to thank Dr. Maria Schneider for the great teamwork in the supervision of the SEC instruments and I am thankful to Pia Lang and Tanja Ohmer for performing NMR measurements at the Institute of Organic Chemistry.

Special thanks go to Anna-Marie Zorn, Astrid Hirschbiel, Azize Ünal, Cesar Rodriguez-Emmenegger, Christiane Lang, Christoph Dürr, Dominik Voll, Doris Abt, Jan Müller, Johannes Willenbacher, Kim Öhlenschläger, and Pieter Derboven

for their friendship during my time in Karlsruhe. I appreciate your support and care for me. I will never forget you and hope to see you again.

I thank my chemistry teacher Hubert Giar for infecting me with his enthusiasm for science, and chemistry in particular. Furthermore, I thank Peter Gerstel for supporting me in scientific matters as well as the more important things in life. If I only had half of the spirit of you two I would be a great man.

Thanks go out to my friends, especially (in chronological order) Youssef Afkir, Martin Krauß, Jan Paul Marschollek, Ali Hartwig, Jan-Eric Teves, and Tobi Rudi. I am very proud to call you my friends.

I thank Anna-Elisabeth Kreuder for her support. She has an essential share in the success of this thesis. Although many things come to an end, some things remain forever and are beyond this thesis.

Most notably, I thank Lisa Cielen for her support before the doctor examination and the time afterwards. I hope to have many more exciting years with you.

Finally, I thank my parents and my sister for their support throughout my life's journey.

Contents

Abbreviations

2VP	2-Vinylpyridine
4VP	4-Vinylpyridine
AA	Acrylic acid
AAm	Acrylamide
Ad	Adamantyl
AFM	Atomic force microscopy
AIBN	2,2′-Azobis(2-methylpropionitrile)
AMPS	2-Acrylamido-2-methylpropanesulfonic acid
arom	Aromatic
ATRP	Atomtransfer radical polymerization
β_{mn}	Overall association constant
β-CD-N_3	Mono azido functionalized β-CD
CBMAA-3	3-(Methacryloylamino-propyl)-(2-carboxy-ethyl)-dimethylammonium carboxybetaine methacrylamide
CD	Cyclodextrin
CL	ϵ-caprolactone
CMP	2-(1-Carboxy-1-methylethylsulfanylthiocarbonylsulfanyl)-2-methylpropionic acid
ConA	Concanavalin A
CPDB	2-Cyano-2-propyl benzodithioate
CTA	Chain transfer agent
C_{tr}	Chain transfer constant
CTP	4-Cyano-4-(phenylcarbonothioylthio)pentanoic acid
CuAAC	Copper (I) catalyzed azide-alkyne cycloaddition
d	Average number of chains formed in a termination reaction
D_h	Hydrodynamic diameter
$Đ_m$	Molar mass dispersity
D_p	Degree of polymerization
DCC	*N*,*N*′-dicyclohexylcarbodiimide
DCM	Dichloromethane
DEAAm	*N*,*N*-diethylacrylamide
DIAD	Diisopropylazodicarboxylate
DLS	Dynamic light scattering
DMF	*N*,*N*-dimethylformamide

DMAAm	*N,N*-dimethylacrylamide
DMAc	*N,N*-dimethylacetamide
DMAEMA	*N,N*-dimethylaminoethyl methacrylate
DMAP	4-Dimethylaminopyridine
DMAPS	3-Dimethyl(methacryloyloxyethyl) ammonium propane sulfonate
DMP	2-(Dodecylthiocarbonothioylthio)-2-methylpropionic acid
DMSO	Dimethylsulfoxide
DNA	Desoxyribonucleic acid
Dopat	2-((Dodecylsulfanyl)carbonothioyl)sulfanyl propionic acid
DOSY	Diffusion-ordered NMR spectroscopy
Dox	Doxorubicin
DPTS	4-(Dimethylamino)-pyridinium *p*-toluenesulfonate
ECD	PEG-*b*-PCL-*b*-PDMAEMA
EDTA	Ethylenediaminetetraacetic acid disodium salt
EMP	2-(((Ethylthio)carbonothioyl)thio)-2-methylpropanoic acid
EPX	Ethyl 2-((ethoxycarbonothioyl)thio)propanoate
eq	Equivalents
ESI-MS	Electrospray ionization mass spectrometry
f	Initiator efficiency
FT-IR	Fourier transform infrared
GAPDH	Glyceraldehyde 3-phosphate dehydrogenase
$\Delta H_{\text{complex}}$	Complex association enthalpy
HEA	Hydroxyethyl acrylate
HPMA	*N*-(2-hydroxypropyl)methacrylamide
ITC	Isothermal titration calorimetry
J	Coupling constant
K_{ij}	Association constant of i and j
k_{add}	Rate coefficient of addition
k_{β}	Rate coefficient of fragmentation
k_{de}	Rate coefficient of initiator decay
k_{ini}	Rate coefficient of initiation
k_{p}	Rate coefficient of propagation
k_{trec}	Rate coefficient of termination by recombination
k_{td}	Rate coefficient of termination by disproportionation
λ	Wavelength
LCST	Lower critical solution temperature
MADIX	Macromolecular design via the interchange of xanthates
Me-β-CD	Randomly methylated β-cyclodextrin
m_{CTA}	Molar mass of CTA
m_{M}	Molar mass of monomer
M_{n}	Number-average molecular weight
MPEG	Methoxy poly(ethylene glycol)
MS	Mass spectrometry
MWCO	Molecular weight cut off
NAS	*N*-acryloxysuccinimide

NCCM	Noncovalently connected micelle
NIPAAm	*N*-isopropylacrylamide
NMP	Nitroxide-mediated polymerization
NMR	Nuclear magnetic resonance
NOESY	Nuclear Overhauser enhancement spectroscopy
OEGMA	Oligo ethylene glycol methacrylate
PAA	Poly(acrylic acid)
PCL	Poly(ϵ-caprolactone)
PDEAAm	Poly(*N,N*-diethylacrylamide)
PDMAAm	Poly(*N,N*-dimethylacrylamide)
PDMAEMA	Poly(2-(dimethylamino)ethyl methacrylate)
pDNA	Plasmid DNA
PEG	Poly(ethylene glycol)
PHEA	Poly(hydroxyethyl acrylate)
PHPMA	Poly(*N*-(2-hydroxypropyl)methacrylamide)
PLA	Poly(lactic acid)
PMDETA	N,N,N',N'',N''-pentamethyldiethyltriamine
PMMA	Poly(methyl methacrylate)
PNIPAAm	Poly(*N*-isopropylacrylamide)
PPG	Poly(propylene glycol)
PSty	Poly(styrene)
R_h	Hydrodynamic radius
RAFT	Reversible addition-fragmentation chain transfer
RI	Refractive index
ROESY	Rotating frame nuclear Overhauser enhancement spectroscopy
ROP	Ring opening polymerization
$\Delta S_{complex}$	Complex association entropy
SEC	Size exclusion chromatography
SEM	Scanning electron microscopy
siRNA	Small interfering ribonucleic acid
SLS	Static light scattering
TEM	Transmission electron microscopy
TFA	Trifluoroacetic acid
TGA	Thermo gravimetric analysis
THF	Tetrahydrofuran
UV	Ultra-violet
UV/Vis	Ultra-violet/visible
V-501	4,4′-Azobis(4-cyanovaleric acid)
VA-044	2,2′-Azobis[2-(2-imidazolin-2-yl)propane]dihydrochloride
XPS	X-ray photoelectron spectroscopy

Chapter 1
Introduction

1.1 Motivation

Polymeric materials play a significant role in contemporary society, e.g. as consumables, as high performance materials or in high-tech applications. The progress in these fields depends to a significant amount on the achievements of polymer science. Especially the development of novel complex macromolecular architectures have driven polymer scientists in recent years [1–3]. The ability to control macromolecular architectures gives rise to the fabrication of materials with novel or improved properties and thus enables the development of new products in a broad range of applications, e.g. microelectronic materials [4], drug/gene delivery [5], biomedical materials [6], supersoft elastomers [7] or hybrid materials [8].

The development of reversible-deactivation radical polymerization techniques, e.g. nitroxide-mediated radical polymerization (NMP) [9, 10], atom transfer radical polymerization (ATRP) [11, 12], and reversible addition-fragmentation chain transfer (RAFT) polymerization [13–15], has provided very suitable and convenient tools for the preparation of complex macromolecular architectures in a controlled fashion. The introduction of *click* chemistry had a further impact on the preparation of complex macromolecular architectures [16–19]. The utilization of complex building blocks with a large diversity, based on the high tolerance of functional groups obtained from reversible-deactivation radical polymerization techniques in highly efficient mild and fast coupling reactions enables the synthesis of complex macromolecular architectures in a modular fashion, e.g. via copper(I)-catalyzed azide-alkyne cycloaddition (CuAAc) [20], thiol-ene [21, 22] or Diels-Alder reactions [23].

Apart from reversible-deactivation radical polymerization techniques and click chemistry, supramolecular chemistry had a significant impact on polymer science. Supramolecular interactions provide a set of new properties that can be utilized in materials design and especially in the formation of complex macromolecular architectures, e.g. reversibility or stimuli-response. Several supramolecular systems have been utilized in polymer chemistry, e.g. hydrogen bonding [24, 25], metal complexes [26] as well as inclusion complexes [27–29]. One of the frequently utilized inclusion

B. V. K. J. Schmidt, *Novel Macromolecular Architectures via a Combination of Cyclodextrin Host/Guest Complexation and RAFT Polymerization*, Springer Theses,
DOI: 10.1007/978-3-319-06077-4_1, © Springer International Publishing Switzerland 2014

complex systems are cyclodextrins (CDs) [30, 31], as they form host/guest complexes with hydrophobic guest molecules/recognition sites (refer to Sect. 2.2). The combination of CD-based host/ guest chemistry and polymer science has been under investigation with regard to a variety of applications, e.g. drug delivery [32], nano-structures [28], supramolecular polymers [33], self-healing materials [34], amphiphiles [35] or bioactive materials [36].

1.2 Thesis Overview

Considering complex macromolecular architectures, CDs offer the opportunity to generate complex macromolecular architectures via supramolecular interactions (refer to Sect. 2.3). To facilitate the formation of complex macromolecular architectures via CD host/guest chemistry, control over polymer end functionality is necessary. End functionalized building blocks can subsequently be applied for the formation of novel architectures via the combination of suitable host and guest functionalized blocks (refer to Fig. 1.1). As different building blocks are utilized, in principle almost unlimited combinations are conceivable, making the formation of complex macromolecular architectures possible in a modular fashion. CD-based supramolecular interactions usually occur in aqueous solution, which restricts the nature of the polymer building blocks to water-soluble polymers. Especially RAFT polymerization is a perfect tool for the formation of water-soluble polymers in a controlled fashion, e.g. with control over end functionality, low molar mass dispersity ($Đ_m$) and control over molar mass (refer to Sect. 2.1). One of the major tasks in the present work is the formation of novel complex macromolecular architectures governed by supramolecular CD host/guest complexes via building blocks synthesized with RAFT polymerization. Thus, the RAFT process is utilized to control polymer functionalities, while supramolecular interactions are utilized to control polymer topology and composition.

In the current thesis, RAFT polymerization was utilized to generate polymers with CD- or guest-endgroups (refer to Fig. 1.1). Therefore, a method was developed to synthesize hydrophilic polymers with hydrophobic guest endgroups directly in water via complexation of guest-functionalized RAFT reagents with CD for the first time. As a direct implication of these results, polymers of that type—namely guest end functionalized poly(*N*,*N*-diethylacrylamide) (PDEAAm)—were investigated with regard to their thermoresponsive behavior. Addition of CD and subsequent complexation of the hydrophobic endgroup led to changes in the cloud point of the polymer solution. Thus, CD host/guest interactions were utilized to modulate the thermoresponsive behavior of PDEAAm. Furthermore, polymers with tailored end functionality were subsequently utilized in the formation of supramolecular macromolecular architectures. Guest functionalized polymers of various types were utilized in the formation of several complex macromolecular architectures. Doubly guest functionalized polymers were connected to CD functionalized polymers via supramolecular interactions to form novel ABA block copolymers. Singly guest endfunctionalized

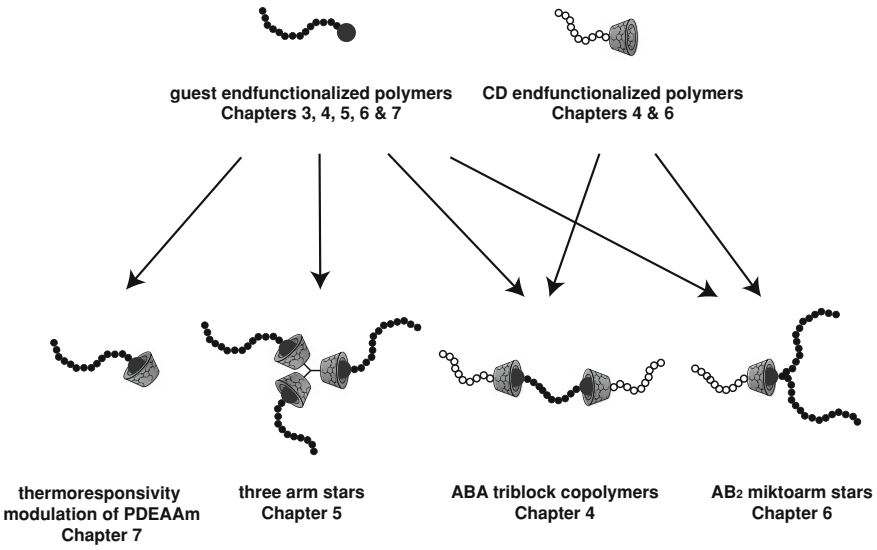

Fig. 1.1 Overview of different projects and building blocks described in the current thesis

polymers were connected to a threefold CD functionalized core to form three-armed star polymers. With mid-chain guest functionalized and a CD end functionalized polymer, supramolecular AB_2 miktoarm star polymers were prepared.

References

1. Hawker CJ, Wooley KL (2005) The convergence of synthetic organic and polymer chemistries. Science 209:1200–1205
2. Hadjichristidis N, Hirao A, Tezuka Y, Du Prez F (eds) Complex macromolecular architectures: synthesis, characterization, and self-assembly. John Wiley & Sons (Asia) Pte Ltd, Singapore (2011)
3. Gregory A, Stenzel MH (2012) Complex polymer architectures via RAFT polymerization: from fundamental process to extending the scope using click chemistry and nature's building blocks. Prog Polym Sci 37:38–105
4. Hedrick JL, Magbitang T, Connor EF, Glauser T, Volksen W, Hawker CJ, Lee VY, Miller RD (2002) Application of complex macromolecular architectures for advanced microelectronic materials. Chem Eur J 8:3308–3319
5. Grayson SM, Godbey WT (2008) The role of macromolecular architecture in passively targeted polymeric carriers for drug and gene delivery. J Drug Target 16:329–356
6. Tian H, Tang Z, Zhuang X, Chen X, Jing X (2012) Biodegradable synthetic polymers: preparation, functionalization and biomedical application. Prog Polym Sci 37:237–280
7. Neugebauer D, Zhang Y, Pakula T, Sheiko SS, Matyjaszewski K (2003) Densely-grafted and double-grafted PEO brushes via ATRP. A route to soft elastomers. Macromolecules 36:6746–6755
8. Soler-Illia GJAA, Azzaroni O (2011) Multifunctional hybrids by combining ordered mesoporous materials and macromolecular building blocks. Chem Soc Rev 40:1107–1150

9. Hawker CJ, Bosman AW, Harth E (2001) New polymer synthesis by nitroxide mediated living radical polymerization. Chem Rev 101:3661–3688
10. Nicolas J, Guillaneuf Y, Lefay C, Bertin D, Gigmes D, Charleux B (2013) Nitroxide-mediated polymerization. Prog Polym Sci 38:63–235
11. Ouchi M, Terashima T, Sawamoto M (2009) Transition Metal-catalyzed living radical polymerization: toward perfection in catalysis and precision polymer synthesis. Chem Rev 109:4963–5050
12. Matyjaszewski K (2012) Atom transfer radical polymerization (ATRP): current status and future perspectives. Macromolecules 45:4015–4039
13. Barner-Kowollik C (2008) Handbook of RAFT-polymerization. Wiley-VCH, Weinheim
14. Barner-Kowollik C, Perrier SJ (2008) The future of reversible addition fragmentation chain transfer polymerization. Polym Sci Part A Polym Chem 46:5715–5723
15. Moad G, Rizzardo E, Thang SH (2012) Living radical polymerization by the RAFT process—a third update. Aust J Chem 65:985–1076
16. Kolb HC, Finn MG, Sharpless KB (2001) Click chemistry: diverse chemical function from a few good reactions. Angew Chem Int Ed 40:2004–2021
17. Barner-Kowollik C, Du Prez FE, Espeel P, Hawker CJ, Junkers T, Schlaad H, Van Camp W (2011) "Clicking" polymers or just efficient linking: what is the difference? Angew Chem Int Ed 50:60–62
18. Kempe K, Krieg A, Becer CR, Schubert US (2012) "Clicking" on/with polymers: a rapidly expanding field for the straightforward preparation of novel macromolecular architectures. Chem Soc Rev 41:176–191
19. Binder WH, Sachsenhofer R (2007) 'Click' chemistry in polymer and materials science. Macromol Rapid Commun 28:15–54
20. Lutz JF (2007) 1,3-dipolar cycloadditions of azides and alkynes: a universal ligation tool in polymer and materials science. Angew Chem Int Ed 46:1018–1025
21. Hoyle C, Bowman C (2010) Thiol-ene click chemistry. Angew Chem Int Ed 49:1540–1573
22. Lowe AB (2010) Thiol-ene "click" reactions and recent applications in polymer and materials synthesis. Polym Chem 1:17–36
23. Tasdelen MA (2011) Diels-Alder "click" reactions: recent applications in polymer and material science. Polym Chem 2:2133–2145
24. Wilson AJ (2007) Non-covalent polymer assembly using arrays of hydrogen-bonds. Soft Matter 3:409–425
25. Bertrand A, Lortie F, Bernard J (2012) Routes to hydrogen bonding chain-end functionalized polymers. Macromol Rapid Commun 33:2062–2091
26. Kurth DG, Higuchi M (2006) Transition metal ions: weak links for strong polymers. Soft Matter 2:915–927
27. Zayed JM, Nouvel N, Rauwald U, Scherman OA (2010) Chemical complexity-supramolecular self-assembly of synthetic and biological building blocks in water. Chem Soc Rev 39:2806–2816
28. Chen G, Jiang M (2011) Cyclodextrin-based inclusion complexation bridging supramolecular chemistry and macromolecular self-assembly. Chem Soc Rev 40:2254–2266
29. Zheng B, Wang F, Dong S, Huang F (2012) Supramolecular polymers constructed by crown ether-based molecular recognition. Chem Soc Rev 41:1621–1636
30. van de Manakker F, Vermonden T, van Nostrum CF, Hennink WE (2009) Cyclodextrin-based polymeric materials: synthesis, properties, and pharmaceutical/biomedical applications. Biomacromolecules 10:3157–3175
31. Yhaya F, Gregory AM, Stenzel MH (2010) Polymers with sugar buckets—the attachment of cyclodextrins onto polymer chains. Aust J Chem 63:195–210
32. Zhou J, Ritter H (2010) Cyclodextrin functionalized polymers as drug delivery systems. Polym Chem 1:1552–1559
33. Harada A, Takashima Y, Yamaguchi H (2009) Cyclodextrin-based supramolecular polymers. Chem Soc Rev 38:875–882

34. Nakahata M, Takashima Y, Yamaguchi H, Harada A (2011) Redox-responsive self-healing materials formed from host/guest polymers. Nat Commun 2:511
35. Zhang X, Wang C (2011) Supramolecular amphiphiles. Chem Soc Rev 40:94–101
36. Chen Y, Liu Y (2010) Cyclodextrin-based bioactive supramolecular assemblies. Chem Soc Rev 39:495–505

Chapter 2
Theoretical Background and Literature Overview

As stated in the introduction, the present thesis is based on a combination of reversible-deactivation radical polymerization via the RAFT process and supramolecular CD host/guest complexes. The RAFT process provides the opportunity to generate polymers with specific endgroups, e.g. guest functionalities for CD. These polymers can subsequently be exploited for the formation of novel complex macromolecular architectures, e.g. block copolymers, star polymers or miktoarm star polymers. The underlying theoretical background is described in the following sections as well as an overview of CD mediated complex macromolecular architectures that have been published in the literature so far.

2.1 Reversible Addition-Fragmentation Chain Transfer Polymerization

2.1.1 Living Polymerization

A living polymerization is strictly speaking a chain propagation reaction that—after full monomer conversion—is still capable of propagation via addition of further monomer [2]. In an ideal case this occurs in polymerization reactions without any chain transfer and termination [3, 4]. Furthermore, the rate of initiation should be fast compared to the rate of propagation, which results in the synthesis of polymer chains with an overall similar degree of polymerization (D_p) [5]. Anionic and some cationic polymerizations are treated as classical/truly living polymerization, while the more recent atom transfer radical polymerization (ATRP) [6–8], nitroxide-mediated polymerization (NMP) [4, 9–11] and the RAFT polymerization [12–16] are treated as

Parts of this chapter were reproduced with permission from Schmidt et al. [1]. Copyright 2014 Elsevier.

B. V. K. J. Schmidt, *Novel Macromolecular Architectures via a Combination of Cyclodextrin Host/Guest Complexation and RAFT Polymerization*, Springer Theses,
DOI: 10.1007/978-3-319-06077-4_2, © Springer International Publishing Switzerland 2014

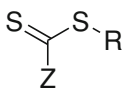

Fig. 2.1 General structure of a CTA/RAFT agent

polymerization with living characteristics, as controlled radical polymerization [17] or reversible-deactivation radical polymerization. All living polymerization techniques have in common that D_p increases linearly with monomer conversion, block copolymers can be formed via sequential monomer addition and low $Đ_m$ are achieved.

In the case of ATRP, radical chain ends are generated via a transition metal catalyzed one electron redox-process that leads to halide terminated dormant chains or radical bearing active chains [6]. An equilibrium between dormant and active species that is centered on dormant species controls the reaction. In NMP, the persistent radical effect is utilized [4]. A nitroxide acts as a radical trap for active chains. As the process of chain termination via a nitroxide is reversible, an activation/deactivation equilibrium is formed. In both processes, ATRP and NMP, a small amount of active species leads to the minimization of radical termination events. The RAFT process is an alternative method to control radical polymerizations and achieves living behavior. Macromolecular design via the interchange of xanthates (MADIX) has an identical mechanism to RAFT yet uses slightly different controlling agents. Both methods were patented in 1998 [18, 19] and are utilized in polymer research very often since then [13, 14]. The RAFT process will be described in detail in the next sections.

RAFT and MADIX differ substantially from the other controlled radical polymerizations, as for the control of the polymerization no persistent radical effect is utilized (refer to Sect. 2.1.2), leading to an increase in propagation rate compared to the other controlled radical polymerization techniques. The process is tolerant to functional monomers, e.g. acrylic acid or vinyl acetate (refer to Sect. 2.1.3), and is especially useful for the preparation of water-soluble polymers (refer to Sect. 2.1.4). The RAFT process, as the other living polymerization techniques, is a tool for the synthesis of complex macromolecular architectures, e.g. block copolymers or star polymers (refer to Sect. 2.1.5).

2.1.2 Mechanism and Kinetics

The central element in the RAFT process is the chain transfer agent (CTA) that allows for control on the polymerization.

The CTA is typically a thiocarbonyl thio compound featuring two substituents that are usually abbreviated as R- and Z-group (refer to Fig. 2.1). These two substituents have a profound influence on the reactivity of the CTA and the RAFT process can be varied via the modification of these substituents. The R-group is also called the radical leaving group and the Z-group is also called the stabilizing group [20, 21].

As depicted in Scheme 2.1 the RAFT equilibria do not create or terminate radicals. Except of the termination reactions, every reaction in the RAFT process

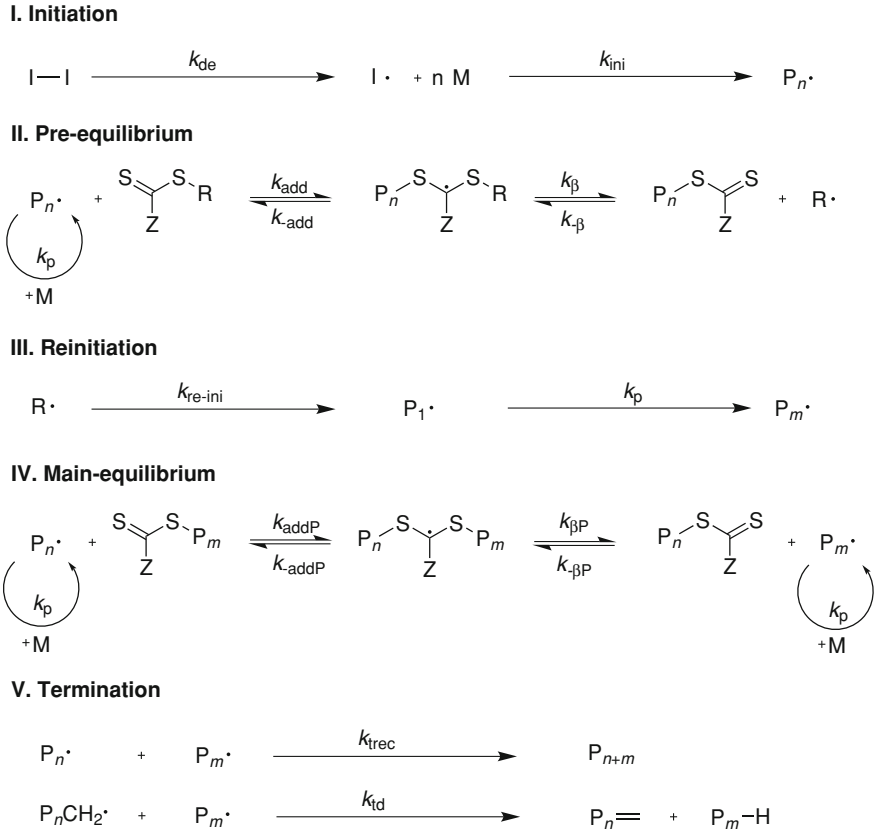

Scheme 2.1 Basic mechanism of the RAFT process

generates a radical. There are only bimolecular cooperative chain transfer reactions [22] and—in contrast to ATRP and NMP—no persistent radicals are involved that are endfunctionalizing polymers in a monomolecular process. Thus, no decrease in the polymerization rate should ideally occur from the RAFT process itself under the assumption that fragmentation and reinitiation are not rate defining. Nevertheless, often inhibition or slower propagation rates compared to conventional free radical polymerization are observed [13, 23]. The RAFT process can be divided into five distinct reaction sequences: Initiation, pre-equilibrium, reinitiation, main-equilibrium and termination. The mechanism of the RAFT process is depicted in Scheme 2.1.

The initiation occurs via the formation of primary radicals I· that form during the decay of a radical initiator I_2 with the rate coefficient k_{de}. The formed radicals react with monomers to short oligomeric chains P_n· with the rate coefficient k_{ini} until a radical reacts with a CTA molecule. The ratio of CTA to initiator should be high, especially when high endgroup functionalization is necessary, e.g. for chain extensions or complex macromolecular architecture formation. Furthermore, a high

Scheme 2.2 Reversible chain transfer in the RAFT process

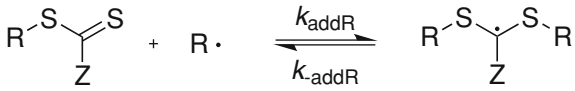

initiator concentration has the drawback of an increased probability of termination reactions due to higher radical concentration [22].

The initiator derived chain adds to a CTA molecule with the rate constant k_{add}. Subsequently the thiocarbonyl centered radical undergoes β-fragmentation with the rate coefficient k_β, which leads to the formation of a free radical R· and a thiocarbonyl thio capped chain. The reaction of the formed radical R· with the rate coefficients k_{addR} and k_{-addR} with another CTA molecule (refer to Scheme 2.2) is usually neglible due to the short life time of the intermediate. In the case of slow fragmentation and side-reactions of the intermediate the reaction should be taken into account [13].

For the description of the chain transfer, the chain transfer constants C_{tr} and C_{-tr} are defined:

$$C_{tr} = \frac{k_{tr}}{k_p} = \frac{k_{add}}{k_p} \cdot \frac{k_\beta}{k_{-add} + k_\beta} \tag{2.1}$$

and

$$C_{-tr} = \frac{k_{-tr}}{k_i} = \frac{k_{-\beta}}{k_i} \cdot \frac{k_{-add}}{k_{-add} + k_\beta} \tag{2.2}$$

The transfer constants depend strongly on the R- and Z-group present in the CTA. The higher the value of C_{tr}, the better is the control of the polymerization [13, 21]. The formed R· radical should reinitiate the polymerization effectively. Furthermore, the R-group has to be a good homolytic leaving group and especially a better leaving group than the radical of the monomer so that fragmentation towards the R-group is preferred. Thus, a balance between reinitiation and leaving group ability has to be found for an effective RAFT process.

The main equilibrium starts when all CTA molecules have reacted. In the equilibrium, the intermediate fragments with the rate coefficient k_{-addP} to the macroradical P_n· or P_m· and a thiocarbonyl thio chain end. With the rate coefficient k_{addP}, the thiocarbonyl thio chain end adds a macroradical again. Whenever a fragmentation takes place, the macroradical can add new monomers with the propagation rate constant k_p. The kinetics of the main equilibrium can be described with the chain transfer constant C_{trP}, which can differ slightly from the chain transfer constant of the pre-equilibrium C_{tr}. If the polymer fragments P_n· or P_m· are treated as identical, the following assumption can be made:

$$k_{-addP} = k_\beta \tag{2.3}$$

which effects the chain transfer constant of the main equilibrium C_{trP} as follows:

$$C_{trP} = \frac{k_{addP}}{2 \cdot k_p} \tag{2.4}$$

For optimal control of the polymerization, C_{trP} should be high [13, 21], i.e. the higher C_{trP} the closer is the plot of D_P against conversion to linearity. Furthermore, $Đ_m$ is decreasing with higher C_{trP}. In the ideal case, there is the same probability for chain growth for all propagating chains, which leads to narrow molecular weight distributions. Following this mechanism a large quantity of the formed polymers should bear the thiocarbonyl thio Z-group on one end and the R-group on the other end. Furthermore initiator derived chains are formed in minor amounts.

Termination reactions occur intrinsically, as in free radical polymerization, radical recombination with k_{trec} and disproportionation with k_{td}.

As with all living polymerization techniques, D_p and the number average molecular mass M_n can be calculated from the conversion and the concentrations of initiator and monomer. D_p is based on the concentration of monomer [M], the concentration of CTA [CTA], the average number of chains that are formed in a termination reaction d, the initiator efficiency f and the initiator concentration [I_2]:

$$D_p = \frac{[M]_0 - [M]_t}{[CTA]_0 + d \cdot f([I_2]_0 - [I_2]_t)} \tag{2.5}$$

With a large excess of CTA compared to initiator follows:

$$D_p \approx \frac{[M]_0 - [M]_t}{[CTA]_0} \tag{2.6}$$

M_n can be calculated analogously with the molar mass of the monomer m_M and the molar mass of the CTA m_{CTA}:

$$M_n = \left(\frac{[M]_0 - [M]_t}{[CTA]_0 + d \cdot f([I_2]_0 - [I_2]_t)} \cdot m_M\right) + m_{CTA} \tag{2.7}$$

A simplification analogous to the calculation of D_p leads to:

$$M_n \approx \left(\frac{[M]_0 - [M]_t}{[CTA]_0} \cdot m_M\right) + m_{CTA} \tag{2.8}$$

In this case a linear relation between M_n or D_p and the monomer conversion is evident, which is characteristic for polymerizations with living character. In an ideal RAFT process the formed thiocarbonyl thio functionalized macromolecule can be reinitiated for chain extension. Too high initiator concentrations lead to the formation of unreactive chains, as the degree of initiator functionalized polymers is increasing. As mentioned earlier, CTAs are often sulfur containing thiocarbonyl thio compounds that have to be chosen according to the monomer. For an efficient RAFT polymerization, the choice of the respective R- and Z-group are crucial. The RAFT agent needs a reactive C–S double bond, which results in high k_{add} values. The intermediate radicals should ideally fragment rapidly, based on a weak S–R bond which leads

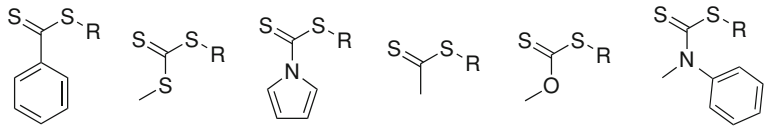

Fig. 2.2 Different types of CTAs [13]

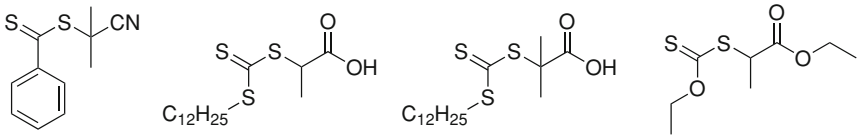

Fig. 2.3 Commonly utilized CTAs (**CPDB** 2-cyano-2-propyl benzodithioate; **Dopat** 2-((dodecylsulfanyl)carbonothioyl)sulfanyl propionic acid; **DMP** 2-(dodecylthiocarbonothioylthio)-2-methylpropionic acid; **EPX** ethyl 2-((ethoxycarbonothioyl)thio)propanoate)

to a large k_β value. Furthermore, the intermediate should partition in favor of the products, i.e. $k_\beta > k_{-\text{add}}$ and R· should effectively reinitiate the polymerization:

In Fig. 2.2 different Z-groups for CTAs are presented, e.g. aromatic (a) or aliphatic (d) dithioesters, trithiocarbonates (b), xanthates (e) and dithiocarbamates (c and f). The rate coefficients for addition and the transfer constants decrease from left ot right [20, 22, 24]. Via the Z-group, the addition and fragmentation rates are modified. The R-group has to be a good radical leaving group that is able to reinitiate the polymerization. Common R-groups include tertiary carbon atoms, e.g. in a cyanoisopropyl group, a cumyl group or an *iso*-butyric acid, or secondary carbon atoms, e.g. in a benzylic group or a *iso*-propionic acid.

2.1.3 Applicability of the Method and Reaction Conditions

The RAFT process gives the opportunity to perform reversible-deactivation radical polymerizations with a large variety of monomers, e.g. styrenic monomers, (meth)acrylates, (meth)acrylamides, vinyl acetate and *N*-vinyl monomers. A tertiary cyanoalkyl dithiobenzoate can act as CTA for styrene (Sty) and methyl methacrylate (MMA) (refer to compound **CPDB** in Fig. 2.3).

Another common class of CTAs are trithiocarbonates connected to tertiary or secondary carboxylic acids or esters (refer to the compounds **Dopat** or **DMP** in Fig. 2.3) that can be used to polymerize styrenics, acrylates or acrylamides. Xanthates (refer to compound **EPX** in Fig. 2.3) or cyanoalkyldithiocarbamates can be utilized

in the polymerization of vinyl acetate or *N*-vinyl monomers, e.g. *N*-vinylpyrrolidone or *N*-vinylcarbazole.

The reaction conditions can usually be adopted from the corresponding conventional free radical polymerization with a commonly used polymerization temperature ranging from ambient temperature to 140 °C. Usually, organic solvents are utilized, yet protic solvents such as alcohols or water can be utilized as well. Furthermore, bulk or emulsion polymerizations are described in the literature [13]. For the initiation every radical source is in principle utilizable [18], but in most cases thermal initiators are employed, e.g. 2,2′-azo-bis-(isobutyronitril) (**AIBN**). Other initiation methods are self-initiation [25, 26], UV-irradiation [27], γ irradiation [28] or a plasma field [29].

2.1.4 Preparation of Water-Soluble Polymers via RAFT Polymerization

RAFT polymerization is arguably the most useful controlled radical polymerization technique for the synthesis of water-soluble polymers [30]. In principle a polymerization in organic solvents or directly in water is possible. For the polymerization in water several water-soluble CTAs and initiators are available (refer to Fig. 2.4). In the case of organic solvents as reaction media a usual RAFT polymerization can be conducted as long as the monomer and polymer are soluble in the respective organic solvent. This is true for some of the mostly used monomers, e.g. *N*-isopropylacrylamide (**NIPAAm**), **DEAAm**, *N*,*N*-dimethylacrylamide (**DMAAm**) or *N*,*N*-dimethylaminoethyl methacrylate (**DMAEMA**). Nevertheless, problems arise when ionic or very hydrophilic monomers are considered that are only soluble in water or at least their corresponding polymers, e.g. styrene sulfonate [31], 2-acrylamido-2-methylpropansulfonic acid (**AMPS**) [32], (3-methacryloylamino-propyl)-(2-carboxy-ethyl)-dimethyl-ammonium (carboxybetaine methacrylamide) (**CBMAA-3**) [33] or acrylamide (**AAm**) [34]. Apart from the monomer choice, water as reaction solvent can have several advantages, when compared to organic solvents. Water is non-toxic, relatively cheap and has a high heat capacity. Some drawbacks are its high boiling point, thus water is not easy to recycle or to remove.

The CTA should be water-soluble in an aqueous polymerization, e.g. 4-cyano-4-(phenylcarbonothioylthio)pentanoic acid (**CTP**), 2-(((ethylthio)carbonothioyl)thio)-2-methylpropanoic acid (**EMP**) or 2-(1-carboxy-1-methylethylsulfanylthiocarbonyl sulfanyl)-2-methylpropionic acid (**CMP**). Nevertheless some side reactions are known that lead to less well defined polymers. McCormick and coworkers spent significant effort to study RAFT polymerization in water. At high temperatures and under neutral or basic conditions the CTA can undergo hydrolysis [30, 35, 36]. In the case of the polymerization of acrylamides, aminolysis can happen after hydrolysis of the respective monomer [30, 35]. Of course, hydrolysis of an amide is not a preferred process, yet when the equivalents of CTA to monomer are considered,

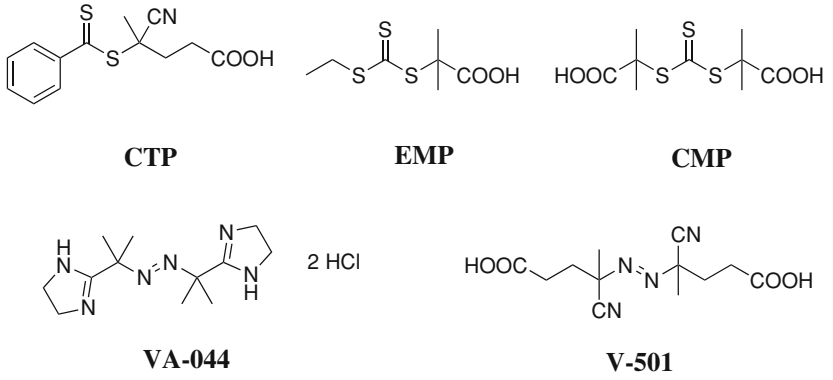

Fig. 2.4 Commonly utilized water-soluble CTAs and radical initiators (**CTP** 4-cyano -4-(phenylcarbonothioylthio)pentanoic acid; **EMP** 2-(((ethylthio)carbonothioyl)thio)-2-methylpropanoic acid; **CMP** 2-(1-carboxy-1-methylethylsulfanylthiocarbonylsulfanyl)-2-methylpropionic acid; **VA-044** 2,2′-azobis[2-(2-imidazolin-2-yl)propane]dihydrochloride; **V-501** 4,4'-azobis(4-cyanovaleric acid))

already a small portion of hydrolysis can lead to loss of CTA and thus control of the polymerization. Usually a higher molecular mass than expected and broader molecular mass distributions are observed. A possibility to overcome these issues is to polymerize in slightly acidic media, e.g. acetic acid buffer, at low temperatures or at best in acidic media and at low temperatures. In these cases even controlled RAFT polymerizations of acrylamides in water are possible [34, 37, 38].

Several monomer classes for water-soluble polymers are available (refer to Fig. 2.5) and can be chosen for the respective application [30, 39]. There are anionic monomers or monomers that can easily be deprotonated, e.g. styrene sulfonate [31], **AMPS** [32] or acrylic acid (**AA**) [40]. Cationic monomers, monomers that can be protonated or quaternized, e.g. 2-vinylpyridine (**2VP**) [41], 4-vinylpyridine (**4VP**) [41, 42] or **DMAEMA** [43, 44], are available as well. Furthermore, zwitterionic monomers, e.g. **CBMAA-3** [33] or 3-dimethyl(methacryloyloxyethyl) ammonium propane sulfonate (**DMAPS**) [45], have been utilized in RAFT polymerizations. A very frequently employed class of monomers are non-ionic monomers, which are mostly acrylamides, e.g. **AAm** [34], **DMAAm** [34], **DEAAm** [46], **NIPAAm** [47] and *N*-(2-hydroxypropyl)methacrylamide (**HPMA**) [33, 48].

2.1.5 Complex Macromolecular Architectures via RAFT Polymerization

The RAFT process is a tool to generate a broad range of macromolecular architectures (refer to Fig. 2.6). As the structure of the CTA is retained in the formed polymer, a modification of the CTA in the R- or Z-part provides the opportunity to incorporate

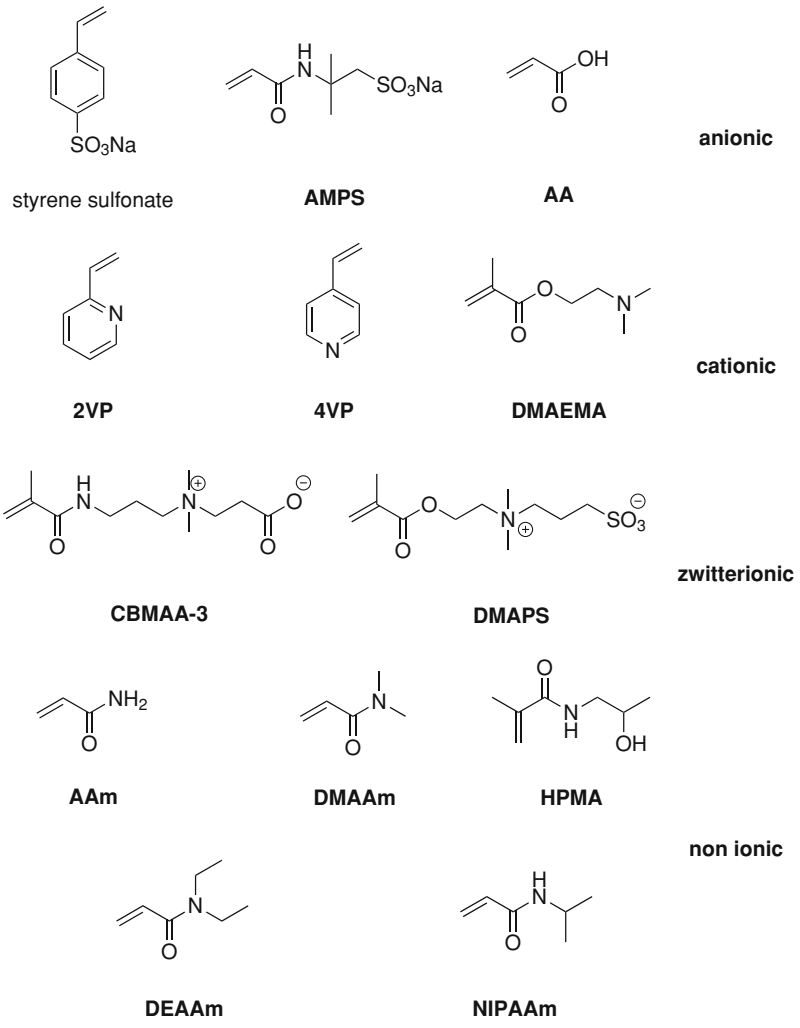

Fig. 2.5 Selection of monomers for the preparation of water-soluble polymers (**AMPS** 2-acrylamido-2-methylpropansulfonic acid; **2VP** 2-vinylpyridine; **4VP** 4-vinylpyridine; **DMAEMA** *N*,*N*-dimethylaminoethyl methacrylate; **CBMAA-3** (3-methacryloylamino-propyl)-(2-carboxy-ethyl)-dimethyl-ammonium (carboxybetaine methacrylamide); **DMAPS** 3-dimethyl(methacryloyloxyethyl) ammonium propane sulfonate; **AAm** acrylamide; **DMAAm** *N*,*N*-dimethylacrylamide; **HPMA** *N*-(2-hydroxypropyl)methacrylamide; **DEAAm** *N*,*N*-diethylacrylamide; **NIPAAm** *N*-isopropylacrylamide)

specific endgroups into polymers [49], e.g. azides [50, 51], alkynes [50], amines [52], alcohols [53] or carboxylic acids [54, 55]. The broad range of possible endgroups leads to a braod range of applications and combinations. Furthermore, several reactive

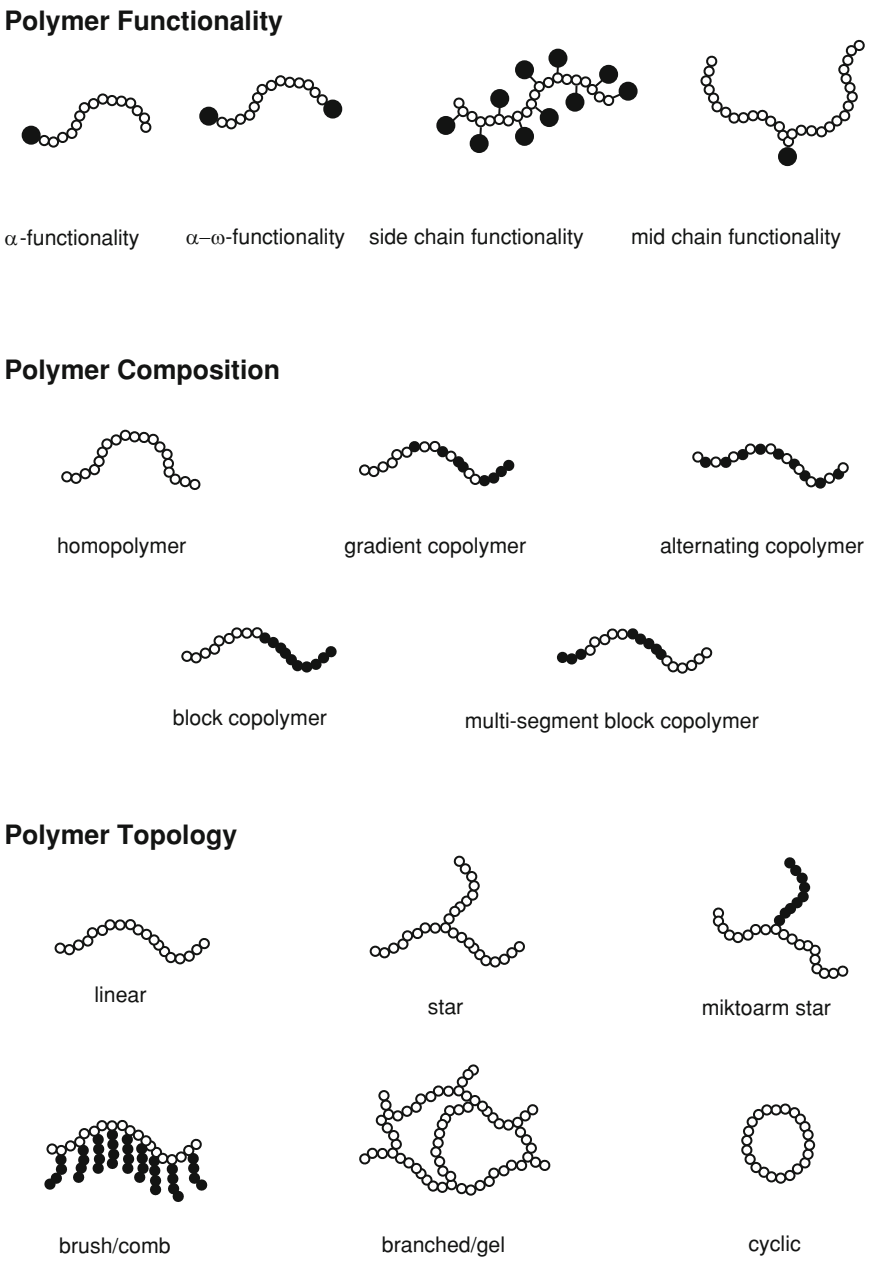

Fig. 2.6 Overview of macromolecular architectures that are accessible via RAFT polymerization

endgroups can be utilized in the formation of complex macromolecular architectures, e.g. in modular ligation reactions [56–59].

An alternative possibility is an endgroup conversion of thiocarbonyl thio endgroups, e.g. thermolysis [60], hydrolysis [61], aminolysis [54] or reduction [62]. Furthermore oxidation [63], radical- [60] and irradiation-induced [64] endgroup removal have been reported in the literature.

Block copolymers can be generated via modular ligation reactions, e.g. CuAAc [49, 50]. Another possibility is the utilization of a macro-CTA, i.e. a polymer that contains a thiocarbonyl thio endgroup. These polymers can be reinitiated and chain extended after initiator and monomer addition [65]. An alternative strategy is the addition of further monomer after high conversion of the first monomer, but in that case gradient block copolymers with tapered transition [17] are obtained [22]. These gradient copolymers are usually not very well suited for microphase separations. A drawback of block copolymer generation via macro-CTAs is that only monomers with similar reactivity can be utilized [49]. A possibility to connect electron rich monomers with electron deficient monomers is the utilization of *N*-(4-pyridinyl)-*N*-methyldithiocarbamate [66]. With this CTA, the formation of block copolymers of methyl methacrylate and vinyl acetate is possible via protonation of the pyridinyl substituent.

Other complex structures can be formed via specially designed CTAs [13, 67], e.g. star polymers [68], polymer brushes [69], dendritic structures [70] or amphiphiles [71].

2.2 Cyclodextrins and Their Complexes

2.2.1 Supramolecular Chemistry

The term of supramolecular chemistry has been defined by Jean-Marie Lehn in 1978. The Nobel laureate of 1987 has defined it as chemistry of non-covalent interactions between host and guest molecules [72, 73]. It can be viewed as chemistry beyond the molecule: While molecular chemistry is based on intramolecular covalent bonds, supramolecular chemistry is based on intermolecular non-covalent bonds [74–76]. Several non-covalent interactions have proven to be versatile in supramolecular chemistry, e.g. hydrogen bonding, metal-ligand interactions or van der Waals interactions [75]. Thus, supramolecular chemistry leads to the formation of supramolecular objects that are defined by the nature of the molecular components and furthermore by the type of interaction between them [75]. In recent years the field of supramolecular chemistry has evolved into areas such as molecular devices and machines or molecular recognition, such as self-assembly and self-organization. One of the frequently utilized host compounds in supramolecular chemistry are CDs that are the focus of the next sections.

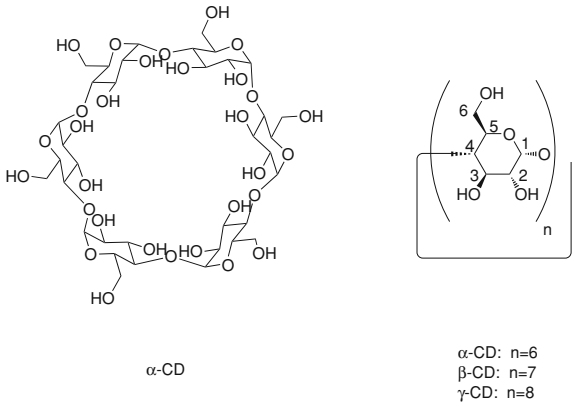

Fig. 2.7 Chemical structure of native CDs and common labelling of C-atoms in the glucose units

2.2.2 Structure and Properties of CDs

CDs are cyclic oligo saccharides of α-D-glucose that are formed through glycosidic α-1,4 bonds [77]. CDs are synthesized in an industrial biochemical process from starch via enzymatic pathways with CD glycosyl transferases, e.g. from *bacillus macerans* [78]. The commonly utilized CDs, also called native CDs, are the ones with n = 6 , 7 or 8 repeating units and are called α-CD, β-CD and γ-CD, respectively (refer to Fig. 2.7 and Table 2.1).

The chemical structure of the CDs resolves in a shallow truncated cone shape of the CD which forms a cavity with openings of two sizes. The exterior of the molecule is very polar/hydrophilic due to many hydroxyl groups whereas the interior is quite nonpolar/hydrophobic. The property of different polarity in different parts of the molecule leads to the most important and utilized ability of CDs: They readily form inclusion complexes with hydrophobic molecules that fit into the cavity in polar environments, mainly in aqueous solution. The complex formation results in several changes of the properties of the guest molecule. First of all, the water solubility of hydrophobic molecules rises significantly. Furthermore, the vapour pressure decreases after complexation as well as the stability against oxidation under air or light induced degradation [79]. In several cases CDs activate chemical reactions, e.g. the hydrolysis of various phenylesters [79, 80]. As CDs are optically active, they are also utilized in chiral catalysis [81]. Other applications include drug delivery [82–84], catalysis [84], chromatography (also for chiral separation) [85] or as food ingredient to mask odours or protect food ingredients against decomposition [84, 86].

CD host/guest complexes can be prepared in solution [87, 88], by coprecipitation [88, 89] or in a slurry [88, 89] as well as in the solid state, e.g. cogrinding or milling [87–89]. In the case of complex formation in solution, sometimes a cosolvent has to be added to enhance the accessibility of the guest, which is depending on the water solubility of the guest molecule.

Table 2.1 Dimensions and water solubility of native CDs

Type of CD	α-CD	β-CD	γ-CD
Number of glucose units	6	7	8
Cavity length (Å)	8	8	8
Approx. cavity diameter (Å)	5.2	6.6	8.4
Water solubility at 25 °C (mol L^{-1})	0.121	0.016	0.168

2.2.3 Thermodynamics and Theory of CD Inclusion Complexation

The complexation of CDs with guest (G) molecules can be considered as a bimolecular process [77]:

$$\begin{aligned} \mathrm{G} + \mathrm{CD} &\rightleftharpoons \mathrm{GCD} \\ \mathrm{GCD} + \mathrm{CD} &\rightleftharpoons \mathrm{GCD_2} \\ \mathrm{GCD} + \mathrm{G} &\rightleftharpoons \mathrm{G_2CD} \end{aligned}$$

These equilibria summarize the formation of CD:G 1:1, 1:2 or 2:1 complexes with the following association constants:

$$K_{11} = \frac{[\mathrm{GCD}]}{[\mathrm{G}][\mathrm{CD}]} \tag{2.9}$$

$$K_{12} = \frac{[\mathrm{GCD_2}]}{[\mathrm{GCD}][\mathrm{CD}]} \tag{2.10}$$

$$K_{21} = \frac{[\mathrm{G_2CD}]}{[\mathrm{G}][\mathrm{GCD}]} \tag{2.11}$$

In general, the formation of more complicated CD host/guest complexes G_mCD_n can be described by the following equilibrium

$$m\mathrm{G} + n\mathrm{CD} \rightleftharpoons \mathrm{G_mCD_n}$$

and equation for the overall association constant β_{mn}:

$$\beta_{mn} = \frac{[\mathrm{G_m}][\mathrm{CD_n}]}{[\mathrm{G}]^m[\mathrm{CD}]^n} \tag{2.12}$$

The driving force for the complex formation is not yet fully understood [77, 87]. Nevertheless, some contributing factors can be identified. The release of water molecules from the cavity leads to an increase in entropy of the system. Furthermore van der Waals interactions and hydrophobic interactions between guest and interior of CD contribute to complex formation. In some cases hydrogen bonding between guest

and the rim of CD takes place. From the temperature dependence of the association constant, enthalpy ($\Delta H_{complex}$) and entropy ($\Delta S_{complex}$) of complexation are obtainable [79]. In most cases, $\Delta H_{complex}$ is negative which leads to complex dissociation at higher temperatures [77, 88, 90, 91], whereas $\Delta S_{complex}$ can have negative or positive values depending on the interactions that take place during complexation. In the complex formation several steps have to be considered [79, 92]:

1. The guest molecule has to approach the CD
2. Enthalpy rich water molecules have to be released from the cavity (results in a rising entropy of the system)
3. The hydration shell of the guest has to be removed at least partly
4. Interactions (mostly weak van der Waals attractions) of the guest molecule with the rim of the CD and the inside (the guest molecule enters the cavity)
5. Possible formation of hydrogen bonds between CD and guest
6. Re-formation of the hydration shell of exposed parts of the guest molecule and around the CD molecule

From the point of complex formation kinetics in steps 1, 4 and 5 the size of the guest molecule plays an important role and no complex formation is observed for guests that extend the cavity size. The assembly of water molecules relies on several factors, e.g. pH value or ionic strength, which is independent from the respective guest molecule. Most likely steps 3 and 4 can be considered rate determining [92]. The size of the guest group is not only a criterion whether it is possible for the guest to enter but also for the stability of the complex. As the interactions between CD and guest are rather weak and of a short range, the complex stability depends strongly on a good fit between CD and guest. In some cases a weak fit between CD and guest can be compensated with the formation of different complex geometries/stoichiometries (refer to Sect. 2.2.4).

2.2.4 Complex Types, Common Host/Guest Pairs and Their Stability

From the geometry of CD two complexation modes are possible. Depending of the dimension of the guest, it can enter the cavity from the primary or the secondary side of CD (refer to Fig. 2.8). The primary side is on the face of C6 and OH-6 and has a slightly smaller opening. The secondary side is on the face of C2 and C3 with a slightly larger opening of the cavity. Complexes with different complexation modes can be identified via multi dimensional NMR spectroscopy [93] and X-ray crystallography [77, 94–96]. Furthermore, different complex stoichiometries are possible [84]. The most common cases are 1:1 CD/guest complexes but 2:1 and 1:2 are described as well, e.g. the complex 1-bromoadamantane with 2 α-CD molecules [97] or the complex of γ-CD with 2 pyrene molecules [98, 99]. The complex stoichiometry can be identified via the method of continuous variation, i.e. Job's plot [93, 97, 100]. In this analysis the product of mole fraction and complexation induced change in the chemical shift

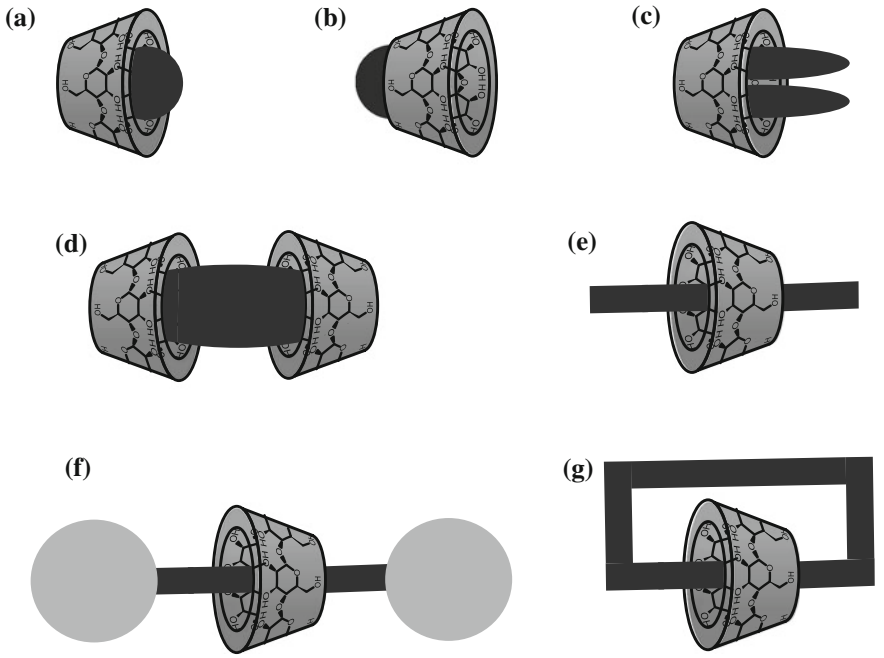

Fig. 2.8 Different types of complexation: **a** 1:1 CD/guest complex from the secondary side, **b** 1:1 CD/guest complex from the primary side, **c** 1:2 CD/guest complex, **d** 2:1 CD/guest complex, **e** pseudo rotaxane, **f** rotaxane, and **g** catenane

in the NMR spectrum is plotted against the mole fraction of guest or CD. The position of the maximum of the obtained curve indicates the complex stoichiometry.

CD complexes with axial shaped guests are called pseudo rotaxanes if they are not fixed via stopper groups (refer to Fig. 2.8) [101]. After fixation with large stopper molecules that suppress the dethreading of CD, complexes of CD with axial guests are called rotaxanes [101, 102]. In that case the CD complexation loses its reversibility and the formed bond between host and guest is a mechanical bond. Another class of mechanically interlocked molecules are catenanes, which are the connection of two or more rings via intertwining (Fig. 2.8) [103].

The different complex types can be transferred to polymers as well, e.g. in poly pseudo rotaxanes [104, 105], polyrotaxanes [106], side chain pseudo polyrotaxanes [107], side chain polyrotaxanes [108] or pseudo rotaxane star polymers [109, 110]. Rotaxane formation can be utilized, e.g. for the formation of supramolecular polymers [111] or hydrogels [112]. The concept of mechanical bonds was utilized for example in the synthesis of mechanically interlocked block copolymers [113, 114].

While the complex stoichiometry can be addressed via Job's plot, the association constant, and thus an equivalent for the complex stability, is accessible via isothermal titration calorimetry [115] or the Benesi-Hildebrand plot [116–118] for instance. In isothermal titration calorimetry the evolution of heat is measured during the addition of guest or host to a host or guest solution, respectively. A fit of the plot of

Table 2.2 Common guests for the native CDs and the respective association constants

Guest	Structure	Type of CD	log β (log M^{-1})
trans-Azobenzene	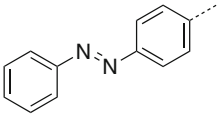	α	4.0 [119]
cis-Azobenzene	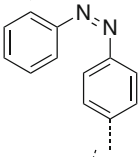	α	0.6 [120]
Indole	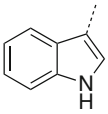	α	7.8 [121]
Phenol	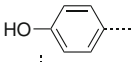	α	4.2 [121]
Adamantyl	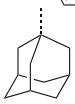	β	4.6 [122]
trans-Azobenzene	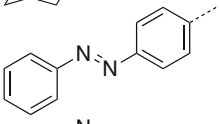	β	2.7 [123]
cis-Azobenzene	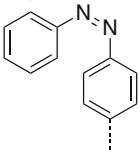	β	0.4 [123]
tert-Butyl phenyl	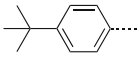	β	4.4 [124]
Phenol	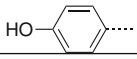	β	3.4 [121]

molar ratio against enthalpy leads to $\Delta G_{\text{complex}}$ and thus the association constant can be derived, while the surface under the curve gives the complexation enthalpy $\Delta H_{\text{complex}}$. The utilization of the Benesi-Hildebrand plot gives the opportunity to obtain association constants via changes of absorption in UV spectra or the chemical shift in NMR spectra.

Table 2.2 shows a selection of different guests with the respective association constant. For, α-CD mono or *para* substituted aromatic structures are commonly utilized, e.g. phenyl or azobenzene with association constants up to 10^4 M^{-1}, as well as aliphatic chains or poly(ethyleneglycol) (PEG). One of the strongest associations are reported between α-CD and indole with an association constant of 10^7 M^{-1} probably due to the formation of additional hydrogen bonds. The adamantyl-group

is a well-known guest group for β-CD with association constants up to 10^5 M^{-1}. Azobenzene and *tert*-butyl phenyl are also utilized in several examples. In the case of γ-CD, very bulky guests are necessary, e.g. two pyrene molecules or cyclododecane.

2.3 Complex Macromolecular Architectures Governed by CD Complexes

In recent years CD complexes have proven to be a perfect tool for the generation of complex macromolecular architectures. Almost every conceivable architecture has been described so far. Especially the development of controlled radical polymerization techniques for the synthesis of endfunctionalized polymers had a very significant impact on the research in this area.

Figure 2.9 shows a compilation of different architectures that were generated via CD host/guest complexes so far. CDs have been utilized for the modification of polymer functionality, polymer composition and polymer topology. CD functionalized polymers are rather readily accessible via living/controlled radical polymerization giving control of end chain and mid chain functionality. Diverse supramolecular polymer compositions can be obtained via incorporation of CD complexes at the interface between different blocks. To achieve more complex topologies, a combination of different functionalized building blocks is necessary, e.g. multi CD functionalized polymer strands. In general, the control over polymer functionality gives rise to the formation of complex supramolecular polymer compositions and topologies.

2.3.1 Common CD Containing Building Blocks

Although CDs possess a large number of functional groups, the reactivity of the primary and secondary hydroxyl groups differs significantly, which gives the opportunity to exclude some of the hydroxyl groups in specific reactions [125, 126]. Nevertheless, at least 6 hydroxyl groups with the same reactivity exist in a CD molecule. To obtain mono functionalization, the reaction conditions have to be monitored carefully. The most commonly used intermediate is the mono tosylate at C6, which can be synthesized in pyridine for all native CDs [127–129] or in aqueous NaOH solution for β-CD and α-CD [130, 131]. The tosylate can be transformed into several useful building blocks, e.g. azide [128, 129], thiol [132] or amine via nucleophilic substitution with a diamine [133]. The azide is available via a nucleophilic substitution of the tosylate with sodium azide [128, 129, 131], whereas the thiol is formed via a nucleophilic substitution with thiourea and subsequent hydrolysis [132, 134]. The azide can be further converted into an amine via reduction [127–129]. With these 3 substituents a large variety of modern polymer conjugation reactions can be utilized, e.g. CuAAc [130, 135] and thiol-ene reactions [136]. CD-functionalized

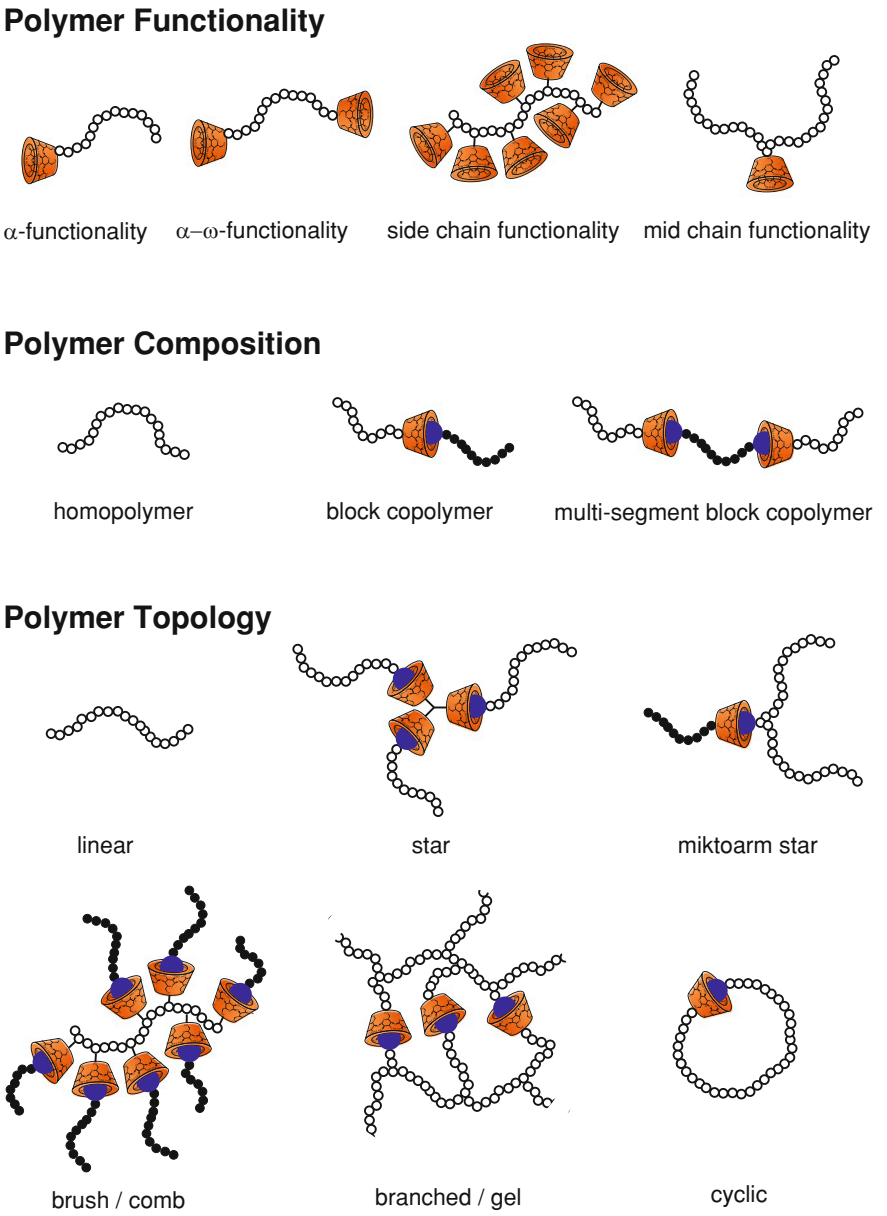

Fig. 2.9 Complex macromolecular architectures via CD-driven supramolecular complexation and macromolecular building blocks with CD moieties (CD is depicted in *orange*; guest groups are depicted in *blue*)

polymerization mediators, e.g. for NMP [137], ATRP [138] or RAFT [139] have been described in the literature as well as post-polymerization conjugation reactions with CDs [138, 140]. Mono functionalizations at C2 are described in the literature as well [141, 142], yet C2 or C3 derivatives are not utilized as frequent as the C6 derivatives. Certainly an esterification of the hydroxyl groups is possible as well, yet the selectivities are usually low. Either full conversions are initially targeted or lower substitution grades are targeted and the obtained mixtures have to be purified in inconvenient procedures.

2.3.2 Block Copolymers

The formation of block copolymers via CD complexes is mainly restricted to AB diblock copolymers so far. Almost exclusively β-CD has been utilized in that regard. The synthesis of supramolecular diblock copolymers is straight forward as only two components are needed: a CD-functionalized polymer and a guest functionalized polymer. These building blocks are commonly obtained via controlled radical polymerization techniques yet in some cases cationic or anionic polymerization have been utilized as well.

One of the first examples is an AB diblock copolymer of PNIPAAm and P4VP synthesized via RAFT polymerization by Zhang and coworkers that has proven to be pH and thermoresponsive [143]. This block copolymer was exploited in temperature- and pH-induced micellization and vesicle formation which was observed via DLS, SLS, fluorescence measurements and TEM. At a pH value over 4.8 and a temperature of 25 °C vesicles were formed and at a pH value of 2.5 and a temperature of 60 °C micelles were formed. Another example of double stimuli responsive block copolymers, i.e. with schizophrenic behavior, has been described by Liu et al. [138]. Again pH- and thermoresponsive behaviour was combined but this time via PDMAEMA and PNIPAAm blocks synthesized via ATRP. Vesicle formation was observed at low pH values and high temperatures (pH 4 and 50 °C), whereas micelles were formed at high pH values and low temperatures (pH 9 and 25 °C), which was proven via TEM, DLS and SLS. Voit and coworkers described a supramolecular diblock copolymer consisting of PNIPAAm synthesized via ATRP and poly(2-methyl-2-oxazoline) synthesized via cationic ring-opening polymerization [144]. The temperature-responsive PNIPAAm block was utilized for temperature-induced aggregation. These examples evidence the impact that CD-based supramolecular chemistry can have in the area of macromolecular architectures.

CD complexes provide another possibility for stimuli response. Not only different polymer types can be utilized in the area of stimuli-responsive materials, yet the supramolecular connection is addressable via external stimuli as well. One of the first examples is the utilization of a voltage responsive connection via a ferrocene endgroup which was described by Yan et al. [145]. A β-CD functionalized PSty and a ferrocene functionalized PEG were utilized. The connection between the blocks can be disrupted, as ferrocene molecules can be oxidized reversibly and the ferrocene

cation does not fit into the β-CD cavity. At first, block copolymer vesicles were obtained that dissociated upon application of an electric current. The rate of dissociation and the release of a test molecule could be adjusted via the amount of the voltage. Another example of diblock copolymers with stimuli responsive linkage was described by the same group [146]. Supramolecular based nanotubes were formed (length ~220 nm and diameter ~90 nm) via a supramolecular poly(ϵ-caprolactone-*b*-AA) (PCL-*b*-PAA) diblock copolymer. The supramolecular complex was formed between azobenzene and α-CD that leads to a light responsive linkage between the blocks. Furthermore, the nanotubes were loaded with Rhodamine B that could be released via light induced disassembly of the nanotubes. Stenzel and coworkers prepared supramolecular core shell nanoparticles with a PMMA core and poly(hydroxy ethylacrylate) (PHEA) shell [136]. The guest functionalized PHEA building block was obtained directly via RAFT polymerization, whereas the CD functionalized PMMA block was obtained via RAFT polymerization of MMA, a Chugaev thermolytic endgroup conversion and a subsequent thiol-ene reaction with mono thiol functionalized β-CD. Core shell nanoparticles (diameter ~150 nm) were obtained after mixing of the building blocks in DMF and subsequent water addition or by the generation of core PMMA nanoparticles in water and addition of the water soluble building blocks. The addition of free β-CD led to the disassembly of the complexes and aggregation of the water insoluble blocks. Recently Yuan and coworkers described a biodegradable diblock copolymer of P(lactide) (PLA) and PEG with a β-CD and ferrocene governed connection [147]. Cyclovoltammetry was utilized to study the redox response of the block copolymer. Furthermore micelles were formed and characterized via TEM and DLS. Cytotoxity and drug-release was investigated with regard to the redox stimulus as well. A block copolymer with pH-responsive supramolecular linkage between β-CD and benzimidazole was described by Zhang et al. [148]. Thus, a diblock copolymer of PCL and dextran was synthesized and supramolecular micelles were formed. The micelles were utilized for in vitro doxorubicin delivery that was supported by the difference of intra and extracelluar pH.

A diblock copolymer with a special linking moiety was described by Quan et al. [130]. In this case a dilinker consisting of α-CD and β-CD connected with a short spacer was utilized to form a diblock copolymer of PNIPAAm and PCL. Furthermore, cell targeting ligands were introduced to enhance cell uptake efficacy. To protect the formed core shell nano-sized assemblies in body fluids, PEG moieties were incorporated as well. The formed assemblies were utilized in drug delivery experiments that showed tumor-triggered release of loaded molecules. This particular example shows how powerful CD complexes are as a tool for the formation of macromolecular architectures with regard to the specific application, e.g. drug delivery [130] or the formation of nano objects [145, 146]. Especially the stimuli-responsive nature of several CD/guest pairs gives the opportunity to disassemble the block copolymer at the junction of the different blocks. Thus, the distinct properties of block copolymers can be utilized but with the additional property of disassembling the blocks. This concept has been utilized recently by Hawker and coworkers in block copolymer lithography with block copolymers that are coupled via hydrogen bonds. This

example shows that supramolecular bonded block copolymers can indeed mimick the behavior of their covalent analogues [149].

2.3.3 Brush Polymers

The synthesis of supramolecular brush polymers can be conducted via two pathways. Either CD molecules are connected to a backbone or surface and a guest endfunctionalized polymer is added or guest molecules are connected to a polymer backbone or surface and CD-endfunctionalized polymers are added. The forming complexes lead to brush-like architectures. Of course the complex formation is governed by equilibria and thus the obtained grafting density strongly depends on the association constants. Furthermore, steric factors play an important role as CDs have a very bulky structure that can suppress high grafting densities.

A supramolecular brush formation in solution has been described by Bernard et al. [140]. A CD-containing backbone was synthesized in a two step procedure. Firstly, trimethyl silyl protected propargyl methacrylate was polymerized via RAFT, subsequently the terminal alkyne groups were deprotected and conjugated with β-CD-N_3 in a CuAAc reaction. Short PAA chains endfunctionalized with an adamantyl-group were synthesized and brushes were formed in aqueous solution. The brush formation was proven via DLS and NOESY (nuclear Overhauser enhancement spectroscopy). Although a dodecyl functional RAFT agent was utilized, no competing complex formation was evident, which was proven via comparison of dodecyl-functional chains with chains after RAFT endgroup removal. Jiang and coworkers presented a supramolecular brush with a copolymer of *N*-vinylpyrolidone and a CD functional monomer and doubly adamantyl endfunctionalized PCL [150]. Interestingly, micellar aggregates were obtained, as shown by TEM and DLS, and no gel formation was observed, although a doubly guest functional polymer was utilized. Later Zhang and coworkers presented a supramolecular brush consisting of a CD-functionalized polymer backbone and adamantyl functionalized oligo ethylene glycol dendrons. The thermoresponsive behavior was studied as a function of several factors, e.g. dendrimer generation or hydrophobicity of the dendrimer endgroups [151]. In that way the LCST could be tuned from 34 to 56 °C. It was found that the dehydration and collapse of the oligo ethylene glycol chains leads to disassembly of the host/guest complexes, which was studied via NMR and ITC. Frey and coworkers investigated the binding strength of PHPMA featuring pendant β-CD functionalities with adamantyl-functionalized hyperbranched and linear poly(glycerols) as well as their block copolymers with PEG [152]. The complex formation was monitored via diffusion-ordered NMR spectroscopy (DOSY), ITC and fluorescence correlation spectroscopy. The steric effect of the hyperbranched grafts resulted in decreased association constants, while the incorporation of PEG spacers led to more stable complexes. Very recently Hetzer et al. [153] showed a supramolecular brush formation of CD end-functionalized PDEAAm with a copolymer consisting of DMAAm and a phenolphthalein-functionalized acrylamide. Due to the complex formation with the

dye functionalized side-chains a color change in the solution was observable during complexation. Another stimuli responsive supramolecular brush polymer was described by Yuan et al. [154]. PEG-*b*-P(glycidyl methacrylate) was prepared via RAFT polymerization and the glycidyl containing block was decorated with β-CD. Addition of a ferrocene endfunctionalized PCL led to the formation of supramolecular brushes that showed redox responsive brush formation coupled with redox responsive micelle formation.

Apart from solution studies several reports regarding surface brushes exist in the literature. Li and coworkers studied the grafting of doubly adamantyl endfunctionalized polymers on CD modified cellulose [155]. After the formation of the supramolecular complexes the grafting was proven via XPS, ellipsometry, TGA and FT-IR. Thus, a supramolecular grafting on the renewable resource cellulose was achieved. Reinhoudt and Huskens introduced the concept of molecular printboards, i.e. mono layers of CD host molecules on a planar surface that are capable of the stable attachment of guest molecules [156]. This concept has been exploited to generate different grafted structures, e.g. on gold [156] or SiO_2 [157]. Furthermore, patterns on the surface have been generated via micro contact printing [157–159]. These molecular printboards have been utilized to immobilize proteins [160, 161], fluorescent dyes [159] or Eu^{3+} luminescent complexes [158]. A similar approach was utilized to graft an azobenzene functionalized cell recognition peptide onto an α-CD functionalized gold surface that showed reversible and photocontrolable cell attachment [162].

2.3.4 Star Polymers

CD-based star polymers can be divided into two categories. Star polymers with CD as a core moiety due to its high concentration of functionality, which is the most frequent utilization of CDs for star polymers. The other possibility is to utilize host/guest complexes to obtain supramolecular star polymers, e.g. via a core molecule with several CD moieties and guest functionalized polymers.

One of the first reports of CD-centered stars is from the work of Haddleton and coworkers, where a 21 arm star polymer consisting of PMMA or PSty arms was synthesized via ATRP with a grafting-from approach [163]. Furthermore, block copolymer stars were formed from the obtained macro initiators. A similiar approach was conducted by Stenzel et al., who described a CD-centered 18 arm PSty star synthesized via living radical polymerization mediated by a half-metallocene iron carbonyl complex [164] and a CD-centered 7 arm star formed via RAFT polymerization of Sty [26, 165], as well as block copolymers with ethyl acrylate [165]. The range of utilized monomers for the arm-forming polymers was subsequently extended later to *tert*-butyl acrylate [166], oligo ethyleneimine [167], azobenzene monomers [168], 2-ethyl-2-oxazoline [169], glycomonomers [170], HEA [170], NIPAAm [171], PNIPAAm-*b*-PDMAAm [172], PS-*b*-P(3-hexylthiophene) [173] and P(L-lysine) dendrons [174] by several research groups. Kakuchi and coworkers

utilized mono amino β-CD to attach a NMP initiator, followed by a living/controlled radical polymerization of Sty [175]. The remaining hydroxyl groups were utilized to attach ATRP initiator via esterification and subsequently MAA or *tert*-butyl acrylate was polymerized to form a CD centered miktoarm structure. Recently Haddleton and coworkers introduced 7 thiols on the secondary face of β-CD for subsequent thiol-ene reactions, e.g. with oligo ethylene glycol methacrylate (OEGMA), and utilized the remaining 14 hydroxyl functions as initiator for the ring-opening polymerization of CL, which leads to the formation of a CD-centered miktoarm star polymer [176]. These examples are of particular interest because the different reactivities of the β-CD hydroxyl groups were utilized to generate a complex macromolecular architecture. A different asymmetric β-CD based star architecture has been described recently by Liu et al. [177]. The primary face of CD was grafted with PDMAEMA, while the secondary face was utilized to attach a magnetic resonance imaging contrast agent. The poly-cationic PDMAEMA was subsequently used to promote polyplex formation with plasmid DNA. Finally in vitro DNA delivery, cytotoxity and magnetic resonance imaging was probed. Moreover, another asymmetric β-CD based star architecture was described by Shen et al. [178]. While the primary face was decorated with PEG, the secondary face of β-CD was grafted with 2-[(methacryloyl)oxy]ethyl acrylate / cysteamine dendrimers that showed the formation of well-defined aggregates in aqueous solution. A γ-CD centered oligo ethyleneimine star was prepared by Li et al. [179]. The γ-CD core was utilized to encapsulate the drug paclitaxel. Furthermore a cell targeting ligand was attached and a polyplex was formed with plasmid DNA. Finally cell viability and gene transfection efficiency were studied. A dumbell-shaped architecture containing of two β-CD centered PNIPAAm stars connected covalently via a PEG backbone was described by Zhang et al. [180]. The thermoresponsive characteristics were studied showing the formation of flower like micelles. An alternative architecture involving CD-core star polymers has been published recently by Wenz and coworkers which is a combination of rotaxane and star architectures [181]. Here α-CD centered PMMA stars were threaded onto a PEG backbone and fixed via large stopper molecules. PMMA chains were grafted from ATRP initiators connected to the threaded α-CD moieties on the rotaxane and were characterized via DOSY, SEC and AFM. An interesting feature of the thus formed brushes is their sensitivity to mechanical forces during SEC measurement, which led to the scission of the PEG thread. A similar approach was followed by Nagahama et al. [182]. PEG was threaded with α-CD to form a polyrotaxane. The remaining hydroxyl groups of the α-CD threads were utilized to grow PLA. Continuous anisotropic phases were formed in the bulk state. The crystallization behavior was studied via DSC, X-ray diffraction and polarized optical microscopy. An accelerated stereo complex formation was found that was attributed to the enhanced moveability due to the rotaxane structure.

Fewer reports are in the literature on star architectures governed by host/guest complexes. An interesting architecture in that regard is the connection of two CD-centered stars with a doubly guest functional polymer, which leads to a dumbbell shape in solution that has been described in two studies [183, 184]. In the first report β-CD centered PNIPAAm with 4 arms was connected with a doubly adamantyl

functionalized PEG, the complex formation was proven via NOESY and the change in the LCST was monitored depending on host/guest ratio or the molecular weight of the employed PEG [183]. Later, β-CD centered PNIPAAm was connected with a doubly adamantyl functionalized poly(propylene glycol) (PPG) [184]. As this system contains two thermoresponsive polymer types, the aggregation behavior was studied depending on the temperature via DLS, NMR, fluorescence measurements, AFM and TEM. The formation of supramolecular block copolymers was evident in cold water, whereas micelle formation was observed at temperatures over 8 °C and above 22 °C micelle destabilization was observed. A similar structure was described by Allcock et al. [185]. A β-CD centered POEGMA star was complexed with an adamantyl endfunctionalized P(bis-(trifluoroethoxy)phosphazene). The formation of micelles was monitored via DLS, TEM and AFM. Furthermore β-CD moieties were introduced into P(phosphazene) side-chains to obtain multiple β-CD grafted polymers. Multiple adamantyl functionalized P(phosphazene)s were prepared as well ans finally the gelation behavior was studied. The formation of an ABC miktoarm star polymer was published recently by Zhu and coworkers that required several functionalization reaction with β-CD [135]. In brief, β-CD was mono tosylated, converted into the azide and mono tosylated again. PEG was conjugated via CuAAc, the remaining tosylate was converted into the azide and subsequently an ATRP initiator was added via CuAAc. DMAEMA was polymerized via ATRP to obtain a miktoarm star with two different arms. A third arm consisting of adamantyl functional PMMA was connected via supramolecular complex formation. Due to the hydrophobic character of PMMA, micelles were obtained in solution and characterized via DLS and TEM. Wu and coworkers utilized a threefold β-CD core to connect three guest functionalized oligo ethylene glycol dendrimer arms [186]. The thermoresponsive behavior of the formed dendrimer stars was investigated showing a variation in the LCST from 43 to 72 °C depending on dendrimer generation, dendrimer endgroup (ethyl or methyl) and ratio of different dendrimer types (with ethyl or methyl endgroup). Furthermore, the effect of salt concentration was investigated as well as the thermally induced decomposition of the supramolecular complexes. An interesting combination of CD-based host/guest chemistry and a protein (concavalin A (ConA))/mannopyranoside interaction was shown by Chen et al. [148]. An α-mannopyranoside and β-CD functionalized dilinker was synthesized and subsequently the supramolecular recognition was probed via ITC. An association constant of 8.4×10^3 M^{-1} was found for the ConA dilinker complex. Addition of adamantyl functionalized PEG showed a further recognition of the β-CD moiety and the adamantyl group with an association constant of 1.1×10^5 M^{-1}. The complex formation was additionally investigated via DLS and SEC evidencing a strong dependence of the number of attached PEG chains on the concentration of the solution. Addition of free α-CD molecules lead to hydrogel formation via a supramolecular interaction of the PEG chains and α-CD. Recently Schmidt et al. showed the formation of supramolecular X- and H-shape star block copolymers. The complex formation was investigated via DLS, NOESY and turbidimetry. Additionally, the temperature induced aggregation behavior was studied via temperature sequenced DLS measurements. A similar aggregation and micelle

destabilization behavior as in the earlier described dumbbell shaped aggregates was found [184].

Jiang and coworkers utilized host guest complexes to form brush-like star architectures with different spherical cores, e.g. SiO_2 nanoparticles [187], CdS quantum dots [188, 189] or gold [190]. In the case of SiO_2 nanoparticles, PEG arms were utilized and subsequently α-CD was added to induce hydrogel formation. In another work quantum dots were utilized as a core for azobenzene or ferrocene endfunctionalized PDMAAm-*b*-PNIPAAm block copolymers [188, 189]. The thermoresponsive nature of the PNIPAAm blocks was utilized to induce hydrogel formation above the LCST. The hydrogels showed a variation of photoluminescence depending on the temperature and thus the gel formation, which can be attributed to the confinement of the quantum dots in the gel. Furthermore, UV-light and electrochemical response was probed. CD-functionalized gold nanoparticles were grafted with azobenzene endfunctionalized PNIPAAm-*b*-PDMAAm, which gave the opportunity to disrupt the supramolecular complex upon UV-irradiation [190]. Heating above the LCST of the PNIPAAm block led to the formation of vesicles. A similar approach was described earlier [191]. In this case gold nanoparticle cores with α-CD shell were utilized as well. Azobenzene endfunctionalized PNIPAAm homopolymer was supramolecularly attached. Subsequently the photoresponsive behavior and the thermal behavior of the aggregates were studied in detail.

2.3.5 Branched Polymers and Gels

The probably most intensively studied field in CD driven macromolecular architectures is the formation of branched structures and hydrogels. Several reviews based on these materials can be found elsewhere [192–196]. Nevertheless, in this section a short overview on polymeric CD-based hydrogels and branched structures that have been synthesized via controlled radical polymerization is presented. In general, the formation of branched structures and hydrogels can be conducted via different pathways. A large amount of host and/or guest functionalities can be incorporated into the side chain of the polymers or as endgroup to induce supramolecular crosslinking. Furthermore, single CD molecules can be utilized as crosslinkers if the guest group is small and two guests can be included, which leads to single-CD crosslinking points. Alternatively CDs can act as crosslinker via aggregation/crystallization.

An example of the latter category utilizes OEGMA based polymers with side chains of POEGMA as a double brush structure that was formed via ATRP. The formation of a hydrogel was induced via addition of α-CD [107]. Interestingly, the formation of hexagonal crystals was observed in the hydrogel which is due to the formation of columnar microcrystalline domains of α-CD. Later P(EG-*co*-DMAEMA) brushes were utilized to form thermo- and pH-responsive gels after α-CD addition [197]. The gelation behavior was altered via copolymer concentration, pH value, PEG branch density and the chain uniformity of the copolymers. With these gels drug release at different pH values and temperatures was studied. The same crosslinking

method was employed with PEG-*b*-PDMAEMA block copolymers, which lead to a series of different microgel morphologies depending on pH value or ionic strength, e.g. hexagonal, bowl or spherical structures that could be visualized via TEM [198]. A recent utilization of α-CD based crosslinking via a poly pseudo rotaxane formation is the supramolecular anchoring of DNA polyplexes in hydrogels formed from PEG-*b*-PCL-*b*-PDMAEMA block copolymers and α-CD [199]. The polymers were synthesized via a combination of ATRP and ring-opening polymerization. Subsequently, DNA polyplexes were formed from blockcopolymer micelles and plasmid DNA. The addition of free PEG chains and α-CD leads to hydrogel formation. The following studies on the release of the incorporated DNA showed sustained release of stable polyplexes with high bioactivity. Yuan and coworkers synthesized a PCL-*b*-POEGMA with pyrene endgroup via a combination of ROP and ATRP [200]. The amphiphilic block copolymer was assembled into micelles and α-CD was added to obtain gelation. Viscoelastic behavior, temperature response and in vivo drug-release were studied with these gels. Furthermore Ji and coworkers described a PEG-*b*-PNIPAAm block copolymer that was utilized to form micelles in solution via heating above the LCST of the PNIPAAm block [201]. Moreover α-CD was added at ambient temperature to induce crystallization due to interactions with the PEG blocks leading to reverse micelles.

A β-CD centered star polymer of PDMAEMA was protonated and utilized to form networks with polyanionic PAA-*b*-PEG di- and triblock copolymers [202]. Depending on the structure of the polyanionic block, fibrillar or spherical microstructured gels were obtained. SEM, TEM, DLS and rheological measurements were carried out to study the obtained materials. Furthermore, the remaining cavity in the β-CD moiety was utilized to include a model drug and study the release behavior. Another example is the temperature induced formation of PNIPAAm hydrogels from a β-CD centered PNIPAAm-*b*-PDMAAm three arm star polymer [172]. Again, the β-CD cavity was utilized for small molecule release. As described before in Sect. 2.3.4, quantum dot centered hydrogels formed due to the LCST of PNIPAAm blocks have been generated as well [188, 189].

Kang and coworkers presented the synthesis of a doubly β-CD functionalized poly(2-(methacryloyloxy)ethyl succinate) via RAFT polymerization [139]. This polymer was utilized in the formation of poly pseudo rotaxanes with an acrylate endfunctionalized PEG-*b*-PPG-*b*-PEG. The acrylate functions were subsequently reacted in a thiol-ene reaction with a multifunctional thiol to form permanent crosslinking points. Thus, a sliding hydrogel was obtained evidencing pH response (from the succinate) and thermoresponse (from the PEG and PPG blocks). Swelling ratios and thermal properties could be adjusted via different chain lengths of the β-CD functionalized polymer which is rather easy via changing the conditions of the RAFT polymerization. Recently Hetzer et al. [203] showed the network formation of a doubly adamantyl functionalized PDMAAm and a three-fold β-CD functionalized linker molecule. Rheological investigations showed increasing viscosities depending on CD/guest ratio, chain length and concentration. Furthermore the viscosity could be reduced drastically via addition of free CD molecules or free guest molecules. Zhang et al. [204] described a redox sensitive network utilizing two- or three-fold β-CD

linker molecules and three- or four-fold ferrocene-functionalized P(ethylene imine). The formed material was analyzed via 2D correlation FT-IR spectroscopy and measurements of the mechanical material properties. Furthermore the addition of oxidants led to dissolution of the material. A redox responsive hydrogel was described by Yuan et al. [205]. DMAAm-based β-CD and ferrocene-containing polymers were formed via RAFT polymerization. A mixture of both polymer types gave a hydrogel that proved to be redox responsive. A photoresponsive hydrogel based on β-CD and azobenzene interactions was described by Guan et al. [206]. A copolymer of NIPAAm and an azobenzene monomer was interacted with a difunctional β-CD containing molecule that has a disulfide connection between the CD moieties. Double stimuli responsive gels were obtained. The azobenzene guest groups allowed for photoresponsive sol-gel transition, where as the disulfide bonds facilitated redox responsive sol-gel transition. Moreover, Gao and coworkers prepared a P(glycidyl methacrylate) via ATRP that was subsequently transformed with diethylenediamine to obtain amine functional polymers [207]. Afterwards β-CD was introduced and complexes with insulin formed. Finally in vitro release of insulin was probed that increased upon addition of competing guests.

2.3.6 Other Architectures

Jiang and coworkers presented a block copolymer-like structure consisting of Frechét-type benzyl ether dendrons (generations 1, 2, and 3) with an azobenzene at the apex and a β-CD functionalized PNIPAAm [208]. These supramolecular block copolymer amphiphiles formed vesicles or micelles in aqueous solution depending on dendron generation. Furthermore, UV-irradiation lead to the disassembly and formation of irregular particles which could be reversed via irradiation of visible light. Heating above the LCST of the PNIPAAm block leads to reversible aggregation of the particles. Vesicles of a doubly CD endfunctionalized P(ether imide) were prepared by Guo et al. [209]. β-CD cavities were present on the inner and outer walls of the vesicle that could be addressed via guest functionalized PEGs depending on the molecular weight, e.g. with 1 and 2 k PEG inner and outer surface was modified, whereas with 5 k PEG the inner surface was modified only partially. Giacomelli et al. [137] formed PSty centered micelles with β-CD surface. The underlying β-CD functionalized PSty was prepared via NMP. The formation of a supramolecular cyclic polymer was described by Inoue et al. [210]. A PEG with azobenzene and β-CD endgroup was utilized in that regard. The formation of cycles could be performed in high dilution, whereas intermolecular complexes were formed at higher concentration. The azobenzene moiety was exploited for UV-light triggered dethreading of the complex. Between the PEG and β-CD a aromatic unit was incorporated that was competing in complexation with the azobenzene depending on the temperature, which was shown via temperature dependent NOESY.

A supramolecular enzyme polymer conjugate was described by Felici et al. [211]. β-CD functionalized PSty was prepared via ATRP that formed vesicles in aqueous

solution. These vesicles bear CD-units on the outer and inner surface. The β-CD moieties were subsequently utilized to conjugate adamantyl-PEG-functionalized horseradish peroxidase that showed catalytical activity although it was connected supramolecularly to the PSty vesicle.

References

1. Schmidt BVKJ, Hetzer M, Ritter H, Barner-Kowollik C (2014) Complex macromolecular architecture design via cyclodextrin host/guest complexes. Prog Polym Sci 39(1):235–249. doi:10.1016/j.progpolymsci.2013.09.006
2. Szwarc M (1983) Living polymers and mechanisms of anionic polymerization. Advances in polymer science, vol 49. Springer, Berlin
3. Hsieh HL, Quirk RP (1996) Anionic polymerization: principles and practical applications, 1st edn. Marcel Dekker, New York
4. Moad G, Rizzardo E, Thang SH (2008) Toward living radical polymerization. Acc Chem Res 41:1133–1142
5. Szwarc M (1993) Ionic polymerization and living polymers, 1st edn. Chapman & Hall, New York
6. Matyjaszewski K, Xia J (2001) Atom transfer radical polymerization. Chem Rev 101:2921–2990
7. Braunecker WA, Matyjaszewski K (2007) Controlled/living radical polymerization: features, developments, and perspectives. Prog Polym Sci 32:93–146
8. Ouchi M, Terashima T, Sawamoto M (2009) Transition metal-catalyzed living radical polymerization: toward perfection in catalysis and precision polymer synthesis. Chem Rev 109:4963–5050
9. Solomon DH, Rizzardo E, Cacioli P (1986) US Patent US4581429
10. Hawker CJ, Bosman AW, Harth E (2001) New polymer synthesis by nitroxide mediated living radical polymerizations. Chem Rev 101:3661–3688
11. Grubbs RB (2011) Nitroxide-mediated radical polymerization: limitations and versatility. Polym Rev 51:104–137
12. Chiefari J, Chong YK, Ercole F, Krstina J, Jeffery J, Le TPT, Mayadunne RTA, Meijs GF, Moad CL, Moad G, Rizzardo E, Thang SH (1998) Living free-radical polymerization by reversible addition/fragmentation chain transfer: the RAFT process. Macromolecules 31:5559–5562
13. Barner-Kowollik C (2008) Handbook of RAFT-polymerization. Wiley-VCH, Weinheim
14. Barner-Kowollik C, Perrier SJ (2008) The future of reversible addition fragmentation chain transfer polymerization. Polym Sci Part A: Polym Chem 46:5715–5723
15. Moad G, Rizzardo E, Thang SH (2008) Radical addition-fragmentation chemistry in polymer synthesis. Polymer 49:1079–1131
16. Moad G, Rizzardo E, Thang SH (2009) Living radical polymerization by the RAFT process—a second update. Aust J Chem 62:1402–1472
17. Odian G (2004) Principles of polymerization, 4th edn. Wiley, New York
18. Le TP, Moad G, Rizzardo E, Thang SH (1998) International Patent WO9801478
19. Corpart P, Charmot D, Biadatti T, Zard SZ, Michelet D (1998) International Patent WO9858974
20. Chiefari J, Mayadunne RTA, Moad CL, Moad G, Rizzardo E, Postma A, Skidmore MA, Thang SH (2003) Thiocarbonylthio compounds (SdC(Z)S-R) in free radical polymerization with reversible addition-fragmentation chain transfer (RAFT polymerization). Effect of the activating Group Z. Macromolecules 36:2273–2283
21. Chong YK, Krstina J, Le TPT, Moad G, Postma A, Rizzardo E, Thang SH (2003) Thiocarbonylthio compounds [SdC(Ph)S-R] in free radical polymerization with reversible addition-fragmentation chain transfer (RAFT polymerization). Role of the free-radical leaving Group (R). Macromolecules 36:2256–2272

22. Perrier S, Takolpuckdee PJ (2005) Macromolecular design via reversible addition-fragmentation chain transfer (RAFT)/xanthates (madix) polymerization. Polym Sci Part A: Polym Chem 43:5347–5393
23. Barner-Kowollik C, Buback M, Charleux B, Coote ML, Drache M, Fukuda T, Goto A, Klumperman B, Lowe AB, Mcleary JB, Moad G, Monteiro MJ, Sanderson RD, Tonge MP, Vana PJ (2006) Mechanism and kinetics of dithiobenzoate-mediated RAFT polymerization. I. The current situation. Polym Sci Part A: Polym Chem 44:5809–5831
24. Moad G, Chiefari J, Chong Y, Krstina J, Mayadunne RT, Postma A, Rizzardo E, Thang SH (2000) Living free radical polymerization with reversible addition—fragmentation chain transfer (the life of RAFT). Polym Int 49:993–1001
25. Mori H, Ookuma H, Nakano S, Endo T (2006) Xanthate-mediated controlled radical polymerization of *N*-Vinylcarbazole. Macromol Chem Phys 207:1005–1017
26. Stenzel-Rosenbaum M, Davis TP, Chen V, Fane AGJ (2001) Star-polymer synthesis via radical reversible addition-fragmentation chain-transfer polymerization. Polym Sci Part A: Polym Chem 39:2777–2783
27. Quinn JF, Barner L, Barner-Kowollik C, Rizzardo E, Davis TP (2002) Reversible addition-fragmentation chain transfer polymerization initiated with ultraviolet radiation. Macromolecules 35:7620–7627
28. Hongand C-Y, You Y-Z, Bai R-K, Pan C-Y, Borjihan GJ (2001) Controlled polymerization of acrylic acid under 60Co irradiation in the presence of dibenzyl trithiocarbonate. Polym Sci Part A: Polym Chem 33:3934–3939
29. Chen G, Zhu X, Zhu J, Cheng Z (2004) Plasma-initiated controlled/living radical polymerization of methyl methacrylate in the presence of 2-cyanoprop-2-yl 1-dithionaphthalate (CPDN). Macromol Rapid Commun 25:818–824
30. Lowe AB, McCormick CL (2007) Reversible addition-fragmentation chain transfer (RAFT) radical polymerization and the synthesis of water-soluble (co)polymers under homogeneous conditions in organic and aqueous media. Prog Polym Sci 32:283–351
31. Mitsukami Y, Donovan MS, Lowe AB, McCormick CL (2001) Water-soluble polymers. 81. Direct synthesis of hydrophilic styrenic-based homopolymers and block copolymers in aqueous solution via RAFT. Macromolecules 34:2248–2256
32. Sumerlin BS, Donovan MS, Mitsukami Y, Lowe AB, McCormick CL (2001) Water-soluble polymers. 84. Controlled polymerization in aqueous media of anionic acrylamido monomers via RAFT. Macromolecules 34:6561–6564
33. Rodriguez-Emmenegger C, Schmidt BVKJ, Sedlakova Z, Subr V, Alles AB, Brynda E, Barner-Kowollik C (2011) Low temperature aqueous living/controlled (RAFT) polymerization of carboxybetaine methacrylamide up to high molecular weights. Macromol Rapid Commun 32:958–965
34. Convertine AJ, Lokitz BS, Lowe AB, Scales CW, Myrick LJ, McCormick CL (2005) Aqueous RAFT polymerization of acrylamide and *N*,*N*-Dimethylacrylamide at room temperature. Macromol Rapid Commun 26:791–795
35. Thomas DB, Convertine AJ, Hester RD, Lowe AB, McCormick CL (2004) Hydrolytic susceptibility of dithioester chain transfer agents and implications in aqueous RAFT polymerizations. Macromolecules 37:1735–1741
36. Levesque G, Arséne P, Fanneau-Bellenger V, Pham T-N (2000) Protein thioacylation: 2. Reagent stability in aqueous media and thioacylation kinetics. Biomacromolecules 1:400–406
37. Thomas DB, Convertine AJ, Myrick LJ, Scales CW, Smith AE, Lowe AB, Vasilieva YA, Ayres N, McCormick CL (2004) Kinetics and molecular weight control of the polymerization of acrylamide via RAFT. Macromolecules 37:8941–8950
38. Thomas DB, Sumerlin BS, Lowe AB, McCormick CL (2003) Conditions for facile, controlled RAFT polymerization of acrylamide in water. Macromolecules 36:1436–1439
39. Smith AE, Xu X, McCormick CL (2010) Stimuli-responsive amphiphilic (co)polymers via RAFT polymerization. Prog Polym Sci 35:45–93

40. Millard P-E, Barner L, Stenzel MH, Davis TP, Barner-Kowollik C, Müller AHE (2006) RAFT polymerization of *N*-Isopropylacrylamide and acrylic acid under-irradiation in aqueous media. Macromol Rapid Commun 27:821–828
41. Convertine AJ, Sumerlin BS, Thomas DB, Lowe AB, McCormick CL (2003) Synthesis of block copolymers of 2- and 4-vinylpyridine by RAFT polymerization. Macromolecules 36:4679–4681
42. Yuan J-J, Ma R, Gao Q, Wang Y-F, Cheng S-Y, Feng L-X, Fan Z-Q, Jiang L (2003) Synthesis and characterization of polystyrene/poly(4-vinylpyridine) triblock copolymers by reversible addition fragmentation chain transfer polymerization and their self-assembled aggregates in water. J Appl Polym Sci 89:1017–1025
43. Sahnoun M, Charreyre M-T, Veron L, Delair T, D'Agosto FJ (2005) Synthetic and characterization aspects of dimethylaminoethyl methacrylate reversible addition fragmentation chain transfer (RAFT) polymerization. Polym Sci Part A: Polym Chem 43:3551–3565
44. Xiong Q, Ni P, Zhang F, Yu Z (2004) Synthesis and characterization of 2-(dimethylamino)ethyl methacrylate homopolymers via aqueous RAFT polymerization and their application in miniemulsion polymerization. Polym Bull 53:1–8
45. Donovan MS, Sumerlin BS, Lowe AB, McCormick CL (2002) Controlled/Living polymerization of sulfobetaine monomers directly in aqueous media via RAFT. Macromolecules 35:8663–8666
46. Delaittre G, Rieger J, Charleux B (2011) Nitroxide-mediated living/controlled radical polymerization of *N*,*N*-diethylacrylamide. Macromolecules 44:462–470
47. Convertine AJ, Lokitz BS, Vasileva Y, Myrick LJ, Scales CW, Lowe AB, McCormick CL (2006) Direct synthesis of thermally responsive DMA/NIPAM diblock and DMA/NIPAM/DMA triblock copolymers via aqueous, room temperature RAFT polymerization. Macromolecules 39:1724–1730
48. Scales CW, Vasilieva YA, Convertine AJ, Lowe AB, McCormick CL (2005) Direct, controlled synthesis of the nonimmunogenic, hydrophilic polymer, poly(*N*-(2-hydroxypropyl)methacrylamide) via RAFT in aqueous media. Biomacromolecules 6:1846–1850
49. Barner L, Davis TP, Stenzel MH, Barner-Kowollik C (2007) Complex macromolecular architectures by reversible addition fragmentation chain transfer chemistry: theory and practice. Macromol Rapid Commun 28:539–559
50. Quémener D, Davis TP, Barner-Kowollik C, Stenzel MH (2006) RAFT and click chemistry: A versatile approach to well-defined block copolymers. Chem Commun 5051–5053
51. Gondi SR, Vogt AP, Sumerlin BS (2007) Versatile pathway to functional telechelics via RAFT polymerization and click chemistry. Macromolecules 40:474–481
52. Postma A, Davis TP, Evans RA, Li G, Moad G, O'Shea MS (2006) Synthesis of well-defined polystyrene with primary amine end groups through the use of phthalimido-functional RAFT agents. Macromolecules 39:5293–5306
53. Liu J, Hong C-Y, Pan C-Y (2004) Dihydroxyl-terminated telechelic polymers prepared by RAFT polymerization using functional trithiocarbonate as chain transfer agent. Polymer 45:4413–4421
54. Lima V, Jiang X, Brokken-Zijp J, Schoenmakers PJ, Klumperman B, Linde RVDJ (2005) Synthesis and characterization of telechelic polymethacrylates via RAFT polymerization. Polym Sci Part A: Polym Chem 43:959–973
55. Lai JT, Filla D, Shea R (2002) Functional polymers from novel carboxyl-terminated trithiocarbonates as highly efficient RAFT agents. Macromolecules 35:6754–6756
56. Lutz JF (2007) 1,3-dipolar cycloadditions of azides and alkynes: a universal ligation tool in polymer and materials science. Angew Chem Int Ed 46:1018–1025
57. Barner-Kowollik C, Inglis AJ (2009) Has click chemistry lead to a paradigm shift in polymer material design? Macromol Chem Phys 210:987–992
58. Kempe K, Krieg A, Becer CR, Schubert US (2012) "Clicking" on/with polymers: a rapidly expanding field for the straightforward preparation of novel macromolecular architectures. Chem Soc Rev 41:176–191

59. Barner-Kowollik C, Du Prez FE, Espeel P, Hawker CJ, Junkers T, Schlaad H, Van Camp W (2011) "Clicking" polymers or just efficient linking: what is the difference? Angew Chem Int Ed 50:60–62
60. Perrier S, Takolpuckdee P, Mars CA (2005) Macromolecular design via reversible addition—fragmentation chain transfer (RAFT)/xanthates (MADIX) polymerization. Macromolecules 38:2033–2036
61. Llauro M, Loiseau J, Boisson F, Delolme F, Ladavière C, Claverie JJ (2004) Unexpected end-groups of poly(acrylic acid) prepared by RAFT polymerization. Polym Sci Part A: Polym Chem 42:5439–5462
62. Lowe AB, Sumerlin BS, Donovan MS, McCormick CL (2002) Facile preparation of transition metal nanoparticles stabilized by well-defined (co)polymers synthesized via aqueous reversible addition-fragmentation chain transfer polymerization. J Am Chem Soc 124:11562–11563
63. Vana P, Albertin L, Barner L, Davis TP, Barner-Kowollik CJ (2002) Reversible addition–fragmentation chain-transfer polymerization: unambiguous end-group assignment via electrospray ionization mass spectrometry. Polym Sci Part A: Polym Chem 40:4032–4037
64. Lu L, Zhang H, Yang N, Cai Y (2006) Toward rapid and well-controlled ambient temperature RAFT polymerization under UV-Vis radiation: effect of radiation wave range. Macromolecules 39:3770–3776
65. Mayadunne RTA, Rizzardo E, Chiefari J, Krstina J, Moad G, Postma A, Thang SH (2000) Living polymers by the use of trithiocarbonates as reversible addition/fragmentation chain transfer (RAFT) agents: ABA triblock copolymers by radical polymerization in two steps. Macromolecules 33:243–245
66. Benaglia M, Chiefari J, Chong YK, Moad G, Rizzardo E, Thang SH (2009) Universal (Switchable) RAFT agents. J Am Chem Soc 131:6914–6915
67. Bernard J, Favier A, Zhang L, Nilasaroya A, Davis TP, Barner-Kowollik C, Stenzel MH (2005) Poly(vinyl ester) star polymers via xanthate-mediated living radical polymerization: from poly(vinyl alcohol) to glycopolymer stars. Macromolecules 38:5475–5484
68. Mayadunne RTA, Jeffery J, Moad G, Rizzardo E (2003) Living free radical polymerization with reversible addition/fragmentation chain transfer (RAFT polymerization): approaches to star polymers. Macromolecules 36:1505–1513
69. Stenzel MH, Zhang L, Huck WTS (2006) Temperature-responsive glycopolymer brushes synthesized via RAFT polymerization using the Z-Group approach. Macromol Rapid Commun 27:1121–1126
70. Darcos V, Duréault A, Taton D, Gnanou Y, Marchand P, Caminade A-M, Majoral J-P, Destarac M, Leising F (2004) Synthesis of hybrid dendrimer-star polymers by the RAFT process. Chem Commun 2110–2111
71. Mertoglu M, Laschewsky A, Skrabania K, Wieland C (2005) New water soluble agents for reversible addition/fragmentation chain transfer polymerization and their application in aqueous solutions. Macromolecules 38:3601–3614
72. Lehn JM (1978) Cryptates: the chemistry of macropolycyclic inclusion complexes. Acc Chem Res 11:49–57
73. Lehn J-M (1988) Supramolecular chemistry—scope and perspectives molecules, supermolecules, and molecular devices (Nobel Lecture). Angew Chem Int Ed 27:89–112
74. Lehn J-M (1995) Supramolecular chemistry. Wiley VCH, Weinheim
75. Lehn J-M (2005) In: Ciferri A (ed) Supramolecular polymers. CRC Press, Boca Raton, Chap. 1, p 3
76. Steed JW, Atwood JL (2009) Supramolecular chemistry. Wiley, New York
77. Connors KA (1997) The stability of cyclodextrin complexes in solution. Chem Rev 97:1325–1358
78. Biwer A, Antranikian G, Heinzle E (2002) Enzymatic production of cyclodextrins. Appl Microbiol Biotechnol 59:609–617
79. Sänger W (1980) Cyclodextrin-einschlussverbindungen in forschung und industrie. Angew Chem 92:343–361

80. van Etten RL, Clowes GA, Sebastian JF, Bender ML (1967) The mechanism of the cycloamylose-accelerated cleavage of phenyl esters. J Am Chem Soc 89:3253–3262
81. da Silva WA, Rodrigues MT, Shankaraiah N, Ferreira RB, Andrade CKZ, Pilli RA, Santos LS (2009) Novel supramolecular palladium catalyst for the asymmetric reduction of imines in aqueous media. Org Lett 11:3238–3241
82. Zhou J, Ritter H (2010) Cyclodextrin functionalized polymers as drug delivery systems. Polym Chem 1:1552–1559
83. Loftsson T, Jarho P, Màsson M, Järvinen T (2005) Cyclodextrins in drug delivery. Expert Opin Drug Deliv 2:335–351
84. Szejtli J (1997) Utilization of cyclodextrins in industrial products and processes. J Mater Chem 7:575–587
85. Nishi H, Fukuyama T, Terabe SJ (1991) Chiral separation by cyclodextrin-modified micellar electrokinetic chromatography. Chrom A 553:503–516
86. Szente L, Szejtli J (2004) Cyclodextrins as food ingredients. Trends Food Sci Technol 15:137–142
87. Dodziuk H (2006) In: Dodziuk H (ed) Cyclodextrins and their complexes. Wiley VCH, Weinheim, Chap. 1, pp 1–26
88. Del Valle EMM (2004) Cyclodextrins and their uses: a review. Process Biochem 39:1033–1046
89. Hedges AR (1998) Industrial applications of cyclodextrins. Chem Rev 98:2035–2044
90. Loftsson T, Brewster ME (1996) Pharmaceutical applications of cyclodextrins. 1. Drug solubilization and stabilization. J Pharm Sci 85:1017–1025
91. Kaya E, Mathias LJJ (2010) Synthesis and characterization of physical crosslinking systems based on cyclodextrin inclusion/host-guest complexation. Polym Sci Part A: Polym Chem 48:581–592
92. Cramer F, Sänger W, Spatz H-C (1967) Inclusion compounds. XIX.1a the formation of inclusion compounds of Ω±-cyclodextrin in aqueous solutions. Thermodynamics and kinetics. J Am Chem Soc 89:14–20
93. Schneider H-J, Hacket F, Rüdiger V, Ikeda H (1998) NMR studies of cyclodextrins and cyclodextrin complexes. Chem Rev 98:1755–1786
94. Béni S, Szakács Z, Csernák O, Barcza L, Noszál B (2007) Cyclodextrin/imatinib complexation: binding mode and charge dependent stabilities. Eur J Pharm Sci 30:167–174
95. Zhang Y, Liu Y, Liu W, Gan Y, Zhou C (2010) Characterization of the inclusion complex of beta-cyclodextrin with sorbic acid in the solid state and in aqueous solution. J Incl Phenom Macrocycl Chem 67:177–182
96. Guo P, Su Y, Cheng Q, Pan Q, Li H (2011) Crystal structure determination of the beta-cyclodextrin/p-aminobenzoic acid inclusion complex from powder X-ray diffraction data. Carbohydr Res 346:986–990
97. Ivanov PM, Salvatierra D, Jaime C (1996) Experimental (NMR) and computational (MD) studies on the inclusion complexes of 1-bromoadamantane with alpha, beta, and gamma-cyclodextrin. J Org Chem 61:7012–7017
98. Chen B, Liu KL, Zhang Z, Ni X, Goh SH, Li J (2012) Supramolecular hydrogels formed by pyrene-terminated poly(ethylene glycol) star polymers through inclusion complexation of pyrene dimers with [gamma]-cyclodextrin. Chem Commun 48:5638–5640
99. Yorozu T, Hoshino M, Imamura M (1982) Fluorescence studies of pyrene inclusion complexes with .alpha.-, beta.-, and .gamma.-cyclodextrins in aqueous solutions. Evidence for formation of pyrene dimer in.gamma.-cyclodextrin cavity. J Phys Chem 86:4426–4429
100. Cruz JR, Becker BA, Morris KF, Larive CK (2008) NMR characterization of the host/guest inclusion complex between beta-cyclodextrin and doxepin. Magn Reson Chem 46:838–845
101. Wenz G, Han B-H, Müller A (2006) Cyclodextrin rotaxanes and polyrotaxanes. Chem Rev 106:782–817
102. Zhao Y-L, Dichtel WR, Trabolsi A, Saha S, Aprahamian I, Stoddart JF (2008) A redox-switchable alpha-cyclodextrin-based [2] rotaxane. J Am Chem Soc 130:11294–11296

103. Armspach D, Ashton PR, Ballardini R, Balzani V, Godi A, Moore CP, Prodi L, Spencer N, Stoddart JF, Tolley MS, Wear TJ, Williams DJ (1995) Catenated cyclodextrins. Chem Eur J 1:31–55
104. Harada A, Kamachi M (1990) Complex formation between poly(ethylene glycol) and alpha-cyclodextrin. Macromolecules 23:2821–2823
105. Harada A, Okada M, Li J, Kamachi M (1995) Preparation and characterization of inclusion complexes of poly(propylene glycol) with cyclodextrins. Macromolecules 28:8406–8411
106. Harada A, Li J, Nakamitsu T, Kamachi M (1993) Preparation and characterization of polyrotaxanes containing many threaded .alpha.-cyclodextrins. J Org Chem 58:7524–7528
107. He L, Huang J, Chen Y, Xu X, Liu L (2005) Inclusion interaction of highly densely PEO grafted polymer brush and alpha-cyclodextrin. Macromolecules 38:3845–3851
108. Born M, Ritter H (1995) Side-chain polyrotaxanes with a tandem structure based on cyclodextrins and a polymethacrylate main chain. Angew Chem Int Ed 34:309–311
109. Gibson HW, Ge Z, Jones JW, Harich K, Pederson A, Dorn HCJ (2009) Supramacromolecular chemistry: Self-assembly of polystyrene-based multi-armed pseudorotaxane star polymers from multi-topic C60 derivatives. Polym Sci Part A: Polym Chem 47:6472–6495
110. Sabadini E, Cosgrove T (2003) Inclusion complex formed between star-poly(ethylene glycol) and cyclodextrins. Langmuir 19:9680–9683
111. Harada A, Takashima Y, Yamaguchi H (2009) Cyclodextrin-based supramolecular polymers. Chem Soc Rev 38:875–882
112. Liao X, Chen G, Liu X, Chen W, Chen F, Jiang M (2010) Photoresponsive pseudopolyrotaxane hydrogels based on competition of host–guest interactions. Angew Chem Int Ed 49:4409–4413
113. De Bo G, De Winter J, Gerbaux P, Fustin C-A (2011) Rotaxane-based mechanically linked block copolymers. Angew Chem Int Ed 50:9093–9096
114. Stoll RS, Friedman DC, Stoddart JF (2011) Mechanically interlocked mechanophores by living-radical polymerization from rotaxane initiators. Org Lett 13:2706–2709
115. Houk KN, Leach AG, Kim SP, Zhang X (2003) Binding affinities of host/uest, protein/ligand, and protein/transition-state complexes. Angew Chem Int Ed 42:4872–4897
116. Benesi HA, Hildebrand JH (1949) A spectrophotometric investigation of the interaction of iodine with aromatic hydrocarbons. J Am Chem Soc 71:2703–2707
117. Kuntz ID, Gasparro FP, Johnston MD, Taylor RP (1968) Molecular interactions and the benesi-hildebrand equation. J Am Chem Soc 90:4778–4781
118. Yang C, Liu L, Mu T-W, Guo Q-X (2000) The performance of the benesi-hildebrand method in measuring the binding constants of the cyclodextrin complexation. Anal Sci 16:537–539
119. Tomatsu I, Hashidzume A, Harada A (2005) Photoresponsive hydrogel system using molecular recognition of alpha-cyclodextrin. Macromolecules 38:5223–5227
120. Tamesue S, Takashima Y, Yamaguchi H, Shinkai S, Harada A (2010) Photoswitchable supramolecular hydrogels formed by cyclodextrins and azobenzene polymers. Angew Chem Int Ed 49:7461–7464
121. Lewis EA, Hansen LD (1973) Thermodynamics of binding of guest molecules to α- and β-cyclodextrins. J Chem Soc, Perkin Trans 2:2081–2085
122. Miyaji T, Kurono Y, Uekama K, Ikeda K (1976) Simultaneous determination of complexation equilibrium constants for conjugated guest species by extended potentiometric titration method: on barbiturate-β-cyclodextrin system. Chem Pharm Bull 24:1155–1159
123. Takashima Y, Nakayama T, Miyauchi M, Kawaguchi Y, Yamaguchi H, Harada A (2004) Complex formation and gelation between copolymers containing pendant azobenzene groups and cyclodextrin polymers. Chem Lett 33:890–891
124. Höfler T, Wenz G (1996) Determination of binding energies between cyclodextrins and aromatic guest molecules by microcalorimetry. J Incl Phenom Macrocycl Chem 25:81–84
125. Boger J, Corcoran RJ, Lehn J-M (1978) Cyclodextrin chemistry. Selective modification of all primary hydroxyl groups of alpha- and beta-cyclodextrins. Helv Chim Acta 61:2190–2218
126. Khan AR, Forgo P, Stine KJ, D'Souza VT (1998) Methods for selective modifications of cyclodextrins. Chem Rev 98:1977–1996

127. Tang W, Ng S-C (2008) Facile synthesis of mono-6-amino-6-deoxy-alpha-, beta-, gamma-cyclodextrin hydrochlorides for molecular recognition, chiral separation and drug delivery. Nat Protoc 3:691–697
128. Hamasaki K, Ikeda H, Nakamura A, Ueno A, Toda F, Suzuki I, Osa T (1993) Fluorescent sensors of molecular recognition. Modified cyclodextrins capable of exhibiting guest-responsive twisted intramolecular charge transfer fluorescence. J Am Chem Soc 115:5035–5040
129. Melton LD, Slessor KN (1971) Synthesis of monosubstitutet cyclodehaxamaylososes. Carbohydr Res 18:29–37
130. Quan C-Y, Chen J-X, Wang H-Y, Li C, Chang C, Zhang X-Z, Zhuo R-X (2010) Core/Shell nanosized assemblies mediated by the alpha/beta cyclodextrin dimer with a tumor-triggered targeting property. ACS Nano 4:4211–4219
131. Amajjahe S, Choi S, Munteanu M, Ritter H (2008) Pseudopolyanions based on poly(NIPAAM-co-Beta-Cyclodextrin Methacrylate) and ionic liquids. Angew Chem Int Ed 47:3435–3437
132. Kuzuya A, Ohnishi T, Wasano T, Nagaoka S, Sumaoka J, Ihara T, Jyo A, Komiyama M (2009) Efficient guest inclusion by beta-cyclodextrin attached to the ends of DNA oligomers upon hybridization to various DNA conjugates. Bioconjug Chem 20:1643–1649
133. Bonomo RP, Cucinotta V, Impellizzeri FDAG, Maccarrone G, Rizzarelli E, Vecchio GJ (1993) Coordination properties of 6-deoxy-6-[1-(2-amino) ethylamino]-beta-cyclodextrin and the ability of its copper(II) complex to recognize and separate amino acid enantiomeric pairs. Incl Phenom Mol Recogn 15:167–180
134. Fujita K, Ueda T, Imoto T, Tabushi I, Toh N, Koga T (1982) Guest-induced conformational change of β-cyclodextrin capped with an environmentally sensitive chromophore. Bioorg Chem 11:72–84
135. Huan X, Wang D, Dong R, Tu C, Zhu B, Yan D, Zhu X (2012) Supramolecular ABC miktoarm star terpolymer based on host/guest inclusion complexation. Macromolecules 45:5941–5947
136. Yhaya F, Binauld S, Callari M, Stenzel MH (2012) One-pot endgroup-modification of hydrophobic RAFT polymers with cyclodextrin by thiol-ene chemistry and the subsequent formation of dynamic core/shell nanoparticles using supramolecular host/guest chemistry. Aust J Chem 65:1095–1103
137. Giacomelli C, Schmidt V, Putaux J-L, Narumi A, Kakuchi T, Borsali R (2009) Aqueous self-assembly of polystyrene chains end-functionalized with beta-cyclodextrin. Biomacromolecules 10:449–453
138. Liu H, Zhang Y, Hu J, Li C, Liu S (2009) Multi-responsive supramolecular double hydrophilic diblock copolymer driven by host-guest inclusion complexation between beta-cyclodextrin and adamantyl moieties. Macromol Chem Phys 210:2125–2137
139. Cai T, Yang WJ, Zhang Z, Zhu X, Neoh K-G, Kang E-T (2012) Preparation of stimuli-responsive hydrogel networks with threaded β-cyclodextrin end-capped chains via combination of controlled radical polymerization and click chemistry. Soft Matter 8:5612–5620
140. Bertrand A, Stenzel M, Fleury E, Bernard J (2012) Host-guest driven supramolecular assembly of reversible comb-shaped polymers in aqueous solution. Polym Chem 3:377–383
141. Martina K, Trotta F, Robaldo B, Belliardi N, Jicsinszky L, Cravotto G (2007) Efficient regioselective functionalizations of cyclodextrins carried out under microwaves or power ultrasound. Tetrahedron Lett 48:9185–9189
142. Casati C, Franchi P, Pievo R, Mezzina E, Lucarini M (2012) Unraveling unidirectional threading of alpha-cyclodextrin in a [2]rotaxane through spin labeling approach. J Am Chem Soc 134:19108–19117
143. Zeng J, Shi K, Zhang Y, Sun X, Zhang B (2008) Construction and micellization of a noncovalent double hydrophilic block copolymer. Chem Commun 3753–3755
144. Stadermann J, Komber H, Erber M, Däbritz F, Ritter H, Voit B (2011) Diblock copolymer formation via self-assembly of cyclodextrin. Macromolecules 44:3250–3259
145. Yan Q, Yuan J, Cai Z, Xin Y, Kang Y, Yin Y (2010) Voltage-responsive vesicles based on orthogonal assembly of two homopolymers. J Am Chem Soc 132:9268–9270

146. Yan Q, Xin Y, Zhou R, Yin Y, Yuan J (2011) Light-controlled smart nanotubes based on the orthogonal assembly of two homopolymers. Chem Commun 47:9594–9596
147. Peng L, Feng A, Zhang H, Wang H, Jian C, Liu B, Gao W, Yuan J (2014) Voltage-responsive micelles based on the assembly of two biocompatible homopolymers. Polym Chem 5:1751–1759
148. Zhang Z, Ding J, Chen X, Xiao C, He C, Zhuang X, Chen L, Chen X (2013) Intracellular pH-sensitive supramolecular amphiphiles based on host-guest recognition between benzimidazole and beta-cyclodextrin as potential drug delivery vehicles. Polym Chem 4:3265–3271
149. Rao J, Paunescu E, Mirmohades M, Gadwal I, Khaydarov A, Hawker CJ, Bang J, Khan A (2012) Supramolecular mimics of phase separating covalent diblock copolymers. Polym Chem 3:2050–2056
150. Ren S, Chen D, Jiang MJ (2009) Noncovalently connected micelles based on a beta-cyclodextrin-containing polymer and adamantane end-capped poly(epsilon-caprolactone) via host/guest interactions. Polym Sci Part A: Polym Chem 47:4267–4278
151. Yan J, Zhang X, Li W, Zhang X, Liu K, Wu P, Zhang A (2012) Thermoresponsive supramolecular dendronized copolymers with tunable phase transition temperatures. Soft Matter 8:6371–6377
152. Moers C, Nuhn L, Wissel M, Stangenberg R, Mondeshki M, Berger-Nicoletti E, Thomas A, Schaeffel D, Koynov K, Klapper M, Zentel R, Frey H (2013) Supramolecular linear-g-hyperbranched graft polymers: topology and binding strength of hyperbranched side chains. Macromolecules 46:9544–9553
153. Hetzer M, Fleischmann C, Schmidt BV, Barner-Kowollik C, Ritter H (2013) Visual recognition of supramolecular graft polymer formation via phenolphthalein/cyclodextrin association. Polymer 54:5141–5147
154. Feng A, Yan Q, Zhang H, Peng L, Yuan J (2014) Electrochemical redox responsive polymeric micelles formed from amphiphilic supramolecular brushes. Chem Commun doi:10.1039/C4CC00463A
155. Zhao Q, Wang S, Cheng X, Yam RCM, Kong D, Li RKY (2010) Surface modification of cellulose fiber via supramolecular assembly of biodegradable polyesters by the aid of host/guest inclusion complexation. Biomacromolecules 11:1364–1369
156. Huskens J, Deij MA, Reinhoudt DN (2002) Attachment of molecules at a molecular printboard by multiple host/guest interactions. Angew Chem Int Ed 41:4467–4471
157. Auletta T et al (2004) Writing patterns of molecules on molecular printboards. Angew Chem Int Ed 43:369–373
158. Hsu S-H, Yilmaz MD, Blum C, Subramaniam V, Reinhoudt DN, Velders AH, Huskens J (2009) Expression of sensitized Eu3+ luminescence at a multivalent interface. J Am Chem Soc 131:12567–12569
159. González-Campo A, Hsu S-H, Puig L, Huskens J, Reinhoudt DN, Velders AH (2010) Orthogonal covalent and noncovalent functionalization of cyclodextrin-alkyne patterned surfaces. J Am Chem Soc 132:11434–11436
160. Ludden MJW, Mulder A, Tampé R, Reinhoudt DN, Huskens J (2007) Molecular printboards as a general platform for protein immobilization: a supramolecular solution to nonspecific adsorption. Angew Chem Int Ed 46:4104–4107
161. Uhlenheuer DA, Wasserberg D, Haase C, Nguyen HD, Schenkel JH, Huskens J, Ravoo BJ, Jonkheijm P, Brunsveld L (2012) Directed supramolecular surface assembly of SNAP-tag fusion proteins. Chem Eur J 18:6788–6794
162. Gong Y-H, Li C, Yang J, Wang H-Y, Zhuo R-X, Zhang X-Z (2011) Photoresponsive smart template via host/guest interaction for reversible cell adhesion. Macromolecules 44:7499–7502
163. Ohno K, Wong B, Haddleton DMJ (2001) Synthesis of well-defined cyclodextrin-core star polymers. Polym Sci Part A: Polym Chem 39:2206–2214
164. Stenzel-Rosenbaum MH, Davis TP, Chen V, Fane AG (2001) Synthesis of poly(styrene) star polymers grown from sucrose, glucose, and cyclodextrin cores via living radical polymerization mediated by a half-metallocene iron carbonyl complex. Macromolecules 34:5433–5438

165. Stenzel MH, Davis TPJ (2002) Star polymer synthesis using trithiocarbonate functional beta-cyclodextrin cores (reversible addition-fragmentation chain-transfer polymerization). Polym Sci Part A: Polym Chem 40:4498–4512
166. Karaky K, Reynaud S, Billon L, François J, Chreim YJ (2005) Organosoluble star polymers from a cyclodextrin core. Polym Sci Part A: Polym Chem 43:5186–5194
167. Yang C, Li H, Goh SH, Li J (2007) Cationic star polymers consisting of alpha-cyclodextrin core and oligoethylenimine arms as nonviral gene delivery vectors. Biomaterials 28:3245–3254
168. He T, Hu T, Zhang X, Zhong G, Zhang H (2009) Synthesis and characterization of a novel liquid crystalline star-shaped polymer based on beta-CD core via ATRP. J Appl Polym Sci 112:2120–2126
169. Fijten MWM, Haensch C, van Lankvelt BM, Hoogenboom R, Schubert US (2008) Clickable poly(2-oxazoline)s as versatile building blocks. Macromol Chem Phys 209:1887–1895
170. Zhang L, Stenzel MH (2009) Spherical glycopolymer architectures using RAFT: from stars with a β-cyclodextrin core to thermoresponsive core–shell particles. Aust J Chem 62:813–822
171. Xu J, Liu SJ (2009) Synthesis of well-defined 7-arm and 21-arm poly(N-isopropylacrylamide) star polymers with beta-cyclodextrin cores via click chemistry and their thermal phase transition behavior in aqueous solution. Polym Sci Part A: Polym Chem 47:404–419
172. Zhang H, Yan Q, Kang Y, Zhou L, Zhou H, Yuan J, Wu S (2012) Fabrication of thermoresponsive hydrogels from star-shaped copolymer with a biocompatible β-cyclodextrin core. Polymer 53:3719–3725
173. Pang X, Feng C, Xu H, Han W, Xin X, Xia H, Qiu F, Lin Z (2014) : Unimolecular micelles composed of inner coil-like blocks and outer rod-like blocks crafted by combination of living polymerization with click chemistry. Polym Chem 5:2747–2755
174. Liu T, Xue W, Ke B, Xie M-Q, Ma D (2014) Star-shaped cyclodextrin-poly(l-lysine) derivative co-delivering docetaxel and MMP-9 siRNA plasmid in cancer therapy. Biomaterials 35:3865–3872
175. Miura Y, Narumi A, Matsuya S, Satoh T, Duan Q, Kaga H, Kakuchi TJ (2005) Synthesis of well-defined AB20-type star polymers with cyclodextrin-core by combination of NMP and ATRP. Polym Sci Part A: Polym Chem 43:4271–4279
176. Zhang Q, Li G-Z, Becer CR, Haddleton DM (2012) Cyclodextrin-centred star polymers synthesized via a combination of thiol-ene click and ring opening polymerization. Chem Commun 48:8063–8065
177. Li Y, Qian Y, Liu T, Zhang G, Hu J, Liu S (2014) Asymmetrically functionalized beta-cyclodextrin-based star copolymers for integrated gene delivery and magnetic resonance imaging contrast enhancement. Polym Chem 5:1743–1750
178. Shao S, Si J, Tang J, Sui M, Shen Y (2014) Jellyfish-shaped amphiphilic dendrimers: synthesis and formation of extremely uniform aggregates. Macromolecules 47:916–921
179. Zhao F, Yin H, Li J (2014) Supramolecular self-assembly forming a multifunctional synergistic system for targeted co-delivery of gene and drug. Biomaterials 35:1050–1062
180. Bai Y, Fan X-d, Tian W, Yao H, Zhuo L-h, tao Zhang H, Fan W-w, Yang Z, Zhang W-b (2013) Synthesis and thermally-triggered self-assembly behaviors of a dumbbell-shaped polymer carrying beta-cyclodextrin at branch points. Polymer 54:3566–3573
181. Teuchert C, Michel C, Hausen F, Park D-Y, Beckham HW, Wenz G (2013) Cylindrical polymer brushes by atom transfer radical polymerization from cyclodextrin/peg polyrotaxanes: synthesis and mechanical stability. Macromolecules 46:2–7
182. Nagahama K, Aoki R, Saito T, Ouchi T, Ohya Y, Yui N (2013) Enhanced stereocomplex formation of enantiomeric polylactides grafted on a polyrotaxane platform. Polym Chem 4:1769–1773
183. Zhang Z-X, Liu X, Xu FJ, Loh XJ, Kang E-T, Neoh K-G, Li J (2008) Pseudo-block copolymer based on star-shaped poly(N-isopropylacrylamide) with a beta-cyclodextrin core and guest-bearing peg: controlling thermoresponsivity through supramolecular self-assembly. Macromolecules 41:5967–5970

184. Zhang Z-X, Liu KL, Li J (2011) Self-assembly and micellization of a dual thermoresponsive supramolecular pseudo-block copolymer. Macromolecules 44:1182–1193
185. Tian Z, Chen C, Allcock HR (2014) Synthesis and assembly of novel poly(organophosphazene) structures based on noncovalent host/guest inclusion complexation. Macromolecules 47. doi:10.1021/ma500020p
186. Yan J, Zhang X, Zhang X, Liu K, Li W, Wu P, Zhang A (2012) Thermoresponsive supramolecular dendrimers via host/guest interactions. Macromol Chem Phys 213:2003–2010
187. Guo M, Jiang M, Pispas S, Yu W, Zhou C (2008) Supramolecular hydrogels made of end-functionalized low-molecular-weight PEG and alpha-cyclodextrin and their hybridization with SiO_2 nanoparticles through host/guest interaction. Macromolecules 41:9744–9749
188. Liu J, Chen G, Guo M, Jiang M (2010) Dual stimuli-responsive supramolecular hydrogel based on hybrid inclusion complex (HIC). Macromolecules 43:8086–8093
189. Du P, Liu J, Chen G, Jiang M (2011) Dual responsive supramolecular hydrogel with electrochemical activity. Langmuir 27:9602–9608
190. Wei K, Li J, Liu J, Chen G, Jiang M (2012) Reversible vesicles of supramolecular hybrid nanoparticles. Soft Matter 8:3300–3303
191. Luo C, Zuo F, Zheng Z, Cheng X, Ding X, Peng Y (2008) Tunable smart surface of gold nanoparticles achieved by light-controlled molecular recognition effection. Macromol Rapid Commun 29:149–154
192. Li J (2009) In: Wenz G (ed) Inclusion polymers. Advances in polymer science, vol 222. Springer, Berlin Heidelberg, pp 175–203
193. Li J, Loh XJ (2008) Cyclodextrin-based supramolecular architectures: Syntheses, structures, and applications for drug and gene delivery. Adv Drug Deliv Rev 60:1000–1017
194. Chen G, Jiang M (2011) Cyclodextrin-based inclusion complexation bridging supramolecular chemistry and macromolecular self-assembly. Chem Soc Rev 40:2254–2266
195. van de Manakker F, Vermonden T, van Nostrum CF, Hennink WE (2009) Cyclodextrin-based polymeric materials: synthesis, properties, and pharmaceutical/biomedical applications. Biomacromolecules 10:3157–3175
196. Li J (2010) Self-assembled supramolecular hydrogels based on polymer–cyclodextrin inclusion complexes for drug delivery. NPG Asia Mater 2:112–118
197. Ren L, He L, Sun T, Dong X, Chen Y, Huang J, Wang C (2009) Dual-responsive supramolecular hydrogels from water-soluble peg-grafted copolymers and cyclodextrin. Macromol Biosci 9:902–910
198. Sui K, Shan X, Gao S, Xia Y, Zheng Q, Xie DJ (2010) Dual-responsive supramolecular inclusion complexes of block copolymer poly(ethylene glycol)-block-poly[(2-dimethylamino)ethyl methacrylate] with alpha-cyclodextrin. Polym Sci Part A: Polym Chem 48:2143–2153
199. Li Z, Yin H, Zhang Z, Liu KL, Li J (2012) Supramolecular anchoring of DNA polyplexes in cyclodextrin-based polypseudorotaxane hydrogels for sustained gene delivery. Biomacromolecules 13:3162–3172
200. Zou H, Guo W, Yuan WJ (2013) Supramolecular hydrogels from inclusion complexation of [small alpha]-cyclodextrin with densely grafted chains in micelles for controlled drug and protein release. J Mater Chem B 1:6235–6244
201. Jin Q, Liu G, Ji J (2014) Supramolecular micelles and reverse micelles based on cyclodextrin polyrotaxanes. Chin J Chem 32:73–77
202. Wu Y, Ni P, Zhang M, Zhu X (2010) Fabrication of microgels via supramolecular assembly of cyclodextrin-containing star polycations and oppositely charged linear polyanions. Soft Matter 6:3751–3758
203. Hetzer M, Schmidt BVKJ, Barner-Kowollik C, Ritter H (2014) Supramolecular polymer networks of building blocks prepared via RAFT polymerization. Polym Chem. 5:2142–2152
204. Wang Y-F, Zhang D-L, Zhou T, Zhang H-S, Zhang W-Z, Zhang A, Luo L, Li B-J, Zhang S (2014) A reversible functional supramolecular materials formed by host-guest inclusion. Polym Chem 5:2922–2927

205. Zhang H, Peng L, Xin Y, Yan Q, Yuan J (2013) Stimuli-responsive polymer networks with beta-cyclodextrin and ferrocene reversible linkage based on linker chemistry. Macromol Symp 329:66–69
206. Guan Y, Zhao H-B, Yu L-X, Chen S-C, Wang Y-Z (2014) Multi-stimuli sensitive supramolecular hydrogel formed by host-guest interaction between PNIPAM-Azo and cyclodextrin dimers. RSC Adv 4:4955–4959
207. Wang L, Yang Y-W, Zhu M, Qiu G, Wu G, Gao H (2014) Beta-cyclodextrin-conjugated amino poly(glycerol methacrylate)s for efficient insulin delivery. RSC Adv 4:6478–6485
208. Zou J, Guan B, Liao X, Jiang M, Tao F (2009) Dual reversible self-assembly of PNIPAM-based amphiphiles formed by inclusion complexation. Macromolecules 42:7465–7473
209. Guo M, Jiang M, Zhang G (2008) Surface modification of polymeric vesicles via host/guest inclusion complexation. Langmuir 24:10583–10586
210. Inoue Y, Kuad P, Okumura Y, Takashima Y, Yamaguchi H, Harada A (2007) Thermal and photochemical switching of conformation of poly(ethylene glycol)-substituted cyclodextrin with an azobenzene group at the chain end. J Am Chem Soc 129:6396–6397
211. Felici M, Marzá-Pérez M, Hatzakis NS, Nolte RJM, Feiters MC (2008) Beta-cyclodextrin-appended giant amphiphile: aggregation to vesicle polymersomes and immobilisation of enzymes. Chem Eur J 14:9914–9920

Chapter 3
CD-Complexed RAFT Agents

3.1 Introduction

RAFT polymerization has emerged as a very efficient tool for the synthesis of water-soluble polymers due to its high tolerance of functional monomers [2–5] (see Sect. 2.1.4). The polymerization itself can be conducted directly in water with a broad range of water-soluble monomers that include methacrylates [6], methacrylamides [7], styrenics [8], acrylates [9] and acrylamides [10–12] so far. Furthermore, the utilization of water is interesting from an environmental and economic point of view as water is non-toxic, non-flammable and readily available. Thus, it is easy to handle safely and low priced. The possibility to solubilize hydrophobic molecules in water is an interesting application of CDs. In this context, hydrophobic monomers were solubilized in water with CDs, e.g. in radical polymerization [13, 14], living radical polymerization [15–17], enzymatic polymerization [18] and Rhodium-catalyzed polymerization [19]. To connect the solubilizing effect of CDs with RAFT polymerization, the aqueous RAFT polymerization of three acrylamido monomers, namely DMAAm, DEAAm and NIPAAm in the presence of a hydrophobic CTA that is solubilized via a host/guest complex was investigated. The employed hydrophobic CTAs bear the 4-*tert*-butyl phenyl-group that is well known to form stable host/guest complexes with β-CDs [20, 21]. Three novel CTAs were synthesized, which contain the guest-group in regions of variable reactivity within the molecule. The guest group can be incorporated in the R-, the Z-group or both. As the CTA allows control over the chain-end functionality in RAFT polymerization, hydrophobic chain ends are obtained directly (as depicted in Scheme 3.1).

The hydrophobic chain ends may have further use as guests in complex self-assemblies with CD-functionalized polymers or surfaces, e.g. to construct supramolecular block copolymers [22, 23] or to obtain supramolecular grafting, e.g. on cellulose

---

ROESY measurements were performed in collaboration with M. Hetzer and Prof. H. Ritter (Heinrich Heine Universität Düsseldorf). Parts of this chapter were reproduced with permission from Schmidt et al. [1]. Copyright 2011 American Chemical Society.

B. V. K. J. Schmidt, *Novel Macromolecular Architectures via a Combination of Cyclodextrin Host/Guest Complexation and RAFT Polymerization*, Springer Theses,
DOI: 10.1007/978-3-319-06077-4_3, © Springer International Publishing Switzerland 2014

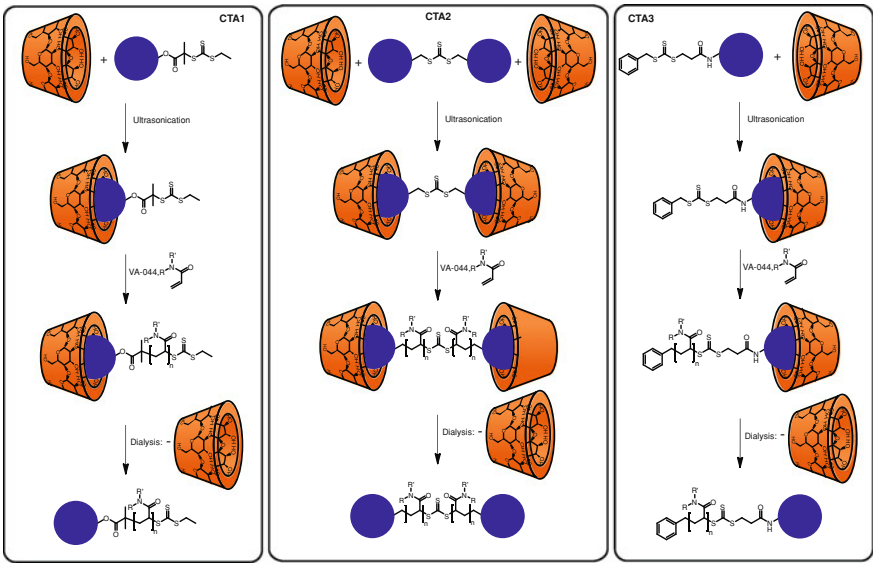

Scheme 3.1 Procedure for the RAFT polymerization of acrylamido-monomers with CD-complexed CTAs (DMAAm: R=R′=Me; DEAAm: R=R′=Et; NIPAAm: R=*i*-Pr, R′=H): R-approach (**1**), combined approach (**2**) and Z-approach (**3**). The guest-substituent, i.e. 4-*tert*-butyl phenyl, is depicted blue

[24]. In the case of thermoresponsive polymers that show T_c behavior such as PNIPAAm or PDEAAm, it is well known that hydrophobic endgroups can induce a change in the observed T_c [25–27]. Therefore a modulation of the thermoresponsivity of these polymers is possible. Furthermore, most water-soluble CTAs contain carboxylic- or sulfonic-acid groups which lead to acid-functionalized polymers [12, 28, 29]. In cases where acid-functionalized water-soluble polymers—e.g. because of unspecific interactions in biological systems—are undesirable, a polymer analogous removal/modification is required which can be complicated depending on the reaction type. Therefore, it is interesting to study the polymerization via hydrophobic guest-functionalized CTA/CD complexes in water. The current approach provides the opportunity to generate hydrophilic polymers without acidic endgroups in one step.

In the present chapter the first aqueous RAFT mediated polymerization of hydrophilic monomers employing a supramolecular CD/CTA host/guest complex utilizing 4-*tert*-butyl phenyl substituted CTAs is described. The presented approach is the first methodology that leads to hydrophilic polymers with hydrophobic endgroups in one step via aqueous RAFT polymerization. High molecular weights and conversions were reached at 25 °C with good control over $Đ_m$ and molecular weight as determined via *N*,*N*-dimethylacetamide (DMAc) SEC. Furthermore, the first living radical polymerization of DEAAm in aqueous solution is described. The structure of the synthesized polymers was confirmed via electrospray ionization-mass

spectrometry (ESI-MS) and ^{1}H-NMR spectroscopy. The living character of the polymer chains was proven via chain extension experiments and the recorded evolution of the full molecular weight distribution with conversion. In addition, several methods for the post-polymerization removal of the employed CDs were studied.

3.2 Results and Discussion

The approach for the utilization of hydrophobic CTAs in aqueous RAFT polymerizations via CD inclusion complexes includes the synthesis of novel hydrophobic CTAs that are subjected to complex formation with randomly methylated CD (Me-β-CD) and are subsequently used in the RAFT polymerization of DMAAm, DEAAm and NIPAAm.

3.2.1 Design and Synthesis of the Chain Transfer Agents

Several trithiocarbonate-CTAs for the aqueous RAFT-polymerization of hydrophilic monomers are mentioned in the literature [12, 28–30]. As R-group, usually the benzyl- or a tertiary-α-carbonyl-group are employed. The synthesis of trithiocarbonates can be carried out via the deprotonation of thiols, their nucleophilic attack on carbon disulfide and nucleophilic attack of the resulting trithiocarbonate salt on bromo-compounds. O'Reilly and coworkers recently presented an elegant way to synthesize trithiocarbonate-CTAs utilizing potassium phosphate as base in acetone [31]. This synthetic route was employed for all of the CTAs described in the current chapter. As guest group the 4-*tert*-butyl phenyl motif was chosen due to its high complexation-constant with β-CD ($K \sim 18{,}000 - 25{,}000\,L \times mol^{-1}$) [21]. From an earlier publication of Wenz and coworker [20] a similar association constant of Me-β-CDwith the 4-*tert*-butyl phenyl-group can be anticipated from a close analog (heptakis-(2,6-di-O-methyl)-β-CD).

As depicted in Scheme 3.2, the synthesis of the guest-functionalized CTAs was accomplished either directly or in two stages to include guest-groups for β-CD-complexes into the CTAs. The guest group was incorporated in the R-group (**1**), Z-group (**3**) or both (**2**). One possibility was the use of DCC-coupling after the synthesis of a precursor CTA (e.g. synthesis of **1**). An alternative route was the synthesis of a guest-functionalized molecule containing a bromine leaving group (e.g. **3**). The direct route utilized guest-functionalized thiols and bromides (e.g. **2**). The synthesized CTAs were characterized via NMR-spectroscopy and ESI-MS.

3.2.2 Complexation of Chain Transfer Agents with Me-β-CD

For the utilization of the guest-functionalized CTAs in aqueous RAFT polymerizations host/guest complexes have to be formed with CD. Me-β-CD was chosen as

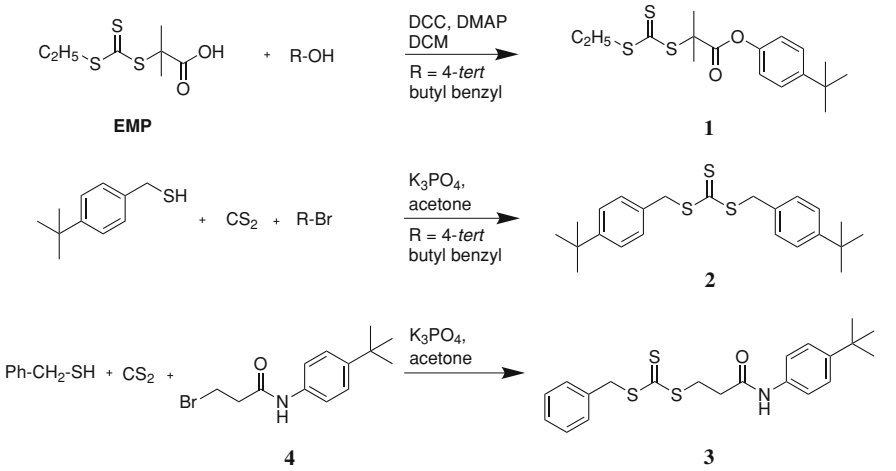

Scheme 3.2 Synthetic routes for the utilized complexable CTAs

host compound due to its increased water solubility compared to β-CD [32]. The complexation was accomplished via mixing the guest-functionalized CTAs with aqueous 40 wt% Me-β-CD-solution and ultrasonication until a clear yellow solution was obtained. Depending on the structure of the CTA the suspension had to be ultrasonicated for variable times, as the ultrasonication time depends on the complex stability and the possibility to disperse the CTA in the aqueous solution.

Figure 3.1 shows CTA/Me-β-CD-solutions and as control CTA/water-solutions before ultrasonication and after ultrasonication at ambient temperature. From the yellow color in the solution after ultrasonication it is obvious that the CTA/Me-β-CD complex was formed. In contrast, the solution in the control experiment shows no yellow color. To ensure complete inclusion, a 5-fold excess was used for all CTAs. For **1** a homogenous solution was obtained after 35 min, for **2** and **3** a homogenous solution was obtained after 100 min of ultrasonication.

A further method to characterize the CTA/Me-β-CDcomplexes is the two-dimenbreaksional ROESY (rotating frame nuclear Overhauser enhancement spectroscopy) NMR-technique [23, 33]. In general there are two modes for the formation of the inclusion complex. The guest can insert into the hydrophobic cavity via the primary, i.e. the side with the smaller opening, or the secondary face of the CD, i.e. the side with the larger opening. From the resonances in the ROESY spectrum it is in principal possible to assign the formed type of the complex. The complexation of **1** with Me-β-CD could be evidenced via the resonance of the *tert*-butyl-protons at 1.33 ppm with the inner protons of Me-β-CD (signal between 3.27 and 3.87 ppm) in D_2O at 25 °C as depicted in Fig. 3.2. Furthermore, the signal of the *tert*-butyl protons is shifted from 1.30 to 1.33 ppm, thus changing place with the signal of the methyl protons from the ethyl-group. Interestingly, the signal for the α-methyl protons of **1** splits into two distinct signals due to chemical inequivalency after complex formation. This signal shows resonance with the C2-methoxy group which is due to a complex

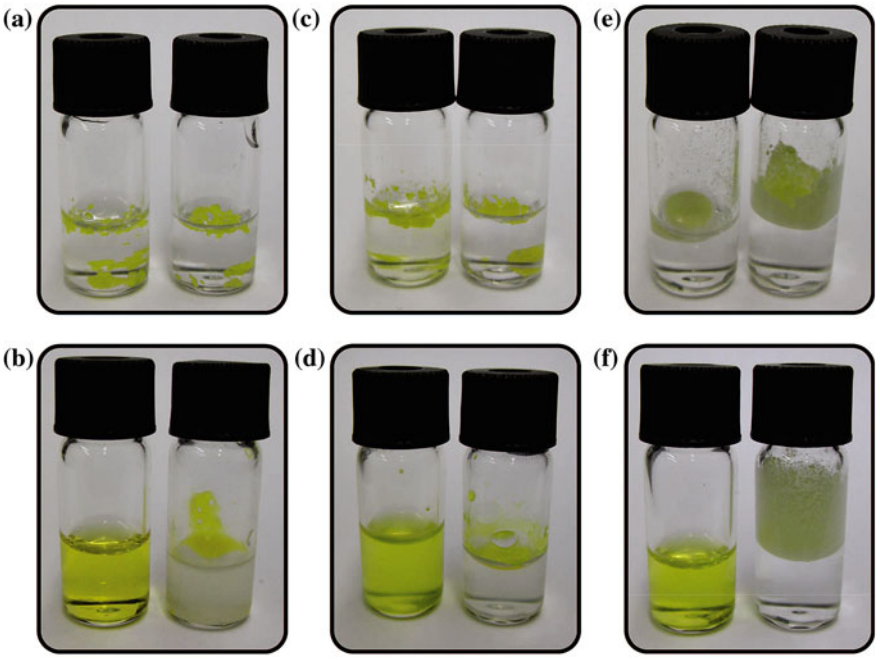

Fig. 3.1 Mixtures of **1** (**a** and **b**), **2** (**c** and **d**) and **3** (**e** and **f**) with aqueous 40 wt% Me-β-CD-solution (*left*) and deionized water (*right*). *Top* before ultrasonication, *bottom* after ultrasonication

with an insertion from the secondary side as shown in Fig. 3.2. Nevertheless, the unspecific resonances between the *tert*-butyl groups with the C2-methoxy- and the C6-methoxy-group suggest a mixture of both inclusion modes.

The 2D ROESY spectrum of **2** and **3** show the interaction between the CTA and Me-β-CD. The direction of the inclusion is not clearly assignable, although weak interaction of the aromatic protons with the C2-methoxy group indicate a complexation via the secondary face of Me-β-CD (refer to Fig. 3.2). For **3**, the resonances of the aromatic protons with the C6-methoxy- and C2-methoxy-protons indicate a complexation on both ends.

A comparison between the different CTAs shows several effects that have an influence on the complex-stability upon monomer addition. One matter is the nature of the monomer, e.g. hydrophobicity and its ability to act as a guest, which is discussed below. An additional point is the hydrophobicity of the CTA with respect to the hydrophobicity of weak guest-groups, e.g. dodecyl-, hexyl- or butyl-groups [34, 35]. Although other CTAs exhibit the possibility to form inclusion-complexes with Me-β-CD, e.g. the analog of **1** with a dodecyl- instead of an ethyl-group, addition of hydrophilic monomers leads to complete demixing due to the loss of the inclusion complex. Most likely, the hydrophobicity of the dodecyl-group is too weakly masked by a CD. Therefore, the complex is lost as competing guest-molecules,

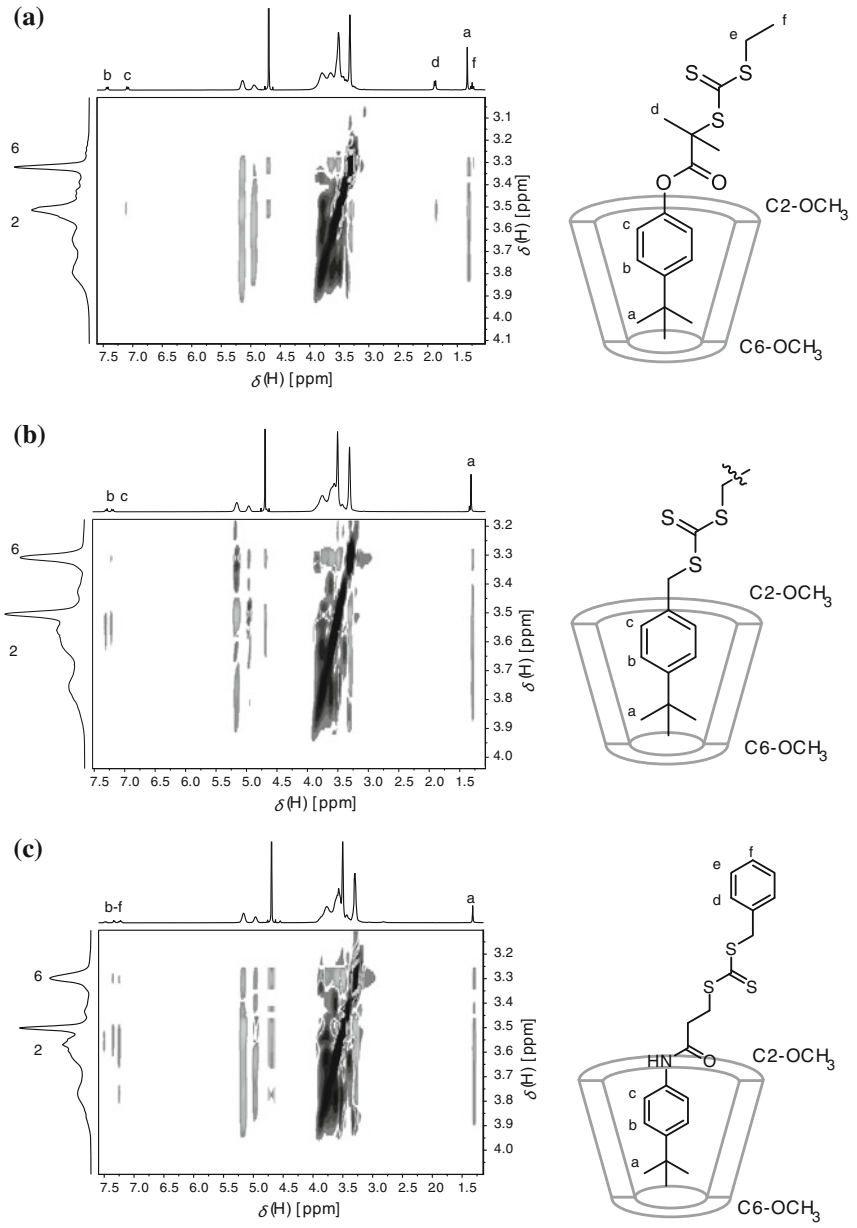

Fig. 3.2 2D ROESY spectrum of a 1:1 molar mixture of **a 1**, **b 2** and **c 3** and Me-β-CD in D_2O at 25 °C and a schematic illustration of the corresponding host/guest complexes

e.g. monomers, are added and the single host/guest complex with the 4-*tert*-butyl phenyl group is not strong enough to keep the whole CTA in solution. It is obvious that the stability of the host/guest complex is additionally correlated with the number of guest-groups incorporated into the CTA. The more guest groups are incorporated, the more stable is the complex. As the host/guest complexes are in equilibrium with the free molecules, it is advantageous to have two complexed groups in one CTA molecule. If one of the two host/guest complexes is lost, the remaining one can keep the entire molecule in solution and accessible for the re-formation of the second complex.

3.2.3 Polymerization with Complexed Chain Transfer Agents

For the polymerization of acrylamido monomers with Me-β-CD complexed CTA three steps were carried out as depicted in Scheme 3.1: Firstly, the complex was formed via ultrasonication of the appropriate CTA in aqueous 40 wt% Me-β-CD-solution. Secondly, monomer, water and initiator were added, the reaction was degassed and the polymerization subsequently commenced. Thirdly, the polymerization mixture was subjected to dialysis to remove residual monomer, initiator and Me-β-CD.

As discussed by McCormick and coworkers a major concern in aqueous RAFT polymerization of acrylamides is the hydrolysis/aminolysis of the CTA during the polymerization [4, 36, 37]. A solution for hydrolysis suppression/prevention is the use of acetic acid/acetate buffer as solvent and low temperature initiators, e.g. VA-044 [30, 37]. Under these conditions McCormick and colleagues evidenced that a controlled polymerization of acrylamide, DMAAm and NIPAAm via the RAFT process in aqueous media is possible [10, 11, 30]. Furthermore, it is well known that low temperatures favour the stability of β-CD-complexes. For these reasons all polymerizations were conducted at 25 °C. As the CTA/Me-β-CD complexes were not soluble in acetic acid/acetate buffer, a series of DMAAm polymerizations—as a test system—were conducted in variable reaction media with **1** or **EMP** to determine the effect of the reaction media on the polymerization. The results are summarized in Fig. 3.3.

Figure 3.3a shows that the polymerization reaction with the complexed **1** (triangles) proceeds slower than the polymerizations with **EMP** in acetic acid/acetate buffer (filled squares) or water (open circles), whereas the **EMP**-mediated polymerizations show comparable reaction rates. Nevertheless, the reaction with **1** leads to a conversion of 70 % in 6 h, while the reactions with **EMP** have a conversion of approximately 80 % within 6 h. It is proposed that the difference in reaction rate is a result of the increasing steric hindrance associated with the bulky CD complex. Although a slower reaction is observed, a superior control over the polymerization with the **1**/CD complex can be noted. Lower $Đ_m$ were observed in these polymerizations as summarized in Fig. 3.3b. In the case of **1** (triangles) the observed molecular weight was higher than the theoretical molecular weight whereas the molecular

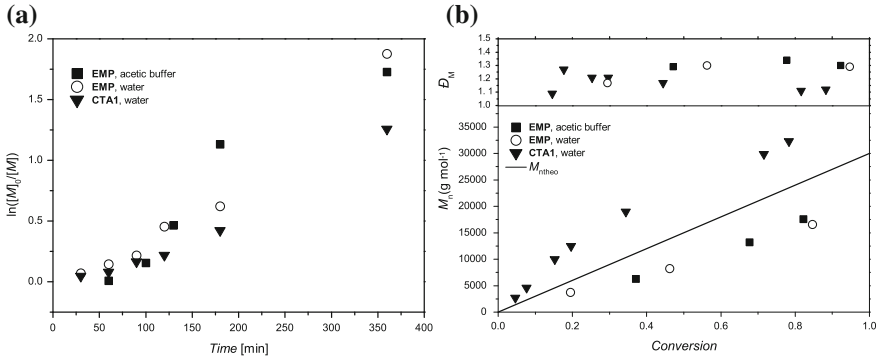

Fig. 3.3 **a** Comparison between the kinetic plots of **EMP**-mediated polymerization in acetic acid/acetate buffer, **EMP**-mediated polymerization in water or **1**/CD-mediated polymerization at 25 °C with a DMAAm/CTA/I ratio of 300/1/0.2 and a DMAAm concentration of 3.5 mol L^{-1}. **b** Comparison of the obtained molecular weights and $Đ_m$ as a function of monomer conversion

weight is lower than the theoretical molecular weight in the case of **EMP** (squares and open circles). As the polymerization has living/controlled character in both acetic acid/acetate buffer and pure water with **EMP** as CTA at 25 °C, there is no need to carry out the polymerization at acidic pH values in the case of complexed CTAs.

3.2.3.1 Removal of the Cyclodextrin After the Polymerization

For the removal of the CD several methods were applied. A test-polymerization with DMAAm and **1** was carried out, divided into several samples and purified in different ways. To compare the residual amounts of the CD in the products, the peak area of the eluting CD in the SEC-analysis was calculated relatively to the peak area of the polymer. The Me-β-CDcontent in the untreated mixture is given in entry 1 of Table 3.1. Dialysis was performed utilizing dialysis tubing with a MWCO of 3,500 Da but the treatment of the samples was varied. One purification method was the treatment of the crude polymerization solution with trifluoroacetic acid for 2 h as CDs are hydrolyzed by strong acids and the solution was dialysed for 3 days at ambient temperature afterwards (entry 2 in Table 3.1). For comparison, the crude polymerization mixture was dialysed for 3 days at ambient temperature (entry 3 in Table 3.1). An alternative method was dialysis for 3 days at ambient temperature and subsequently dialysis for 1 day or 2 days at 45 °C (entries 4 and 5 in Table 3.1). Furthermore enzymatic treatment with Taka-Diastase in acetic acid/acetate buffer at 37 °C for 1 day was employed after dialysis for 3 days at ambient temperature and another dialysis for 3 days at ambient temperature after the enzymatic treatment (entry 6 in Table 3.1). The enzymatic treatment with Taka Diastase from *Aspergillus oryzae* should lead to degradation of the CDs as it contains the enzyme α-amylase which is known to hydrolyse the α-1,4-glycosidic bond of the CDs [38–40].

Table 3.1 Results for the different purification methods quantified with the residual amount of Me-β-CD according to SEC measurements

Entry	Purification procedure	Me-β-CD (% area)
1	No purification	29.1
2	CF_3COOH 2 h, dialysis 3 d ambient temp.	7.5
3	Dialysis 3 d ambient temp.	8.4
4	Dialysis 3 d ambient temp., dialysis 1 d 45 °C	5.4
5	Dialysis 3 d ambient temp., dialysis 2 d 45 °C	3.3
6	Dialysis 3 d ambient temp., Taka-Diastase acetate buffer 1 d 37 °C, dialysis 3 d ambient temp.	4.1

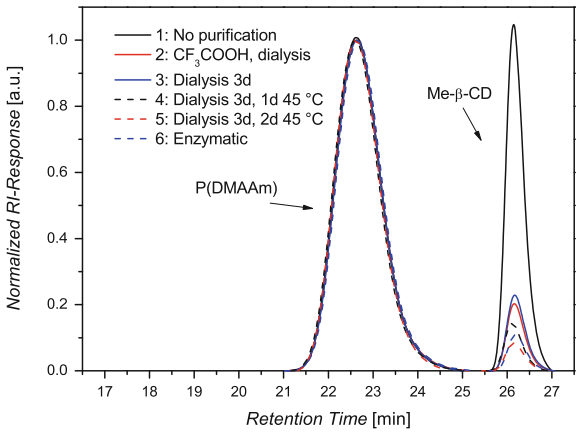

Fig. 3.4 Elugrams of the purification methods study depicting the PDMAAm peak and the peaks of the residual Me-β-CD

As listed in Table 3.1 dialysis at elevated temperatures, e.g. 45 °C, provides the best results with only 3.3 % Me-β-CD remaining (entry 5 in Table 3.1). Nevertheless, enzymatic treatment has a very similar performance with 4.1 % Me-β-CD remaining (entry 6 in Table 3.1; the corresponding elugrams can be found in Fig. 3.4). In the case of PDEAAm and PNIPAAm, dialysis at elevated temperatures leads to the precipitation of the polymers that supports the removal of residual CD. Generally, it should be noted that dialysis leads to a loss of low molecular weight polymers and oligomers. Especially in the case of low target molecular weights, the molecular weight distributions are thus to some extent affected.

3.2.3.2 Polymerization of *N,N*-Dimethylacrylamide with Complexed Chain Transfer Agents

DMAAm is very frequently employed in polymer chemistry. In the living/controlled radical polymerization with complexed CTAs the best control is obtained with **1** compared to **2** and **3** (see Tables 3.2, 3.3 and 3.4). This can be mostly attributed to

Table 3.2 Results for the living/controlled RAFT polymerization of DMAAm at 25 °C in aqueous solution with **1**

DMAAm/CTA/I	Time/h	*Conv.*	M_{ntheo}/g mol^{-1}	M_{nSEC}/g mol^{-1}	$Đ_m$
107/1/0.2	6	65	7,300	10,500	1.17
198/1/0.2	6	88	18,000	17,000	1.09
294/1/0.2	12	>99	29,500	36,500	1.08
585/1/0.2	12	94	55,000	62,000	1.06
1018/1/0.2	12	98	99,300	94,000	1.06

Table 3.3 Results for the living/controlled RAFT polymerization of DMAAm at 25 °C in aqueous solution with **2**

DMAAm/CTA/I	Time/h	*Conv.*	M_{ntheo}/g mol^{-1}	M_{nSEC}/g mol^{-1}	$Đ_m$
56/1/0.2	6	80	4,800	13,000	1.24
99/1/0.2	6	95	9,500	22,000	1.35
203/1/0.2	6	87	17,400	32,000	1.29
340/1/0.2	6	>99	29,100	49,500	1.42
603/1/0.2	12	>99	59,800	82,500	1.32
1184/1/0.2	12	>99	117,300	141,000	1.51

Table 3.4 Results for the living/controlled RAFT polymerization of DMAAm at 25 °C in aqueous solution with **3**

DMAAm/CTA/I	Time/h	*Conv.*	M_{ntheo}/g mol^{-1}	M_{nSEC}/g mol^{-1}	$Đ_m$
51/1/0.2	6	76	4,600	14,000	1.31
108/1/0.2	6	70	7,700	19,500	1.27
203/1/0.2	6	78	15,600	38,000	1.43
306/1/0.2	12	93	27,900	70,000	1.53
588/1/0.2	12	>99	58,000	102,500	1.46
1002/1/0.2	12	>99	100,000	156,500	1.54

the complex stability and the tertiary α-ester R-group in **1**. A monomer concentration of 3.0 mol L^{-1} was chosen and the CTA/initiator ratio was held constant at 1/0.2. The complex of **1** with Me-β-CD was stable throughout the reaction time and even at high monomer/CTA ratios up to 1,000/1. Therefore molecular weights ranging from 10,000 to 94,000 g mol^{-1} were obtained in good agreement with theoretical values. High conversion was reached in short reaction times even at the low polymerization temperature of 25 °C. The resulting $Đ_m$ lie between 1.06 and 1.17 (see Table 3.2 and Fig. 3.5d). Although the polymers were purified as described in the experimental section a small residue of unremoved CD (approx. 0.4–5.5 %) remained. Apart from residual CD, the SEC traces are unimodal, show only minor low molecular weight tailing and no high molecular weight coupling products.

Time resolved experiments with regard to conversion and molecular weight were carried out to confirm the living character of the polymerization (refer to

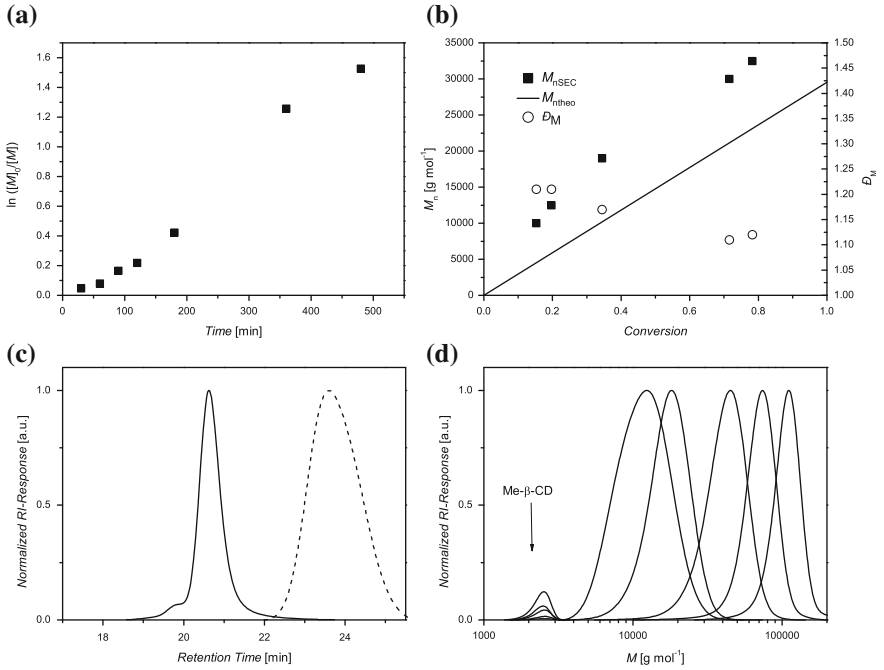

Fig. 3.5 **a** Kinetic plot for the polymerization of DMAAm at 25 °C with **1**. **b** Evolution of M_n with conversion at 25 °C with DMAAm/**1**/I: 297/1/0.2. **c** Chain-extension at 25 °C for 24 h. **d** Molecular weight distributions for different monomer/CTA ratios [(DMAAm/**1** (conversion) from *left* to *right*: 107/1 (65 %); 198/1 (88 %); 294/1 (>99 %); 585/1 (94 %); 1018/1 (98 %)]

Appendix A.1 for a collection of NMR-spectra). As depicted in Fig. 3.5, the kinetic first order plot shows linearity which confirms a constant radical concentration during the reaction and evidences a short induction period (<30 min). The molecular weights are increasing linearly with conversion which evidences the living character of the polymerization and the $Đ_m$ is decreasing with increasing conversion. Further proof for the living radical polymerization comes from the chain extension of purified macro-CTAs with DMAAm. A quantitative reinitiation was observed that leads to a shift in molecular weight from 10,500 to 97,500 g mol^{-1} with a final $Đ_m$ of 1.08. Nevertheless, small amounts of chain-chain coupling products were observed in the high molecular weight region.

The molecular structure of low molecular weight samples was confirmed via ESI-MS (M_n = 3,000 g mol^{-1}) and ^{1}H-NMR (M_n = 10,500 g mol^{-1}) (see Appendices A.2/A.3), evidencing the incorporation of the hydrophobic endgroups into the hydrophilic polymer. The mass spectrometric data shows no signals from initiator terminated polymer which is in accord with highly efficient chain-extension experiments.

With **2** turbidity was observed upon monomer addition that vanished in the beginning of the polymerization. In the polymerizations with **3** turbidity was observed

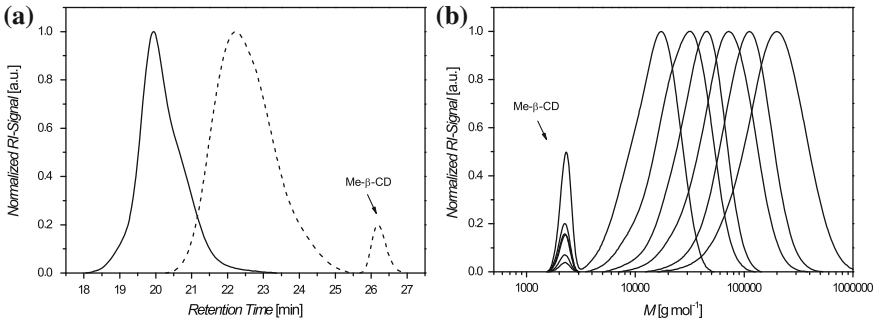

Fig. 3.6 **a** Chain-extension with DMAAm at 25 °C for 24 h. **b** Molecular weight distributions for different monomer/**2** ratios [DMAAm/**2** from *left* to *right* (conversion): 56/1 (80 %); 99/1 (95 %); 203/1 (87 %); 340/1 (>99 %); 603/1 (>99 %); 1184/1 (>99 %)]

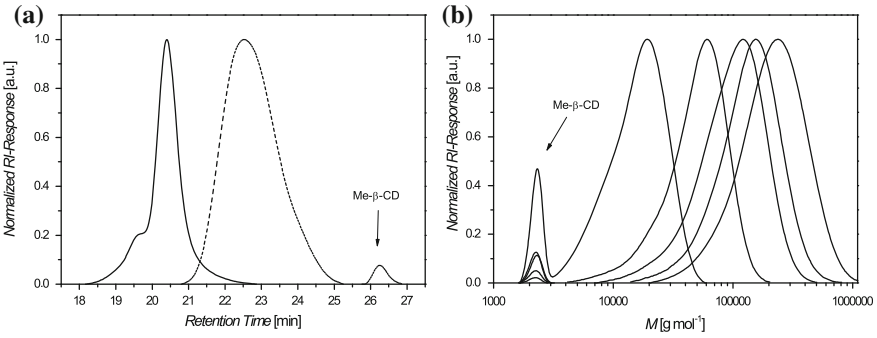

Fig. 3.7 **a** Chain-extension with DMAAm at 25 °C for 24 h. **b** Molecular weight distributions for different monomer/**3** ratios [DMAAm/**3** from *left* to *right* (conversion): 51/1 (76 %); 108/1 (70 %); 203/1 (78 %); 306/1 (93 %); 588/1 (>99 %); 1002/1 (>99 %)]

at monomer/CTA ratios exceeding 300/1. Nevertheless, molecular masses of up to 156,000 g mol^{-1} were reached with $Đ_m$ ranging from 1.31 to 1.54 (refer to Tables 3.3, 3.4 and Figs. 3.6, 3.7) with high conversions in short reaction times. As stated above, less control over the polymerization is observed with **2** and **3**. The less stable complexes of Me-β-CD with **2** and **3** lead to partial demixing on monomer and water addition as observed via a turbidity of the solution. Such a demixing explains the higher disagreement of experimental molecular weights compared to theoretical molecular weights, as less CTA molecules are accessible in the solution in the case of turbidity, thus leading to higher molecular weights. The broader molar-mass dispersity of the polymers prepared with **2** and **3** can be also attributed to the partial demixing as the undissolved CTA molecules react on a slower time scale. Therefore, low molecular weight tailing is observed which leads to higher $Đ_m$. Nevertheless, chain-extension experiments were conducted that proof the living character of the polymerization based on a high reinitiation efficiency.

Table 3.5 Results for the living/controlled RAFT polymerization of DEAAm at 25 °C in aqueous solution with **1**

DEAAm/CTA/I	Time/h	*Conv.*	M_{ntheo}/g mol^{-1}	M_{nSEC}/g mol^{-1}	$Đ_m$
12/1/0.2	12	>99	1,900	2,500	1.10
42/1/0.2	12	>99	5,800	5,000	1.11
80/1/0.2	12	>99	10,600	10,000	1.09
163/1/0.2	12	>99	21,100	18,000	1.08
248/1/0.2	12	>99	32,000	29,000	1.07
426/1/0.2	18	>99	54,600	55,000	1.06
813/1/0.2	18	>99	103,800	87,000	1.05

3.2.3.3 Polymerization of *N,N*-Diethylacrylamide with Complexed Chain Transfer Agents

PDEAAm is a polymer that exhibits a very low T_c of around 30 °C [41]. At a reaction temperature of 25 °C it should be possible to polymerize DEAAm in aqueous media via the RAFT process. Although the living radical polymerization in organic media has been described [42], a living/controlled radical polymerization of this monomer in aqueous solution has not been accomplished yet. **1**, **2** and **3** were employed for the polymerization of DEAAm. The monomer concentration was held constant at 3.5 mol L^{-1}, the temperature at 25 °C and the CTA/initiator ratio at 1/0.2. As with DMAAm, **1** shows the best control over the polymerizations. No turbidity or demixing is noticed for monomer/CTA ratios up to 200/1 and only a slight turbidity is observed for higher CTA/monomer ratios in the case of **1**. Molecular weights from 2,500 up to 87,000 g mol^{-1} that were in good agreement with the theoretical values were reached in short reaction times, e.g. 12 or 18 h, with quantitative conversions and $Đ_m$ ranging from 1.05 to 1.11 (see Table 3.5 and Fig. 3.8d). The resulting molecular weight distributions are unimodal and display no evidence for high molecular weight termination products or low molecular weight tailing, except for the lowest target molecular weight where low molecular weight (<1,000 g mol^{-1}) species are observed.

To confirm the living character of the polymerization, time resolved experiments with regard to conversion and molecular mass were carried out (refer to Appendix A.4 for a collection of NMR-spectra) and chain extensions were performed as depicted in Fig. 3.8. Besides a constant radical concentration as evidenced by a linear first-order plot with a short induction period below 30 min, the molecular weight grows linearly with conversion as expected for polymerizations with living character. Furthermore, the experimental molecular weights are in good agreement with the theory and the $Đ_m$ are decreasing with increasing conversion. The chain extension affords a very high reinitiation efficiency with a growth in molecular weight from 8,500 to 83,000 g mol^{-1} and a $Đ_m$ of 1.13 for the resulting polymer with a small amount of chain-chain coupling products.

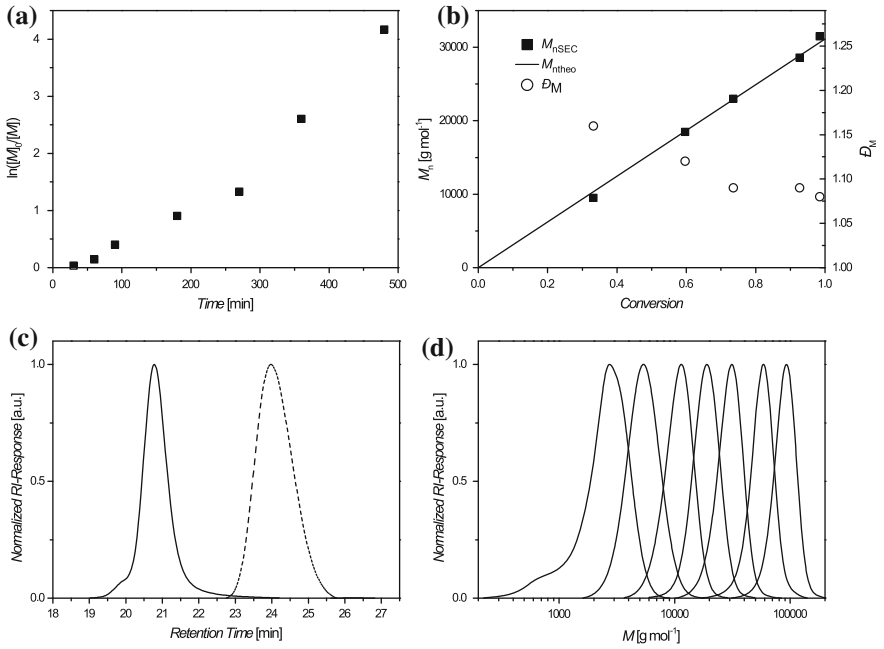

Fig. 3.8 **a** Kinetic plot for the polymerization of DEAAm at 25 °C with **1**. **b** Evolution of M_n with conversion at 25 °C with DEAAm/**1**/I: 241/1/0.2. **c** Chain-extension at 25 °C for 24 h. **d** Molecular weight distributions for different monomer/CTA ratios [DEAAm/**1** from *left* to *right* (conversion >99 %): 12/1; 42/1; 80/1; 163/1; 248/1; 426/1; 813/1]

ESI-MS and ^{1}H-NMR were recorded of a low molecular weight sample (M_n = 4,000 g mol^{-1}) to confirm the structure of the synthesized polymers. The results are in agreement with the expected polymer structure proving the incorporation of the hydrophobic endgroups into the hydrophilic polymer (refer to Appendices A.5/A.6). Furthermore, there is no indication of initiator derived chains in the ESI-MS spectrum which explains the high reinitiation efficiency.

For the other CTAs (**2** and **3**) turbid solutions were observed upon water addition. Nevertheless, high conversions were reached in short reaction times and molecular weights ranging from 4,000 to 116,000 g mol^{-1} were reached with $Đ_m$ from 1.10 to 1.39 (see also Tables 3.6, 3.7 and Figs. 3.9, 3.10). Similar to the polymerizations of DMAAm with **2** and **3** a disagreement of the experimental molecular weights with those theoretically predicted was noted that could be due to the turbid nature of the solution at the beginning of the polymerization process. It is also worth noting that the polymers remained in solution throughout the entire reaction time with all three CTAs although it is known from literature that hydrophobic endgroups lead to a lower T_c in PDEAAm [27].

Table 3.6 Results for the living/controlled RAFT polymerization of DEAAm at 25 °C in aqueous solution with **2**

DEAAm/CTA/I	Time/h	*Conv.*	M_{ntheo}/g mol^{-1}	M_{nSEC}/g mol^{-1}	$Đ_m$
13/1/0.2	12	>99	1,700	4,000	1.13
51/1/0.2	6	94	5,600	10,500	1.22
81/1/0.2	6	>99	10,300	13,000	1.32
158/1/0.2	12	>99	20,100	28,000	1.30
481/1/0.2	12	97	59,200	73,500	1.23
799/1/0.2	12	>99	101,000	107,000	1.23

Table 3.7 Results for the living/controlled RAFT polymerization of DEAAm at 25 °C in aqueous solution with **3**

DEAAm/CTA/I	Time/h	*Conv.*	M_{ntheo}/g mol^{-1}	M_{nSEC}/g mol^{-1}	$Đ_m$
13/1/0.2	12	92	1,500	4,500	1.14
40/1/0.2	12	89	4,500	14,000	1.36
79/1/0.2	12	97	15,300	15,500	1.39
160/1/0.2	12	>99	20,300	23,500	1.27
243/1/0.2	12	99	30,700	41,000	1.09
505/1/0.2	12	>99	62,700	59,000	1.23
810/1/0.2	12	99	102,000	116,000	1.10

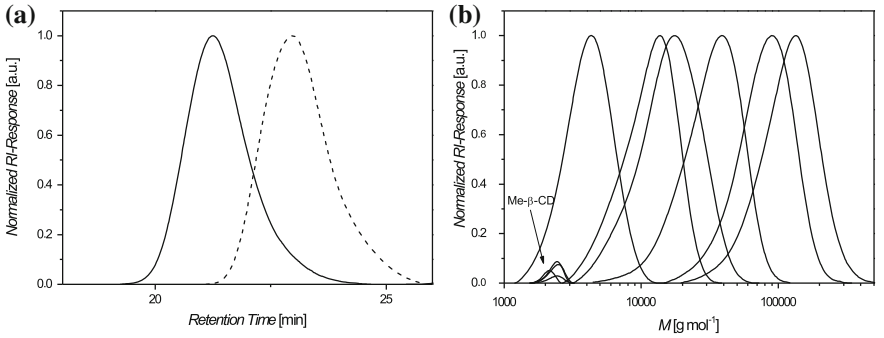

Fig. 3.9 **a** Chain-extension with DEAAm at 25 °C for 24 h. **b** Molecular weight distributions for different monomer/**2** ratios [DEAAm/**2** from *left* to *right* (conversion): 12/1 (>99 %); 51/1 (94 %); 81/1 (>99 %); 158/1 (>99 %); 481/1 (97 %); 799/1 (>99 %)]

3.2.3.4 Polymerization of *N*-Isopropylacrylamide with Complexed Chain Transfer Agents

Another important acrylamido monomer is NIPAAm. Due to the T_c of PNIPAAm that is close to human body temperature, many efforts have been made for its synthesis [2, 26, 30]. As the T_c of PNIPAAm is close to 31 °C [43], which is comparable to the T_c of PDEAAm, a controlled polymerization of NIPAAm is feasible at 25 °C in

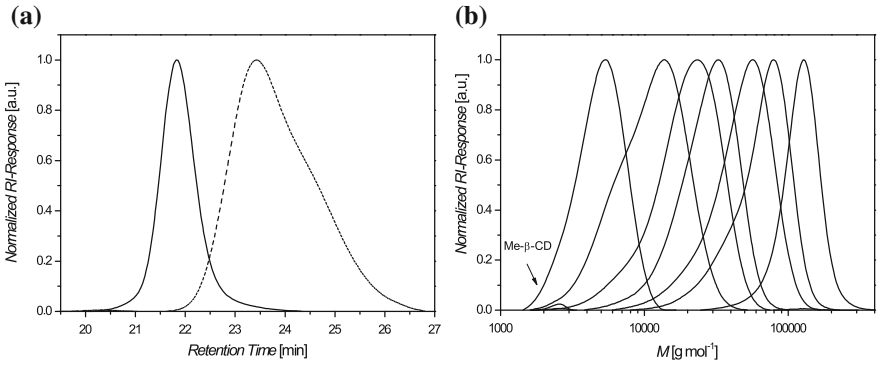

Fig. 3.10 **a** Chain-extension with DEAAm at 25 °C for 24 h. **b** Molecular weight distributions for different monomer/**3** ratios [DEAAm/**3** from *left* to *right* (conversion): 13/1 (92 %); 40/1 (89 %); 79/1 (97 %); 160/1 (>99 %); 243/1 (99 %); 505/1 (>99 %); 810/1 (99 %)]

Table 3.8 Results for the living/controlled RAFT polymerization of NIPAAm at 25 °C in aqueous solution with **1**

NIPAAm/CTA/I	Time/h	*Conv.*	M_{ntheo}/g mol^{-1}	M_{nSEC}/g mol^{-1}	$Đ_m$
15/1/0.2	18	>99	2,100	4,000	1.15
39/1/0.2	18	>99	4,800	7,500	1.29
44/1/0.2	18	>99	5,500	9,000	1.15
260/1/0.2	20	>99	30,100	50,000	1.46

aqueous media [30]. Therefore it should be possible to polymerize NIPAAm with CD-complexed CTAs at 25 °C in aqueous media as well.

In the case of NIPAAm, a controlled polymerization was only possible with **1**. The other CTAs showed complete demixing upon addition of the monomer and water, which is further discussed in the subsequent section. Nevertheless, with **1** polymers up to 50,000 g mol^{-1}were synthesized with $Đ_m$ ranging from 1.15 to 1.46 with quantitative conversions in 18 or 20 h. The monomer concentration was held constant at 2.5 mol L^{-1}, the polymerization temperature at 25 °C and the CTA/initiator ratio at 1/0.2. The results are summarized in Table 3.8. A significant excess of the experimental molecular weights compared to the theoretically predicted ones by a factor of 1.5–2.0 was evidenced that could be due to a partial disassembly of the CTA/CD complex. The obtained polymers show unimodal molecular weight distributions with no significant tailing in the low molecular region. Furthermore, no high molecular weight termination products are visible.

A constant radical concentration is supported by a linear first-order plot evidencing a short induction period of approximately 30 min (refer to Appendix Fig. A.7 for a collection of NMR-spectra). A confirmation of living radical polymerization was accomplished via a chain-extension experiment and a time resolved experiment that indicated a linear increase of molecular weight with conversion (see Fig. 3.11).

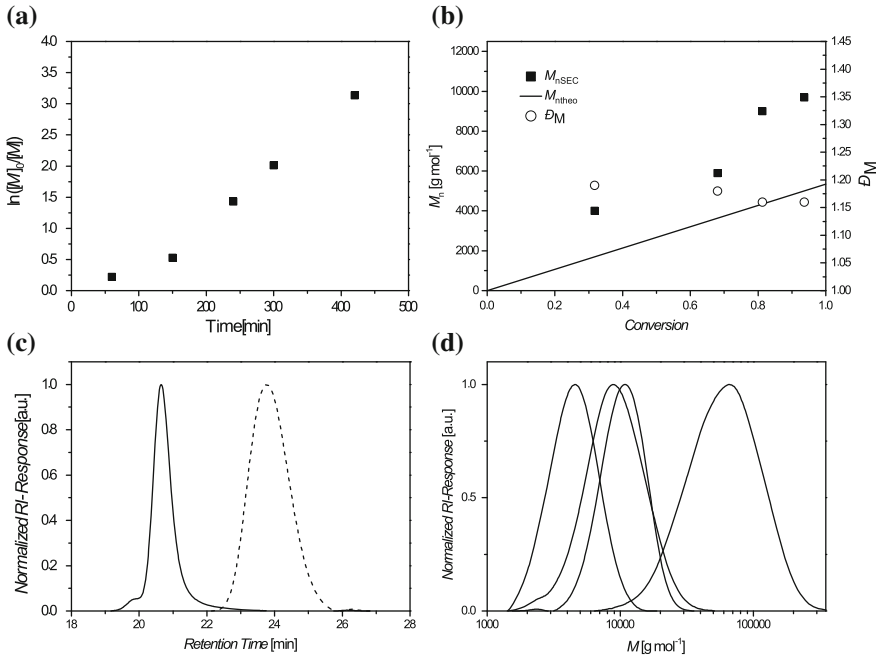

Fig. 3.11 **a** Kinetic plot for the polymerization of NIPAAm at 25 °C with **1**. **b** Evolution of M_n with conversion at 25 °C with NIPAAm/**1**/I: 44/1/0.2. **c** Chain-extension at 25 °C for 24 h. **d** Molecular weight distributions for different monomer/CTA ratios [NIPAAm/**1** from *left* to *right* (conversion >99 %): 15/1; 39/1; 44/1; 260/1]

Higher experimental molecular weights compared to the theoretical molecular weights are observed, as discussed above. The chain extension shows that the amount of dead chains is neglible as chain-extension from 9,000 to 90,000 g mol^{-1} was performed with very high efficiency leading to a $Đ_m$ of 1.11 showing only minor chain-chain coupling products.

In addition to the kinetic studies, ESI-MS was performed to evidence the structure of the obtained polymers. As depicted in the Appendix (Fig. A.8) the results fit very well to the expected values indicating the incorporation of the hydrophobic endgroups into the hydrophilic polymers. Furthermore, there is no indication of initiator derived chains that matches with the observed high reinitiation efficiency. ^{1}H-NMR was measured (refer to Appendix A.9) indicating the incorporation of the hydrophobic endgroup in the aromatic region of the spectrum.

3.2.3.5 Effect of the Monomer Structure on the RAFT Polymerization with Complexed Chain Transfer Agents

A comparison of the studied monomers evidences that with increasing guest-character the complexation of the CTAs decreases. With DMAAm no turbidity was observed for **1** and only slight turbidity for **2** and **3**. This effect is also reflected in the control over molecular weights and $Đ_m$ as the best control is achieved with **1**. In the polymerization of DEAAm, only slight turbidity was observed with CTA **1** where DEAAm/**1** ratios exceeded 300/1. With **2** and **3** turbidity was observed with DEAAm/CTA ratios from 13/1 to 813/1. In analogy to the polymerization of DMAAm the **1** mediated polymerizations of DEAAm show the best control over molecular weight and $Đ_m$. The overall trend is continuing in the polymerization with NIPAAm as it could only be conducted with **1** and only short chains up to 50,000 g mol^{-1} could be synthesized with an increasing $Đ_m$ towards longer chains. It appears that the substituents in the acrylamido monomers have a significant effect on the stability of the CTA/CD complex. DMAAm disturbs the complex only weakly whereas DEAAm leads to a significant expulsion of CTA molecules from the CD cavity. NIPAAm leads to expulsion in all cases with **2** or **3** and complexes with **1** were only stable up to a monomer/CTA ratio of 260/1. The complex stability is increasing from NIPAAm over DEAAm to DMAAm which is in contrast to the ability of the substituent in the acrylamido monomer to act as a competing guest in the CD. The more hydrophobic and bulky *iso*-propyl group in NIPAAm has a more pronounced effect on the CTA/CD complex stability than the ethyl group in DEAAm which itself has a larger effect on the CTA/CD complex than the methyl-group in DMAAm. We propose that this effect is due to a shift in the host/guest equilibrium towards disassembly of the complex induced by additional guest molecules. These can be either monomers or additional water molecules. As monomers have to be employed in higher equivalents to synthesize high molecular weight polymers in living/controlled radical polymerizations the possibility that the monomer leads to expulsion of the CTA from the Me-β-CD rises with increasing target molecular weights. An increasing amount of water may also lead to a loss of the CTA/CD complex [44]. The amount of water increases with increasing target chain length as more water is needed to retain a solution-polymerization. Therefore, the decrease in the complexation efficiency in the case of higher targeted molecular weights can be explained by the increasing employed amount of monomer and water molecules in these cases.

3.3 Conclusions

The utilization of CDs provides new opportunities for the synthetic methodology of living/controlled radical polymerization. Based on the concept of supramolecular chemistry, host/guest complexes seem to be attractive as controlling agents in living radical polymerizations. The first aqueous RAFT polymerization of acry-

lamido monomers, e.g. DMAAm, DEAAm and NIPAAm, with a supramolecular complex of CD and hydrophobic CTAs, could be performed. The solubility of three novel guest-functionalized CTAs in water was enhanced drastically via a CD/CTA inclusion complex. These complexes were thereafter utilized in living/controlled radical polymerizations at 25 °C in water leading to hydrophilic polymers with hydrophobic endgroups in one step. The polymerization leads to polymers with high molar masses and low $Đ_m$ ($7{,}500 \leq M_n \leq 116{,}000$ g mol^{-1}; $1.06 \leq Đ_m \leq 1.54$ for PDMAAm, $2{,}500 \leq M_n \leq 150{,}000$ g mol^{-1}; $1.05 \leq Đ_m \leq 1.39$ for PDEAAm and $4{,}000 \leq M_n \leq 50{,}000$ g mol^{-1}; $1.15 \leq Đ_m \leq 1.46$ for PNIPAAm). Furthermore, the first living radical polymerization of DEAAm in water was described. The living character of the polymerizations was confirmed by a linear increase of the molecular weight with conversion and chain extensions showed very high reinitiation efficiencies. ESI mass spectra as well as ^{1}H-NMR-spectra were in good agreement with the expectations evidencing the incorporation of hydrophobic endgroups in the hydrophilic acrylamido polymers. Thus, the first living/controlled polymerization of hydrophilic acrylamido monomers with hydrophobic CTA leading directly to hydrophobic endfunctionalized polymers in aqueous solution is provided.

3.4 Experimental Part

3.4.1 Synthesis of 4-(tert-butyl)phenyl 2-(((ethylthio)carbonothioyl) thio)-2-methylpropanoate (1)

In a 50 mL Schlenk-flask **EMP** (1.02 g, 4.55 mmol, 1.0 eq.), 4-*tert*-butyl phenol (1.71 g, 11.38 mmol, 2.5 eq.) and DMAP (0.22 g, 1.80 mmol, 0.4 eq.) were dissolved in anhydrous DCM (20 mL). At 0 °C a solution of DCC (1.90 g, 9.21 mmol, 2.0 eq.) in anhydrous DCM (12 mL) was added. After 1 h the solution was warmed to ambient temperature, stirred overnight, filtered and concentrated under reduced pressure. The residual yellow oil was purified via column chromatography on silica-gel with *n*-hexane:ethyl acetate 20:1 as eluent. The product was obtained as yellow oil which solidified upon cooling (1.54 g, 4.32 mmol, 95 %).

^{1}H-NMR (400 MHz, $CDCl_3$): [δ, ppm] = 1.30 (s, 9H, (C***H***$_3$)$_3$), 1.34 (t, 3H, ^3J = 7.4 Hz, CH$_2$–C***H***$_3$), 1.83 (s, 6H, C–(C***H***$_3$)$_2$), 3.32 (q, 2H, ^3J = 7.4 Hz, C***H***$_2$), 7.00 (d, 2H, ^3J = 8.8 Hz, C***H***–C–O), 7.37 (d, 2H, ^3J = 8.8 Hz, C***H***–C–C(CH$_3$)$_3$). **^{13}C-NMR** (100 MHz, $CDCl_3$): [δ, ppm] = 12.9 (***C***H$_3$), 25.4 ((***C***H$_3$)$_2$), 31.3 ((***C***H$_3$)$_3$), 31.4 (***C***H$_2$), 34.5 (***C***–(CH$_3$)$_3$), 55.8 (***C***–(CH$_3$)$_2$), 120.7 (***C***H–C–O), 126.2 (***C***H–C–C–(CH$_3$)$_3$), 148.7 (CH–***C***–O; ***C***–C(CH$_3$)$_3$), 171.8 (***C***=O), 221.1 (***C***=S). **ESI-MS**: $[M + Na^+]_{exp}$ = 379.11 m/z and $[M + Na^+]_{calc}$ = 379.04 m/z.

3.4.2 Synthesis of bis(4-(tert-butyl)benzyl) carbonotrithioate (2)

In a 50 mL round-bottom-flask, 4-*tert*-butylbenzyl mercaptan (1.0 mL, 5.36 mmol, 1.0 eq.) was dissolved in a suspension of $K_3PO_4 \cdot H_2O$ (1.39 g, 6.02 mmol, 1.1 eq.) in acetone (20 mL) at ambient temperature. After stirring for 10 min at ambient temperature carbon disulfide (1.0 mL, 16.56 mmol, 3.1 eq.) was added and the solution turned yellow. 4-*Tert*-butyl benzylbromide (1.0 mL, 5.44 mmol, 1.0 eq.) was added after 10 min and the mixture stirred at ambient temperature overnight. The mixture was filtered and the filtrate concentrated under reduced pressure. The yellow oily residue was purified via column chromatography on silica-gel with *n*-hexane as eluent. A yellow oil was obtained which solidified upon cooling (1.82 g, 4.52 mmol, 84 %).

^{1}H-NMR (400 MHz, $CDCl_3$): [δ, ppm] = 1.30 (s, 18H, C–(C***H***$_3$)$_3$), 4.59 (s, 4H, C***H***$_2$–S), 7.25–7.29 (m, 4H, C***H***), 7.31–7.36 (m, 4H, C***H***). **^{13}C-NMR** (100 MHz, $CDCl_3$): [δ, ppm] = 31.3 (***C***H$_3$), 34.6 (***C***–(CH$_3$)$_3$), 41.3 (***C***H$_2$), 125.7 (***C***H), 128.97(***C***H), 131.8 (***C***–C–(CH$_3$)$_3$), 150.8 (***C***–CH$_2$), 223.2 (***C***=S). **ESI-MS**: $[M + Na^+]_{exp}$ = 424.99 m/z and $[M + Na^+]_{calc}$ = 425.14 m/z.

3.4.3 Synthesis of 3-bromo-N-(4-(tert-butyl)phenyl) propanamide (4)

In a 100 mL Schlenk-flask 4-*tert*-butyl aniline (1.5 mL, 9.42 mmol, 1.0 eq.) and triethylamine (1.9 mL, 13.60 mmol, 1.4 eq.) were dissolved in anhydrous THF (30 mL). At 0 °C 3-bromopropionyl chloride (1.3 mL, 13.14 mmol, 1.4 eq.) in anhydrous THF (15 mL) was added dropwise and stirred at ambient temperature overnight. Sat. $NaHCO_3$-solution (180 mL) was added and extracted with DCM (2 × 180 mL). The combined organic extracts were washed with deionized H_2O (180 mL) and brine (180 mL), dried over Na_2SO_4, filtered and concentrated under reduced pressure. The solid residue was recrystallized twice from *n*-hexane:ethyl acetate 5:1 to give the product as pale yellow crystals (1.37 g, 4.83 mmol, 51 %).

^{1}H-NMR (400 MHz, $CDCl_3$): [δ, ppm] = 1.30 (s, 9H, (C***H***$_3$)$_3$), 2.92 (t, 2H, ^3J = 6.6 Hz, C***H***$_2$–C=O), 3.71 (t, 2H, ^3J = 6.6 Hz, C***H***$_2$Br), 7.34, (d, 2H, ^3J = 8.5 Hz, C***H***–C–(CH$_3$)$_3$), 7.38 (N***H***), 7.44 (d, 2H, ^3J = 8.5 Hz, C***H***–CNH). **^{13}C-NMR** (100 MHz, $CDCl_3$): [δ, ppm] = 27.2 (***C***H$_2$–Br), 31.3 (C–(***C***H$_3$)$_3$), 34.4 (***C***–(CH$_3$)$_3$), 40.7 (***C***H$_2$–C=O), 119.9 (***C***H–C–NH), 125.9 (***C***H–C–C–(CH$_3$)$_3$), 134.8 (***C***–NH), 147.8 (***C***–C–(CH$_3$)$_3$), 167.9 (***C***=O). **ESI-MS**: $[M + Na^+]_{exp}$ = 306.12 m/z and $[M + Na^+]_{calc}$ = 307.18 m/z.

3.4.4 Synthesis of benzyl (3-((4-(tert-butyl)phenyl) amino)-3-oxopropyl) carbonotrithioate (3)

In a 50 mL round-bottom-flask benzylmercaptan (498 µl, 4.23 mmol, 1.0 eq.) was dissolved in a suspension of $K_3PO_4 \cdot H_2O$ (1.08 g, 4.69 mmol, 1.1 eq.) in 25 mL acetone at ambient temperature. After stirring for 10 min at ambient temperature carbon disulfide (766 µl, 12.69 mmol, 3.0 eq.) was added and the solution turned yellow. 3-Bromo-*N*-(4-(*tert*-butyl)phenyl)propanamide (**4**) (1.20 g, 4.23 mmol, 1.0 eq.) was added after 10 min and the mixture stirred at ambient temperature overnight. 1M HCl (160 mL) were added and extracted twice with DCM (2 × 160 mL). The combined organic extracts were washed with deionized H_2O (160 mL), brine (160 mL), dried over Na_2SO_4, filtered and concentrated under reduced pressure. The solid residue was recrystallized from *n*-hexane:ethyl acetate 1:1 to give the product as a yellow solid in two fractions (1.21 g, 3.00 mmol, 71 %).

^{1}H-NMR (400 MHz, $CDCl_3$): [δ, ppm] = 1.30 (s, 9H, (CH_3)$_3$), 1.60 (s, 1H, N***H***), 2.79 (t, 2H, ^3J = 7.0 Hz, C=O–C***H***$_2$), 3.73 (t, 2H, ^3J = 7.0 Hz, S–C***H***$_2$–CH$_2$), 4.61 (s, 2H, C***H***$_2$), 7.25–7.45 (m, 9H, ***H***$_{arom}$). **^{13}C-NMR** (100 MHz, $CDCl_3$): [δ, ppm] = 31.3 (C–(***C***H$_3$)$_3$), 32.0 (***C***H$_2$–C=O), 34.4 (***C***–(CH$_3$)$_3$), 36.1 (CH$_2$-***C***H$_2$-S), 41.5 (***C***H$_2$), 119.8 (***C***H–C–NH), 125.9 (***C***H–C–C(CH$_3$)$_3$), 127.8 (***C***H), 128.7 (CH–***C***H–C–CH$_2$), 129.3 (***C***H–C–CH$_2$), 134.8, 134.9 (***C***–NH, ***C***–CH$_2$), 147.6 (***C***–C–(CH$_3$)$_3$), 168.5 (***C***=O), 223.7 (***C***=S). **ESI-MS**: [M + Na$^+$]$_{exp}$ = 426.27 m/z and [M + Na$^+$]$_{calc}$ = 426.100 m/z.

3.4.5 Exemplary Procedure for the Polymerization of DMAAm

1 (4.9 mg, 0.014 mmol, 1.0 eq.) and Me-β-CD-solution (40 wt% in deionized H_2O, 228 mg, 0.070 mmol, 5.0 eq.) were added to a Schlenk-tube. The two-phase mixture was ultrasonicated until a clear yellow solution was obtained. Subsequently, a stirring-bar, DMAAm (274 mg, 2.77 mmol, 198.9 eq.), VA-044 (1.0 mg, 0.003 mmol, 0.2 eq.) and deionized H_2O (0.8 mL) were added. After three freeze-pump-thaw cycles the tube was sealed and placed into an oil bath at 25 °C and removed after 6 h. The tube was subsequently cooled with liquid nitrogen to stop the reaction. A NMR-sample was withdrawn for the determination of conversion, inhibited with a pinch of hydroquinone (approx. 5 mg) and D_2O was added. A conversion of 88 % was calculated based on the NMR data (see Sect. 9.3 for details of the calculation). The residue was dialysed with a SpectraPor3 membrane (MWCO = 3,500 Da) for 3 days at ambient temperature and for 2 days at 45 °C. The solvent was removed in vacuo to yield the polymer as a yellow solid (96 mg, 39 %, SEC(DMAc): M_{nSEC} = 17,000 g mol^{-1}, $Đ_m$ = 1.09).

In the case of short-chain polymers (with targeted M_n below 3,500 g mol^{-1}) the reaction mixture was dialysed with a SpectraPor3 membrane (MWCO =1,000 Da)

for three days at ambient temperature. The polymer sample was subsequently diluted with acetic acid/acetate buffer, the α-amylase containing enzyme-mixture Taka-Diastase was added to degrade the residual CDs, the mixture was incubated at 37 °C for 24 h and boiled for 10 min [38, 40]. Finally, the mixture was dialysed against water for 3 days at ambient temperature and the solvent removed in vacuo. For the other polymerizations the Me-β-CD/CTA/initiator ratio was kept constant at 5/1/0.2. The DMAAm/CTA ratio was altered and water was added to keep the concentration constant at 3.0 mol L^{-1}. The experiments with **2** and **3** were conducted in an analogous fashion.

3.4.6 Exemplary Procedure for the Chain Extension of PDMAAm

PDMAAm (M_{nSEC} = 10,500 g mol^{-1}, $Đ_m$ = 1.17, 20.0 mg, 0.002 mmol, 1.0 eq.) as macro-CTA, DMAAm (183 mg, 1.85 mmol, 925.0 eq.), VA-044 (0.3 mg, 0.001 mmol, 0.5 eq.) and deionized H_2O (0.6 mL) were added to a Schlenk-tube. After three freeze-pump-thaw cycles the tube was placed into an oil bath at 25 °C and kept there for 24 h. The reaction-mixture was cooled with liquid nitrogen, subjected to air and dialysed for 3 days at ambient temperature. The solvent was removed in vacuo to give the polymer as a yellow solid (197 mg, 97 %, **SEC(DMAc)**: M_{nSEC} = 97,500 g mol^{-1}, $Đ_m$ = 1.08).

3.4.7 Exemplary Procedure for Kinetic Measurements of DMAAm

1 (12.2 mg, 0.034 mmol, 1.0 eq.) and Me-β-CD-solution (40 wt% in deionized H_2O, 551 mg, 0.168 mmol, 4.9 eq.) were added to a Schlenk-tube. The two-phase mixture was ultrasonicated until a clear yellow solution was obtained. Subsequently, DMAAm (1.00 g, 10.10 mmol, 297.1 eq.), VA-044 (2.2 mg, 0.007 mmol, 0.2 eq.) and deionized H_2O (2.7 mL) were added. The solution was separated into several tubes with a stirring-bar and three freeze-pump-thaw cycles were applied. Subsequently, the tubes were sealed and placed into an oil bath at 25 °C. After specific time intervals the tubes were cooled with liquid nitrogen. Samples for NMR analysis were withdrawn, a pinch of hydroquinone (approx. 5 mg) was added to inhibit further polymerization and D_2O was added. The conversion was calculated via comparison of the vinyl-proton integrals with the appropriate integrals of the backbone or side chains of the polymers (see Sect. 9.3 for details). The residual sample in each tube was purified by dialysis for 3 days at ambient temperature and 1 day at 45 °C. The solvent was removed in vacuo and the polymer subjected to SEC-analysis.

3.4.8 Exemplary Procedure for the Polymerization of DEAAm

1 (5.0 mg, 0.014 mmol, 1.0 eq.) and Me-β-CD-solution (40 wt% in deionized H_2O, 228 mg, 0.070 mmol, 5.0 eq.) were added to a Schlenk-tube. The two-phase mixture was ultrasonicated until a clear yellow solution was obtained. Subsequently, a stirring bar, DEAAm (142 mg, 1.12 mmol, 80.0 eq.), VA-044 (0.9 mg, 0.003 mmol, 0.2 eq.) and deionized H_2O (0.2 mL) were added. After three freeze-pump-thaw cycles the tube was sealed and placed into an oil bath at 25 °C and removed after 12 h. The tube was subsequently cooled with liquid nitrogen to stop the reaction. A NMR-sample was withdrawn for the determination of conversion, inhibited with a pinch of hydroquinone (approx. 5 mg) and acetone-D_6 was added. A conversion of >99 % was calculated based on the NMR data (see Sect. 9.3 for details). The residue was dialysed with a SpectraPor3 membrane (MWCO = 3,500 Da) for 3 days at ambient temperature and for 1 day at 45 °C. The solvent was removed in vacuo to yield the polymer as a yellow solid (110 mg, 75 %, **SEC(DMAc)**: M_{nSEC} = 10,000 g mol^{-1}, $Đ_m$ = 1.09).

In the case of short-chain polymers (with targeted M_n below 3,500 g mol^{-1}) the reaction mixture was dialysed with a SpectraPor3 membrane (MWCO = 1,000 Da) for three days at ambient temperature. The polymer sample was subsequently diluted with acetic acid/acetate buffer, the α-amylase containing enzyme-mixture Taka-Diastase was added to degrade the residual CDs, the mixture incubated at 37 °C for 24 h and boiled for 10 min. Finally, the mixture was dialysed against water for 3 days at ambient temperature and the solvent removed in vacuo. For the other polymerizations the Me-β-CD/CTA/initiator ratio was kept constant at 5/1/0.2. The DEAAm/CTA ratio was altered and water was added to keep the concentration constant at 3.5 mol L^{-1}. The experiments with **2** and **3** were conducted in an analogous fashion.

3.4.8.1 Exemplary Procedure for the Chain Extension of PDEAAm

PDEAAm (M_{nSEC} = 8,500 g mol^{-1}, $Đ_m$ = 1.11, 20.0 mg, 0.002 mmol, 1.0 eq.) as macro-CTA, DEAAm (204 mg, 1.60 mmol, 925.0 eq.), VA-044 (0.4 mg, 0.001 mmol, 0.5 eq.), deionized H_2O (0.3 mL) and acetone (0.3 mL) were added to a Schlenk-tube. After three freeze-pump-thaw cycles the tube was placed into an oil bath at 25 °C and kept there for 24 h. The reaction-mixture was cooled with liquid nitrogen, subjected to air and dialysed for 3 days at ambient temperature. The solvent was removed in vacuo to give the polymer as a yellow solid (182 mg, 81 %, **SEC(DMAc)**: M_{nSEC} = 83,000 g mol^{-1}, $Đ_m$ = 1.13).

3.4.9 Exemplary Procedure for Kinetic Measurements of the Polymerization of DEAAm

1 (17.4 mg, 0.049 mmol, 1.0 eq.) and Me-β-CD-solution (40 wt% in deionized H_2O, 820 mg, 0.250 mmol, 5.1 eq.) were added to a Schlenk-tube. The two-phase mixture was ultrasonicated until a clear yellow solution was obtained. Afterwards DEAAm (1.50 g 11.78 mmol, 240.5 eq.), VA-044 (3.2 mg, 0.010 mmol, 0.2 eq.) and deionized H_2O (3.3 mL) were added. The solution was separated into several tubes containing a stirring-bar and three freeze-pump-thaw cycles were applied. Subsequently the tubes were sealed and placed into an oil bath at 25 °C. After specific time intervals the tubes were cooled with liquid nitrogen. Samples for NMR analysis were withdrawn, a pinch of hydroquinone (approx. 5 mg) was added to inhibit further polymerization and acetone-D_6 was added. The conversion was calculated via comparison of the vinyl-proton integrals with the appropriate integrals of the backbone or side chains of the polymers (see Sect. 9.3 for details). The residual sample in each tube was purified by dialysis for 3 days at ambient temperature and 1 day at 45 °C. The solvent was removed in vacuo and the polymer subjected to SEC-analysis.

3.4.10 Exemplary Procedure for the Polymerization of NIPAAm

1 (7.0 mg, 0.020 mmol, 1.0 eq.) and Me-β-CD-solution (40 wt% in deionized H_2O, 326 mg, 0.100 mmol, 5.0 eq.) were added to a Schlenk-tube. The two-phase mixture was ultrasonicated until a clear yellow solution was obtained. Afterwards stirring-bar, NIPAAm (100 mg, 0.88 mmol, 44.0 eq.), VA-044 (1.3 mg, 0.004 mmol, 0.2 eq.) and deionized H_2O (0.2 mL) were added. After three freeze-pump-thaw cycles the tube was sealed and placed into an oil bath at 25 °C and removed after 18 h. The tube was subsequently cooled with liquid nitrogen to stop the reaction. A NMR-sample was withdrawn for the determination of conversion, inhibited with a pinch of hydroquinone (approx. 5 mg) and acetone-D_6 was added. A conversion of >99 % was calculated based on the NMR data (see Sect. 9.3 for details). The residue was dialysed with a SpectraPor3 membrane (MWCO = 3,500 Da) for 3 days at ambient temperature and for 1 day at 45 °C. The solvent was removed in vacuo to yield the polymer as a yellow solid (64 mg, 60 %, **SEC(DMAc)**: M_{nSEC} = 9,000 g mol^{-1}, $Đ_m$ = 1.15).

In the case of short-chain polymers (with targeted M_n below 3,500 g mol^{-1}) the reaction mixture was dialysed with a SpectraPor3 membrane (MWCO = 1,000 Da) for 3 days at ambient temperature. The polymer sample was subsequently diluted with acetic acid/acetate buffer, the α-amylase containing enzyme-mixture Taka-Diastase was added to degrade the residual CDs, the mixture incubated at 37 °C for 24 h and boiled for 10 min. Finally, the mixture was dialysed against water for 3 days at ambient

temperature and the solvent removed in vacuo. For the other polymerizations the Me-β-CD/CTA/initiator ratio was kept constant at 5/1/0.2. The NIPAAm/CTA ratio was altered and water was added to keep the concentration constant at 2.5 mol L^{-1}.

3.4.11 Exemplary Procedure for the Chain Extension of PNIPAAm

PNIPAAm (M_{nSEC} = 9,000 g mol^{-1}, $Đ_m$ = 1.15, 20.0 mg, 0.002 mmol, 1.0 eq.) as macro-CTA, NIPAAm (172 mg, 1.52 mmol, 760.0 eq.), VA-044 (0.4 mg, 0.001 mmol, 0.5 eq.), deionized H_2O (0.8 mL) and 1,4-dioxane (0.6 mL) were added to a Schlenk-tube. After three freeze-pump-thaw cycles the tube was placed into an oil bath at 25 °C and kept there for 24 h. The reaction-mixture was cooled with liquid nitrogen, subjected to air and dialysed for 3 days at ambient temperature. The solvent was removed in vacuo to give the polymer as a yellow solid (180 mg, 94 %, **SEC(DMAc)**: M_{nSEC} = 90,000 g mol^{-1}, $Đ_m$ = 1.11).

3.4.12 Exemplary Procedure for Kinetic Measurements of the Polymerization of NIPAAm

1 (35.8 mg, 0.101 mmol, 1.0 eq.) and Me-β-CD-solution (40 wt% in deionized H_2O, 1.65 g, 0.504 mmol, 5.0 eq.) were added to a Schlenk-tube. The two-phase mixture was ultrasonicated until a clear yellow solution was obtained. Afterwards NIPAAm (500 mg, 4.42 mmol, 43.8 eq.), VA-044 (6.5 mg, 0.020 mmol, 0.2 eq.) and deionized H_2O (0.8 mL) were added. The solution was separated into several tubes containing a stirring-bar and three freeze-pump-thaw cycles were applied. Subsequently, the tubes were sealed and placed into an oil bath at 25 °C. After specific time intervals the tubes were cooled with liquid nitrogen. Samples for NMR analysis were withdrawn, a pinch of hydroquinone (approx. 5 mg) was added to inhibit further polymerization and acetone-D_6 was added. The conversion was calculated via comparison of the vinyl-proton integrals with the appropriate integrals of the backbone or side chains of the polymers (see Sect. 9.3 for details). The residual sample in each tube was purified by dialysis for 3 days at ambient temperature and 1 day at 45 °C. The solvent was removed in vacuo and the polymer subjected to SEC-analysis.

References

1. Schmidt BVKJ, Hetzer M, Ritter H, Barner-Kowollik C (2011) Cyclodextrin-complexed RAFT agents for the ambient temperature aqueous living/controlled radical polymerization of acrylamido monomers. Macromolecules 44(18): 7220–7232. doi:10.1021/ma2011969

2. Millard P-E, Barner L, Stenzel MH, Davis TP, Barner-Kowollik C, Müller AHE (2006) RAFT polymerization of N-Isopropylacrylamide and acrylic acid under -irradiation in aqueous media. Macromol Rapid Commun 27:821–828
3. Millard P-E, Barner L, Reinhardt J, Buchmeiser MR, Barner-Kowollik C, Müller AHE (2010) Synthesis of water-soluble homo- and block-copolymers by RAFT polymerization under [gamma]-irradiation in aqueous media. Polymer 51:4319–4328
4. Lowe AB, McCormick CL (2007) Reversible addition-fragmentation chain transfer (RAFT) radical polymerization and the synthesis of water-soluble (co)polymers under homogeneous conditions in organic and aqueous media. Prog Polym Sci 32:283–351
5. Smith AE, Xu X, Kirkland-York SE, Savin DA, McCormick CL (2010) "Schizophrenic" self-assembly of block copolymers synthesized via aqueous RAFT polymerization: from micelles to vesicles. Macromolecules 43:1210–1217
6. Xiong Q, Ni P, Zhang F, Yu Z (2004) Synthesis and characterization of 2-(dimethylamino)ethyl methacrylate homopolymers via aqueous RAFT polymerization and their application in miniemulsion polymerization. Polym Bull 53:1–8
7. Scales CW, Vasilieva YA, Convertine AJ, Lowe AB, McCormick CL (2005) Direct, controlled synthesis of the nonimmunogenic, hydrophilic polymer, poly(N-(2-hydroxypropyl)methacrylamide) via RAFT in aqueous media. Biomacromolecules 6:1846–1850
8. Mitsukami Y, Donovan MS, Lowe AB, McCormick CL (2001) Water-soluble polymers. 81. Direct synthesis of hydrophilic styrenic-based homopolymers and block copolymers in aqueous solution via RAFT. Macromolecules 34:2248–2256
9. Garnier S, Laschewsky A (2005) Synthesis of new amphiphilic diblock copolymers and their self-assembly in aqueous solution. Macromolecules 38:7580–7592
10. Thomas DB, Convertine AJ, Myrick LJ, Scales CW, Smith AE, Lowe AB, Vasilieva YA, Ayres N, McCormick CL (2004) Kinetics and molecular weight control of the polymerization of acrylamide via RAFT. Macromolecules 37:8941–8950
11. Convertine AJ, Lokitz BS, Lowe AB, Scales CW, Myrick LJ, McCormick CL (2005) Aqueous RAFT polymerization of acrylamide and N,N-dimethylacrylamide at room temperature. Macromol Rapid Commun 26:791–795
12. Glatzel S, Badi N, Pach M, Laschewsky A, Lutz J-F (2010) Well-defined synthetic polymers with a protein-like gelation behavior in water. Chem Commun 46:4517–4519
13. Schwarz-Barac S, Ritter H (2003) Cyclodextrins in polymer synthesis: free radical polymerization of a tert-butylmethacrylate-cyclodextrin host-guest system in aqueous medium. J Macromol Sci. Part A: Pure Appl Chem A40:437–448
14. Ritter H, Mondrzik BE, Rehahn M, Gallei M (2010) Free radical homopolymerization of a vinylferrocene/cyclodextrin complex in water. Beilstein J Org Chem 60:6
15. Storsberg J, Hartenstein M, Müller AHE, Ritter H (2000) Cyclodextrins in polymer synthesis: polymerization of methyl methacrylate under atom-transfer conditions (ATRP) in aqueous solution. Macromol Rapid Commun 21: 1342–1346
16. Köllisch HS, Barner-Kowollik C, Ritter H (2006) Living free radical polymerization of cyclodextrin host-guest complexes of styrene via the reversible addition fragmentation chain transfer (RAFT) process in aqueous solution. Macromol Rapid Commun 27:848–853
17. Köllisch HS, Barner-Kowollik C, Ritter H (2009) Amphiphilic block copolymers based on cyclodextrin host-guest complexes via RAFT-polymerization in aqueous solution. Chem Commun, pp 1097–1099.
18. Pang Y, Ritter H, Tabatabai M (2003) Cyclodextrins in polymer chemistry: enzymatically catalyzed oxidative polymerization of para-functionalized phenol derivatives in aqueous medium by use of horseradish peroxidase. Macromolecules 36:7090–7093
19. Ding L, Li Y, Deng J, Yang W (2011) Preparation of hydrophobic helical poly(N-propargylamide)s in aqueous medium via a monomer/cyclodextrin inclusion complex. Polym Chem 2:694–701

20. Höfler T, Wenz G (1996) Determination of binding energies between cyclodextrins and aromatic guest molecules by microcalorimetry. J Inclusion Phenom Macrocyclic Chem 25:81–84
21. Weickenmeier M, Wenz G, Huff J (1997) Association thickener by host guest interaction of a beta-cyclodextrin polymer and a polymer with hydrophobic side-groups. Macromol Rapid Commun 18:1117–1123
22. Zeng J, Shi K, Zhang Y, Sun X, Zhang B (2008) Construction and micellization of a noncovalent double hydrophilic block copolymer. Chem Commun, pp 3753–3755.
23. Stadermann J, Komber H, Erber M, Däbritz F, Ritter H, Voit B (2011) Diblock copolymer formation via self-assembly of cyclodextrin and adamantyl end-functionalized polymers. Macromolecules 44:3250–3259
24. Zhao Q, Wang S, Cheng X, Yam RCM, Kong D, Li RKY (2010) Surface modification of cellulose fiber via supramolecular assembly of biodegradable polyesters by the aid of host/guest inclusion complexation. Biomacromolecules 11:1364–1369
25. Kujawa P, Segui F, Shaban S, Diab C, Okada Y, Tanaka F, Winnik FM (2005) Impact of end-group association and main-chain hydration on the thermosensitive properties of hydrophobically modified telechelic poly(N-isopropylacrylamides) in water. Macromolecules 39:341–348
26. Vogt AP, Sumerlin BS (2008) Tuning the temperature response of branched poly(N-isopropylacrylamide) prepared by RAFT polymerization. Macromolecules 41:7368–7373
27. Li H, Yu B, Matsushima H, Hoyle CE, Lowe AB (2009) The thiol/isocyanate click reaction: facile and quantitative access to omega-end-functional poly(N,N-diethylacrylamide) synthesized by RAFT radical polymerization. Macromolecules 42:6537–6542
28. Mertoglu M, Laschewsky A, Skrabania K, Wieland C (2005) New water soluble agents for reversible addition/fragmentation chain transfer polymerization and their application in aqueous solutions. Macromolecules 38:3601–3614
29. Smith AE, Xu X, McCormick CL (2010) Stimuli-responsive amphiphilic (co)polymers via RAFT polymerization. Prog Polym Sci 35:45–93
30. Convertine AJ, Lokitz BS, Vasileva Y, Myrick LJ, Scales CW, Lowe AB, McCormick CL (2006) Direct synthesis of thermally responsive DMA/NIPAM diblock and DMA/NIPAM/DMA triblock copolymers via aqueous, room temperature RAFT polymerizatio. Macromolecules 39:1724–1730
31. Skey J, O'Reilly RK (2008) Facile one pot synthesis of a range of reversible addition-fragmentation chain transfer (RAFT) agents. Chem Commun, pp 4183–4185.
32. Loftsson T, Jarho P, Màsson M, Järvinen T (2005) Cyclodextrins in drug delivery. Expert Opin Drug Deliv 2:335–351
33. Glockner P, Schollmeyer D, Ritter H (2002) X-ray diffraction analysis of butyl- and isobornyl acrylate/heptakis(2,6-di-O-methyl)-beta-cyclodextrin complexes and correlation to H-1 NMR-spectra. Des Monomers Polym 5:163–172
34. Funasaki N, Yodo H, Hada S, Neya S (1992) Stoichiometries and equilibrium constants of cyclodextrin-surfactant complexations. Bull Chem Soc Jpn 65:1323–1330
35. Rekharsky MV, Inoue Y (1998) Complexation thermodynamics of cyclodextrins. Chem Rev 98:1875–1918
36. Baussard J-F, Habib-Jiwan J-L, Laschewsky A, Mertoglu M, Storsberg J (2004) New chain transfer agents for reversible addition-fragmentation chain transfer (RAFT) polymerisation in aqueous solution. Polymer 45:3615–3626
37. Thomas DB, Convertine AJ, Hester RD, Lowe AB, McCormick CL (2004) Hydrolytic susceptibility of dithioester chain transfer agents and implications in aqueous raft polymerizations. Macromolecules 37:1735–1741
38. Suetsugu N, Koyama S, Takeo K, Kuge T (1974) Kinetic studies on the hydrolyses of alpha, beta, and gamma-cyclodextrins by Taka-amylase A. J Biochem 76:57–63
39. Jodái I, Kandra L, Harangi J, Nánási P, Szejtli J (1984) Hydrolysis of cyclodextrin by aspergillus oryzae alpha-amylase. Starch-Stärke 36:140–143
40. Fetzner A, Böhm S, Schreder S, Schubert R (2004) Degradation of raw or film-incorporated [beta]-cyclodextrin by enzymes and colonic bacteria. Eur J Pharm Biopharm 58:91–97

41. Gan LH, Cai W, Tam KC (2001) Studies of phase transition of aqueous solution of poly(N,N-diethylacrylamide-co-acrylic acid) by differential scanning calorimetry and spectrophotometry. Eur Polym J 37:1773–1778
42. Delaittre G, Rieger J, Charleux B (2011) Nitroxide-mediated living/controlled radical polymerization of N,N-diethylacrylamide. Macromolecules 44:462–470
43. Heskins M, Guillet JE (1968) Solution properties of poly(*N*-isopropylacrylamide). J Macromol Sci. Part A: Pure Appl Chem 2:1441–1455
44. Del Valle EMM (2004) Cyclodextrins and their uses: a review. Process Biochem 39:1033–1046

Chapter 4
Supramolecular ABA Triblock Copolymers

4.1 Introduction

Complex macromolecular architectures constitute an important field in contemporary polymer chemistry. Block copolymers belong to the most studied materials in this field and are subjected to manifold applications [2, 3]. Apart from classical anionic [4] and cationic [5] polymerization, reversible-deactivation radical polymerizations, e.g. NMP [6], ATRP [7, 8], and RAFT polymerization [9, 10] have proven to be a very versatile tool for the generation of new block copolymers with a large variety of different blocks via convenient synthetic procedures. Furthermore, modular ligation chemistry had a strong impact on the field of block copolymer synthesis [11–13], e.g. via the CuAAc [14], the Diels-Alder [15] or the RAFT hetero Diels-Alder reaction [16], which provide numerous opportunities to generate block copolymers as well as more complex architectures [15, 17].

A common application of CDs in polymer chemistry is the utilization as a linker molecule for the formation of supramolecular block copolymers. Hereby, reversible-deactivation radical polymerization techniques and modular conjugation have proven to be a very powerful tool set for the incorporation of CD-endgroups into polymers. The most frequently applied ligation reaction is CuAAc based on the convenient synthesis of mono azido functionalized β-CD (β-CD–N_3). So far, mostly AB diblock copolymers with different properties have been described, e.g. with a light responsive linkage [18], with a redox responsive linkage [19], with a thermoresponsive block [20] and even with schizophrenic behavior of the blocks [21, 22]. A further example is a CD-centered star polymer, where two cores are coupled using supramolecular interactions [23, 24]. The variety of possible building blocks and guest-moieties gives the opportunity for several applications. For example, light-controlled supramolecular nanotubes have been described [18] as well as vesicular nanocontainers with voltage-

NOESY measurements were performed in collaboration with M. Hetzer and Prof. H. Ritter (Heinrich Heine Universität Düsseldorf). Parts of this chapter were reproduced with permission from Schmidt et al. [1]. Copyright 2013 American Chemical Society.

B. V. K. J. Schmidt, *Novel Macromolecular Architectures via a Combination of Cyclodextrin Host/Guest Complexation and RAFT Polymerization*, Springer Theses,
DOI: 10.1007/978-3-319-06077-4_4, © Springer International Publishing Switzerland 2014

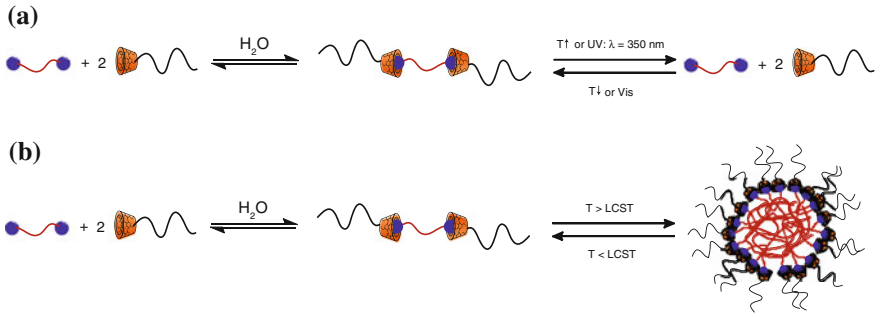

Scheme 4.1 Schematic representation of the formation of supramolecular ABA triblock copolymers via CD host/guest complexation (β-CD is depicted *orange*; the guest groups are depicted *blue*; the outer PHPMA block is depicted *black*; the inner PDMAAm- and PDEAAm-blocks are depicted *red*): **a** PDMAAm based supramolecular block copolymers with temperature- and light-responsive complexation via azobenzene guest groups and **b** PDEAAm based supramolecular block copolymers with T_c triggered aggregate formation

triggered release [19] or supramolecular linkages for the generation of dynamic core-shell nanoparticles [25]. A further example is a core-shell nano-assembly that shows tumor-trigged release [26]. One can imagine many applications that can be derived from conventional covalently bound block copolymers, e.g. self-assembly of supramolecular block copolymers coupled via hydrogen bonding motifs in thin-films that mimick the behavior of their covalent analogues [27].

In the current approach, two PHPMA outer blocks are connected with a PDMAAm or PDEAAm inner block via a CD host/guest complex to generate a novel supramolecular macromolecular architecture (see Scheme 4.1). PHPMA was chosen due to its potential application in drug delivery [28]. PDMAAm was selected to study the thermoresponsive behavior of the host/guest complexation (refer to Scheme 4.1a), whereas PDEAAm was chosen due to its T_c of close to 30 °C [29] and therefore close to physiological temperatures. The T_c of PDEAAm can be utilized to form aggregates in aqueous solution upon heating that are connected via supramolecular interactions (see Scheme 4.1b).

In this chapter the formation of a novel supramolecular ABA triblock copolymer consisting of a PDMAAm or PDEAAm inner block and a biocompatible PHPMA outer block is reported. The inner building block was synthesized via RAFT polymerization employing novel doubly guest-functionalized CTAs featuring adamantyl or photoresponsive azobenzene guest groups. The outer building block was synthesized via RAFT polymerization with an alkyne containing CTA and subsequent CuAAc with β-CD–N_3. The building blocks were characterized via ^{1}H-NMR, ESI-MS and SEC. The complex formation was investigated with DLS, turbidimetry measurements and NOESY.

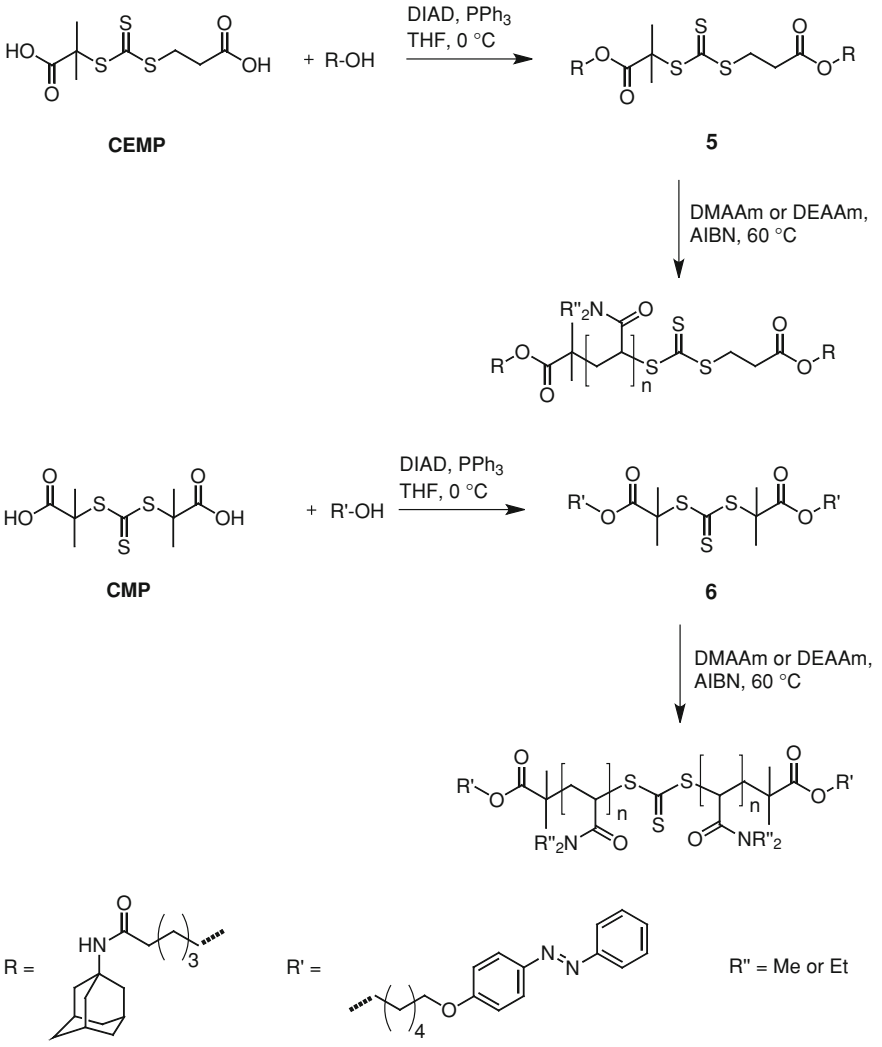

Scheme 4.2 Overview of the synthetic pathway leading to the doubly guest-functionalized inner building block featuring adamantyl- or azobenzene-guest groups

4.2 Results and Discussion

4.2.1 Synthesis of the Building Blocks

For the synthesis of the inner building blocks two doubly guest-functionalized CTAs based on trithiocarbonates were designed. **5** contains two adamantyl groups and **6** contains two azobenzene groups. The adamantyl group was chosen due to its high

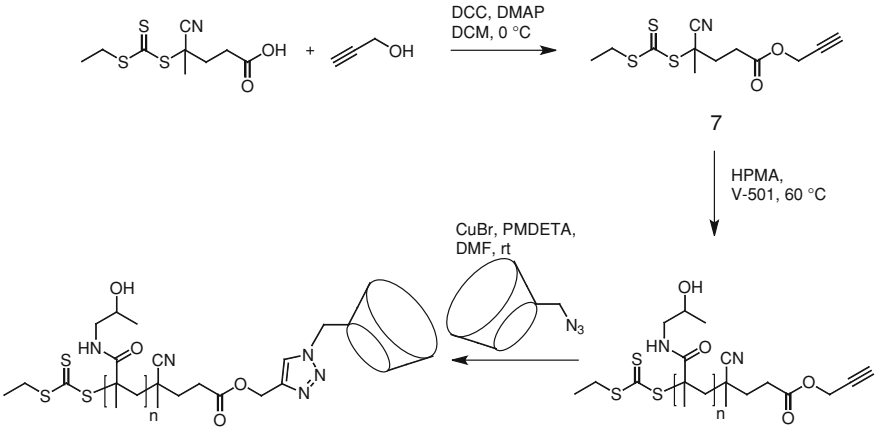

Scheme 4.3 Overview of the synthetic pathway leading to the β-CD-functionalized outer PHPMA building block

complexation constant of up to 10^5 M^{-1} with β-CD [30]. The azobenzene group was chosen due to its ability to change the conformation from *trans* to *cis* in response to light irradiation. This change in conformation leads to a significant change in the complexation constant with β-CD, i.e. the guest is expelled from the host-molecule upon irradiation with UV-light. The guest molecules were attached to the core CTA molecule via a short spacer group to support its availability in the complex formation. As shown in Scheme 4.2, both guest-functionalized CTAs were synthesized via a Mitsunobu reaction from the corresponding acids, **CEMP** in the case of **5** and **CMP** in the case of **6**.

Subsequently, the novel CTAs were employed in the RAFT polymerization of DMAAm and DEAAm in DMF at 60 °C with AIBN as initiator. DMAAm was selected to investigate the temperature response of the complex formation whereas DEAAm was chosen due to it's T_c, providing the opportunity to study the formation of block copolymer aggregates in solution due to a coil to globule transition of PDEAAm above the T_c. For PDMAAm, molecular masses of 6,400 and 15,700 g mol^{-1} with a $Đ_m$ of 1.06 and 1.11, respectively, were achieved with **5**, while a molecular weight of 5,400 and 11,000 g mol^{-1} with a $Đ_m$ of 1.08 and 1.11, respectively, were reached with **6** (refer to Fig. 4.1a, b and Table 4.1). The polymerization of DEAAm with **5** afforded polymers with molecular masses ranging from 6,500 to 12,100 g mol^{-1} and $Đ_m$ ranging from 1.11 to 1.27 (refer to Fig. 4.1c and Table 4.1). Furthermore, PDEAAms with molecular weights ranging from 5,400 to 11,000 g mol^{-1} and $Đ_m$ ranging from 1.16 to 1.33 (refer to Fig. 4.1d and Table 4.1) were synthesized with **6**. The structures of the polymers were verified via ^{1}H-NMR and ESI-MS (refer to Appendix Figs. B.1, B.2, B.3, B.4, B.5, B.6, B.7, B.8).

For the outer building block the biocompartible monomer HPMA was utilized [28]. Therefore, a trithiocarbonate CTA with an alkyne moiety was synthesized (refer to Scheme 4.3). A dithiobenzoate CTA, the first choice for methacrylamide

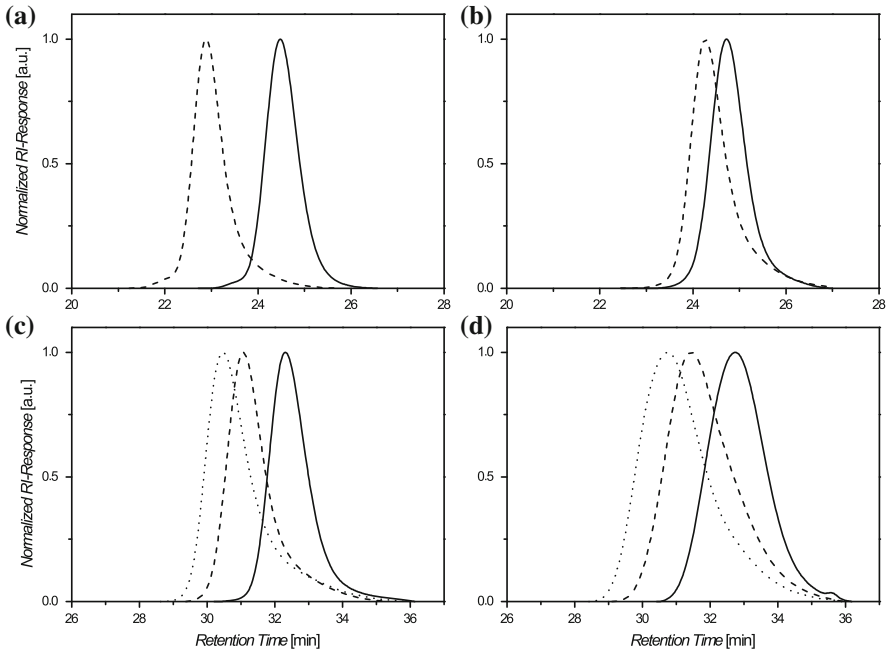

Fig. 4.1 SEC traces for **a** PDMAAm polymerized with **5** (*dashed line* $PDMAAm_{151}$-Ad_2; *solid line* $PDMAAm_{57}$-Ad_2), **b** PDMAAm polymerized with **6** (*dashed line* $PDMAAm_{103}$-Azo_2; *solid line* $PDMAAm_{46}$-Azo_2), **c** PDEAAm polymerized with **5** (*dotted line* $PDEAAm_{89}$-Ad_2; *dashed line* $PDEAAm_{78}$-Ad_2; *solid line* $PDEAAm_{45}$-Ad_2), **d** PDEAAm polymerized with **6** (*dotted line* $PDEAAm_{80}$-Azo_2; *dashed line* $PDEAAm_{59}$-Azo_2; *solid line* $PDEAAm_{36}$-Azo_2)

and methacrylate monomers, was not further considered as the complex formation between the phenyl-group and β-CD cannot be ruled out. As the utilized CTA contains an unprotected alkyne moiety, the conversion in the RAFT polymerizations was kept at low values to suppress radical transfer to the terminal alkyne.

The polymerization of HPMA was conducted in a mixture of DMF and acetic acid/sodium acetate buffer with V-501 as initiator at 70 °C . The utilization of **7** afforded narrowly distributed alkyne-functionalized PHPMA, e.g. a molecular mass of 6,500 g mol^{-1} and a $Đ_m$ of 1.17 (refer to Fig. 4.2 and Table 4.2). The structure of the polymer was proven via ESI-MS and ^{1}H-NMR measurements (refer to Appendix B.9/B.10).

The subsequent functionalization with β-CD was accomplished via a CuAAc reaction of the alkyne-functionalized PHPMA and β-CD–N_3. In the SEC trace a shift of the RI-signal to lower retention times is evident, thus proving the increased hydrodynamic volume of the β-CD conjugated PHPMA in comparison with the alkyne-functionalized PHPMA (refer to Fig. 4.2a–d), e.g. the M_n of the molecular weight distribution of $PHPMA_{44}$ increases from 6,500 to 7,300 g mol^{-1}, which fits the theory as the β-CD–N_3 moiety has a molecular weight of 1,159 g mol^{-1}.

Table 4.1 Results for the living/controlled RAFT polymerization of DMAAm or DEAAm at 60 °C in DMF

DMAAm/CTA/I	Time/h	*Conv.*	M_{ntheo}/g mol^{-1}	M_{nSEC}/g mol^{-1}	$Đ_m$	D_p
5: 34/1/0.2	24	>99	4,200	6,400	1.06	57
5: 100/1/0.2	24	>99	10,700	15,700	1.11	151
6: 35/1/0.2	24	79	3,500	5,400	1.08	46
6: 100/1/0.2	24	65	7,300	11,000	1.15	103
5: 56/1/0.2	24	>99	7,900	6,500	1.11	45
5: 107/1/0.2	24	98	14,300	10,700	1.16	78
5: 159/1/0.2	24	97	20,900	12,100	1.27	89
6: 55/1/0.2	24	76	6,100	5,400	1.16	36
6: 110/1/0.2	24	72	10,900	8,300	1.26	59
6: 172/1/0.2	24	76	22,800	11,000	1.33	80

Table 4.2 Results for the living/controlled RAFT polymerization of HPMA at 70 °C in DMF/acetic acid sodium acetate buffer with **7**

HPMA/CTA/I	Time/h	*Conv.*	M_{ntheo}/g mol^{-1}	M_{nSEC}/g mol^{-1}	$Đ_m$	D_p
35/1/0.2	2	15	1,100	3,900	1.17	26
35/1/0.2	2	28	1,700	4,300	1.15	28
36/1/0.2	2	23	5,400	6,500	1.17	44
71/1/0.2	13	81	8,400	9,200	1.40	63

Table 4.3 Results for the CuAAc conjugation of alkyne-functionalized PHPMA and β-CD–N_3

Alkyne-PHPMA			β-CD-PHPMA		
M_{nSEC}/g mol^{-1}	M_{pSEC}/g mol^{-1}	$Đ_m$	M_{nSEC}/g mol^{-1}	M_{pSEC}/g mol^{-1}	$Đ_m$
3,900	4,400	1.17	3,800	5,800	1.41
4,300	4,700	1.15	3,800	5,800	1.46
6,500	7,700	1.17	7,300	8,900	1.29
9,200	13,900	1.4	10,600	15,200	1.44

In other cases with lower molecular weight PHPMA (refer to Table 4.3), the M_n of the distribution remains close to unchanged. Nevertheless, the peak maximum molecular weight (M_p) increases as expected (Table 4.3) and a shift of the full molecular weight distribution is visible (Fig. 4.2a–d). In all cases a broadening of the molecular weight distribution is evident that could be attributed to adsorptive interactions of the β-CD moiety with the SEC column. The distributions have small shoulders at higher molecular weights that could be due to the conjugation of small amounts of difunctional azido β-CD.

Furthermore, ^{1}H-NMR spectroscopy shows the formation of the triazole ring as the new signal at 8.1 ppm can be assigned to the triazole-proton (Fig. 4.2e inset). Additionally, the ^{1}H-NMR spectrum shows signals that can be assigned to both β-CD and PHPMA, e.g. the anomeric CD protons between 4.3 and 4.6 ppm,

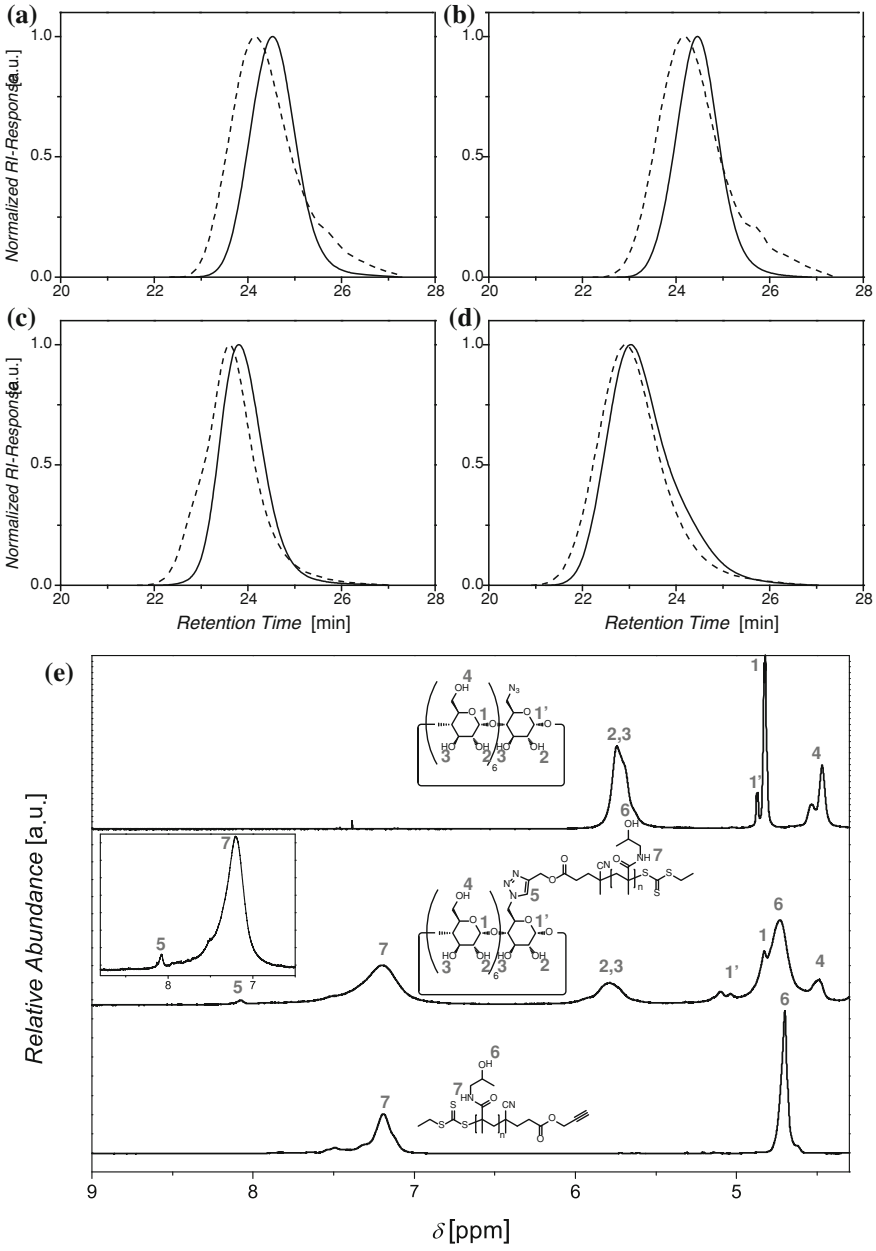

Fig. 4.2 **a** SEC traces for PHPMA polymerized with **7** (*solid line*) and the product of the conjugation with β-CD–N_3 (*dashed line*): **a** for $PHPMA_{26}$-alkyne; **b** for $PHPMA_{28}$-alkyne; **c** for $PHPMA_{44}$-alkyne; **d** for $PHPMA_{63}$-alkyne and **e** comparison of the ^{1}H-NMR spectra of β-CD–N_3 (*top*), the β-CD-functionalized PHPMA click product (*middle* $PHPMA_{28}$-β-CD) and alkyne-functionalized PHPMA (*bottom* $PHPMA_{28}$-alkyne)

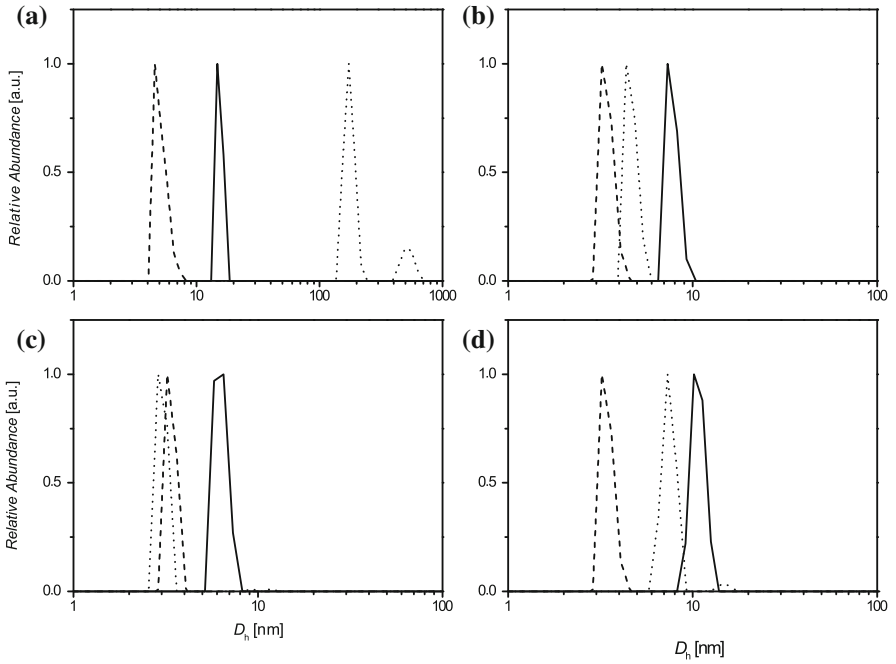

Fig. 4.3 Comparison of the number averaged particle size distributions obtained from DLS measurements of the building blocks (*dashed line* PHPMA and *dotted line* PDMAAM) and the supramolecular block copolymer (*solid line*) at a concentration of 1 mg mL^{-1} and at 25 °C : **a** $PHPMA_{44}$-β-CD, $PDMAAm_{57}$-Ad_2 and $PDMAAm_{57}$-Ad_2-*b*-$(PHPMA_{44}$-β-$CD)_2$; **b** $PHPMA_{26}$-β-CD, $PDMAAm_{151}$-Ad_2 and $PDMAAm_{151}$-Ad_2-*b*-$(PHPMA_{26}$-β-$CD)_2$; **c** $PHPMA_{26}$-β-CD, $PDMAAm_{46}$-Azo_2 and $PDMAAm_{46}Azo_2$-*b*-$(PHPMA_{26}$-β-$CD)_2$; **d** $PHPMA_{26}$-β-CD, $PDMAAm_{103}$-Azo_2 and $PDMAAm_{103}Azo_2$-*b*-$(PHPMA_{26}$-β-$CD)_2$

the 2-hydroxyl and the 3-hydroxyl protons between 5.5 and 6.0 ppm, the hydroxyl protons of PHPMA between 4.6 and 4.8 ppm or the amide proton of PHPMA between 7.0 and 7.5 ppm (see Fig. 4.2e).

4.2.2 Formation of ABA Triblock Copolymers via Self-Assembly

To ensure the availability of the hydrophobic guest groups for the complex formation, the self-assembly of the building blocks was accomplished via the dialysis method. In brief, both polymer building blocks were dissolved in an organic solvent, e.g. DMF, one solution was added dropwise to the other under vigorous stirring and the organic solvent was removed via dialysis. The complexes were finally lyophilized and subsequently characterized via DLS and NOESY.

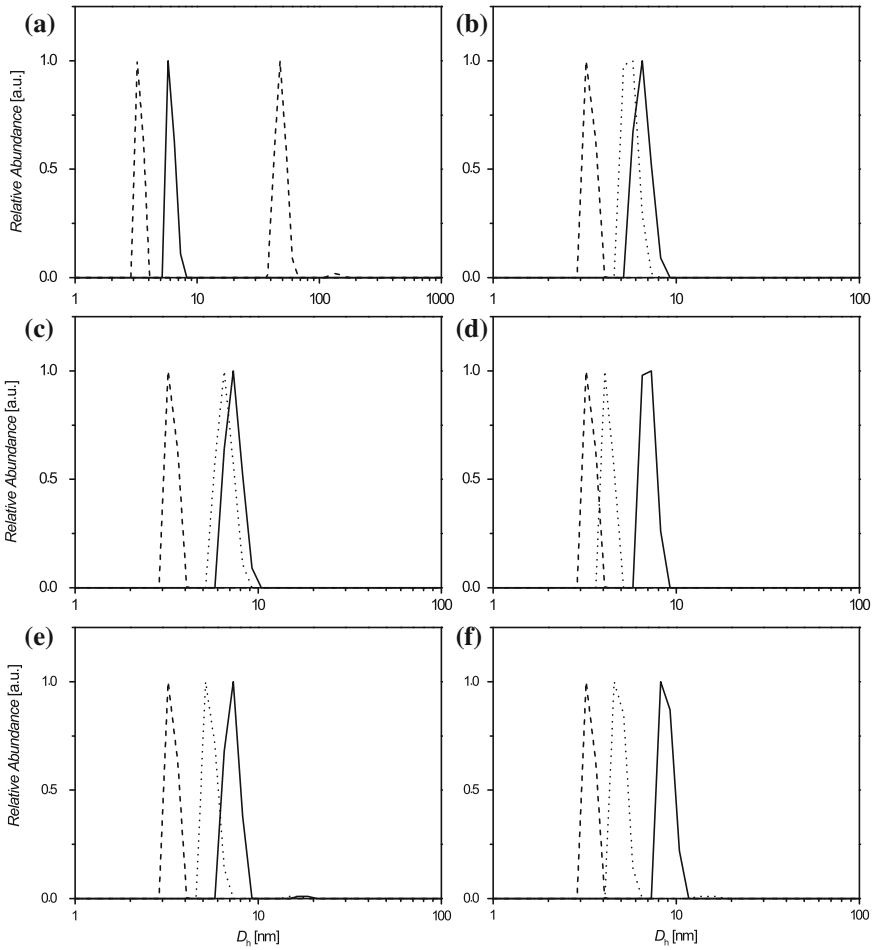

Fig. 4.4 Comparison of the number averaged particle size distributions obtained from DLS measurements of the building blocks (*dashed line* PHPMA and *dotted line* PDEAAM) and the supramolecular block copolymer (*solid line*) at a concentration of 1 mg mL^{-1}at 10 °C : **a** $PHPMA_{28}$-β-CD, $PDEAAm_{45}$-Ad_2 and $PDEAAm_{45}$-Ad_2-b-$(PHPMA_{28}$-β-$CD)_2$; **b** $PHPMA_{28}$-β-CD, $PDEAAm_{78}$-Ad_2 and $PDEAAm_{78}Ad_2$-*b*-$(PHPMA_{28}$-β-$CD)_2$; **c** $PHPMA_{28}$-β-CD, $PDEAAm_{89}$-Ad_2 and $PDEAAm_{89}$-Ad_2-*b*-$(PHPMA_{28}$-β-$CD)_2$; **d** $PHPMA_{28}$-β-CD, $PDEAAm_{36}$-Azo_2 and $PDEAAm_{36}Azo_2$-*b*-$(PHPMA_{28}$-β-$CD)_2$; **e** $PHPMA_{28}$-β-CD, $PDEAAm_{59}$-Azo_2 and $PDEAAm_{59}Azo_2$-*b*-$(PHPMA_{28}$-β-$CD)_2$; **f** $PHPMA_{28}$-β-CD, $PDEAAm_{80}$-Azo_2 and $PDEAAm_{80}Azo_2$-*b*-$(PHPMA_{28}$-β-$CD)_2$

DLS is a versatile tool to investigate the complex formation in solution. In the current investigation DLS was employed to obtain the hydrodynamic diameter (D_h) of the polymer coils in solution. In principle, the D_h should increase upon complex formation as three polymer chains are included in the complex. The PDMAAm based complexes were measured at 25 °C and the complexes show larger D_h than the

individual parts (refer to Figs. 4.3 and 4.4), e.g. PHPMA$_{26}$-β-CD has a D_h of 3.4 nm, PDMAAm$_{151}$-Ad$_2$ has a D_h of 4.7 nm and the supramolecular complex features a D_h of 7.8 nm. An exception is the doubly adamantyl-functionalized PDMAAm with low molecular weight, which has a D_h of 175.0 nm for PDMAAm$_{57}$-Ad$_2$, a D_h of 5.1 for PHPMA$_{44}$-β-CD and a D_h of 15.4 nm for the supramolecular complex PDMAAm$_{57}$-Ad$_2$-*b*-(PHPMA$_{44}$-β-CD)$_2$. In this case, the hydrophobic guest groups lead to aggregation of or within the homopolymer. The complex shows a smaller D_h, yet the value of 15.4 nm suggests further aggregation probably due to more complicated structures in solution (refer to Fig. 4.3a). An example for doubly azobenzene-functionalized PDEAAm is PDEAAm$_{80}$Azo$_2$-*b*-(PHPMA$_{28}$-β-CD)$_2$ with a D_h of 8.9 nm. The individual building blocks PDEAAm$_{80}$Azo$_2$ and PHPMA$_{28}$-β-CD have a D_h of 4.9 and 3.4 nm, respectively. Due to the T_c of PDEAAm the DLS measurements were performed at 10 °C . A significant increase in D_h was evident in most of the cases (refer to Fig. 4.4). An example for doubly adamantyl-functionalized PDEAAm PDEAAm$_{89}$-Ad$_2$-*b*-(PHPMA$_{28}$-β-CD)$_2$ with a D_h of 7.4 nm consisting of PDEAAm$_{89}$-Ad$_2$ with a D_h of 6.6 nm and PHPMA$_{28}$-β-CD with a D_h of 3.4 nm. Similar to PDMAAm of lower molecular weight, doubly adamantyl-functionalized PDEAAm shows very large D_h (48.4 nm for PDEAAm$_{45}$-Ad$_2$) for the homopolymer and a D_h of 6.1 nm after complexation with PHPMA$_{28}$-β-CD (Fig. 4.4a). For doubly azobenzene-functionalized PDEAAm an increase in D_h from 4.9 nm for the middle-block PDEAAm$_{80}$-Azo$_2$ and 3.4 nm for the outer PHPMA$_{28}$-β-CD blocks to 8.9 nm is observed for the complex. In the case of azobenzene functionalized polymers no higher aggregates were observed for the homopolymers or complexes, which can be attributed to the higher polarity of the azobenzene moiety compared to the adamantyl group.

To evidence the molecular nature of the complex formation NOESY was utilized, which is a well suited tool to study host/guest complex formation. The adamantyl-based systems PDMAAm$_{151}$Ad$_2$-*b*-(PHPMA$_{26}$-β-CD)$_2$ and PDEAAm$_{78}$Ad$_2$-*b*-(PHPMA$_{28}$-β-CD)$_2$ show cross correlation peaks that correspond to the signals of the adamantyl moiety at 1.7, 2.0 and 2.2 ppm and the inner protons of β-CD between 3.5 and 3.8 ppm (Fig. 4.5a, e). This proves the close spatial proximity of the adamantyl moiety and the inner CD protons, which is the case for inclusion complexes. NOESY spectra of the azobenzene-based systems show weak cross correlation peaks originating from the azobenzene protons between 7.0 and 7.5 ppm and the inner CD protons (refer to Fig. 4.5c, f). The azobenzene-moiety shows weaker cross correlation peaks in comparison with adamantyl-systems which can be explained with the weaker complexation and the larger distance between the CD protons and the aromatic protons in the azobenzene. Nevertheless, the spectra are a strong hint for inclusion complex formation. In general, the observed cross correlation peaks are weaker in the case of PDEAAm containing samples as the concentration of the NMR samples was lower due to less solubility of the block copolymer in D_2O compared to the PDMAAm based copolymers. It should be noted that the described supramolecular ABA block copolymer is in equilibrium with the building blocks due to its non-covalent nature. Therefore, the existence of AB block copolymers and non-connected building blocks cannot be excluded. However, the formation of the desired structure is governed by

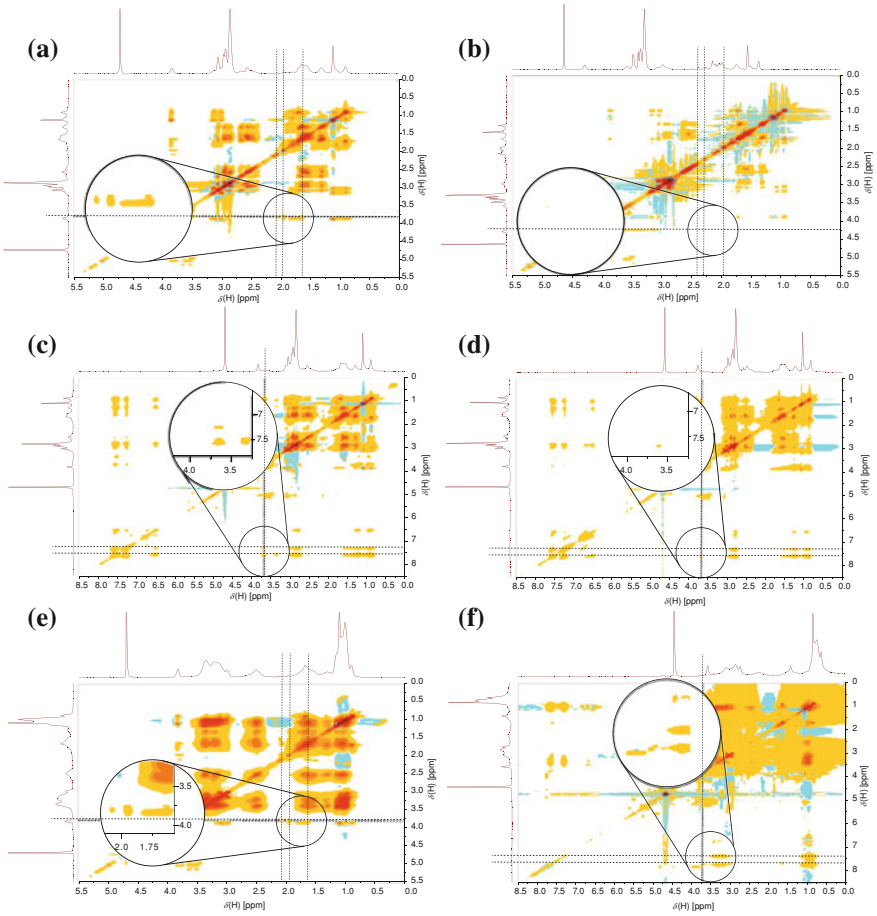

Fig. 4.5 2D NOESY spectra of the supramolecular triblock copolymers in D_2O: **a** $PDMAAm_{151}Ad_2$-*b*-$(PHPMA_{26}$-β-$CD)_2$ at 25 °C ; **b** $PDMAAm_{151}Ad_2$-*b*-$(PHPMA_{26}$-β-$CD)_2$ at 70 °C ; **c** $PDMAAm_{103}Azo_2$-*b*-$(PHPMA_{26}$-β-$CD)_2$ at 25 °C ; **d** $PDMAAm_{103}Azo_2$-*b*-$(PHPMA_{26}$-β-$CD)_2$ after UV irradiation for 7 min at 25 °C ; **e** $PDEAAm_{78}Ad_2$-*b*-$(PHPMA_{28}$-β-$CD)_2$ at 25 °C and **f** $PDEAAm_{80}Azo_2$-*b*-$(PHPMA_{28}$-β-$CD)_2$ at 25 °C

the association constants that are rather high in the described systems. Thus, the ABA block copolymer should almost exclusively be present in solution.

4.2.3 Investigations of the Stimuli-Responsive Behavior

The prepared CD-based host/guest complexes show thermoresponsivity due to the usually negative enthalpy of complex formation (refer to Sect. 2.2.3) [31, 32]. To evidence the thermoresponsivity of the host/guest supramolecular triblock copolymers guest-functionalized PDMAAm was synthesized that features no T_c. As shown in

Fig. 4.6, both the adamantyl- and azobenzene-based triblock copolymers show a significant decrease in D_h from 7.8 to 4.2 nm for an adamantyl-guest in the case of PDMAAm$_{151}$Ad$_2$-*b*-(PHPMA$_{26}$-β-CD)$_2$ and from 11.2 to 5.4 nm in the case of azobenzene in PDMAAm$_{103}$Azo$_2$-*b*-(PHPMA$_{26}$-β-CD)$_2$ upon heating to 70 °C . Furthermore, the complexes form again after remaining at ambient temperature which is proven by an increase in D_h close to the original values. In the case of lower molecular weight PDMAAm, the D_h increases with heating which is due to the formation of aggregates in solution as the complex dissociates (Fig. 4.6a, b). These aggregates could be formed due to the hydrophobic guest-groups that are unmasked which changes the solubility of the PDMAAm. In analogy to the higher molecular weight PDMAAms, the complexes re-form again after remaining at ambient temperature for 3–4 days and the D_h decreases. The rate of the re-formation of the complexes can be followed by DLS. It seems that azobenzene-based complexes form faster, which may be attributed to the increased polarity of azobenzene compared to adamantane, which enhances the accessibility of the guest moiety in aqueous solution. Moreover, the re-formation of the complexes is faster with a higher degree of polymerization of PDMAAm. An explanation for the effect is the overall solubility of the polymer chain that changes drastically after the complex dissociation for lower molecular weight polymers and the earlier mentioned aggregates disturb the complex re-formation.

Furthermore, The temperature triggered dissociation of the supramolecular complexes could be observed via 2D NOESY at 70 °C (see Fig. 4.5b). In comparison with the sample at 25 °C , no relevant cross-correlation peaks are observable. It should be noted that due to the increased temperature the chemical shifts of the respective signals change.

In addition to the thermoresponsivity of the employed host/guest complexes, azobenzenes provide the opportunity to generate structures that are sensitive to light irradiation, as azobenzenes show a transition from the thermodynamically more stable *trans*- to the *cis*-conformation at wavelengths close to 360 nm. This photoisomerization is reversible and the reisomerization can be induced by heat or light with wavelengths close to 430 nm. Furthermore, the complexation constants are higher for the *trans*-conformation compared to the *cis*-conformation (460 M^{-1} for a *trans*-azobenzene test-compound and 2.5 M^{-1} for a *cis* azobenzene test-compound) [33]. In general, higher complexation constants (up to 10^4 M^{-1}) [34] and differences between *cis* and *trans*-conformations could be achieved via the utilization of α-CD instead of β-CD. In here, azobenzene-based β-CD complexes were irradiated with UV light at 350 nm for 30 min and the change in D_h was monitored via DLS. A significant decrease was evident, e.g. from 8.9 to 4.8 nm after irradiation in the case of PDEAAm$_{80}$Azo$_2$-*b*-(PHPMA$_{28}$-β-CD)$_2$ (see Fig. 4.7), evidencing that the block copolymers are debonded in a photoresponsive fashion. After keeping the samples at ambient temperature and daylight, the block copolymers formed again as proven by an increased D_h value, e.g. 8.2 nm compared to the original value of 8.9 nm in the case of PDEAAm$_{80}$Azo$_2$-*b*-(PHPMA$_{28}$-β-CD)$_2$ and 10.1 nm compared to 11.2 nm before in the case of PDMAAm$_{103}$Azo$_2$-*b*-(PHPMA$_{26}$-β-CD)$_2$. In almost all cases the D_h after standing in daylight is close to the initial value. As shown in

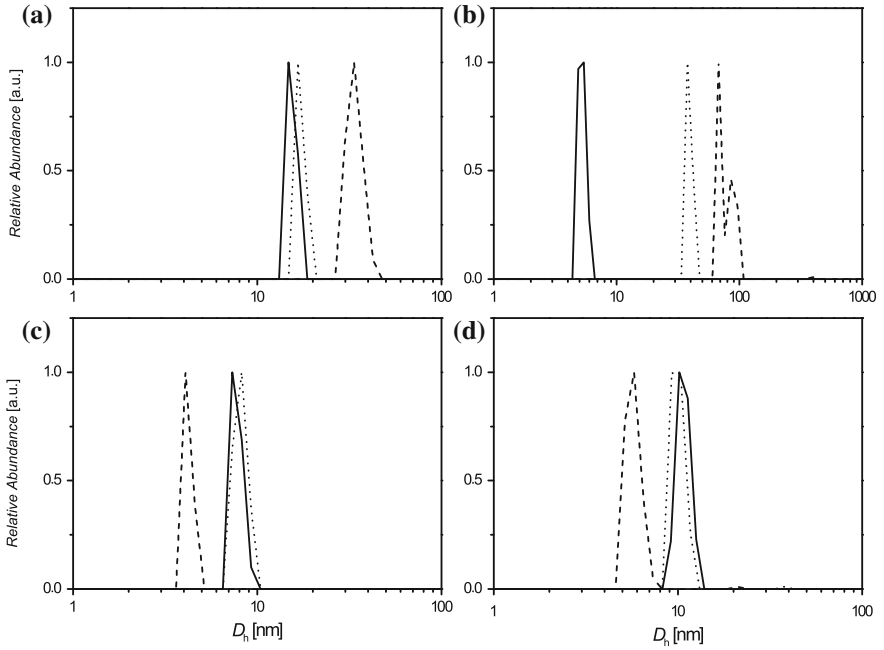

Fig. 4.6 Number averaged particle size distributions obtained from DLS measurements before heating to 70 °C (*solid line*), at 70 °C (*dashed line*) and after keeping at ambient temperature for the specified time (*dotted line*): **a** complex $PDMAAm_{57}Ad_2$-*b*-$(PHPMA_{44}$-β-$CD)_2$ before heating, at 70 °C and after 4 days; **b** complex $PDMAAm_{46}Azo_2$-*b*-$(PHPMA_{26}$-β-$CD)_2$ before heating, at 70 °C and after 3 days; **c** complex $PDMAAm_{151}Ad_2$-*b*-$(PHPMA_{26}$-β-$CD)_2$ before heating, at 70 °C and after 3 days; **d** complex $PDMAAm_{103}Azo_2$-*b*-$(PHPMA_{26}$-β-$CD)_2$ before heating, at 70 °C and after 1 day

Figs. 4.6 and 4.7, the azobenzene-based PDMAAm block copolymers are double responsively bound as their supramolecular connection is sensitive to heat and light.

The light triggered complex dissociation could be observed furthermore via 2D NOESY (see Fig. 4.5d). The intensity of the corresponding cross correlation peaks decreases significantly after irradiation of UV light for 7 min. Nevertheless, the peaks do not vanish completely. This can be attributed to the fact that the complexes could re-form during the NOESY measurement with a measuring time of around 9 h. Furthermore an equilibrium between *cis*- and *trans*-azobenzenes is formed where small amounts of *trans*-azobenzenes with higher association constant remain in the solution and the irradiation time is limited as RAFT polymers are sensitive to UV irradiation.

The formation of *cis*-azobenzenes can be monitored via UV spectroscopy as well. The UV spectra of all samples show a significant increase of the absorption at 440nm after irradiation at 350 nm for 30 min (see Fig. 4.8 and Appendix B.11 and B.12). Concomitantly, the absorption of *trans*-azobenzene moieties at 340 nm decreases drastically. As the absorption of *trans*-azobenzene is overlapping with the absorption

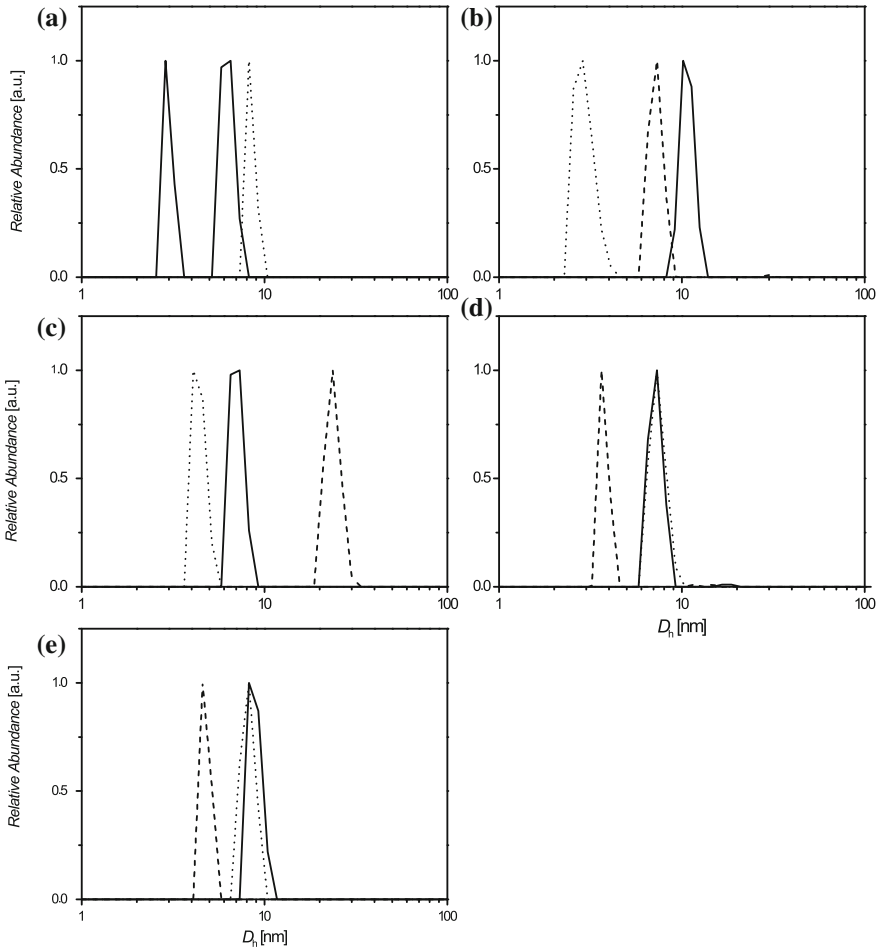

Fig. 4.7 Number averaged particle size distributions obtained from DLS measurements before applying the stimulus (*solid line*), directly after UV irradiation at 350 nm for 30 min (*dashed line*) and in daylight for the specified time (*dotted line*): **a** complex PDMAAm$_{46}$Azo$_2$-*b*-(PHPMA$_{26}$-β-CD)$_2$ before irradiation, directly after irradiation and after 3 days; **b** complex PDMAAm$_{103}$Azo$_2$-*b*-(PHPMA$_{26}$-β-CD)$_2$ before irradiation, directly after irradiation and after 1 day; **c** complex PDEAAm$_{36}$Azo$_2$-*b*-(PHPMA$_{28}$-β-CD)$_2$ before irradiation, directly after irradiation and after 3 days; **d** complex PDEAAm$_{59}$Azo$_2$-*b*-(PHPMA$_{28}$-β-CD)$_2$ before irradiation, directly after irradiation and after 2 days; **e** complex PDEAAm$_{80}$Azo$_2$-*b*-(PHPMA$_{28}$-β-CD)$_2$ before irradiation, directly after irradiation and after 2 days

of the trithiocarbonate, a quantitative statement with respect to the *trans*- and *cis*-azobenzene content in solution is difficult. Nevertheless, judging from the shape of the absorption band after irradiation, only minor amounts of *trans*-azobenzene remain.

The utilization of PDEAAm as the inner block provides the opportunity for temperature-induced aggregation [21, 22, 24]. As shown in Fig. 4.9, the block copoly-

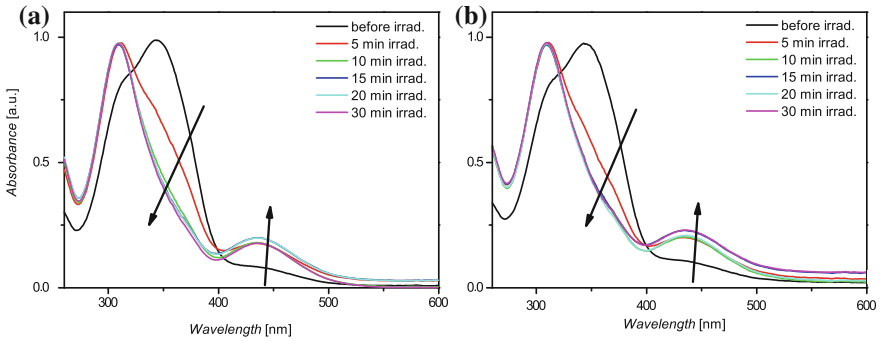

Fig. 4.8 Overlay of the UV spectra before irradiation (*black curve*), after irradiation at 350 nm for 5 min (*red curve*) and after irradiation at 350 nm for longer than 5 min (*other curves*) at 10 °C : **a** PDEAAm$_{59}$Azo$_2$; **b** PDEAAm$_{59}$Azo$_2$-*b*-(PHPMA$_{28}$-β-CD)$_2$

mers are present as random coils at lower temperatures, e.g. a D_h of around 7 nm for PDEAAm$_{78}$Ad$_2$-*b*-(PHPMA$_{28}$-β-CD)$_2$ up to 30 °C or a D_h around 8 nm for PDEAAm$_{59}$Azo$_2$-*b*-(PHPMA$_{28}$-β-CD)$_2$ up to 20 °C (Fig. 4.9a/b). The situation changes upon heating over the T_c where aggregates are formed. In the case of PDEAAm$_{78}$Ad$_2$-*b*-(PHPMA$_{28}$-β-CD)$_2$ aggregates with D_h between 24 and 90 nm are formed between 31 and 36 °C . A broader temperature range from 21 to 34 °C is covered with PDEAAm$_{59}$Azo$_2$-*b*-(PHPMA$_{28}$-β-CD)$_2$, where D_h between 54 and 222 nm are observed. With further heating these aggregates agglomerate, leading to particles with sizes over 1,000 nm. The other examined block copolymers show similar behavior. In the first stage, unimers were observed, whereas aggregates with D_h ranging from 37 to 210 nm were observed after heating above the T_c. The onset of the aggregate formation varies with different chain length of the middle block as well as the nature of the guest group. Agglomerate sizes ranging from $D_h = 1{,}000-1{,}700$ nm were found in the third stage of the temperature sequenced DLS measurements except of PDEAAm$_{36}$Azo$_2$-*b*-(PHPMA$_{28}$-β-CD)$_2$ where particles between 500 and 1,000 nm are found (refer to Appendix Fig. B.13). In general all samples show the described D_h profile with a change of the temperature. The behavior of these triblock copolymers resembles the behavior of literature known systems where a plateau as well as further agglomeration is described [22, 24]. One possible explanation for agglomeration at higher temperatures is the decreased complex stability, making a dynamic exchange of the building blocks possible. Thus, the stabilization effect of the PHPMA corona on the PDEAAm cores is decreasing and finally the aggregates begin to agglomerate. The DLS data are in agreement with the plots of turbidimetry, which is evident via the direct comparison in Fig. 4.9a/c and b/d.

Turbidity measurements show in almost all cases an increased T_c of the complexes compared to the uncomplexed PDEAAm blocks (refer to Fig. 4.9 and Appendix B.14), which is an expected behavior of supramolecular block copolymers with a thermoresponsive block [22, 24]. A possible explanation for such a behavior is the shielding of the hydrophobic endgroups by the CD moiety. In the case of doubly

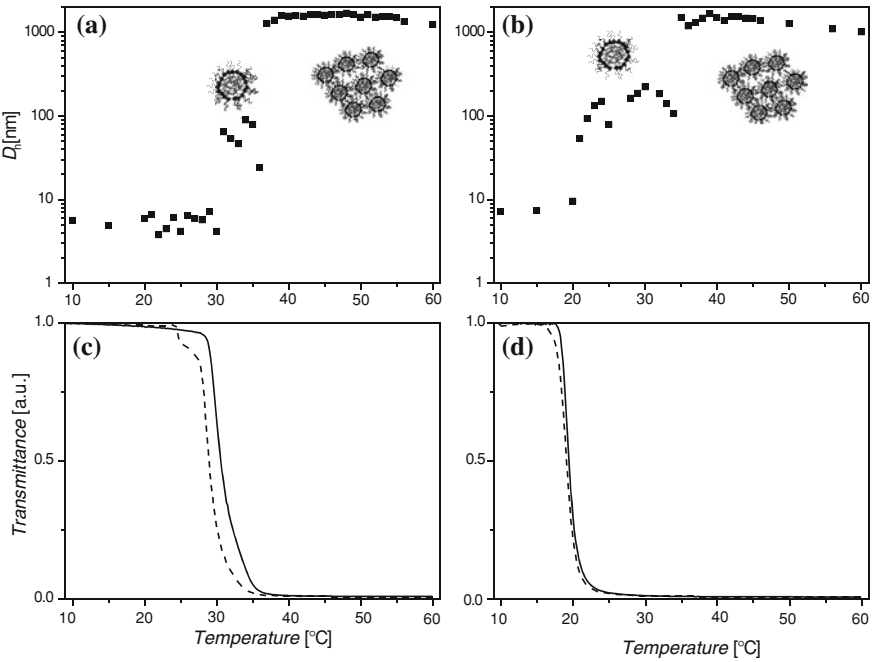

Fig. 4.9 **a** Temperature sequenced DLS measurement of $PDEAAm_{78}Ad_2$-*b*-$(PHPMA_{28}$-β-$CD)_2$ at a heating rate of 0.2 °C min^{-1} and a concentration of 1 mg mL^{-1}; **b** temperature sequenced DLS measurement of $PDEAAm_{59}Azo_2$-*b*-$(PHPMA_{28}$-β-$CD)_2$ at a heating rate of 0.2 °C min^{-1} and a concentration of 1 mg mL^{-1}; **c** turbidity measurements for $PDEAAm_{78}Ad_2$ (*dashed line*) and the supramolecular triblock copolymer $PDEAAm_{78}Ad_2$-*b*-$(PHPMA_{28}$-β-$CD)_2$ (*solid line*) at a cooling rate of 0.32 °C min^{-1} and a concentration of mg mL^{-1}; **d** turbidity measurements for $PDEAAm_{59}Azo_2$ (*dashed line*) and the supramolecular triblock copolymer $PDEAAm_{59}Azo_2$-*b*-$(PHPMA_{28}$-β-$CD)_2$ (*solid line*) at a cooling rate of 0.32 °C min^{-1} and a concentration of 1 mg mL^{-1}

adamantyl-functionalized polymers the difference in the T_cs lies between 4 and 2 °C whereas the difference with azobenzene-functionalized polymers is rather small and the T_cs are almost the same. A reason for the different behavior of the guest groups may be the enhanced polarity of the azobenzene moiety and the weaker association with β-CD. Furthermore an increase of the T_c with molecular weight is evident as well.

4.3 Conclusions

The synthesis of a novel macromolecular architecture based on CD host/guest chemistry, i.e. an ABA triblock copolymer was accomplished. A doubly guest-functionalized, namely adamantyl- and azobenzene-functionalized inner block was synthesized via RAFT polymerization of DMAAm and DEAAm. The host functionalized block was synthesized via RAFT polymerization of the monomer HPMA,

affording the biocompatible PHPMA, and a CuAAc conjugation with β-CD–N_3. The individual blocks were characterized via SEC, ^{1}H-NMR and ESI-MS. Subsequently, the triblock copolymers were formed in aqueous solution and the complex formation was evidenced via DLS, 2D NOESY as well as turbidity measurements. Furthermore, the triblock copolymer formation was responsive to temperature and in the case of azobenzene-guests to irradiation of light at 350 nm in a reversible fashion as disassembly after the stimuli and reassembly of the triblock copolymers was unambiguously evidenced. In the case of PDEAAm, the temperature induced aggregation was investigated after heating above the T_c of the PDEAAm block.

4.4 Experimental Part

4.4.1 Synthesis of 6-(adamantan-1-ylamino)-6-oxohexyl 2-((((3-((6-(-adamantan-1-ylamino)-6-oxohexyl)oxy)-3-oxopropyl)thio)carbonothioyl)thio)-2-methylpropanoate (5)

According to a literature procedure [35], **CEMP** (0.61 g, 2.26 mmol, 1.0 eq.), *N*-(adamantan-1-yl)-6-hydroxyhexanamide (**8**) (1.50 g, 5.65 mmol, 2.5 eq.) and triphenylphosphine (1.48 g, 5.65 mmol, 2.5 eq.) were dissolved in anhydrous THF (15mL). At 0 °C DIAD (1.3 mL, 5.65 mmol, 2.5 eq.) in anhydrous THF (5 mL) was added dropwise. The reaction mixture was stirred at ambient temperature over night and subsequently for 3 h at 40 °C . After cooling to ambient temperature, DCM (50 mL) was added and the organic phase was washed twice with saturated $NaHCO_3$-solution (50 mL). The organic phase was dried over Na_2SO_4, filtered and the solvent evaporated in vacuo. The residue was subjected to column chromatography on silica-gel with *n*-hexane:ethyl acetate as eluent that was gradually changed from 1:1 to 1:2. The product was obtained as a yellow oil (0.88 g, 1.15 mmol, 51 %).

^{1}H-NMR (400 MHz, $CDCl_3$): [δ, ppm] = 1.15−1.28 (m, 4H, 2x C***H***$_2$–CH_2–CH_2–C=O), 1.28−1.46 (m, 4H, 2x C***H***$_2$–CH_2–O), 1.48–1.75 (m, 28H, 4x (C***H***$_3$)$_2$–C, 2x C***H***$_2$–CH_2–C=O; 6x C***H***$_{2,adamantyl}$), 1.92−2.01 (m, 12H, 6x C***H***$_{2,adamantyl}$–C–NH), 2.04–2.10 (m, 10 H, 6x C***H***$_{adamantyl}$; 2x C***H***$_2$–C=O), 2.70 (t, ^3J = 6.9 Hz, C***H***$_2$–CH_2–S), 3.52 (t, 2H, ^3J = 6.9 Hz, C***H***$_2$–S), 4.08 (q, 4H, ^3J = 6.4 Hz, C***H***$_2$–O–C=O), 5.19 (m, 2H, N***H***). **^{13}C-NMR** (100 MHz, $CDCl_3$): [δ, ppm] = 25.5, 25.7 and 25.8 (2x ***C***H_2–CH_2–CH_2–C=O; 2x ***C***H_2–CH_2–C=O, 2x (***C***H_3)$_2$–C), 28.3 and 28.5 (2x ***C***H_2–CH_2–O–C=O), 29.6 (6x ***C***$H_{adamantyl}$), 31.4 (***C***H_2–CH_2–S), 33.2 (***C***H_2–S), 36.5 (6x ***C***$H_{2,adamantyl}$, 37.7 (2x ***C***H_2–C=O), 41.9 (6x ***C***$H_{2,adamantyl}$–C–NH), 51.9 (2x ***C***–NH), 56.4 (2x ***C***$(CH_3)_2$), 65.0 and 66.1 (2x ***C***H_2–O–C=O), 171.5, 172.0, 172.1 and 172.9 (4x ***C***=O), 220.9 (***C***=S). **ESI-MS**: $[M + Na^+]_{exp}$ = 785.58 m/z and $[M + Na^+]_{calc}$ = 785.37 m/z.

4.4.2 Synthesis of bis(6-(4-(phenyldiazenyl)phenoxy)hexyl) 2,2′-(thiocarbonylbis(sulfanediyl))bis(2-methylpropanoate) (6)

Based on a literature procedure [35], **CMP** (1.00 g, 3.54 mmol, 1.0 eq.), 6-(4-(phenyldiazenyl)phenoxy)hexan-1-ol (**9**) (3.38 g, 11.33 mmol, 3.2 eq.) and triphenylphosphine (2.97 g, 11.32 mmol, 3.2 eq.) were dissolved in anhydrous THF (20 mL). At 0 °C DIAD (2.2 mL, 11.21 mmol, 3.2 eq.) in anhydrous THF (20 mL) was added dropwise. The reaction mixture was stirred at ambient temperature over night and subsequently for 3 h at 40 °C . After cooling to ambient temperature, DCM (100 mL) was added and the organic phase was washed twice with saturated $NaHCO_3$-solution (100 mL). The organic phase was dried over Na_2SO_4, filtered and the solvent evaporated in vacuo. The residue was subjected to column chromatography on silica-gel with *n*-hexane:ethyl acetate as eluent that was gradually changed from 10:1 to 8:1. The product was obtained as an orange oil which solidified on cooling (2.77 g, 3.30 mmol, 93 %).

^{1}H-NMR (400 MHz, $CDCl_3$):): [δ, ppm] = 1.37−1.57 (m, 4H, 2x C***H***$_2$–CH_2–CH_2–O), 1.58–1.72 (m, 16H, 4x C–C***H***$_3$; 2x O=C–O–CH_2–C***H***$_2$), 1.77–1.87 (m, 4H, 2x O–CH_2–C***H***$_2$), 4.03 (t, 4H, ^3J = 6.5 Hz, 2x C***H***$_2$–O), 4.09 (t, 4H, ^3J = 6.5 Hz, 2x C***H***$_2$–O–C=O), 7.00 (d, 4H, ^3J = 9.0 Hz, 4x C***H***$_{arom}$), 7.40−7.46 (m, 2H, 2x C***H***$_{arom}$), 7.47−7.56 (m, 4H, 4x C***H***$_{arom}$), 7.82−7.97 (m, 8H, 8x C***H***$_{arom}$). **^{13}C-NMR** (100 MHz, $CDCl_3$): [δ, ppm] = 25.3 (4x ***C***H_3–C), 25.8 and 25.9 (4x ***C***H_2–CH_2–CH_2–O), 28.4 (2x O–CH_2–***C***H_2), 29.2 (2x O=C–O–CH_2–***C***H_2), 56.3 (2x ***C***$(CH_3)_2$), 66.1 (2x O=C–O–***C***H_2), 68.3 (2x O–***C***H_2), 114.8 (2x O–C_{arom}–***C***H_{arom}), 122.7 (2x ***C***H_{arom}), 124.9 (4x ***C***H_{arom}), 129.2 (4x ***C***H_{arom}), 130.4 (2x ***C***H_{arom}), 147.0 (2x ***C***$_{arom}$–N=N), 152.9 (2x ***C***$_{arom}$–N=N), 161.8 (2x O–***C***$_{arom}$), 172.9 (2x ***C***=O), 218.6 (***C***=S). **ESI-MS**: $[M + H^+]_{exp}$ = 843.33 m/z and $[M + H^+]_{calc}$ = 843.33 m/z.

4.4.3 Synthesis of prop-2-yn-1-yl 4-cyano-4-(((ethylthio) carbonothioyl)thio)pentanoate (7)

In a 100 mL Schlenk-flask, **CEP** (1.00 g, 3.80 mmol, 1.0 eq.), propargylalcohol (0.5 mL, 8.65 mmol, 2.3 eq.) and DMAP (0.09 g, 0.77 mmol, 0.2 eq.) were dissolved in anhydrous DCM (20 mL). At 0 °C a solution of DCC (1.57 g, 7.61 mmol, 2.0 eq.) in anhydrous DCM (10 mL) was added. After 1 h the solution was warmed to ambient temperature, stirred overnight, filtered and concentrated under reduced pressure. The residue was purified via column chromatography on silica-gel with *n*-hexane:ethyl acetate 10:1 as eluent. The product was obtained as a yellow oil (0.94 g, 3.13 mmol, 82 %).

^{1}H-NMR (400 MHz, $CDCl_3$): [δ, ppm] = 1.35 (t, 3H, ^3J = 7.4 Hz, CH_2–C***H***$_3$), 1.87 (s, 3H, C–C***H***$_3$), 2.27–2.59 (m, 3H, C***H***, C***H***$_2$–COO), 2.62–2.76 (m, 2H, C–C***H***$_2$), 3.34 (q, 2H, ^3J = 7.4 Hz, CH_3–C***H***$_2$), 4.71 (d, 2H, ^4J = 2.5 Hz, C***H***$_2$–C–CH). **^{113}**C-NMR (100 MHz, $CDCl_3$): [δ, ppm] = 12.9 (***C***H_3), 25.0 (C–***C***H_3), 29.7 (***C***H_2–

COO), 31.5 (C–***C***H_2), 33.8 (CH_3–***C***H_2), 46.4 (***C***–CH_2), 52.6 (***C***H_2–C–CH), 75.4 (CH_2–C–***C***H), 77.4 (CH_2–***C***–CH), 119.0 (***C***–N), 170.8 (***C***=O), 216.8 (***C***=S). **ESI-MS**: $[M + Na^+]_{exp}$ = 324.08 m/z and $[M + Na^+]_{calc}$ = 324.02 m/z.

4.4.4 Exemplary Procedure for the RAFT Polymerization of DEAAm

5 (54.9 mg, 0.07 mmol, 1.0 eq.), DEAAm (500.0 mg, 3.94 mmol, 56.3 eq.), AIBN (4.2 mg, 0.03 mmol, 0.4 eq.), DMF (3.3 mL) and a stirring-bar were added into a Schlenk-tube. After three freeze-pump-thaw cycles the tube was backfilled with argon, sealed, placed into an oil bath at 60 °C and removed after 24 h. The tube was subsequently cooled with liquid nitrogen to stop the reaction. An NMR-sample was withdrawn for the determination of conversion, inhibited with a pinch of hydroquinone (approx. 5 mg) and $CDCl_3$ was added. Quantitative conversion was estimated based on the NMR data (see Sect. 9.3 for details of the calculation). The residue was dialyzed against deionized water with a SpectraPor3 membrane (MWCO = 1,000 Da) for 3 days at ambient temperature. The solvent was removed in vacuo to yield the polymer as a yellow solid (422.0 mg, 76 %, **SEC(THF)**: M_{nSEC} = 6,500 g mol^{-1}, $Đ_m$ = 1.11).

4.4.5 Exemplary Procedure for the RAFT Polymerization of HPMA

7 (60.5 mg, 0.20 mmol, 1.0 eq.), HPMA (2.00 g, 14.18 mmol, 35.5 eq.), V-501 (11.6 mg, 0.04 mmol, 0.2 eq.), DMF (6.0 mL), acetic acid/sodium acetate buffer (pH 5.2, 0.27 M acetic acid and 0.73 M sodium acetate; 6.0 mL) and a stirring-bar were added into a Schlenk-tube. After three freeze-pump-thaw cycles the tube was backfilled with argon, sealed, placed into an oil bath at 70 °C and removed after 2 h. The tube was subsequently cooled with liquid nitrogen to stop the reaction. A NMR-sample was withdrawn for the determination of conversion, inhibited with a pinch of hydroquinone (approx. 5 mg) and D_2O was added. A conversion of 23 % was estimated based on the NMR data (see Sect. 9.3 for details of the calculation). The residue was dialyzed against deionized water with a SpectraPor3 membrane (MWCO = 1,000 Da) for 3 days at ambient temperature. The solvent was removed in vacuo to yield the polymer as a yellow solid (0.37 g, 80 %, **SEC(DMAc)**: M_{nSEC} = 6,500 g mol^{-1}, $Đ_m$ = 1.17).

4.4.6 Exemplary Click-Reaction of Alkyne-Functionalized PHPMA with β-CD–N_3

Alkyne-functionalized PHPMA (M_{nSEC} = 6,500 g mol^{-1}; 150.0 mg, 0.023 mmol, 1.0 eq.), β-CD–N_3 (133.8 mg, 0.115 mmol 5.0 eq.), PMDETA (34 µl, 0.163 mmol, 7.1 eq.), DMF (5.3 mL) and a stirring-bar were introduced into a Schlenk-tube. After three freeze-pump-thaw cycles the tube was filled with argon and CuBr (19.8 mg, 0.138 mmol, 6.0 eq.) was added under a stream of argon. Subsequently, two freeze-pump-thaw cycles were performed, the tube was backfilled with argon and the mixture stirred at ambient temperature for 24 h. EDTA-solution (5 wt%, 1 mL) was added and the residue was dialyzed against deionized water with a SpectraPor3 membrane (MWCO = 2,000 Da) for 3 days at ambient temperature. The solvent was removed in vacuo to yield the CD-functionalized polymer as a yellow solid (96.0 mg, 55 %, **SEC(DMAc)**: M_{nSEC} = 7,300 g mol^{-1}, $Đ_m$ = 1.29).

4.4.7 Exemplary Supramolecular ABA Block Copolymer-Formation via CD/Guest Interaction

CD-functionalized PHPMA (M_{nSEC} = 7,300 g mol^{-1}; 70.0 mg, 0.0096 mmol, 2.0 eq.) was dissolved in DMF (4 mL) and added dropwise to a solution of doubly adamantyl-functionalized PDMAAm (M_{nSEC} = 6,400 g mol^{-1}; 30.0 mg, 0.0047 mmol, 1.0 eq.) in DMF (2 mL) under vigorous stirring. The resulting solution was dialysed against a deionized water/DMF-mixture with a SpectraPor3 (MWCO = 1,000 Da) membrane at 4 °C . The water-content was gradually changed from 70 to 100 % over 1 day and the dialysis was continued for 3 days with deionized water at 4 °C . The solvent was removed in vacuo to yield the supramolecular complex in quantitative yield.

References

1. Schmidt BVKJ, Hetzer M, Ritter H, Barner-Kowollik C (2013) UV Light and Temperature Responsive Supramolecular ABA Triblock Copolymers via Reversible Cyclodextrin Complexation. Macromolecules 46(3):1054–1065. doi:10.1021/ma302386w
2. Lodge TP (2003) Block copolymers: past successes and future challenges. Macromol Chem Phys 204:265–273
3. Ruzette A-V, Leibler L (2005) Block copolymers in tomorrow's plastics. Nat Mater 4:19–31
4. Ishizone T, Hirao A (2012) In synthesis of polymers: new structures and methods. In: Schlüter A D, Hawker CJ, Sakamoto J (eds) Chapter anionic polymerization: recent advances, Wiley-VCH, Weinheim, pp 81–134
5. Aoshima S, Kanaoka S (2009) A renaissance in living cationic polymerization. Chem Rev 109:5245–5287
6. Hawker CJ, Bosman AW, Harth E (2001) New polymer synthesis by nitroxide mediated living radical polymerizations. Chem Rev 101:3661–3688

7. Ouchi M, Terashima T, Sawamoto M (2009) Transition metal-catalyzed living radical polymerization: toward perfection in catalysis and precision polymer synthesis. Chem Rev 109:4963–5050
8. Matyjaszewski K (2012) Atom Transfer Radical Polymerization (ATRP): current status and future perspectives. Macromolecules 45:4015–4039
9. Chiefari J, Chong YK, Ercole F, Krstina J, Jeffery J, Le TPT, Mayadunne RTA, Meijs GF, Moad CL, Moad G, Rizzardo E, Thang SH (1998) Living free-radical polymerization by reversible addition/fragmentation chain transfer: the RAFT process. Macromolecules 31:5559–5562
10. Barner-Kowollik C (2008) Handbook of RAFT-polymerization. Wiley-VCH, Weinheim
11. Lutz JF (2007) 1,3-dipolar cycloadditions of azides and alkynes: a universal ligation tool in polymer and materials science. Angew Chem Int Ed 46:1018–1025
12. Barner-Kowollik C, Inglis AJ (2009) Has click chemistry lead to a paradigm shift in polymer material design? Macromol Chem Phys 210:987–992
13. Kempe K, Krieg A, Becer CR, Schubert US (2012) "Clicking" on/with polymers: a rapidly expanding field for the straightforward preparation of novel macromolecular architectures. Chem Soc Rev 41:176–191
14. Opsteen JA, van Hest JCM (2005) Modular synthesis of block copolymers via cycloaddition of terminal azide and alkyne functionalized polymers. Chem Commun 41:57–59
15. Hizal G, Tunca U, Sanyal AJ (2011) Discrete macromolecular constructs via the diels alder click reaction. Polym Sci Part A Polym Chem 49:4103–4120
16. Inglis AJ, Stenzel MH, Barner-Kowollik C (2009) Ultra-fast RAFT-HDA click conjugation: an efficient route to high molecular weight block copolymers. Macromol Rapid Commun 30:1792–1798
17. Schmidt BVKJ, Fechler N, Falkenhagen J, Lutz JF (2011) Controlled folding of synthetic polymer chains through the formation of positionable covalent bridges. Nat Chem 3:234–238
18. Yan Q, Xin Y, Zhou R, Yin Y, Yuan J (2011) Light-controlled smart nanotubes based on the orthogonal assembly of two homopolymers. Chem Commun 47:9594–9596
19. Yan Q, Yuan J, Cai Z, Xin Y, Kang Y, Yin Y (2010) Voltage-responsive vesicles based on orthogonal assembly of two homopolymers. J Am Chem Soc 132:9268–9270
20. Stadermann J, Komber H, Erber M, Däbritz F, Ritter H, Voit B (2011) Diblock copolymer formation via self-assembly of cyclodextrin and adamantyl end-functionalized polymers. Macromolecules 44:3250–3259
21. Zeng J, Shi K, Zhang Y, Sun X, Zhang B (2008) Construction and micellization of a noncovalent double hydrophilic block copolymer. Chem Commun 44:3753–3755
22. Liu H, Zhang Y, Hu J, Li C, Liu S (2009) Multi-responsive supramolecular double hydrophilic diblock copolymer driven by host-guest inclusion complexation between beta-cyclodextrin and adamantyl moieties. Macromol Chem Phys 210:2125–2137
23. Zhang Z-X, Liu X, Xu FJ, Loh XJ, Kang E-T, Neoh K-G, Li J (2008) Pseudo-block copolymer based on star-shaped poly(N-isopropylacrylamide) with a beta-cyclodextrin core and guest-bearing PEG: controlling thermoresponsivity through supramolecular self-assembly. Macromolecules 41:5967–5970
24. Zhang Z-X, Liu KL, Li J (2011) Self-assembly and micellization of a dual thermoresponsive supramolecular pseudo-block copolymer. Macromolecules 44:1182–1193
25. Yhaya F, Binauld S, Callari M, Stenzel MH (2012) One-pot endgroup-modification of hydrophobic RAFT polymers with cyclodextrin by thiol-ene chemistry and the subsequent formation of dynamic core-shell nanoparticles using supramolecular host/guest chemistry. Aust J Chem 65:1095–1103
26. Quan C-Y, Chen J-X, Wang H-Y, Li C, Chang C, Zhang X-Z, Zhuo R-X (2010) Core/shell nanosized assemblies mediated by the alpha/beta cyclodextrin dimer with a tumor-triggered targeting property. ACS Nano 4:4211–4219
27. Rao J, Paunescu E, Mirmohades M, Gadwal I, Khaydarov A, Hawker CJ, Bang J, Khan A (2012) Supramolecular mimics of phase separating covalent diblock copolymers. Polym Chem 3:2050–2056

28. Fleige E, Quadir MA, Haag R (2012) Stimuli-responsive polymeric nanocarriers for the controlled transport of active compounds: concepts and applications. Adv Drug Delivery Rev 64:866–884
29. Gan LH, Cai W, Tam KC (2001) Studies of phase transition of aqueous solution of poly(N,N-diethylacrylamide-co-acrylic acid) by differential scanning calorimetry and spectrophotometry. Eur Polym J 37:1773–1778
30. Rekharsky MV, Inoue Y (1998) Complexation thermodynamics of cyclodextrins. Chem Rev 98:1875–1918
31. Ross PD, Rekharsky MV (1996) Thermodynamics of hydrogen bond and hydrophobic interactions in cyclodextrin complexes. Biophys J 71:2144–2154
32. Del Valle EMM (2004) Cyclodextrins and their uses: a review. Process Biochem 39:1033–1046
33. Takashima Y, Nakayama T, Miyauchi M, Kawaguchi Y, Yamaguchi H, Harada A (2004) Complex formation and gelation between copolymers containing pendant azobenzene groups and cyclodextrin polymers. Chem Lett 33:890–891
34. Tomatsu I, Hashidzume A, Harada A (2005) Photoresponsive hydrogel system using molecular recognition of alpha-cyclodextrin. Macromolecules 38:5223–5227
35. Kwak RNY, Matyjaszewski K (2008) Dibromotrithiocarbonate iniferter for concurrent ATRP and RAFT polymerization. Effect of monomer, catalyst, and chain transfer agent structure on the polymerization mechanism. Macromolecules 41:4585–4596

Chapter 5
Supramolecular Three Armed Star Polymers

5.1 Introduction

Star polymers are an important class of polymers that have attracted significant attention in the last years [2–4]. This can be attributed to unique properties originating from their condensed structure, non-linear shape, and multiple chain ends per macromolecule. Many applications for such systems have been discussed in the literature, e.g. as unimolecular nanocontainers [5], for drug-delivery [6] or in organic light-emitting diodes [7].

Traditionally, the synthesis of star polymers has been carried out via living polymerization techniques, i.e. anionic [4] or cationic [8, 9] methodologies. According to these synthetic strategies, one can distinguish between multifunctional initiators, i.e. the core-first approach [10], or multifunctional termination agents, i.e. the arm-first approach [11]. Especially the introduction of controlled radical polymerization techniques, i.e. NMP [12], ATRP [13], and RAFT polymerization [14, 15], have led to the generation of a broad range of star polymers in core-first approaches via multifunctional initiators or CTAs [16–18]. As an alternative, modular conjugation reactions can be employed for the synthesis of such architectures, e.g. via click chemistry [3, 19] in an arm-first approach. Several methods have been employed in that regard benefiting from high efficiency, short reaction times, and possible equimolarity of the reactions that fulfil the respective criteria [20]. Some examples include the copper-catalyzed azide-alkyne cycloaddition (CuAAc) [21, 22], the thiolene reaction [23], or the RAFT hetero Diels–Alder reaction [24]. As these strategies represent orthogonal approaches, they are nowadays also widely employed for the synthesis of miktoarm star polymers [3, 19, 25].

DLS measurements were performed in collaboration with T. Rudolph and Prof. F. H. Schacher (Friedrich Schiller Universität Jena). ROESY measurements were performed in collaboration with M. Hetzer and Prof. H. Ritter (Heinrich Heine Universität Düsseldorf). Parts of this chapter were reproduced from Schmidt et al. [1] with permission from the Royal Society of Chemistry.

B. V. K. J. Schmidt, *Novel Macromolecular Architectures via a Combination of Cyclodextrin Host/Guest Complexation and RAFT Polymerization*, Springer Theses,
DOI: 10.1007/978-3-319-06077-4_5, © Springer International Publishing Switzerland 2014

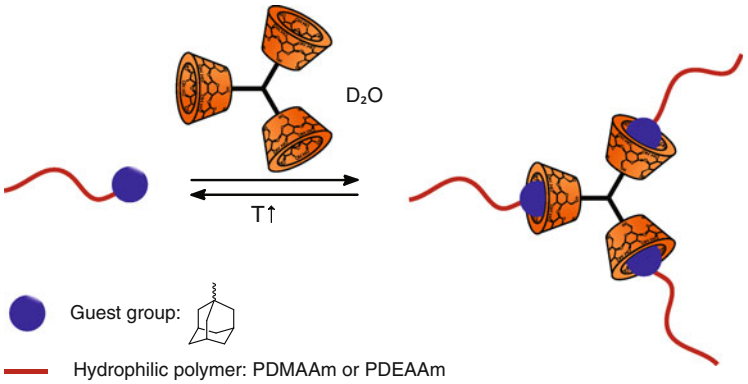

Scheme 5.1 Schematic representation of supramolecular star polymer formation via host/guest inclusion complexes between adamantyl-functionalized polyacrylamides (polymer *red*; adamantyl-group *blue*) and a three-pronged β-CD linker (*orange*)

New opportunities arise from the synthesis of supramolecular star polymers. Here, the formation of the star polymer is driven by supramolecular interactions that offer reversible and potentially stimuli-responsive bond-formation amongst other properties. The mainly utilized types of supramolecular interactions comprise hydrogen-bonding [26–28], metal-ligand-coordination [29–31] or host/guest complexation [32]. An important class of hosts in the realm of host/guest complexations are CDs due to their availability and the ease of chemical modification. Considering star polymer synthesis the ability of CDs to form inclusion complexes with hydrophobic guest molecules enables the formation of new materials. Apart from the formation of new macromolecular architectures, this ability is widely used in polymer chemistry, e.g. for drug- or siRNA-delivery [33–35], or to solubilize hydrophobic monomers [36–38]. In the case of star polymers CD has been mainly used as a core molecule in the past, e.g. in ATRP [39], RAFT [40], or in a combination of ATRP and NMP [41]. Here, however, the arms were covalently attached to the CD core. In an alternative example CD-centered star polymers were reported, where two cores are bound employing supramolecular interactions [42, 43].

In this chapter the formation of supramolecular three-armed star polymers using CD host/guest interactions is presented. The materials consist of adamantyl-functionalized polyacrylamides as arms and a threefold β-CD-functionalized core molecule (refer to Scheme 5.1). An adamantyl-functionalized CTA was utilized in the RAFT polymerization of DMAAm and DEAAm for the synthesis of the arms, which were subsequently characterized via ESI-MS, NMR and SEC. In aqueous solution, supramolecular complexes were formed and the existence of three-armed star polymers was proven via ROESY as well as DLS.

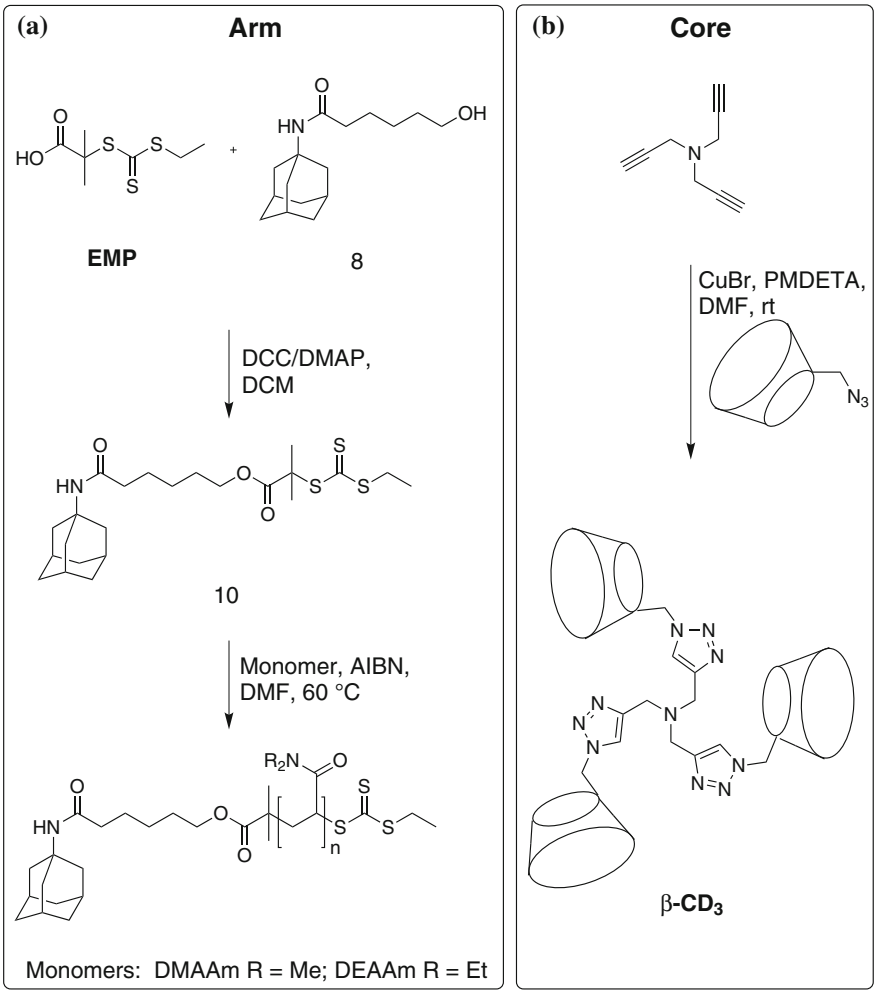

Scheme 5.2 Synthesis of the building blocks utilized for star polymer formation: **a** adamantyl-functionalized RAFT-agent (**10**), followed by the synthesis of polyacrylamides; **b** synthesis of the three-pronged β-CD core (β-**CD$_3$**)

5.2 Results and Discussion

5.2.1 Synthesis and Characterization of the Building Blocks

For the formation of supramolecular star polymers two types of building blocks were synthesized (Scheme 5.2): adamantyl end-functionalized polymers as arms (guest) and a three-pronged β-CD-functionalized core as the host.

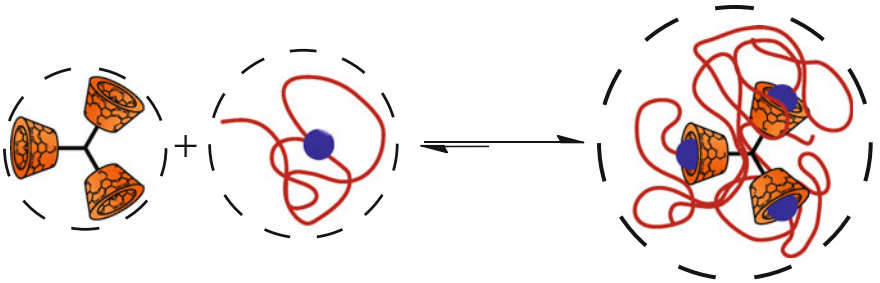

Scheme 5.3 Schematic representation of the formation of supramolecular star polymers, indicating the expected changes in hydrodynamic radius (R_h *dashed circles*)

Table 5.1 Results for the RAFT polymerization of DMAAm (top) and DEAAm (bottom) with **10** at 60 °C in DMF with AIBn as initiator

DMAAm/**10**/I	Time/(h)	*Conv.*	M_{ntheo}/(g mol^{-1})	M_{nSEC} /(g mol^{-1})	$Đ_m$	D_p
21/1/0.1	24	quant.	2,550	3,500	1.08	31
100/1/0.2	24	quant.	10,370	14,600	1.12	143
241/1/0.2	24	96 %	23,400	20,500	1.23	202
101/1/0.2	24	quant.	13,300	11,500	1.11	87

The adamantyl-functionalized polymers were synthesized via RAFT-polymerization using a trithiocarbonate-containing CTA **10**. The prominent adamantyl moiety was chosen as guest-group due to its high complexation constants with β-CD of up to 10^5 M^{-1} [44]. The CTA was synthesized starting from an adamantyl-containing alcohol via DCC-coupling with **EMP** as shown in Scheme 5.2a. The adamantyl moiety was separated from the trithiocarbonate group with a C_5-spacer to improve its accessibility for the inclusion process. Subsequently, RAFT polymerizations were conducted with DMAAm and DEAAm utilizing several CTA/monomer ratios. Polymerization degrees ranging from 31 to 202 with M_n ranging from 3,500 to 20,500 g mol^{-1} and low $Đ_m < 1.25$ were achieved for PDMAAm. Furthermore, the thermoresponsive adamantyl-functionalized PDEAAm was prepared via RAFT polymerization with **10** affording a polymerization degree of 87 with a M_n of 11,500 g mol^{-1} and a low $Đ_m$ (see Table 5.1).

The RAFT polymerization of DMAAm and DEAAm with **10** yielded unimodal molecular mass distributions (Fig. 5.1). For higher molecular masses a certain tailing to higher elution volumes was observed, presumably due to interactions with the column during SEC. The structure of the obtained polymers was verified via ^{1}H-NMR and ESI-MS (refer to the Appendix Figs. C.1–C.4).

The three-pronged CD-functional building block β-CD_3 was synthesized via CuAAc starting from tripropargylamine and β-CD-N_3 (Scheme 5.2b) [45]. The product was analyzed via ^{1}H-NMR and ESI-MS (Appendix C.5/C.6).

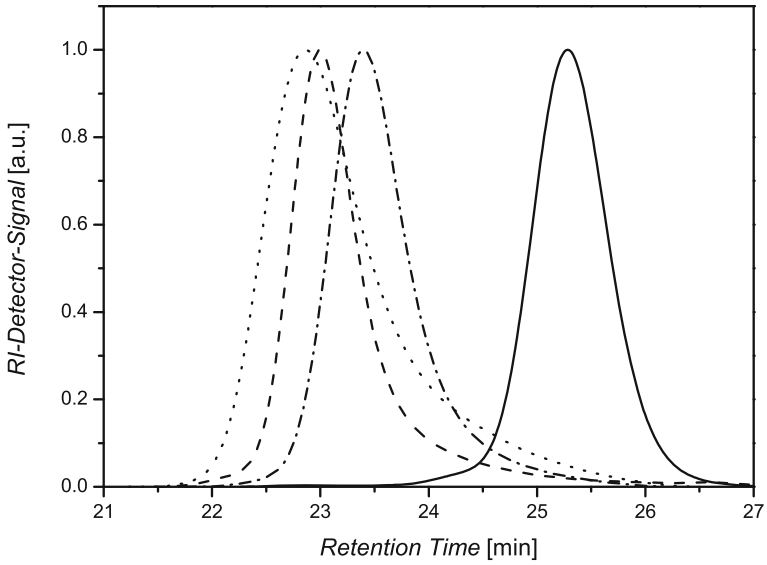

Fig. 5.1 SEC-traces for $PDMAAm_{31}$-Ad (*solid black line*), $PDMAAm_{143}$-Ad (*dashed black line*), $PDMAAm_{202}$-Ad (*dotted black line*), and $PDEAAm_{87}$-Ad (*solid dashed-dotted line*)

5.2.2 *Star Polymer Formation: Investigations Using Light Scattering*

Light scattering experiments are a powerful method for the in situ investigation of polymeric systems in solution. Before mixing the arms and the core moiety, all individual compounds were analyzed via DLS at ambient temperature in H_2O and D_2O. Surprisingly, all polyacrylamide-compounds seemed to be better soluble in D_2O, resulting in an increase of ~20 % of the hydrodynamic radius (R_h) (Fig. 5.2), while for **β-CD_3** no difference was observed. Such an effect has also been observed for PNIPAAm [46–48], although the reason was not fully understood. The increased hydrodynamic volumes of the polymer chains should, however, lead to a better accessibility of the adamantyl moiety for the inclusion process with the β-CD_3 core. Therefore, all following experiments were performed in D_2O at a polymer concentration of 5 mg mL^{-1}. In addition, control experiments in H_2O were carried out (Fig. 5.3a).

Adamantyl-functionalized PDMAAm with three different molar masses were combined in stoichiometric amounts (3:1) with the **β-CD_3** core, dissolved in D_2O, stirred and analyzed using DLS after 12 and 24 h (also after several days, Fig. 5.5), showing a clear shift to higher hydrodynamic radii with time. For $PDMAAm_{31}$ (M_{nSEC} = 3,500 g mol^{-1}) an apparent hydrodynamic radius R_h = 1.8 nm was observed, while the β-CD_3 exhibits a radius of R_h = 1.3 nm. After 12 h at ambient temperature, an increase in size to R_h = 2.3 nm was found, which remained constant over several days. This corresponds to an expansion ratio of 1.3. The same

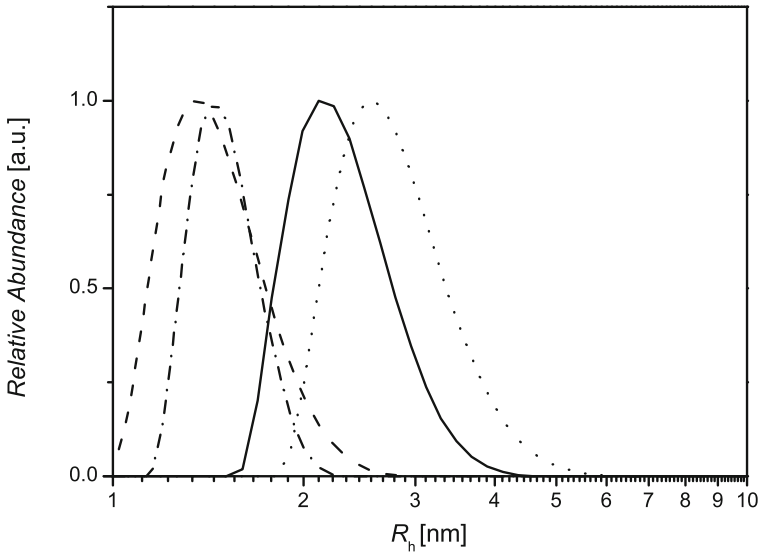

Fig. 5.2 Comparison of the number averaged hydrodynamic radii for the core β-CD_3 in H_2O (*dashed line*) and D_2O (*dashed-dotted line*) and $PDMAAm_{143}$-Ad in H_2O (*solid line*) and in D_2O (*dotted line*) at 25 °C

procedure was utilized for $PDMAAm_{143}$ and $PDMAAm_{202}$ and a R_h of 2.5 and 3.3 nm for the unimolecular polymer chains was observed, respectively. After stoichiometric mixing in a molar ratio of 3:1 with the CD-core moiety, a distinct increase in size can be observed in both cases. For $PDMAAm_{143}$, supramolecular star polymers with R_h = 3.7 nm were observed whereas in case of $PDMAAm_{202}$ the aggregate size was even larger, with R_h = 4.6 nm, owing to longer polyacrylamide arms. An expansion ratio of 1.5 and 1.4 (Table 5.2) was deduced. In all cases, monomodal number-weighted size distributions were observed, indicating full inclusion of the guest-polymer chains into the CD core (Fig. 5.4). The proposed structure formation mechanism is depicted in Scheme 5.3, which also illustrates the rather small observed expansion ratios. As the arms of the formed supramolecular star polymers form coils in solution in three dimensions, the observed R_h of the star polymers is smaller than the sum of the individual parts.

For all investigated combinations of the arms with the core, an increase of the hydrodynamic radius was observed, hinting at the formation of star-shaped aggregates. The expansion ratio (Table 5.2) yields comparable values for all polymers investigated. Adamantyl-functionalized polymers with higher a molecular mass leads to higher hydrodynamic radii. Furthermore, the size distributions of the adamantyl-functionalized polymers were measured after the addition of crude β-CD (refer to Fig. 5.3b) to prove that the increase in R_h is due to the three-pronged nature of **β-CD_3**.

For control experiments, the linear polymer was dissolved together with the linker molecule **β-CD_3** in H_2O and analyzed over several days without any change in the

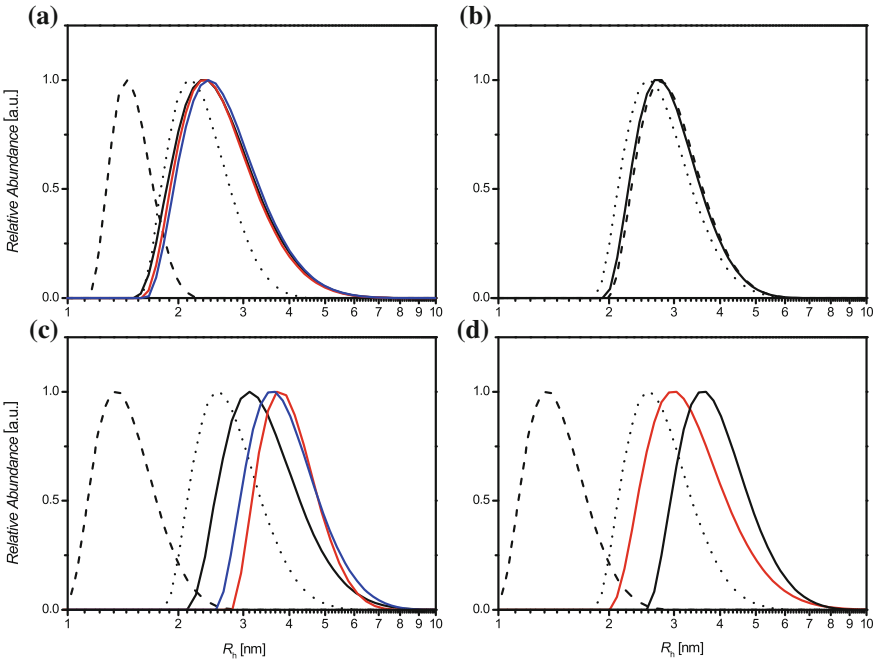

Fig. 5.3 Number averaged hydrodynamic radii obtained from DLS measurements **a** for PDMAAm$_{143}$-Ad (*black dotted line*) mixed with the *β*-**CD$_3$** core (*black dashed line*) and the resulting supramolecular star polymers over several days in H_2O at 25 °C (1 day *black solid line*; 5 days *red solid line*; 9 days *blue solid line*); **b** for PDMAAm$_{143}$-Ad mixed (*dotted line*) with *β*-CD at 25 °C in D_2O (stoichiometric *β*-CD *solid line*; excess *β*-CD *dashed line*); **c** for PDMAAm$_{143}$-Ad (*black dotted line*) mixed with the *β*-**CD$_3$** core (*black dashed line*) in a time dependent investigation of the self-assembly process (10 min *black solid line*; 1 h *red solid line*; 12 h *blue solid line*); **d** for PDMAAm$_{143}$-Ad (*black dotted line*) mixed with the *β*-**CD$_3$** core (*black dashed line*) for a 1:1 mixture of PDMAAm$_{143}$-Ad (*red solid line*) and the *β*-**CD$_3$** core with a molar ratio of 3:1 (*black solid line*) (D_2O, 25 °C)

R_h being observed (Fig. 5.3a). In Fig. 5.3c the increase of R_h with time is depicted. A growth of R_h with time is visible. After 10 min the complex formation progressed to a large extend and after 5 h the complex formation is finished. As a further control the *β*-**CD$_3$** was mixed in an excess with the polymer (Fig. 5.3d), which shows no significant increase in R_h. This can be attributed to a formation of only one supramolecular connection per guest functionalized chain and thus the size of the aggregate is smaller compared to the incorporation of three guest functionalized polymer chains in the complex.

The reversibility of star polymer formation at higher temperatures was also investigated via DLS (Fig. 5.4d). Therefore, the temperature was increased from 25 to 70 °C in 2 h and the sample was kept at this temperature for further 30 min. As a result, a decrease of the R_h from 3.7 to 2.8 nm was observed. This might well correspond to the expulsion of the adamantyl moiety from the *β*-**CD$_3$** core

Table 5.2 DLS results (number averaged hydrodynamic radii) for the individual building blocks, the supramolecular star polymers after self-assembly, and the respective expansion ratio at 25 °C in D_2O

Polymer	$R_{h,\text{crude polymer}}$/(nm)	$R_{h,\text{polymer@}\beta\text{-CD}_3}$/(nm)	Expansion ratio
β-CD$_3$	1.3	–	–
PDMAAm$_{31}$-Ad	1.8	2.3	1.3
PDMAAm$_{143}$-Ad	2.5	3.7	1.5
PDMAAm$_{202}$-Ad	3.3	4.6	1.4
PDEAAm$_{87}$-Ad	2.4	3.8	1.6

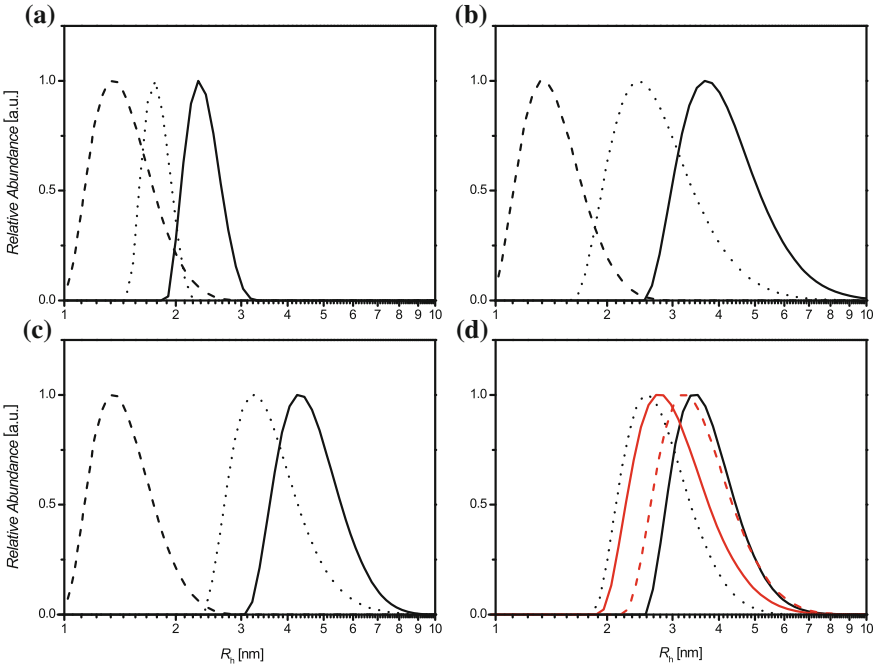

Fig. 5.4 Number averaged hydrodynamic radii obtained from DLS measurements for PDMAAm$_x$: **a** x = 31, **b** x = 143 and **c** x = 202 (*dotted lines*), the **β-CD$_3$** core molecule (*dashed lines*), and the resulting supramolecular star polymers in a molar ratio of 3:1 after 24 h in D_2O at 25 °C (*solid lines*); **d** Investigations regarding the reversibility of the inclusion process by heating the complex from 25 °C (*black solid line*) to 70 °C (*red solid line*), followed by cooling and re-formation of the aggregates (*red dotted line*) (*black dotted line* arm polymer for comparison)

(Fig. 5.4d, red solid line). Afterwards, the sample solution was cooled down to 25 °C and, subsequently, the R_h increased again.

Comparable investigations were carried out using PDEAAm$_{87}$ (Fig. 5.5a), a polymer which exhibits cloud point behaviour [49]. Depending on the molar mass and the respective end group, PDEAAm materials undergo a coil-to-globule transition

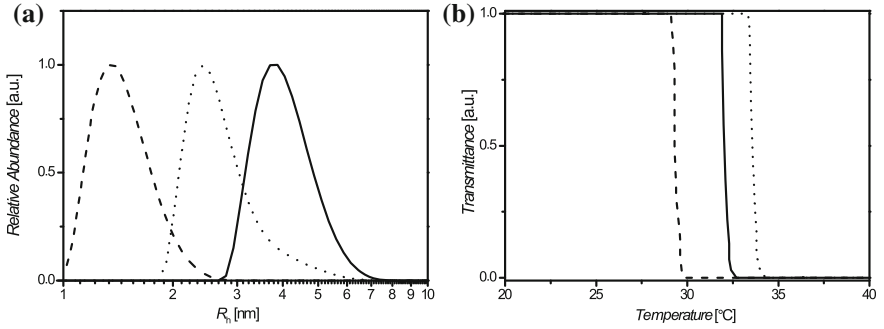

Fig. 5.5 **a** Number averaged size distributions obtained from DLS measurements for the supramolecular star polymer (*solid line*), PDEAAm$_{87}$-Ad (*dotted line*), and the β-**CD$_3$** core (*dashed line*) in a molar ratio of 3:1 after 24 h at 25 °C; **b** turbidity measurements for PDEAAm$_{87}$-Ad (*dotted line*), the supramolecular star polymer (*solid line*), and a mixture of PDEAAm$_{87}$-Ad and β-CD (*dashed line*) mixture in D_2O

in the temperature range of 25–40 °C [49, 50]. Again, stoichiometric amounts of PDEAAm$_{87}$-Ad and the CD-core were mixed in D_2O and the resulting assemblies were investigated using DLS. An increase in R_h from 2.4 to 3.8 nm was observed, corresponding to an expansion ratio of 1.6, similar values if compared to the earlier discussed PDMAAm systems (Fig. 5.5a).

To elucidate the temperature-dependent solubility of the PDEAAM-based supramolecular star polymers in water, turbidimetry measurements were carried out. Any changes in temperature were performed with a heating/cooling rate of 1 °C min^{-1}. The cloud point temperature (T_c) was determined at a transmittance of 50 %. Three samples, PDEAAm$_{87}$-Ad, the supramolecular star polymer, and a mixture of β-CD and PDEAAm$_{87}$, were investigated in a temperature range of 5−100 °C in D_2O. For PDEAAm$_{87}$, a T_c of 29.3 °C was found, while the mixture with CD led to a higher value (T_c = 33.6 °C). Such an observation can be explained by the complexation of the adamantyl moiety by β-CD and therefore the formation of a less hydrophobic endgroup. In case of the star-shaped system a cloud point at 32.0 °C was observed in between the values for PDEAAm$_{87}$-Ad and the β-CD containing mixture (Fig. 5.5b). This might be explained by a shielding of the hydrophobic adamantyl groups due to the inclusion complex formation and—at the same time—a decrease in the conformational freedom of the individual polymer chains by connecting three arms to one core moiety. The sharp decrease of the transmittance and the reversibility of the turbidimetry measurements (at least three times) are an additional indication for the successful formation of supramolecular star polymers via host/guest inclusion complexes. The collapse of the PDEAAm arms leads to an inclusion of the β-**CD$_3$** into the collapsed polymer coil at a temperature far below the dissociation of the host/guest complex (∼70 °C), as demonstrated using DLS in Fig. 5.4d.

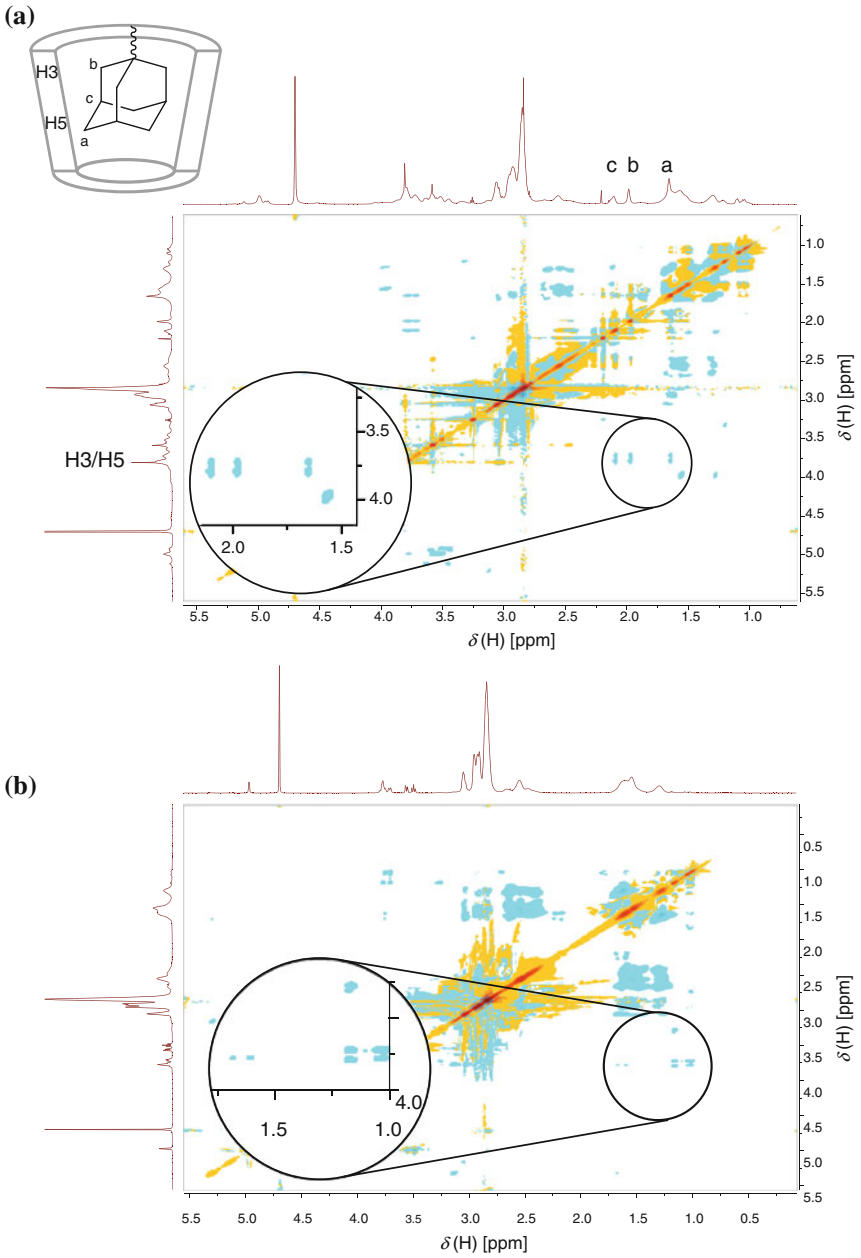

Fig. 5.6 2D ROESY spectrum (the *insets* show a magnification of the relevant peaks) in D_2O at 25 °C of **a** 3:1 molar mixture of $PDMAAm_{31}$-Ad (M_{nSEC} = 3,500 g mol^{-1}, $Đ_m$ = 1.08) and the **β-CD$_3$** core; **b** 1:1.1 molar mixture of PDMAAm (M_{nSEC} = 12,800 g mol^{-1}, $Đ_m$ = 1.10) polymerized with **EMP** and β-CD

5.2.3 Investigations of the Self-Assembly via ROESY

ROESY is a perfectly suitable tool to investigate the formation of inclusion complexes. The cross-correlation peaks in the ROESY spectrum can be assigned to protons that are closely situated (<4 Å) [51]. While DLS experiments probe the molecular nature of the star polymers, ROESY was performed to demonstrate the formation of the inclusion complex between the adamantyl moiety of polymer arms and the **β-CD$_3$** core.

The 2D ROESY spectrum (Fig. 5.6a) shows six cross-correlation peaks that can be assigned to the adamantyl moiety and the β-CD moiety. The a, b and c protons of the adamantyl group feature resonances at 1.7, 2.0 and 2.1 ppm, respectively, whereas the inner protons H3 and H5 of β-CD have resonances at 3.7 and 3.8 ppm. In the 2D spectrum, the signals are located at the corresponding intersections that are expected for an inclusion complex of β-CD and the adamantyl moiety. Thus, a close distance between the protons of the adamantyl and β-CD moiety can be concluded, confirming the formation of an inclusion complex [52]. To exclude complex formation between the CD and the side chains of PDMAAm, a control sample of PDMAAm polymerized with **EMP** without the adamantyl moiety and β-CD was investigated as well, where the respective cross-correlation peaks were absent in the 2D NMR (Fig. 5.6b). Instead cross-correlation peaks between CD and the isobutyric acid or ethyl endgroups arise (cross-correlation peaks at 1.0–1.3 and 1.7 with 3.7 and 3.8 ppm). Nevertheless these signals are not present, when adamantyl functionalized polymers are added. This could be due to the increased association constant of the adamantyl moiety compared to an isobutyric acid or ethyl group.

5.3 Conclusions

In summary, the formation of supramolecular star polymers via the formation of inclusion complexes between adamantyl-functionalized polyacrylamides and a three-pronged CD-core was performed. The synthesis of PDMAAm-Ad and PDEAAm-Ad was carried out via RAFT polymerization with a novel adamantyl-functionalized chain transfer agent (**10**). The core, **β-CD$_3$**, was synthesized via CuAAc techniques. All building blocks were characterized via SEC, ^{1}H-NMR and ESI-MS.

The formation of supramolecular star polymers was carried out in D_2O and evidenced via a combination of DLS and 2D ROESY. In the case of star polymers with PDEAAm arms, additional turbidity measurements revealed a change in temperature-dependent solution behaviour. The star polymer formation was shown to be reversible, as heating to 70 °C leads to an expulsion of the individual polymer arms and cooling to 25 °C to re-formation of the complex.

5.4 Experimental Part

5.4.1 Synthesis of 6-(Adamantan-1-ylamino)-6-oxohexyl 2-(((ethylthio)carbonothioyl)thio)-2-methylpropanoate (10)

In a 50 mL Schlenk-flask, **EMP** (0.84 g, 3.75 mmol, 1.0 eq.), *N*-(adamantan-1-yl)-6-hydroxyhexanamide (**8**)(1.00 g, 3.77 mmol, 1.0 eq.) and DMAP (0.09 g, 0.74 mmol, 0.2 eq.) were dissolved in anhydrous DCM (15 mL). At 0 °C a solution of DCC (1.17 g, 5.67 mmol, 1.5 eq.) in anhydrous DCM (10 mL) was added. After 1 h the solution was warmed to ambient temperature, stirred overnight, filtered and concentrated under reduced pressure. The residual oil was purified via column chromatography on silica-gel with a 5:1 mixture of *n*-hexane:ethyl acetate as eluent. The product was obtained as yellow oil (1.08 g, 2.29 mmol, 61 %).

^{1}H-NMR (400 MHz, $CDCl_3$): [δ, ppm] = 1.27–1.43 (m, 5H, C***H***$_3$–CH_2; C***H***$_2$–CH_2–CH_2–O), 1.53–1.73 (m, 16H, 2x C–C***H***$_3$; C***H***$_2$–CH_2–O; C***H***$_2$–CH_2–C=O; 3x C***H***$_{2,adamantyl}$), 1.98 (d, 6H, ^3J = 2.8 Hz, 3x NH–C–C***H***$_{2,adamantyl}$), 2.02–2.10 (m, 5H, 3x C***H***$_{adamantyl}$; C***H***$_2$–C=O–NH), 3.28 (q, 2H, ^3J = 7.4 Hz, C***H***$_2$–CH_3), 4.08 (t, 2H, ^3J = 6.5 Hz, C***H***$_2$–O), 5.11 (br s, 1H, N***H***). **^{13}C-NMR** (100 MHz, $CDCl_3$): δ, ppm = 13.1 (***C***H_3–CH_2), 25.5, 25.7 and 28.3 (***C***H_2–CH_2–C=O; ***C***H_2–CH_2–CH_2–C=O; ***C***H_2–CH_2–C=O–NH; 2x ***C***H_3–C=O), 29.6 (3x ***C***$H_{adamantyl}$), 31.3 (CH_3–***C***H_2), 36.5 (3x ***C***$H_{2,adamantyl}$), 37.8 (***C***H_2–C=O–NH), 41.9 (3x ***C***$CH_{2,adamantyl}$–C–NH), 52.0 (***C***–NH), 56.2 (***C***$(CH_3)2$), 66.0 (CH_2–***C***H_2–O), 172.1 (NH–***C***=O), 173.1 (O–***C***=O), 221.4 (***C***=S). **ESI-MS**: $[M + Na^+]_{exp}$ = 494.42 m/z and $[M + Na^+]_{calc}$ = 494.18 m/z.

5.4.2 Synthesis of N,N,N-(Tris-1-(mono-(6-desoxy)-β-CD)-1H-1,2,3-triazol-4-yl)methanamine (β-CD$_3$)

The preparation of this compound was modified from a literature procedure [45]. In a 50 mL Schlenk-tube tripropargylamine (34 mg, 0.26 mmol, 1.0 eq.), PMDETA (0.16 mL, 0.77 mmol, 3.0 eq.) and β-CD-N_3 (1.00 g, 0.86 mmol, 3.3 eq.) were dissolved in DMF (11 mL). After three freeze–pump–thaw cycles the tube was backfilled with argon and CuBr (112 mg, 0.78 mmol, 3.0 eq.) was added under a flow of argon. The tube was sealed again and subjected to two freeze–pump–thaw cycles. Subsequently the tube was backfilled with argon and immersed in an oil bath at 70 °C for 4 days. After cooling to ambient temperature the product was precipitated in an excess of acetone. The product was filtered, dissolved in 10 mL EDTA-solution (5 wt%) and dialyzed with a SpectraPor3 membrane (MWCO = 2,000 Da) for 3 days at ambient temperature. Finally the solvent was removed in vacuo to yield **β-CD$_3$** (574 mg, 0.16 mmol, 61 %) as an off-white solid.

^{1}H-NMR (400 MHz, D_2O): [δ, ppm] = 3.18 (d, 3H, ^3J = 11.5 Hz, N–NC***H***(gem)$_2$), 3.32 (t, 3H, ^3J = 6.3 Hz, N–NC***H***(gem)$_2$), 3.37–4.14 (m, 124H, CD–***H***$_{2,3,4,5,6}$), 4.24 (t, 3H, ^3J = 8.8 Hz, NC***H***(gem)$_2$–C), 4.66 (dd, 3H, ^3J = 14.2, 8.4 Hz, NC***H***(gem)$_2$–C), 4.93–5.25 (m, 21H, CD–***H***1), 8.02 (s, 3H, ***H***$_{\text{triazole}}$). **ESI-MS**: [M + 2Na^{2+}]$_{\text{exp}}$ = 1,828.33 m/z and [M + 2Na^{2+}]$_{\text{calc}}$ = 1,828.09 m/z (refer to Appendix Fig. C.6 for a more detailed ESI-MS characterization)

5.4.3 Exemplary Procedure for the RAFT Polymerization

10 (60.0 mg, 0.13 mmol, 1.0 eq.), DMAAm (1.26 g, 12.72 mol, 97.9 eq.), AIBN (4.2 mg, 0.03 mmol, 0.2 eq.), DMF (6.0 mL) and a stirring-bar were added into a Schlenk-tube. After three freeze–pump–thaw cycles the tube was backfilled with argon, sealed, placed into an oil bath at 60 °C and removed after 24 h. The tube was subsequently cooled with liquid nitrogen to stop the reaction. A NMR-sample was withdrawn for the determination of conversion, inhibited with a pinch of hydroquinone (approx. 5 mg) and $CDCl_3$ was added. A quantitative conversion was calculated based on the NMR data (see Sect. 9.3 for details). The residue was dialyzed with a SpectraPor3 membrane (MWCO = 1,000 Da) for 3 days at ambient temperature. The solvent was removed in vacuo to yield the polymer as a yellow solid (1.20 g, 99 %, **SEC(DMAc)**: M_{nSEC} = 14,600 g mol^{-1}, $Đ_{\text{m}}$ = 1.12).

5.4.4 Exemplary Procedure for the Self-Assembly of the Adamantyl-Functionalized PDMAAm with β-CD$_3$

Adamantyl-functionalized PDMAAm (M_{nSEC} = 13,200 g mol^{-1}, 55.4 mg, 0.0042 mmol, 3.0 eq.) and β-CD_3 (5.0 mg, 0.0014 mmol, 1.0 eq.) were dissolved in D_2O (0.5 mL, c = 120 mg mL^{-1}) and stirred at ambient temperature overnight. Subsequently, the formed complex was characterized via 2D ROESY.

5.4.5 Preparation for Dynamic Light Scattering Experiments

Adamantyl-functionalized polymer, e.g. PDMAAm (M_{nSEC} = 14,600 g mol^{-1}, 12.4 mg, 3.0 eq.) and β-CD_3 (1.4 mg, 1.0 eq.) were dissolved in D_2O or Milli-Q water (1 mL, c = 5 mg mL^{-1}) and stirred at 25 °C.

References

1. Schmidt BVKJ, Rudolph T, Hetzer M, Ritter H, Schacher FH, Barner-Kowollik C (2012) Supramolecular three-armed star polymers via cyclodextrin host/guest self-assembly. Polym Chem 3:3139–3154. doi:10.1039/C2PY20293J
2. Inoue K (2000) Functional dendrimers, hyperbranched and star polymers. Prog Polym Sci 25:453–571
3. Khanna K, Varshney S, Kakkar A (2010) Miktoarm star polymers: advances in synthesis, self-assembly, and applications. Polym Chem 1:1171–1185
4. Higashihara T, Hayashi M, Hirao A (2011) Synthesis of well-defined star-branched polymers by stepwise iterative methodology using living anionic polymerization. Prog Polym Sci 36:323–375
5. Kreutzer G, Ternat C, Nguyen TQ, Plummer CJG, Månson J-AE, Castelletto V, Hamley IW, Sun F, Sheiko SS, Herrmann A, Ouali L, Sommer H, Fieber W, Velazco MI, Klok H-A (2006) Water-soluble, unimolecular containers based on amphiphilic multiarm star block copolymers. Macromolecules 39:4507–4516
6. Liu J, Duong H, Whittaker MR, Davis TP, Boyer C (2012) Synthesis of functional core, star polymers via RAFT polymerization for drug delivery applications. Macromol Rapid Commun 33:760–766
7. Chen L, Li P, Tong H, Xie Z, Wang L, Jing X, Wang FJ (2012) White electroluminescent single-polymer achieved by incorporating three polyfluorene blue arms into a star-shaped orange core. Polym Sci Part A Polym Chem 50:2854–2862
8. Kanaoka S, Sawamoto M, Higashimura T (1991) Star-shaped polymers by living cationic polymerization. 1. Synthesis of star-shaped polymers of alkyl and vinyl ethers. Macromolecules 24:2309–2313
9. Schlaad H, Diehl C, Gress A, Meyer M, Demirel AL, Nur Y, Bertin A (2010) Poly(2-oxazoline)s as smart bioinspired polymers. Macromol Rapid Commun 31:511–525
10. Hirano T, Yoo HS, Ozama Y, El-Magd AA, Sugiyama K, Hirao A (2010) Precise synthesis of novel ferrocene-based star-branched polymers by using specially designed 1,1-diphenylethylene derivatives in conjunction with living anionic polymerization. J Inorg Organomet Polym Mater 20:445–456
11. Roovers JEL, Bywater S (1974) Preparation of six-branched polystyrene. Thermodynamic and hydrodynamic porperties of four- and six-branched star polystyrenes. Macromolecules 7:443–449
12. Hawker CJ, Bosman AW, Harth E (2001) New polymer synthesis by nitroxide mediated living radical polymerizations. Chem Rev 101:3661–3688
13. Braunecker WA, Matyjaszewski K (2007) Controlled/living radical polymerization: features, developments, and perspectives. Prog Polym Sci 32:93–146
14. Chiefari J, Chong YK, Ercole F, Krstina J, Jeffery J, Le TPT, Mayadunne RTA, Meijs GF, Moad CL, Moad G, Rizzardo E, Thang SH (1998) Living free-radical polymerization by reversible addition/fragmentation chain transfer: the RAFT process. Macromolecules 31:5559–5562
15. Barner-Kowollik C (2008) Handbook of RAFT-polymerization. Wiley-VCH, Weinheim
16. Hawker CJ (1995) Architectural control in "living" free radical polymerizations: preparation of star and graft polymers. Angew Chem Int Ed 34:1456–1459
17. Jankova K, Bednarek M, Hvilsted SJ (2005) Star polymers by ATRP of styrene and acrylates employing multifunctional initiators. Polym Sci Part A Polym Chem 43:3748–3759
18. Barner-Kowollik C, Davis TP, Stenzel MH (2006) Synthesis of star polymers using RAFT polymerization: what is possible? Aust J Chem 59:719–727
19. Altintas O, Vogt AP, Barner-Kowollik C, Tunca U (2012) Constructing star polymers via modular ligation strategies. Polym Chem 3:34–45
20. Barner-Kowollik C, Du Prez FE, Espeel P, Hawker CJ, Junkers T, Schlaad H, Van Camp W (2011) "Clicking" polymers or just efficient linking: what is the difference? Angew Chem Int Ed 50:60–62

21. Gao H, Matyjaszewski K (2006) Synthesis of star polymers by a combination of ATRP and the “click” coupling method. Macromolecules 39:4960–4965
22. Fijten MWM, Haensch C, van Lankvelt BM, Hoogenboom R, Schubert US (2008) Clickable poly(2-oxazoline)s as versatile building blocks. Macromol Chem Phys 209:1887–1895
23. Chan, JW, Yu B, Hoyle CE, Lowe AB (2008) Convergent synthesis of 3-arm star polymers from RAFT-prepared poly(N,N-diethylacrylamide) via a thiol-ene click reaction. Chem Commun 44:4959–4961
24. Inglis AJ, Sinnwell S, Stenzel MH, Barner-Kowollik C (2009) Ultrafast click conjugation of macromolecular building blocks at ambient temperature. Angew Chem Int Ed 48:2411–2414
25. Iskin B, Yilmaz G, Yagci Y (2011) Synthesis of ABC type miktoarm star copolymers by triple click chemistry. Polym Chem 2:2865–2871
26. Bernard J, Lortie F, Fenet B (2009) Design of heterocomplementary H-bonding RAFT agents towards the generation of supramolecular star polymers. Macromol Rapid Commun 30:83–88
27. Likhitsup A, Yu S, Ng Y-H, Chai CLL, Tam EKW (2009) Controlled polymerization and self-assembly of a supramolecular star polymer with a guanosine quadruplex core. Chem Commun 45:4070–4072
28. Altintas O, Muller T, Lejeune E, Plietzsch O, Bräse S, Barner-Kowollik C (2012) Combining modular ligation and supramolecular self-assembly for the construction of star-shaped macromolecules. Macromol Rapid Commun 33:977–983
29. Wu X, Fraser CL (2000) The importance of macroligand molecular weight and solvent polarity in modulating metal core reactivity in heteroleptic polymeric ruthenium tris(bipyridine) complex synthesis. Macromolecules 33:7776–7785
30. Schubert US, Heller M (2001) Metallo-supramolecular initiators for the preparation of novel functional architectures. Chem Eur J 7:5252–5259
31. Gadwal I, De S, Stuparu MC, Amir RJ, Jang SG, Khan AJ (2012) Supramolecular star polymers with compositional heterogeneity. Polym Sci Part A Polym Chem 50:1844–1850
32. Huang F, Nagvekar DS, Slebodnick C, Gibson HW (2004) A supramolecular triarm star polymer from a homotritopic tris(crown ether) host and a complementary monotopic paraquat-terminated polystyrene guest by a supramolecular coupling method. J Am Chem Soc 127:484–485
33. Davis ME (2009) The first targeted delivery of siRNA in humans via a self-assembling, cyclodextrin polymer-based nanoparticle: from concept to clinic. Mol Pharm 6:659–668
34. Zhou J, Ritter H (2010) Cyclodextrin functionalized polymers as drug delivery systems. Polym Chem 1:1552–1559
35. Yhaya F, Lim J, Kim Y, Liang M, Gregory AM, Stenzel MH (2011) Development of micellar novel drug carrier utilizing temperature-sensitive block copolymers containing cyclodextrin moieties. Macromolecules 44:8433–8445
36. Köllisch HS, Barner-Kowollik C, Ritter H (2009) Amphiphilic block copolymers based on cyclodextrin host-guest complexes via RAFT-polymerization in aqueous solution. Chem Commun 45:1097–1099
37. Ritter H, Mondrzik BE, Rehahn M, Gallei M (2010) Free radical homopolymerization of a vinylferrocene/cyclodextrin complex in water. Beilstein J Org Chem 6(60)
38. Ding L, Li Y, Deng J, Yang W (2011) Preparation of hydrophobic helical poly(N-propargylamide)s in aqueous medium. Polym Chem 2:694–701
39. Ohno K, Wong B, Haddleton DMJ (2001) Synthesis of well-defined cyclodextrin-core star polymers. Polym Sci Part A Polym Chem 39:2206–2214
40. Stenzel MH, Davis TPJ (2002) Star polymer synthesis using trithiocarbonate functional beta-cyclodextrin cores (reversible addition/fragmentation chain-transfer polymerization). Polym Sci Part A Polym Chem 40:4498–4512
41. Miura Y, Narumi A, Matsuya S, Satoh T, Duan Q, Kaga H, Kakuchi TJ (2005) Synthesis of well-defined AB20-type star polymers with cyclodextrin-core by combination of NMP and ATRP. Polym Sci Part A Polym Chem 43:4271–4279

42. Zhang Z-X, Liu X, Xu FJ, Loh XJ, Kang E-T, Neoh K-G, Li J (2008) Pseudo-block copolymer based on star-shaped poly(N-isopropylacrylamide) with a beta-cyclodextrin core and guest-bearing PEG: controlling thermoresponsivity through supramolecular self-assembly. Macromolecules 41:5967–5970
43. Zhang Z-X, Liu KL, Li J (2011) Self-assembly and micellization of a dual thermoresponsive supramolecular pseudo-block copolymer. Macromolecules 44:1182–1193
44. Rekharsky MV, Inoue Y (1998) Complexation thermodynamics of cyclodextrins. Chem Rev 98:1875–1918
45. Dong R, Liu Y, Zhou Y, Yan D, Zhu X (2011) Photo-reversible supramolecular hyperbranched polymer based on host-guest interactions. Polym Chem 2:2771–2774
46. Wang X, Wu C (1999) Light-scattering study of coil-to-globule transition of a poly(N-isopropylacrylamide) chain in deuterated water. Macromolecules 32:4299–4301
47. Kujawa P, Winnik FM (2001) Volumetric studies of aqueous polymer solutions using pressure perturbation calorimetry: a new look at the temperature-induced phase transition of poly(N-isopropylacrylamide) in water and D_2O. Macromolecules 34:4130–4135
48. Mao H, Li C, Zhang Y, Furyk S, Cremer PS, Bergbreiter DE (2004) High-throughput studies of the effects of polymer structure and solution components on the phase separation of thermoresponsive polymers. Macromolecules 37:1031–1036
49. Gan LH, Cai W, Tam KC (2001) Studies of phase transition of aqueous solution of poly(N,N-diethylacrylamide-co-acrylic acid) by differential scanning calorimetry and spectrophotometry. Eur Polym J 37:1773–1778
50. Kujawa P, Segui F, Shaban S, Diab C, Okada Y, Tanaka F, Winnik FM (2005) Impact of end-group association and main-chain hydration on the thermosensitive properties of hydrophobically modified telechelic poly(N-isopropylacrylamides) in water. Macromolecules 39:341–348
51. Schneider H-J, Hacket F, Rüdiger V, Ikeda H (1998) NMR studies of cyclodextrins and cyclodextrin complexes. Chem Rev 98:1755–1786
52. Liu H, Zhang Y, Hu J, Li C, Liu S (2009) Multi-responsive supramolecular double hydrophilic diblock copolymer driven by host-guest inclusion complexation between beta-cyclodextrin and adamantyl moieties. Macromol Chem Phys 210:2125–2137

Chapter 6
AB_2 Miktoarm Star Polymers

6.1 Introduction

The generation of novel macromolecular architectures utilizing the concept of supramolecular chemistry has driven synthetic polymer chemistry significantly in the last years [2]. Hydrogen bonding [3, 4], metal complexes [5] and inclusion complexes [6] are widely employed. An important class of supramolecular hosts that have the ability to form inclusion complexes are CDs. This ability has found manifold utilization in polymer chemistry, e.g. for drug-delivery [7] or to dissolve hydrophobic monomers [8]. From the view of macromolecular architectures, CDs give the opportunity for the formation of macromolecular architectures that are governed by supramolecular interactions in an aqueous environment [9]. Examples for the utilization of CDs for the formation of complex macromolecular architectures cover a broad range of architectures e.g. linear diblockcopolymers [10–14], supramolecular gels [15, 16], CD-centered star polymers connected to linear polymers [17, 18] or supramolecular grafts for polymer brushes [19, 20].

In this chapter the formation of supramolecular miktoarm star polymers is presented, i.e. star polymers that have arms consisting of more than one polymer type, utilizing CD- and adamantyl-functionalized acrylamido polymers. The precursor polymers were synthesized via RAFT polymerization—based on a novel two-arm adamantyl bearing trithiocarbonate—of DMAAm and DEAAm and were thoroughly characterized via ESI-MS, NMR and SEC in DMAc. The subsequent formation of the supramolecular complex in water was proven via 2D ROESY and is supported by DLS data.

ROESY measurements were performed in collaboration with M. Hetzer and Prof. H. Ritter (Heinrich Heine Universität Düsseldorf). Parts of this chapter were reproduced from Schmidt et al. [1] with permission from the Royal Society of Chemistry.

B. V. K. J. Schmidt, *Novel Macromolecular Architectures via a Combination of Cyclodextrin Host/Guest Complexation and RAFT Polymerization*, Springer Theses,
DOI: 10.1007/978-3-319-06077-4_6, © Springer International Publishing Switzerland 2014

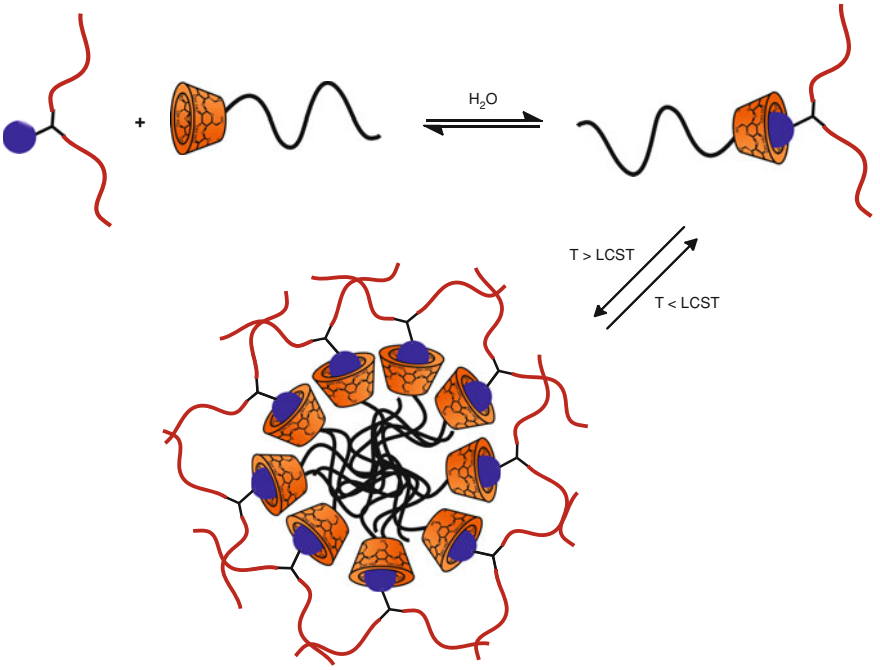

Scheme 6.1 Synthetic pathway for the supramolecular miktoarm star polymer (PDEAAm is depicted in *black*, PDMAAm is depicted in *red*, the β-CD moiety is depicted *orange* and the adamantyl group is depicted in *dark blue*)

6.2 Results and Discussion

6.2.1 Synthesis of the Building Blocks

A RAFT agent with an adamantyl moiety between two trithiocarbonate-groups was synthesized (Schemes 6.1 and 6.2), to achieve a mid-chain guest-functionalized polymer,. The prominent adamantyl moiety was chosen as guest-group due to its high complexation constants of up to 10^5 M^{-1} [21]. To increase the mobility and accessibility of the pendant adamantyl-group a C_5-spacer was incorporated. The adamantyl moiety was coupled to isopropylidene-2,2-bis(methoxy)propionic acid **13** with DCC. After deprotection, an acid-functionalized trithiocarbonate RAFT-agent was attached via DCC-coupling to yield **11**.

The subsequent RAFT-polymerizations of DMAAm with were conducted in DMF employing AIBN as initiator at 60 °C leading to narrow unimodal molecular weight distributions with low $Đ_m$ (Scheme 6.3, Fig. 6.1 and Table 6.1). The tailing of the elugram is probably due to adsorptive interactions of the polymers with the SEC column. The molecular structure of the polymers was verified via ESI-MS and ^{1}H-NMR (Appendix D.1/D.2). The ability of the adamantyl-functionalized PDMAAm

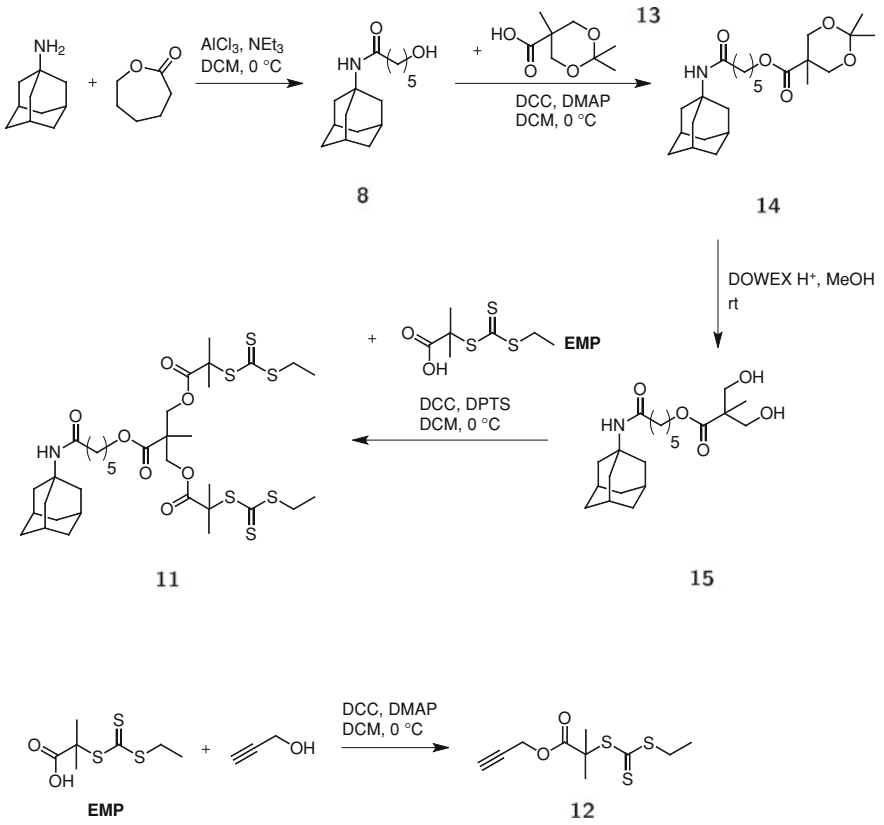

Scheme 6.2 Synthesis of the utilized CTAs [**EMP**: 2-(((ethylthio)carbonothioyl)thio)-2-methyl-propanoic acid]

to form an inclusion complex with β-CD was proven via 2D ROESY (Fig. 6.7b). The resonances between the adamantyl-protons (1.65, 1.95 and 2.05 ppm) and the inner protons of β-CD (3.7 and 3.8ppm) show the inclusion of the guest-group. Furthermore, a minor correlation between the methyl-endgroups and the inner CD protons is visible. A mixture of β-CD and non-adamantyl-functionalized PDMAAm displays no comparable peaks (Fig. 6.7a) evidencing that no other protons in PDMAAm show correlation signals in the region of the adamantyl protons.

An alkyne-endfunctionalized PDEAAm was synthesized with a terminal alkyne-containing RAFT-agent (**12**) in DMF with AIBN as initiator at 60 °C (Scheme 6.2). It should be noted that the monomer conversion was kept low to avoid undesired side-reactions, e.g. radical transfer to the alkyne-moiety. Unimodal molecular weight distributions with narrow $Đ_m$ were achieved according to SEC in DMAc (Fig. 6.1 and Table 6.1).

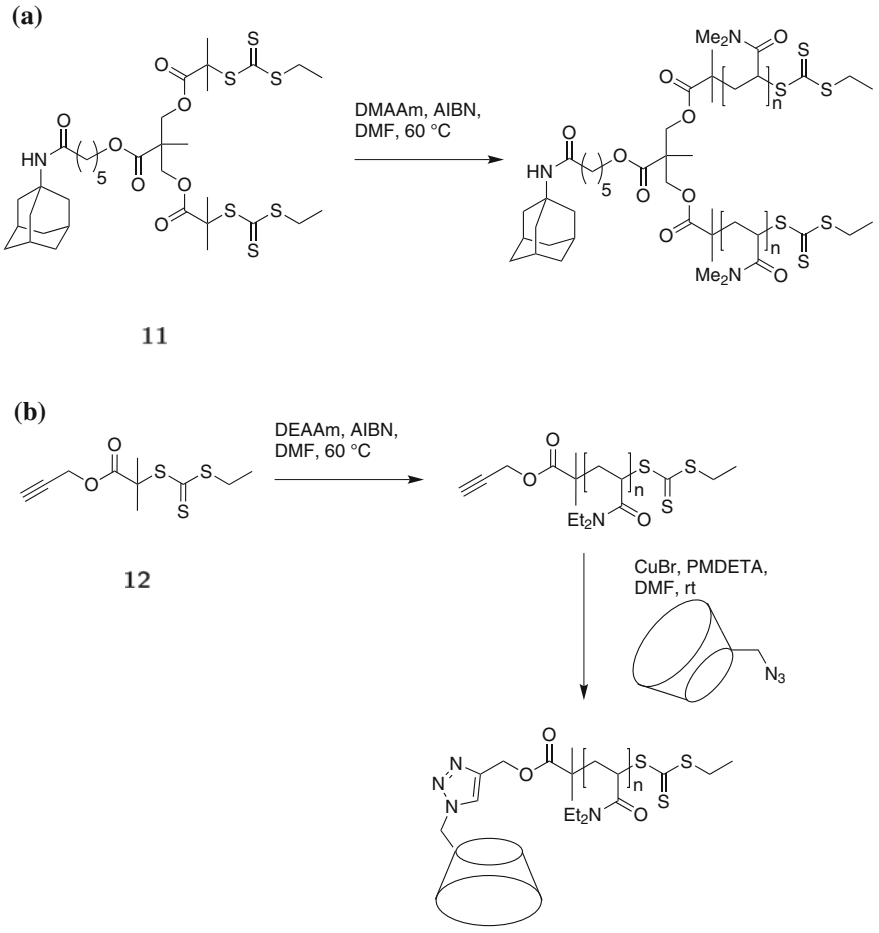

Scheme 6.3 RAFT polymerization for the synthesis of **a** mid-chain adamantyl-functionalized PDMAAm; **b** alkyne-functionalized PDEAAm and the subsequent CuAAc to form β-CD-functionalized PDEAAm

Table 6.1 Results for the RAFT polymerization of DMAAm (*top*) with **11** and DEAAm (*bottom*) with **12** at 60 °C in DMF

Monomer/CTA/I	Time/(h)	*Conv.* (%)	M_{ntheo}/(g mol^{-1})	M_{nSEC}/(g mol^{-1})	$Đ_m$	D_p
199/1/0.1	24	90	18,300	15,800	1.41	155
76/1/0.1	6	60	6,000	7,500	1.14	57

The alkyne-functionalized PDEAAm was further characterized via ^{1}H-NMR and ESI-MS showing a high endgroup fidelity (Appendix D.3/D.4). The host-functionalized polymer was subsequently synthesized via CuAAc of the

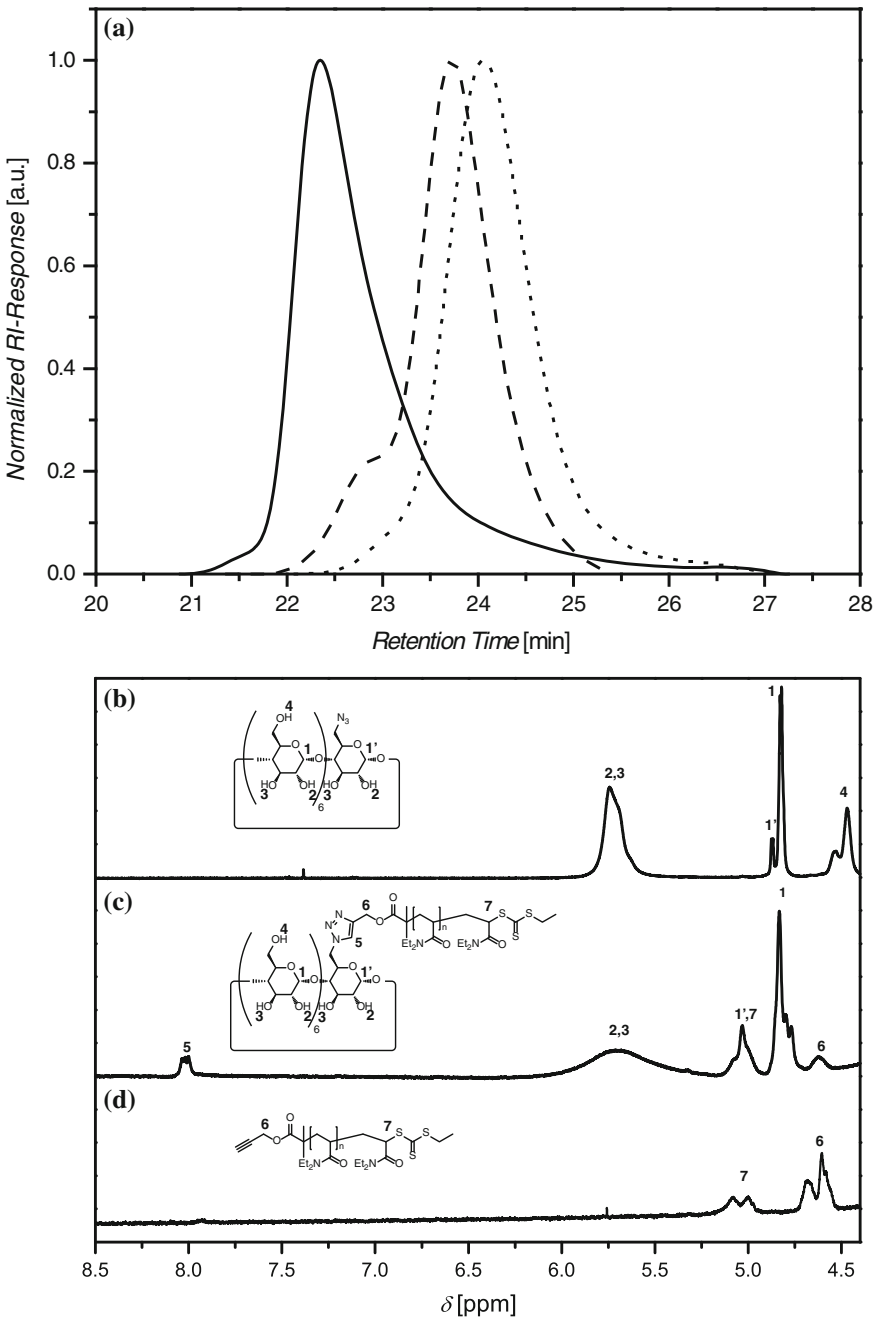

Fig. 6.1 **a** SEC-traces of the utilized PDMAAm$_{155}$-Ad (*solid line* M_{nSEC} = 15,800 g mol^{-1}, $Đ_m$ = 1.41), PDEAAm$_{57}$-alkyne (*dotted line* M_{nSEC} = 7,500 g mol^{-1}, $Đ_m$ = 1.14) and PDEAAm$_{57}$-β-CD (*dashed line* M_{nSEC} = 10,300 g mol^{-1}, $Đ_m$ = 1.12) in DMAc; comparison of the ^{1}H-NMR region from 4.3 ppm to 8.5 ppm, **b** β-CD-N$_3$, **c** the click-product PDEAAm$_{57}$-β-CD (M_{nSEC} = 8,000 g mol^{-1}, $Đ_m$ = 1.27) and **d** PDEAAm$_{57}$-alkyne (M_{nSEC} = 7,500 g mol^{-1}, $Đ_m$ = 1.14)

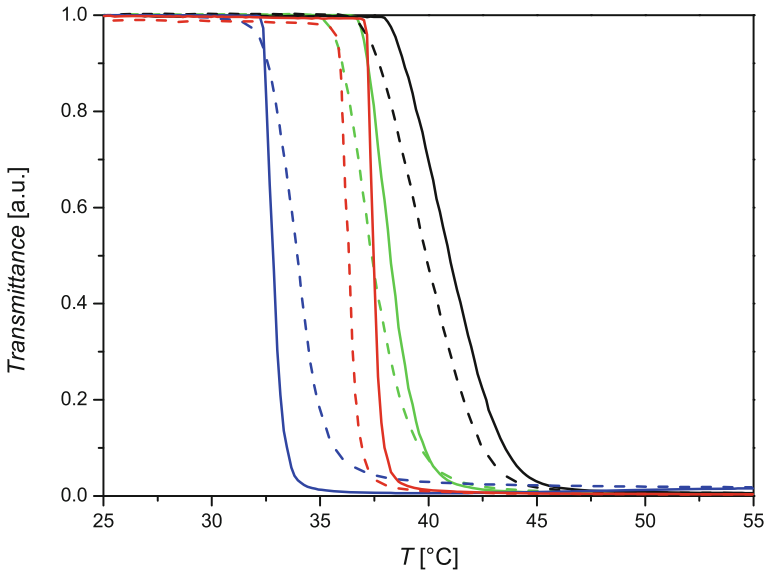

Fig. 6.2 Turbidimetry measurement (cooling *dotted line*; heating *solid line*) of the supramolecular miktoarm star complex (*black curves*), $PDEAAm_{57}$-β-CD (*green curves*; M_{nSEC} = 10,300 g mol^{-1}, $Đ_m$ = 1.12); $PDEAAm_{57}$-alkyne (*blue curves* M_{nSEC} = 7,500 g mol^{-1}, $Đ_m$ = 1.14) and acid-functionalized PDEAAm (*red curves* M_{nSEC} = 7,900 g mol^{-1}, $Đ_m$ = 1.20) at a concentration of 1 mg mL^{-1}

alkyne-endfunctionalized polymer with β-CD-N_3 (Scheme 6.2). The successful ligation can be followed by the shift of the full molecular weight distribution determined by SEC in DMAc (Fig. 6.1) as well as the emerging peak at 8 ppm from the triazole proton in the ^{1}H-NMR and the new peaks corresponding to the β-CD moiety (Fig. 6.1c). The SEC elugram indicates a shoulder at higher molecular weights that may be attributed to coupling products due to small amounts of difunctional β-CD-N_3.

Turbidimetry measurements show an increase in the T_c from 32.5 to 38.1 °C (heating ramp) upon addition of the strongly hydrophilic β-CD moiety (Fig. 6.2). Furthermore, a slower transition is observed, which gives an indication that the β-CD moiety also has an effect on the kinetics of the thermoresponsive behavior of PDEAAm.

6.2.2 *Characterization of the Supramolecular Miktoarm Star Polymer*

The supramolecular miktoarm star polymer was prepared via the dialysis method. Both blocks (Table 6.1) were dissolved in THF and one solution was added

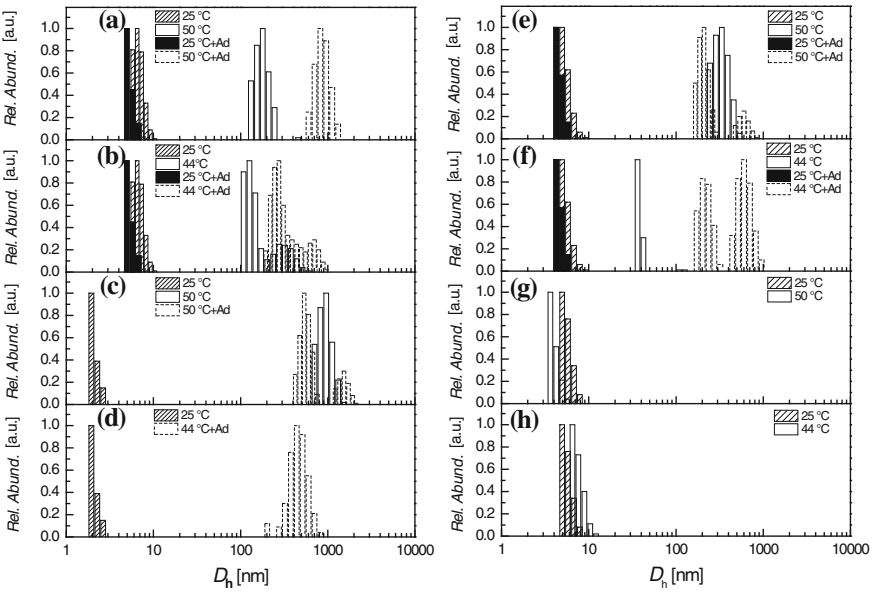

Fig. 6.3 Comparison of the number averaged particle size distributions obtained from DLS measurements at a concentration of 1 mg mL^{-1} with or without 1-adamantylamine hydrochloride (*Ad*): **a** the supramolecular complex at 25 and 50 °C; **b** the supramolecular complex at 25 and 44 °C; **c** $PDEAAm_{57}$-β-CD at 25 and 50 °C; **d** $PDEAAm_{57}$-β-CD at 25 and 44 °C; **e** the control sample P4 at 25 and 50 °C; **f** the control sample P4 at 25 and 44 °C; **g** $PDMAAm_{155}$-Ad at 25 and 50 °C; **h** $PDMAAm_{155}$-Ad at 25 and 44 °C

dropwise to the other under vigorous stirring. The organic solvent was removed via dialysis. After lyophilization of the sample the complex was dissolved in D_2O or H_2O to perform ROESY or DLS. The measurement of the T_cs of the supramolecular complex and the β-CD functionalized PDEAAm show a difference of 2.3 °C from 38.1 to 40.4 °C (heating ramp) (Fig. 6.2). The above is an expected result, as the non-thermoresponsive PDMAAm block leads to an increased hydrophilicity of the complex and thus the T_c is shifted to higher values. The supramolecular complex also shows a slower transition in contrast to non-CD functionalized PDEAAm featuring a rather sharp transition (Fig. 6.2), which can be attributed to the interactions of both the CD moiety and the PDMAAm block with the PDEAAm-block.

DLS gives the opportunity to study the properties of the formed supramolecular complexes in solution (Fig. 6.3). A comparison of the D_h of the single parts and the complex in water at 25 °C shows only minor differences (Fig. 6.3). The adamantyl-functionalized PDMAAm shows a D_h at 25 °C of 5.6 nm and the β-CD-functionalized PDEAAm shows a D_h of 2.1 nm at 25 °C whereas the supramolecular miktoarm star polymer shows a D_h of 6.8 nm at 25 °C. A variation of the molar ratios of the two utilized building blocks shows a maximum diameter at a molar ratio of 1:1 (Fig. 6.4). This gives an indication for complex formation at 25 °C.

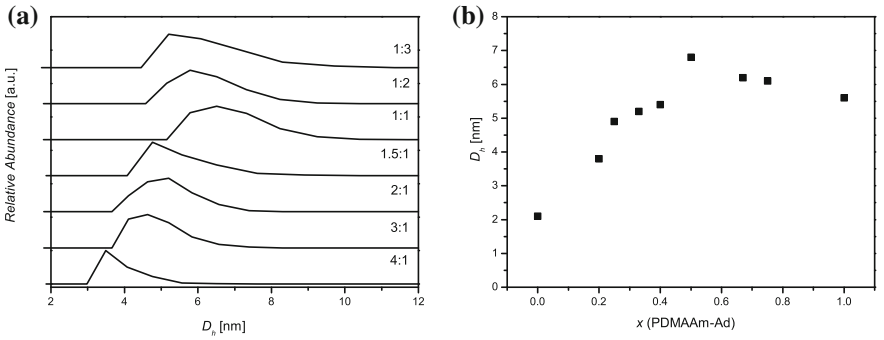

Fig. 6.4 **a** Comparison of the number averaged particle size distributions obtained from DLS measurements at 1 mg mL^{-1} at 25 °C and different molar ratios of $PDMAAm_{155}$-Ad:$PDEAAm_{57}$-β-CD and **b** comparison of the number averaged hydrodynamic diameter at 1 mg mL^{-1} at 25 °C of mixtures of $PDMAAm_{155}$-Ad and $PDEAAm_{57}$-β-CD in dependence of the molar fraction x of $PDMAAm_{155}$-Ad

A significant difference between the building blocks and the supramolecular complex is observed when the samples are heated above the T_c of the thermoresponsive PDEAAm-block (Appendix D.5). Micellization of thermoresponsive supramolecular block copolymers has been used in the literature relatively often, e.g. to prove the formation of the desired architectures or to generate multi-stimuli responsive micelles [10, 11, 22]. At 44 and 50 °C the D_h of the adamantyl-functionalized PDMAAm is not changing significantly as expected for a non T_c-polymer (Fig. 6.3). The β-CD-functionalized PDEAAm shows large aggregates with a D_h of 937 nm at 50 °C. In contrast, the complex has a D_h of 132 and 275 nm at 44 and 50 °C respectively. A control sample that was prepared from a non adamantyl-functionalized PDMAAm and the β-CD-functionalized PDEAAm features a D_h of 38 nm at 44 °C and 333 nm at 50 °C. The comparison indicates that the supramolecular miktoarm star polymer forms larger aggregates than the control sample. As it has been concluded from the turbidimetry measurements, the PDEAAm block interacts with both the β-CD moiety and the PDMAAm. This is apparent again from the DLS results, where heating of the control sample leads to one distribution, giving rise to the assumption that the free PDMAAm is associated with the PDEAAm aggregates. Keeping that in mind, the difference in D_h between the supramolecular miktoarm star polymer and the control sample has to be considered carefully. Nevertheless, the difference is still significant and a strong indication for complex formation. The observed particle sizes are larger than expected for a usual micellar system. It is possible that at 44 °C agglomeration of the formed aggregates already commences. On the other hand, in the literature micellar systems with similar size are described [18, 23].

The addition of an excess of 1-adamantylamine hydrochloride (Ad) leads to an insignificant decrease of the D_h at 25 °C of 1.4 nm whereas large differences are observed at elevated temperatures. Instead of 132 and 275 nm larger particles with D_h of 275 and 881 nm are found upon heating at 44 and 50 °C, respectively. At

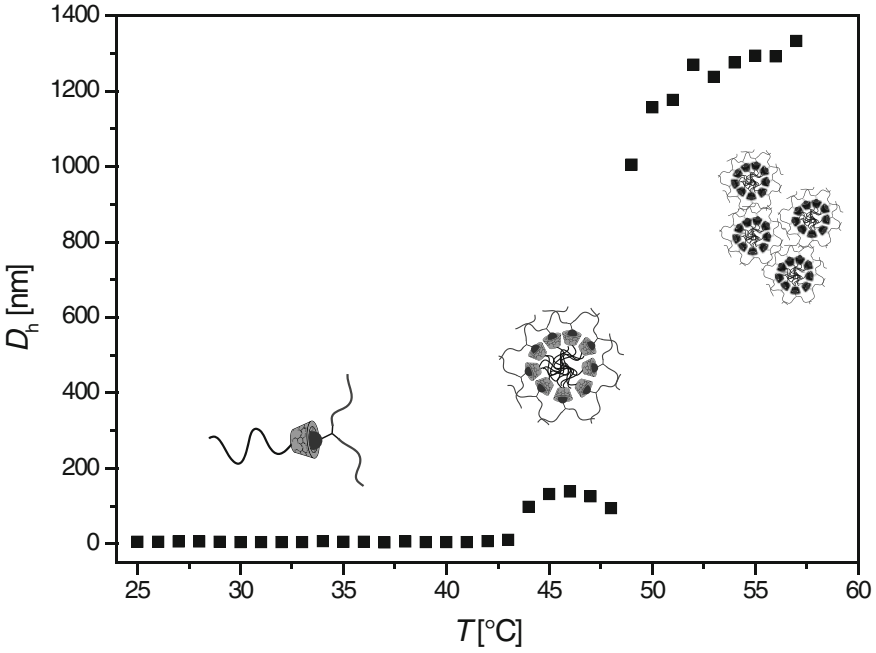

Fig. 6.5 Temperature sequenced DLS measurement showing the relation between the D_h from the number averaged particle size distribution and the temperature

50 °C a D_h of 881 nm is formed, which is close to the D_h of β-CD-functionalized PDEAAm with 937 nm. This result is in agreement with the expectation that the addition of an excess of guest molecules leads to the disruption of the supramolecular miktoarm star polymer complex and therefore different aggregates are formed in solution upon heating. It should be noted that the addition of guest molecules also alters the thermoresponsive behavior of the control sample. In this case also larger aggregates are formed with multi-modal particle size distributions, which can be attributed to a change in the hydrophilicity of the CD endgroups when an inclusion complex is formed (Fig. 6.3).

To further investigate the formation of the aggregates a temperature sequenced DLS measurement of the supramolecular complex was performed which shows three regimes (Fig. 6.5). From 25 to 43 °C, the complexes are present as unimolecular coils with an average D_h of 5.4 nm. From 44 to 48 °C defined aggregates are formed with an average D_h of 118 nm as the PDEAAm-block becomes insoluble due to its T_c. The formation of defined aggregates is a strong hint for the supramolecular connection between both blocks. A further increase in temperature leads to further agglomeration (>1,000 nm) as it has been discussed in the literature with a similar system consisting of a linear linker with an adamantyl-group on every end and two β-CD-centered stars attached via supramolecular interactions [18]. This effect could be attributed to the weaker complexation at elevated temperatures, which leads to

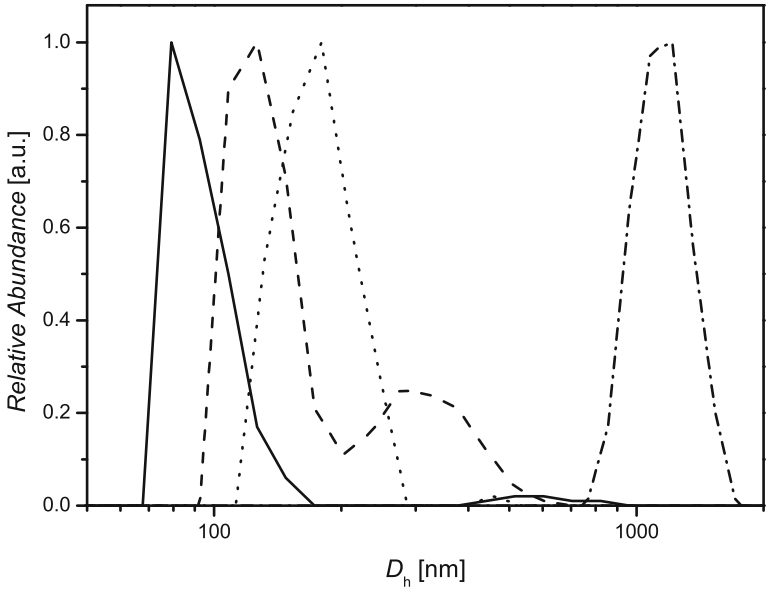

Fig. 6.6 Comparison of the number averaged particle size distributions of the supramolecular miktoarm star polymer obtained from DLS measurements with slow heating at 44 °C (*solid line*) and 50 °C (*dashed-dotted line*) and after fast heating at 44 °C (*dashed line*) and 50 °C (*dotted line*)

partial disruption of the complexes, a loss or rearrangement of stabilizing PDMAAm chains in the corona and agglomeration of multiple particles. It is striking that the size of the formed aggregates depends strongly on the heating rate (Fig. 6.6). Direct heating from 25 to 50 °C leads to smaller aggregates (275 nm) than slow heating (>1,000 nm). The above behavior could be due to effects of the kinetics of the aggregate formation [24].

The DLS results are an indication that the expected supramolecular complex is formed. Nevertheless, the connection of both blocks via the CD/adamantyl pair has to be proven. ROESY is a powerful tool to study inclusion complexes. The ROESY spectrum of the supramolecular complex proves the inclusion of the mid-chain adamantyl moiety in the PDMAAm into the pendant CD units of the PDEAAm thus proving the formation of a supramolecular miktoarm star polymer (Fig. 6.7c). Six correlation peaks at 1.72, 2.04 and 2.16 ppm can be assigned to the interaction of the adamantyl group with the inner protons of β-CD at 3.7 and 3.8 ppm [11]. No other significant correlation peaks are found in the respective regions, which proves that no other interactions are present that could lead to different architectures. A similar spectrum was found with the adamantyl-functionalized PDMAAm and native β-CD (Fig. 6.7b). Furthermore the additional correlation peaks between 1.2 ppm and 3.7 and 3.8 ppm that were found with native β-CD are absent in the ROESY spectrum of the miktoarm star polymer. Thus, the formation of the miktoarm star architecture can be assumed.

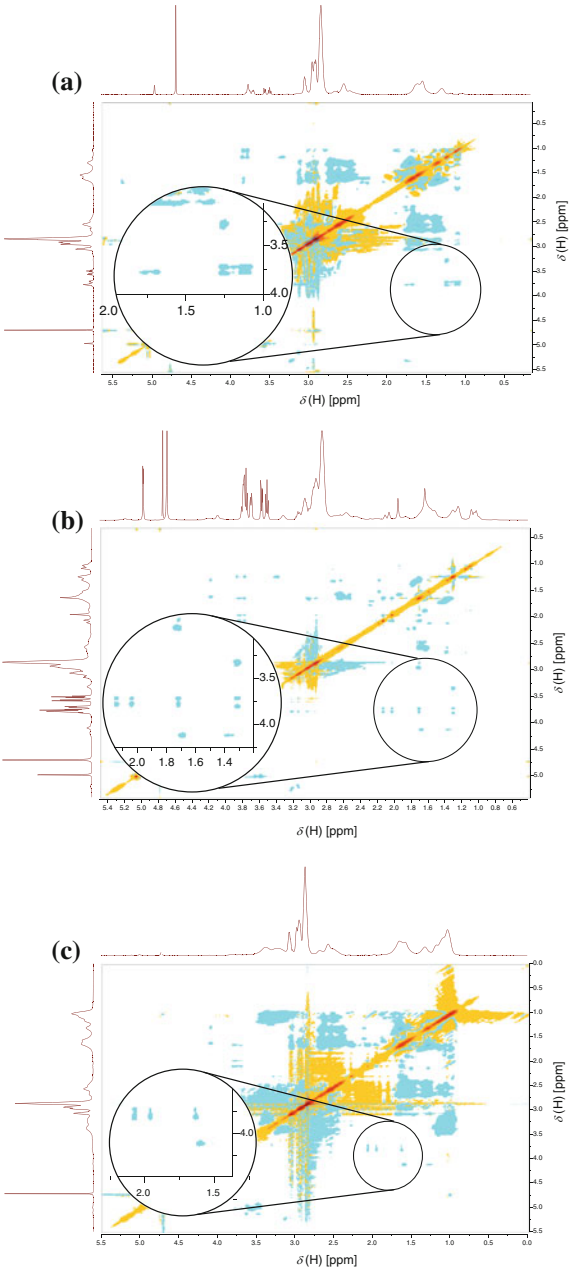

Fig. 6.7 2D ROESY spectra in D_2O at 25 °C with magnification of the relevant signals of **a** 1:1.1 molar mixture of PDMAAm (M_{nSEC} = 12,800 g mol^{-1}, $Đ_m$ = 1.10) polymerized with **EMP** and β-CD; **b** 1:1.1 molar mixture of a mid-chain adamantyl-functionalized PDMAAm (M_{nSEC} = 4,000 g mol^{-1}, $Đ_m$ = 1.09) polymerized with **11** and β-CD; **c** the supramolecular miktoarm star polymer in D_2O at 25 °C

6.3 Conclusions

The formation of a novel supramolecular miktoarm star polymer that is based on CD-host/guest chemistry was described. A mid-chain adamantyl-containing PDMAAm and an alkyne-endgroup-containing PDEAAm were prepared via the RAFT process. The terminal alkyne was transferred into a β-CD-endgroup via CuAAc with β-CD-N_3. The supramolecular miktoarm star polymer architecture was formed subsequently via a CD/adamantyl inclusion-complex. The complex formation was proven via DLS and ROESY. The thermoresponsive behavior of the formed supramolecular miktoarm star polymers were studied via turbidimetry measurements showing significant changes in the T_cs of complexed polymers and the native building blocks. Furthermore, temperature sequenced DLS was performed to study the temperature induced micellization of the supramolecular miktoarm star polymers with regard to the size of formed aggregates. It could be shown that addition of free guest molecules leads to disruption of the formed supramolecular complexes with significant changes in the thermoresponsive behavior.

6.4 Experimental Part

6.4.1 Synthesis of 6-(Adamantan-1-ylamino)-6-oxohexyl-2,2,5-trimethyl-1,3-dioxane-5-carboxylate (14)

In a 50 mL Schlenk-flask isopropylidene-2,2-bis(methoxy)propionic acid (**13**) (1.04 g, 8.04 mmol, 1.2 eq.), *N*-(adamantan-1-yl)-6-hydroxyhexanamide (**8**) (1.78 g, 6.72 mmol, 1.0 eq.) and DMAP (0.16 g, 1.31 mmol, 0.2 eq.) were dissolved in anhydrous DCM (14 mL). At 0 °C a solution of DCC (1.66 g, 8.04 mmol, 1.2 eq.) in anhydrous DCM (8 mL) was added. After 1 h the solution was warmed to ambient temperature, stirred overnight, filtered and concentrated under reduced pressure. The residual oil was purified via column chromatography on silica-gel with a mixture of *n*-hexane:ethyl acetate as eluent that was gradually changed from 5:1 to 4:1. The product was obtained as colorless oil (2.70 g, 6.41 mmol, 95 %).

^{1}H-NMR (400 MHz, $CDCl_3$): [δ, ppm] = 1.18 (s, 3H, C***H***$_3$–C–C=O), 1.30–1.50 (m, 8H, 2x C–C***H***$_3$, C***H***$_2$–CH_2–C–O), 1.56–1.73 (m, 10H, 2x C***H***$_{2,alkyl}$; 3x C***H***$_{2,adamantyl}$), 1.97 (d, 6H, ^3J = 2.8 Hz, 3x NH–C–C***H***$_{2,adamantyl}$), 2.02–2.12 (m, 5H, 3x C***H***$_{adamantyl}$; C***H***$_2$–C=O–NH), 3.62 (d, 2H, J = 11.8 Hz, C***H***$_2$–O–C), 3.98–4.36 (m, 4H, 2x C***H***$_2$–O–C), 5.10 (br s, 1H, N***H***). **^{13}C-NMR** (100 MHz, $CDCl_3$): [δ, ppm] = 18.9 (C–***C***H_3), 23.0 and 24.6 (2x CH_3–C–O), 25.4 and 25.6 (***C***H_2–CH_2–C=O; ***C***H_2–CH_2–CH_2–C=O), 28.5 (***C***H_2–CH_2–C=O–NH), 29.6 (3x ***C***$H_{adamantyl}$), 36.5 (3x ***C***$H_{2,adamantyl}$), 37.7 (***C***H_2–C=O–NH), 41.8 (3x ***C***$H_{2,adamantyl}$–C–NH), 41.9 (O–CH_2–***C***–C=O), 51.9 (***C***–NH), 64.9 (CH_2–***C***H_2–O), 66.2 (2x C–***C***H_2–O), 98.2 (CH_2–O–***C***$(CH_3)2$–O–CH_2), 172.0 (NH–***C***=O), 174.4 (O–***C***=O). **ESI-MS**: $[M + Na^+]_{exp}$ = 444.48 m/z and $[M + Na^+]_{calc}$ = 444.27 m/z.

6.4.2 Synthesis of 6-(Adamantan-1-ylamino)-6-oxohexyl 3-hydroxy-2-(hydroxymethyl)-2-methylpropanoate (15)

6-(Adamantan-1-ylamino)-6-oxohexyl-2,2,5-trimethyl-1,3-dioxane-5-carboxylate (**14**) (2.50 g, 5.94 mmol, 1.0 eq.) was dissolved in methanol (20 mL). Subsequently one spoon of Dowex H^+ resin was added and the mixture stirred at ambient temperature over night. The mixture was filtered and washed with methanol. After evaporation of the solvent in vacuo 2.15 g (5.64 mmol, 95 %) of the product were obtained as colorless oil.

^{1}H-NMR (400 MHz, $CDCl_3$): [δ, ppm] = 1.06 (s, 3H, C***H***$_3$–C–C=O), 1.29–1.50 (m, 2H, C***H***$_2$–CH_2–C–O), 1.52–1.77 (m, 10H, 2x C***H***$_{2,alkyl}$; 3x C***H***$_{2,adamantyl}$), 1.97–2.14 (m, 11H, 3x C***H***$_{adamantyl}$; C***H***$_2$–C=O–NH; 3x NH–C–C***H***$_{2,adamantyl}$), 2.83 (br s, 2H, O***H***), 3.72 (d, 2H, ^3J = 11.2 Hz, C***H***$_2$–O–C), 3.87 (d, 2H, ^3J = 11.2 Hz, C***H***$_2$–O–C), 4.16 (t, 2H, ^3J = 6.4 Hz, CH_2–C***H***$_2$–O–C), 5.21 (br s, 1H, N***H***). **^{13}C-NMR** (100 MHz, $CDCl_3$): [δ, ppm] = 17.4 (C–***C***H_3), 25.2 and 25.7 (***C***H_2–CH_2–C=O; ***C***H_2–CH_2–CH_2–C=O), 28.3 (***C***H_2–CH_2–C=O–NH), 29.6 (3x ***C***$H_{adamantyl}$), 36.5 (3x ***C***$H_{2,adamantyl}$), 37.5 (***C***H_2–C=O–NH), 41.8 (3x ***C***$H_{2,adamantyl}$–C–NH), 49.4 (O=C–***C***–(CH_2–O)2), 52.1 (***C***–NH), 64.9 (CH_2–***C***H_2–O), 68.3 (2x C–***C***H_2–O), 172.3 (NH–***C***=O), 176.2 (O–***C***=O). **ESI-MS**: $[M + Na^+]_{exp}$ = 404.44 m/z and $[M + Na^+]_{calc}$ = 404.50 m/z.

6.4.3 Synthesis of 2-(((6-(Adamantan-1-ylamino)-6-oxohexyl)oxy)carbonyl)-2-methylpropane-1,3-diyl bis(2-(((ethylthio)carbonothioyl)thio)-2-methylpropanoate (11)

In a 50 mL round bottom-flask 6-(adamantan-1-ylamino)-6-oxohexyl 3-hydroxy-2-(hydroxymethyl)-2-methylpropanoate (**15**) (2.00 g, 5.25 mmol, 1.0 eq.), **EMP** (2.47 g, 11.02 mmol, 2.1 eq.) and DPTS (0.62 g, 2.11 mmol, 0.4 eq.) were dissolved in anhydrous DCM (20 mL). At 0 °C a solution of DCC (3.25 g, 15.75 mmol, 3.0 eq.) in anhydrous DCM (20 mL) was added. After 1 h the solution was warmed to ambient temperature, stirred for 2 days, filtered and concentrated under reduced pressure. The residual oil was purified via column chromatography on silica-gel with a mixture of *n*-hexane:ethyl acetate as eluent that was gradually changed from 4:1 to 3:1. The product was obtained as yellow oil (2.25 g, 2.84 mmol, 54 %).

^{1}H-NMR (400 MHz, $CDCl_3$): [δ, ppm] = 1.02–1.47 (m, 11H, C***H***$_2$–CH_2–C–O; C***H***$_3$–C–C=O; 2x C***H***$_3$–CH_2), 1.51–1.85 (m, 22H, 2x C***H***$_{2,alkyl}$; 3x C***H***$_{2,adamantyl}$; 4x C–C***H***$_3$), 1.89–2.22 (m, 11H, 3x C***H***$_{adamantyl}$; C***H***$_2$–C=O–NH; 3x NH–C–C***H***$_{2,adamantyl}$), 3.26 (q, 4H, ^3J = 7.4 Hz, C***H***$_2$–S), 3.31–3.90 (m, 6H, C***H***$_2$–O–C, C***H***$_2$–O–C; CH_2–C***H***$_2$–O–C), 5.15 (br s, 1H, N***H***). **^{13}C-NMR** (100 MHz, $CDCl_3$): [δ, ppm] = 13.0 (4x CH_2–***C***H_3), 17.9 (C–***C***H_3), 25.4, 25.5 and 25.7 (4x C-***C***H_3; ***C***H_2–CH_2–C=O; ***C***H_2–CH_2–CH_2–C=O), 28.5 (***C***H_2–CH_2–C=O–NH), 29.6

(3x ***C***$H_{adamantyl}$), 31.3 (2x ***C***H_2–S), 36.5 (3x ***C***$H_{2,adamantyl}$), 37.6 (***C***H_2–C=O–NH), 41.8 (3x ***C***$H_{2,adamantyl}$–C–NH), 46.2 (O=C–***C***–(CH_2–O)2), 52.0 (***C***–NH), 56.0 (***C***–(CH_3)2), 65.3 and 67.0 (CH_2–***C***H_2–O; 2x C–***C***H_2–O), 172.0, 172.4 and 172.6 (2x O–***C***=O, NH–***C***=O), 221.4 (2x ***C***=S). **ESI-MS**: $[M + Na^+]_{exp}$ = 816.32 m/z and $[M + Na^+]_{calc}$ = 816.22 m/z.

6.4.4 Synthesis of prop-2-yn-1-yl 2-(((ethylthio)carbonothioyl)-thio)-2-methylpropanoate (12)

In a 250 mL Schlenk-flask **EMP** (4.00 g, 17.86 mmol, 1.0 eq.), propargyl alcohol (2.1 mL, 36.34 mmol, 2.0 eq.) and DMAP (0.88 g, 7.20 mmol, 0.4 eq.) were dissolved in anhydrous DCM (80 mL). At 0 °C a solution of DCC (7.40 g, 35.86 mmol, 2.0 eq.) in anhydrous DCM (40 mL) was added. After 1 h the solution was warmed to ambient temperature, stirred overnight, filtered and concentrated under reduced pressure. The residual oil was purified via column chromatography on silica-gel with a 20:1 mixture of *n*-hexane:ethyl acetate. The product was obtained as yellow oil (3.92 g, 14.94 mmol, 84 %).

^{1}H-NMR (400 MHz, $CDCl_3$): [δ, ppm] = 1.32 (t, 3H, ^3J = 7.4 Hz, C***H***$_3$–CH_2), 1.70 (s, 6H, 2x C–C***H***$_3$), 2.46 (t, ^3J = 2.5 Hz, 1H, C***H***), 3.28 (q, 2H, ^3J = 7.4 Hz, CH_3–C***H***$_2$), 4.69 (d, ^3J = 2.5 Hz, 2H, C***H***$_2$–O). **^{13}C-NMR** (100 MHz, $CDCl_3$): [δ, ppm] = 13.0 (CH_2–***C***H_3), 25.3 (2x C–***C***H_3), 31.4 (***C***H_2–CH_3), 53.5 (***C***–CH_3), 55.7 (***C***H_2–O), 75.2 (***C***H), 77.4 (***C***–CH), 172.5 (***C***=O), 221.0 (***C***=S). **ESI-MS**: $[M + Na^+]_{exp}$ = 284.88 m/z and $[M + Na^+]_{calc}$ = 285.01 m/z.

6.4.5 Exemplary Synthesis of Mid-Chain Adamantyl-Functionalized PDMAAm

11 (60.0 mg, 0.076 mmol, 1.0 eq.), DMAAm (1.50 g, 15.14 mmol, 199.2 eq.), AIBN (2.5 mg, 0.015 mmol, 0.2 eq.), DMF (15.0 mL) and a stirring-bar were added into a Schlenk-tube. After three freeze–pump–thaw cycles the tube was backfilled with argon, sealed, placed in an oil bath at 60 °C and removed after 24 h. The tube was subsequently cooled with liquid nitrogen to stop the reaction. A NMR-sample was withdrawn for the determination of conversion, inhibited with a pinch of hydroquinone (approx. 5 mg) and $CDCl_3$ was added. A conversion of 90 % was calculated based on the NMR data (see Sect. 9.3 for details of the calculation). The residue was dialyzed against deionized water with a SpectraPor3 membrane (MWCO = 1,000 Da) for 3 days at ambient temperature. The solvent was removed in vacuo to yield the polymer as a yellow solid (1.40 g, 99 %, M_{ntheo} = 18,500 g mol^{-1}, **SEC(DMAc)**: M_{nSEC} = 15,800 g mol^{-1}, $Đ_m$ = 1.41).

6.4.6 Exemplary Synthesis of Alkyne-Functionalized PDEAAm

12 (269.0 mg, 1.03 mmol, 1.0 eq.), DEAAm (10.00 g, 78.62 mmol, 76.3 eq.), AIBN (15.0 mg, 0.091 mmol, 0.1 eq.), DMF (45 mL) and a stirring-bar were added into a Schlenk-tube. After three freeze–pump–thaw cycles the tube was backfilled with argon, sealed, placed in an oil bath at 60 °C and removed after 6 h. The tube was subsequently cooled with liquid nitrogen to stop the reaction. A NMR-sample was withdrawn for the determination of conversion, inhibited with a pinch of hydroquinone (approx. 5 mg) and $CDCl_3$ was added. A conversion of 82 % was calculated based on the NMR data (see Sect. 9.3 for details of the calculation). The residue was dialyzed against deionized water with a SpectraPor3 membrane (MWCO = 1,000 Da) for 3 days at ambient temperature. The solvent was removed in vacuo to yield the polymer as yellow solid (7.34 g, 87 %, M_{ntheo} = 8,200 g mol^{-1}, **SEC(DMAc)**: M_{nSEC} = 7,500 g mol^{-1}, $Đ_{\mathrm{m}}$ = 1.14).

6.4.7 Exemplary Click-Reaction of Alkyne-Functionalized PDEAAm with β-CD-N_3

Alkyne functionalized PDEAAm (M_{nSEC} = 7,500 g mol^{-1}; 2.00 g, 0.27 mmol, 1.0 eq.), β-CD-N_3 (1.25 g, 1.08 mmol 4.0 eq.), PMDETA (56 µl, 0.27 mmol, 1.0 eq.), DMF (25 mL) and a stirring-bar were introduced into a Schlenk-tube. After three freeze–pump–thaw cycles the tube was filled with argon and CuBr (38.0 mg, 0.27 mmol, 1.0 eq.) was added under a stream of argon. Subsequently, two freeze–pump–thaw cycles were performed, the tube backfilled with argon and the mixtures stirred at ambient temperature for 24 h. EDTA-solution (5 wt%, 1 mL) was added and the residue was dialysed against deionized water with a SpectraPor3 membrane (MWCO = 2,000 Da) for 3 days at ambient temperature. The solvent was removed in vacuo to yield the CD-functionalized polymer as a yellow solid (1.58 g, 68 %, **SEC(DMAc)**: M_{nSEC} = 10,300 g mol^{-1}, $Đ_{\mathrm{m}}$ = 1.12).

6.4.8 Exemplary Supramolecular Miktoarm Star Polymer-Formation via CD/Guest Interaction

Mid-chain adamantyl functionalized PDMAAm (M_{nSEC} = 15,800 g mol^{-1}; 100.0 mg, 0.006 mmol, 1.0 eq.) was dissolved in THF (2 mL) and added dropwise to a solution of CD-functionalized PDEAAm (M_{nSEC} = 8,000 g mol^{-1}; 50.6 mg, 0.006 mmol, 1.0 eq.) under vigorous stirring. The resulting solution was dialyzed against a deionized water/THF-mixture. The water-content was gradually changed from 70 to 100 % over 1 day and the dialysis was continued for 3 days with deionized water at ambient

temperature. The solvent was removed in vacuo to yield the supramolecular complex in quantitative yield. In a similar manner a control sample was prepared consisting of a CD-functionalized PDEAAm (M_{nSEC} = 8,000 g mol^{-1}; 25.0 mg, 0.003 mmol, 1.0 eq.) and non-adamantyl functionalized PDMAAm (M_{nSEC} = 12,300 g mol^{-1}; 38.4 mg, 0.003 mmol, 1.0 eq.) that was polymerized with **EMP**.

References

1. Schmidt BVKJ, Hetzer M, Ritter H, Barner-Kowollik C (2012) Miktoarm star polymers via cyclodextrin-driven supramolecular self-assembly. Polym Chem 3:3064–3067. doi:10.1039/C2PY20214J
2. Zayed JM, Nouvel N, Rauwald U, Scherman OA (2010) Chemical complexity-supramolecular self-assembly of synthetic and biological building blocks in water. Chem Soc Rev 39:2806–2816
3. Chen S, Bertrand A, Chang X, Alcouffe P, Ladaviére C, Gèrard J-F, Lortie F, Bernard J (2010) Heterocomplementary H-Bonding RAFT agents as tools for the preparation of supramolecular miktoarm star copolymers. Macromolecules 43:5981–5988
4. Altintas O, Tunca U, Barner-Kowollik C (2011) Star and miktoarm star block (co)polymers via self-assembly of ATRP generated polymer segments featuring Hamilton wedge and cyanuric acid binding motifs. Polym Chem 2:1146–1155
5. Fustin CA, Guillet P, Schubert US, Gohy JF (2007) Metallo-supramolecular block copolymers. Adv Mater 19:1665–1673
6. Rauwald U, Scherman O (2008) Supramolecular block copolymers with cucurbit[8]uril in water. Angew Chem Int Ed 47:3950–3953
7. Yhaya F, Lim J, Kim Y, Liang M, Gregory AM, Stenzel MH (2011) Development of micellar novel drug carrier utilizing temperature-sensitive block copolymers containing cyclodextrin moieties. Macromolecules 44:8433–8445
8. Köllisch HS Barner-Kowollik C, Ritter H (2009) Amphiphilic block copolymers based on cyclodextrin host-guest complexes via RAFT-polymerization in aqueous solution. Chem Commun 1097–1099
9. Chen G, Jiang M (2011) Cyclodextrin-based inclusion complexation bridging supramolecular chemistry and macromolecular self-assembly. Chem Soc Rev 40:2254–2266
10. Zeng J, Shi K, Zhang Y, Sun X, Zhang B (2008) Construction and micellization of a noncovalent double hydrophilic block copolymer. Chem Commun 3753–3755
11. Liu H, Zhang Y, Hu J, Li C, Liu S (2009) Multi-responsive supramolecular double hydrophilic diblock copolymer driven by host-guest inclusion complexation between beta-cyclodextrin and adamantyl moieties. Macromol Chem Phys 210:2125–2137
12. Yan Q, Xin Y, Zhou R, Yin Y, Yuan J (2011) Light-controlled smart nanotubes based on the orthogonal assembly of two homopolymers. Chem Commun 47:9594–9596
13. Stadermann J, Komber H, Erber M, Däbritz F, Ritter H, Voit B (2011) Diblock copolymer formation via self-assembly of cyclodextrin and adamantyl end-functionalized polymers. Macromolecules 44:3250–3259
14. Yan Q, Yuan J, Cai Z, Xin Y, Kang Y, Yin Y (2010) Voltage-responsive vesicles based on orthogonal assembly of two homopolymers. J Am Chem Soc 132:9268–9270
15. Kretschmann O, Choi SW, Miyauchi M, Tomatsu I, Harada A, Ritter H (2006) Switchable hydrogels obtained by supramolecular cross-linking of adamantyl-containing LCST copolymers with cyclodextrin dimers. Angew Chem Int Ed 45:4361–4365
16. Nakahata M, Takashima Y, Yamaguchi H, Harada A (2011) Redox-responsive self-healing materials formed from host/guest polymers. Nat Commun 2:511

17. Zhang Z-X, Liu X, Xu FJ, Loh XJ, Kang E-T, Neoh K-G, Li J (2008) Pseudo-block copolymer based on star-shaped poly(N-isopropylacrylamide) with a beta-cyclodextrin core and guest-bearing PEG: controlling thermoresponsivity through supramolecular self-assembly. Macromolecules 41:5967–5970
18. Zhang Z-X, Liu KL, Li J (2011) Self-assembly and micellization of a dual thermoresponsive supramolecular pseudo-block copolymer. Macromolecules 44:1182–1193
19. Zhao Q, Wang S, Cheng X, Yam RCM, Kong D, Li RKY (2010) Surface modification of cellulose fiber via supramolecular assembly of biodegradable polyesters by the aid of host/guest inclusion complexation. Biomacromolecules 11:1364–1369
20. Bertrand A, Stenzel M, Fleury E, Bernard J (2012) Host-guest driven supramolecular assembly of reversible comb-shaped polymers in aqueous solution. Polym Chem 3:377–383
21. Rekharsky MV, Inoue Y (1998) Complexation thermodynamics of cyclodextrins. Chem Rev 98:1875–1918
22. Bigot J, Charleux B, Cooke G, Delattre F, Fournier D, Lyskawa J, Sambe L, Stoffelbach F, Woisel P (2010) Tetrathiafulvalene end-functionalized poly(N-isopropylacrylamide): a new class of amphiphilic polymer for the creation of multistimuli responsive micelles. J Am Chem Soc 132:10796–10801
23. Li L-Y, He W-D, Li J, Zhang B-Y, Pan T-T, Sun X-L, Ding Z-L (2010) Shell-cross-linked micelles from PNIPAM-b-(PLL)2 Y-shaped miktoarm star copolymer as drug carriers. Biomacromolecules 11:1882–1890
24. Sakai F, Chen G, Jiang M (2012) A new story of cyclodextrin as a bulky pendent group causing uncommon behaviour to random copolymers in solution. Polym Chem 3:954–961

Chapter 7
Modulation of the Thermoresponsitivity of PDEAAm via CD Addition

7.1 Introduction

Thermoresponsive water soluble polymers have attracted much attention in the last years [2–5]. This is especially due to a broad range of envisaged applications, in e.g. drug [6] or gene delivery [7]. Several polymer classes have been in the focus of polymer scientists, e.g. poly(oxazolines) [8], poly(acrylamides) or poly(acrylates) with oligo(ethyleneglycol) sidechains [9]. In addition thermoresponsive blocks have been utilized in polymers with multiple stimuli responses, i.e. schizophrenic behavior [10]. A common property of thermoresponsive water soluble polymers is a coil to globule transition at a certain critical temperature, i.e. the cloud point T_c. Either the polymers lose their water solubility upon heating to a certain temperature (LCST) or they dissolve upon heating (UCST). There are manifold examples of these two classes, e.g. PNIPAAm [11] for LCST-polymers or poly(*N*-acryloylglycinamide) [12] for UCST-polymers. The T_c is governed by several factors such as ionic strength [13], polymer endgroups [14], polymer concentration, polymer topology [15] or the addition of supramolecular hosts, e.g. β-CD via complexation of endgroups [16, 17] or polymer sidegroups [18]. The variation of the polymer endgroup gives rise to modulations of the T_c, which can also be combined with external triggers or additional compounds, e.g. the masking of a hydrophobic endgroup with cucurbit[8]uril [19], the cleavage of a disulfide to remove a hydrophobic endgroup [20] or the photoisomerization of polymer endgroups [21] via UV-light.

In the present chapter the modulation of the T_c of PDEAAm via the formation of supramolecular inclusion complexes between the guest-functionalized polymers and Me-β-CD or β-CD (Scheme 7.1) is described. The change in the T_c upon complexation was determined via turbidimetry measurements. Furthermore, the complexes were characterized via 2D NOESY. The modulation of the T_c could be reversed via

NOESY measurements were performed in collaboration with M. Hetzer and Prof. H. Ritter (Heinrich Heine Universität Düsseldorf). Parts of this chapter were reproduced with permission from Schmidt et al. [1]. Copyright 2013 John Wiley & Sons.

B. V. K. J. Schmidt, *Novel Macromolecular Architectures via a Combination of Cyclodextrin Host/Guest Complexation and RAFT Polymerization*, Springer Theses,
DOI: 10.1007/978-3-319-06077-4_7, © Springer International Publishing Switzerland 2014

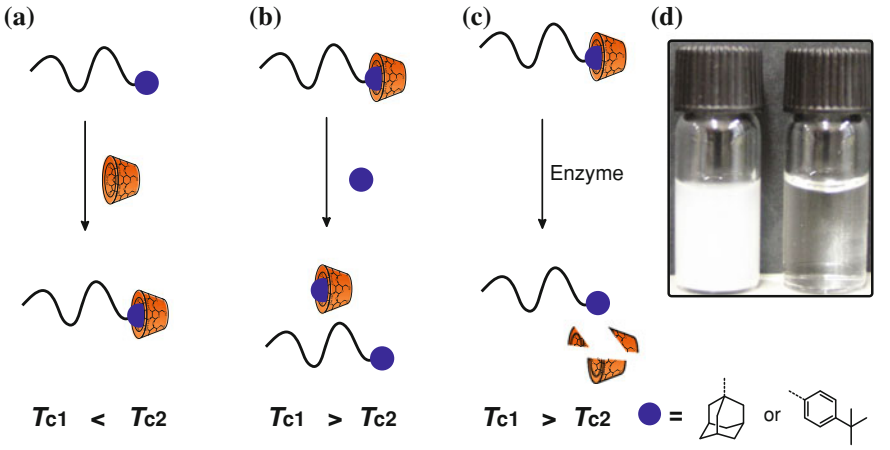

Scheme 7.1 Overview of the examined concept. **a** Increase of the T_c of PDEAAm (*black*) via addition of Me-β-CD or β-CD (*orange*); **b** decrease of T_c after addition of competing guest molecules; **c** decrease of T_c after degradation of CD upon enzyme addition; **d** picture of crude doubly adamantyl functionalized PDEAAm (M_n = 3,000 g mol^{-1}) (*left*) and the polymer after complex formation with 2 eq. of Me-β-CD (*right*) at 10 °C

addition of competing guest molecules or for the first time via enzymatic degradation of the added CDs, which is an outstanding property with regard to biomedical applications.

In the research on CD-complexed RAFT reagents for the reversible-deactivation radical polymerization of various acrylamides in aqueous solution (refer to Chap. 3) it was noticed that in the case of DEAAm a homogenous polymerization mixture was retained throughout the reaction time. Nevertheless, some of the obtained polymers showed no water solubility after the removal of Me-β-CD. This effect was assigned to the masking of the hydrophobic endgroups by the CD moiety and is investigated further in the present chapter.

7.2 Results and Discussion

7.2.1 Synthesis of Guest Endfunctionalized PDEAAm

PDEAAm with different chain lengths and endgroups was prepared via RAFT polymerization in DMF at 60 °C using AIBN as initiator (Scheme 7.2). As endgroups for single and double functionalized polymers *tert*-butyl phenyl (via **1** and **2**), adamantyl (via **10** and **5**) or azobenzene (via **16** and **6**) were utilized (Fig. 7.1). The obtained polymers were analyzed via SEC and subsequently subjected to measurements of the T_c (refer to Appendix E.1–E.7).

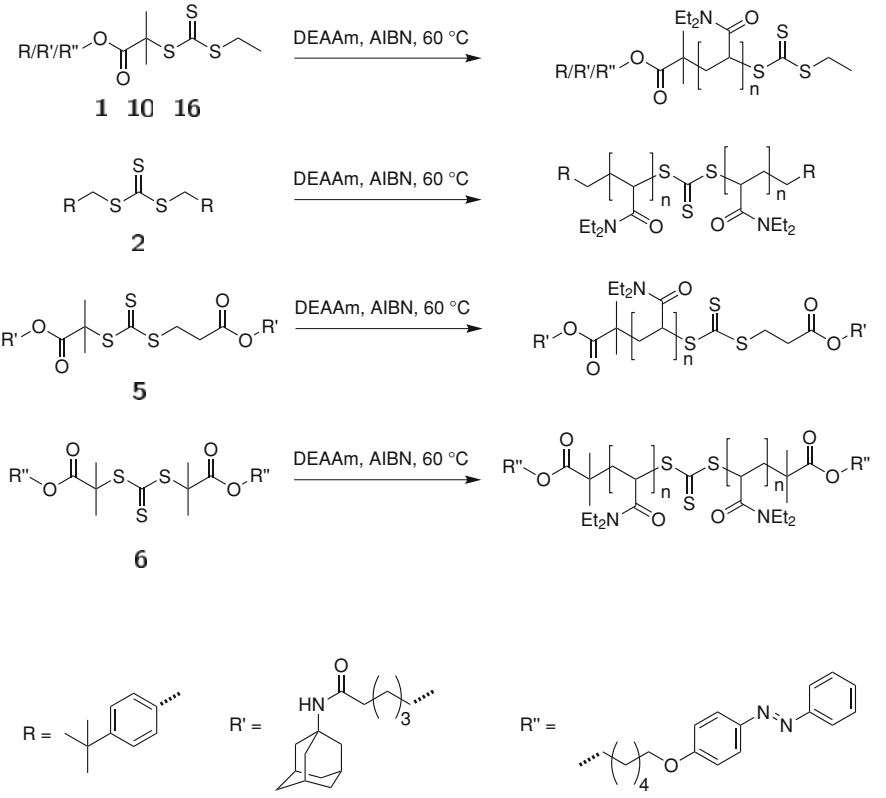

Scheme 7.2 Polymerization of DEAAm in DMF at 60 °C with the respective CTA to generate the desired endfunctionalized polymers

The effect of CDs on the solubility of PDEAAm can be readily visualized when a short chain PDEAAm with hydrophobic guest groups is considered, e.g. double adamantyl functionalized PDEAAm (M_n = 3,000 g mol^{-1}). Without the addition of Me-β-CD, the polymer is insoluble in water even at 4 °C, whereas after addition of Me-β-CD a clear solution of PDEAAm in water is obtained (refer to Scheme 7.1d). The inclusion complex formation of the polymer endgroup with Me-β-CD can be proven via NOESY. In the case of *tert*-butyl phenyl guests, the expected cross correlation peaks between the signals of the inner CD protons at 3.6 and 3.8 ppm and the *tert*-butyl phenyl-protons at 1.3, 6.9 and 7.3 ppm (refer to Fig. 7.2a, b) are observed. For adamantyl guests cross correlation peaks between the inner CD protons and the adamantyl protons at 1.7, 2.0 and 2.2 ppm are evident (refer to Fig. 7.2c, d). Mixtures of azobenzene functionalized PDEAAm with Me-β-CD or α-CD show cross correlation peaks between the inner CD protons and the signals of the protons of the azobenzene moiety between 7.0 and 7.5 ppm. A control sample of carboxyl terminated PDEAAm shows no cross correlation peaks in the respective regions (refer to Appendix E.1).

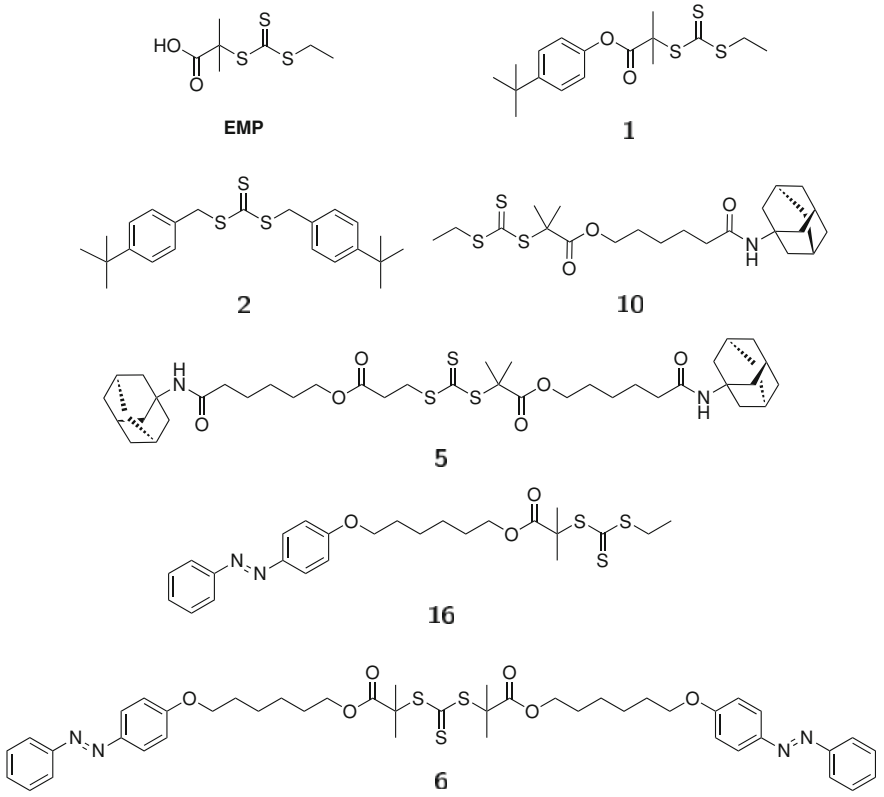

Fig. 7.1 Structures of the utilized CTAs

7.2.2 Turbidimetric Measurements: Influence of Guest Groups, Chain Length and CD/Endgroup Ratio

Apart from macroscopic observations, the apparent T_cs were measured via turbidimetry with and without the addition of Me-β-CD. Firstly, the effect of different guest-groups and their quantity was probed. Transmittance versus temperature plots of exemplary chain lengths close to 5,000 g mol^{-1} are depicted in Fig. 7.4a. As expected, doubly guest functionalized PDEAAm exhibits a lower T_c compared to single functionalized PDEAAm due to the increased hydrophobicity of the chains, e.g. a T_c of 28.4 °C is observed for single *tert*-butyl phenyl functionalization and a T_c of 26.8 °C for double *tert*-butyl phenyl functionalization. Single adamantyl functionalized PDEAAm has a T_c of 29.8 °C and double adamantyl functionalized PDEAAm is not soluble in water over 4 °C. After addition of Me-β-CD, an increase of the T_c is observed that is also dependent on the respective guest group. For adamantyl guest groups, large changes are evident, e.g. from 29.8 to 35.1 °C in the case of $M_n = 4{,}900$ g mol^{-1}. A completely different situation is observed in the

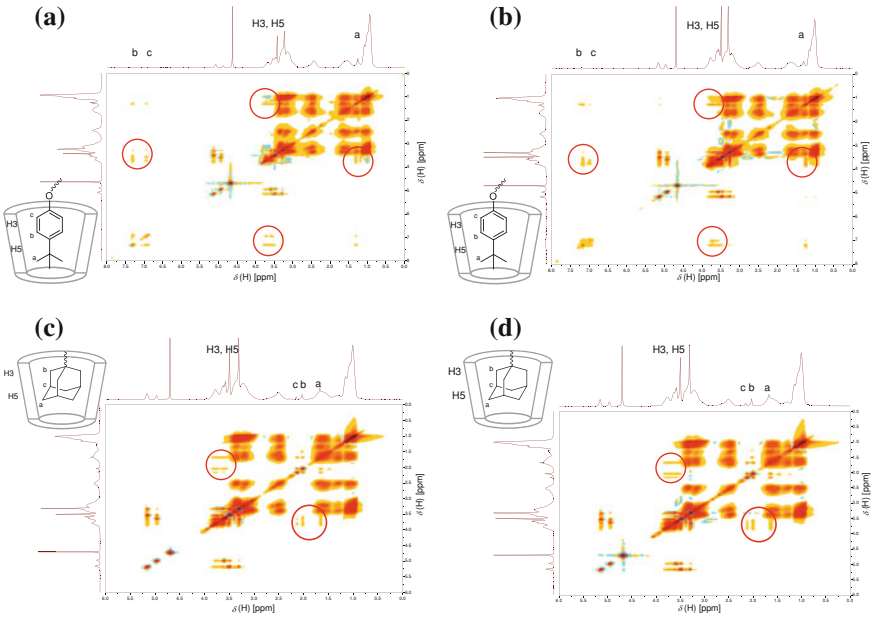

Fig. 7.2 NOESY spectrum in D_2O at 25 °C of a mixture of **a** single *tert*-butyl phenyl functionalized PDEAAm (M_n = 6,500 g mol^{-1}) and 2 eq. of Me-β-CD; **b** double *tert*-butyl phenyl functionalized PDEAAm (M_n = 5,600 g mol^{-1}) and 4 eq. of Me-β-CD; **c** single adamantyl functionalized PDEAAm (M_n = 4,900 g mol^{-1}) and 2 eq. of Me-β-CD; **d** double adamantyl functionalized PDEAAm (M_n = 7,700 g mol^{-1}) and 4 eq. of Me-β-CD

case of azobenzene guests, as no significant changes in the T_c upon complexation are evident. This effect could be due to the more hydrophilic nature of azobenzenes and the weaker complexation with β-CD (refer to Appendices E.6 and E.7). Thus, the effect of addition of α-CD on the T_c of azobenzene functionalized PDEAAm was investigated due to higher association constants of α-CD with azobenzenes.2 After addition of α-CD, similar T_cs of non-complexed and Me-β-CD complexed PDEAAm were observed (refer to Appendices E.8 and E.9). The observed T_c is increasing with increasing chain length. Nevertheless the T_c is not rising over 30 °C even for molecular masses over 10,000 g mol^{-1}.

Furthermore, the dependence of the T_c from the polymer chain length was investigated (Fig. 7.4b). In general, T_c increases with increasing chain length for guest functionalized systems, e.g. the T_c comprises a range from insoluble at 4–33.0 °C from a molecular mass of 1,800–11,200 g mol^{-1} in the case of single *tert*-butyl phenyl functionalized PDEAAm without the addition of Me-β-CD. The complex formation with Me-β-CD leads to an increase of the T_c from 6.0 to 1.5 °C resulting in a range of observed T_cs from 22.9 to 34.5 °C (refer to Fig. 7.4b). The differences in the T_c between Me-β-CD associated and non-associated PDEAAm decrease with molar mass of the polymers. This is due to the weaker influence of the

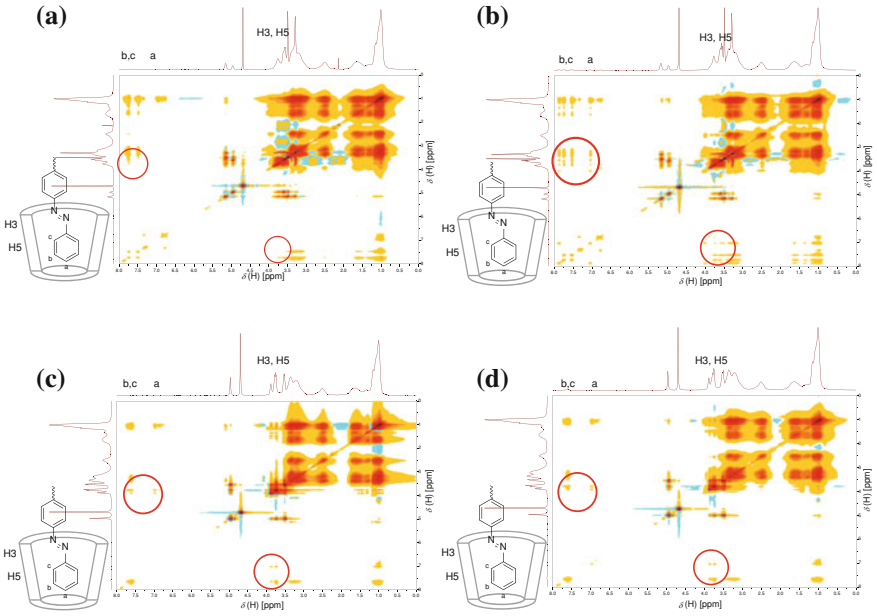

Fig. 7.3 NOESY spectrum in D_2O at 25 °C of a mixture of **a** single azobenzene functionalized PDEAAm (M_n = 5,000 g mol^{-1}) and 2 eq. of Me-β-CD; **b** double azobenzene functionalized PDEAAm (M_n = 11,500 g mol^{-1}) and 4 eq. of Me-β-CD; **c** single azobenzene functionalized PDEAAm (M_n = 5,000 g mol^{-1}) and 2 eq. of α-CD; **d** double azobenzene functionalized PDEAAm (M_n = 11,500 g mol^{-1}) and 4 eq. of α-CD

hydrophobic endgroups with a larger hydrophilic fraction in the polymer. In the case of carboxylic acid functionalized PDEAAm, the T_c is almost constant around 37.5–41.1 °C regardless of the addition of Me-β-CD which leads to T_cs from 38.8 to 41.6 °C. In general, the possible ranges of T_c modulation with CD complexes is dependent on the chain length, the hydrophobicity of the guest group and the number of guest groups (Fig. 7.5). As stated already, T_c increases with increasing chain length of PDEAAm. In the case of double *tert*-butyl phenyl functionalized PDEAAm, the observed T_c increases from insoluble with a M_n of 1,800 g mol^{-1} to 30.7 °C for a M_n of 7,400 g mol^{-1}. After addition of 2 equivalents of Me-β-CD, the T_c shifts to 33.5 °C for a M_n of 1,800 g mol^{-1} and to 36.7 °C for a M_n of 7,400 g mol^{-1}. Single adamantyl functionalized PDEAAm shows T_cs of 27.3 °C for a M_n of 3,200 g mol^{-1} and 33.7 °C for a M_n of 8,300 g mol^{-1}. The association of the endgroups with Me-β-CD leads to a T_c of 33.4 °C for a M_n of 3,200 g mol^{-1} and 35.6 °C for a M_n of 8,300 g mol^{-1}. For the double adamantyl functionalized PDEAAm samples only PDEAAm with higher molecular mass of 12,700 g mol^{-1} is soluble in water with a T_c of 33.0 °C. The addition of Me-β-CD leads to solubilization of all samples. For a M_n of 5,100 g mol^{-1}, a T_c of 27.8 °C is observed, while a T_c of 36.1 °C is observed for a M_n of 12,700 g mol^{-1}. Similar trends are observable for both guest systems.

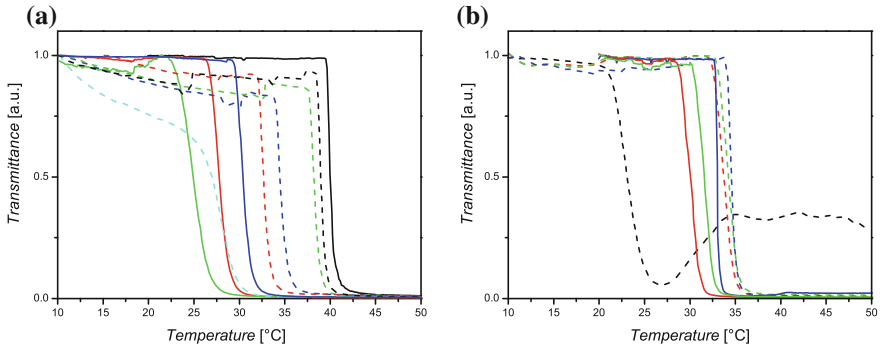

Fig. 7.4 **a** Turbidimetric measurements of PDEAAm with different guest groups (*solid line* without Me-β-CD; *dashed line* with Me-β-CD) and a M_n of approx. 5,000 g mol^{-1}: carboxylic acid (*black*), double *tert*-butyl phenyl (*green*), single adamantyl (*blue*), single *tert*-butyl phenyl (*red*) and double adamantyl (turquoise, note: without Me-β-CD the T_c is below 4 °C); **b** Turbidimetric measurements of PDEAAm with different M_n and single *tert*-butyl phenyl endgroup (*solid line* without Me-β-CD; *dashed line* with Me-β-CD): M_n = 1,800 g mol^{-1} (*black*, note: without Me-β-CD the T_c is below 4 °C), 6,500 g mol^{-1} (*red*), 7,700 g mol^{-1} (*green*) and 11,200 g mol^{-1} (*blue*)

In the case of the *tert*-butyl phenyl and adamantyl endgroups, the T_c converges at molecular masses exceeding 8,000 g mol^{-1} to a value of approximately 33 °C, which is close to the reported value in the literature [22]. It is noteworthy that carboxylic acid functionalized PDEAAm has even higher T_cs close to 40 °C, probably due to additional hydrogen bonding interactions. The addition of Me-β-CD leads to a shift in the observed T_c from approximately 37–40 °C. For shorter chain polymers with M_n below 8,000 g mol^{-1}, T_cs of approximately 33 °C are observed. Interestingly, at chain lengths over 8,000 g mol^{-1} the T_c still increases after Me-β-CD and converges to the value of carboxylic acid functionalized PDEAAm, which shows that the addition of CDs does not only shield the hydrophilic endgroups but also increases the hydrophilicity of the chain ends (Fig. 7.5).

The dependence of endgroup/Me-β-CD ratio on the T_c was investigated as well (Fig. 7.6 and Appendix E.10). Initially for short chain guest functionalized polymers (M_n = 3,800 g mol^{-1}) upon Me-β-CD addition the transmittance versus temperature plot shows the expected sharp increase in turbidity at the T_c. Unexpectedly, the turbidity decreases again after further heating (see also Figs. 7.4b and 7.7b: black dashed line). The variation of the Me-β-CD/polymer endgroup ratio reveals an unexpected behavior. For short chain guest functionalized polymers with pendant complexed Me-β-CD (M_n = 3,800 g mol^{-1}), the transmittance versus temperature plot shows the expected sharp increase in turbidity at the T_c. The turbidity decreases again after further heating, whereas control samples with carboxylic acid endfunctionalization and comparable M_n do not show such a behavior. This effect clearly indicates that the behavior is due to host/guest complexation. The cooling curve does not show such a behavior, yet a slower transition is observed resulting in a large discrepancy of the T_c from heating ramp and cooling ramp. With a longer chain guest functional

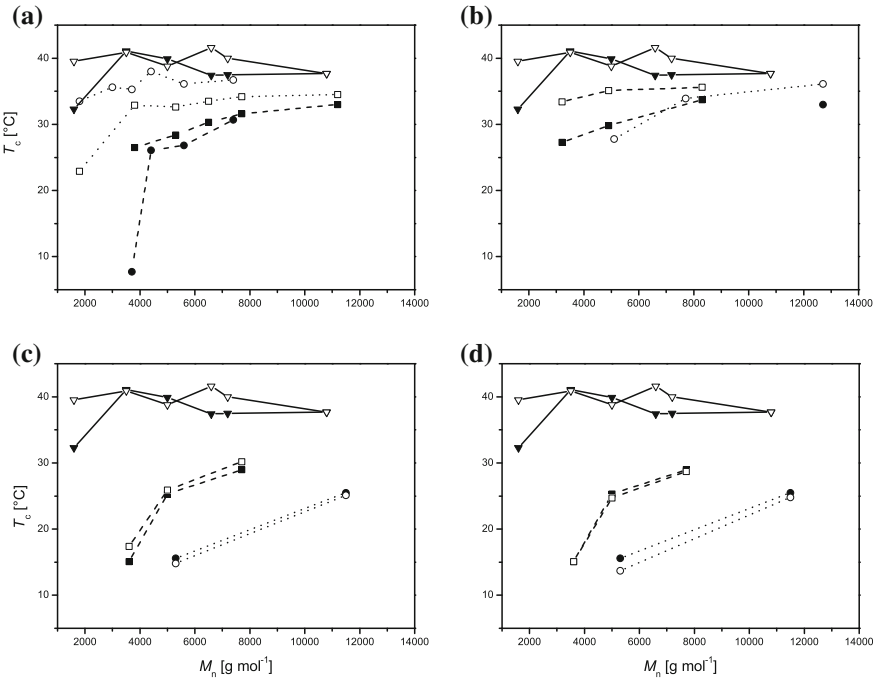

Fig. 7.5 Observed T_cs as a function of M_n for PDEAAm (*filled symbols*) and complexed PDEAAm (*open symbols* **a**–**c** Me-β-CD addition and **d** α-CD addition): **a** single *tert*-butyl phenyl guest (*squares*), double *tert*-butyl phenyl guests (*circles*) and carboxylic acid functionalization (*triangles*); **b** single adamantyl guest (*squares*), double adamantyl guests (*circles*) and carboxylic acid functionalization (*triangles*); **c** and **d** single azobenzene guest (*squares*), double azobenzene guests (*circles*) and carboxylic acid functionalization (*triangles*)

PDEAAm ($M_n = 6{,}500$ g mol^{-1}), only minor discrepancies of the T_c between the heating and cooling ramp are observed. Nevertheless, the decreasing turbidity after the first sharp increase is observed, yet to a weaker extent as well. A possible explanation is that after the phase transition at the T_c the complexes begin to break up, which leads to free Me-β-CD molecules in solution that interact with the insoluble polymers and change the turbidity of the solution.

7.2.3 Reversal of the Effect via External Stimuli

As the addition of Me-β-CD leads to significant changes in the observed T_cs, removal of the CD moieties should give the opportunity to decrease the T_c again or even to precipitate the uncomplexed PDEAAm strands. One possibility is the addition of an excess of guest molecules that should shift the equilibrium to uncomplexed

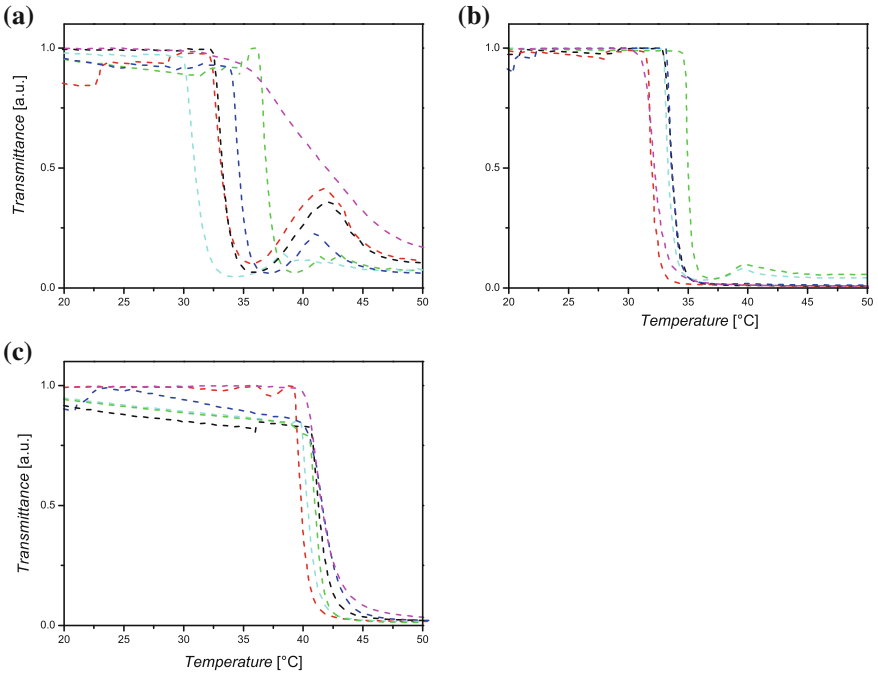

Fig. 7.6 Turbidimetric measurements of PDEAAm with different Me-β-CD equivalents (heating ramps: 1.0 eq. *red curve*; 1.5 eq. *turquoise curve*; 2.0 eq. *black curve*; 3.0 eq. *blue curve*; 5.0 eq. *green curve*; cooling ramp: 2.0 eq. *magenta curve*): **a** single *tert*-butyl phenyl group ($M_n = 3{,}800$ g mol^{-1}), **b** single *tert*-butyl phenyl group ($M_n = 6{,}500$ g mol^{-1}) and **c** carboxylic acid group ($M_n = 3{,}500$ g mol^{-1})

polymers and therefore change the observed T_c (refer to Fig. 7.7a, b). As an example, single *tert*-butyl phenyl ($M_n = 3{,}800$ g mol^{-1}) and double *tert*-butyl phenyl ($M_n = 5{,}600$ g mol^{-1}) functionalized PDEAAm was complexed with 2 equiv. of Me-β-CD and an excess of 16 equiv. 1-adamantyl amine hydrochloride was added. A decrease in the T_c towards the T_c of uncomplexed PDEAAm was observed, i.e. from 32.9 to 27.9 °C for single *tert*-butyl phenyl functionalized PDEAAm ($M_n = 3{,}800$ g mol^{-1}) (refer to Appendix E.11).

Apart from the addition of competing guests, destruction of the added CD molecules should lead to a shift in T_c as well. An enzymatic pathway is a valid and biocompatible choice, e.g. via hydrolysis of the α-1,4-glycosidic bond in CD with α-amylase. Incubation of beforehand β-CD complexed PDEAAm with Taka diastase from *Aspergillus oryzae* leads to a significant shift in T_c from 30.4 to 26.5 °C in the case of double *tert*-butyl phenyl functionalized PDEAAm ($M_n = 4{,}400$ g mol^{-1}) (refer to Fig. 7.7c and Appendix E.12), which is close to the obtained T_c for the respective uncomplexed sample. For a control sample with non-guest functionalized

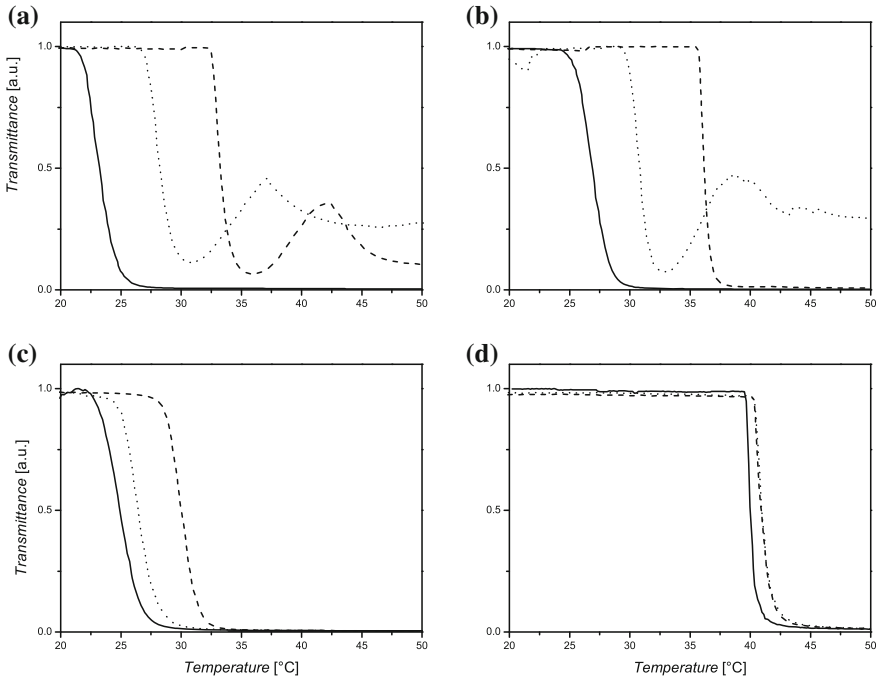

Fig. 7.7 **a** Turbidimetric measurements of PDEAAm with single *tert*-butyl phenyl group (M_n = 3,800 g mol^{-1}): without Me-β-CD (*solid line*), with 2 eq. Me-β-CD (*dashed line*) and after addition of 16 eq. 1-adamantylamine hydrochloride (*dotted line*); **b** turbidimetric measurements of PDEAAm with double *tert*-butyl phenyl group (M_n = 5,600 g mol^{-1}): without Me-β-CD (*solid line*), with 2 eq. Me-β-CD (*dashed line*) and after addition of 16 eq. 1-adamantyl amine hydrochloride (*dotted line*); **c** turbidimetric measurements of PDEAAm with double *tert*-butyl phenyl group (M_n = 4,400 g mol^{-1}): without β-CD (*solid line*), with 2 eq. β-CD (*dashed line*) and after enzymatic treatment (*dotted line*); **d** turbidimetric measurements of PDEAAm with carboxylic acid group (M_n = 5,000 g mol^{-1}): without β-CD (*solid line*), with 2eq. β-CD (*dashed line*) and after enzymatic treatment (*dotted line*)

PDEAAm, no shift was observed (Fig. 7.7d). Thus not only an increase in T_c upon complex formation was observed, but the situation could be reversed via addition of a competing guest or enzymatically.

7.3 Conclusions

In summary, we have evidenced that the T_c of aqueous guest functionalized PDEAAm solutions is responsive to the addition of CD host molecules. The formation of supramolecular host/guest complexes of the hydrophobic polymer endgroups with CDs leads to a shielding of the hydrophobic nature of the pendant guests. Further-

more, the effect of different guest groups, the chain length and the endgroup/CD ratio was investigated, showing a broad tuneability of the T_c. Addition of competing guest molecules or CD degrading enzymes gives the opportunity to reverse the observed change of the T_c in a straightforward and—in the case of enzymatic treatment—biocompatible fashion.

7.4 Experimental Part

7.4.1 Synthesis of 6-(4-(phenyldiazenyl)phenoxy)hexyl 2-(((ethylthio)carbonothioyl)thio)-2-methylpropanoate (16)

In a 50 mL Schlenk-flask **EMP** (0.75 g, 3.35 mmol, 1.0 eq.), 6-(4-(phenyldiazenyl)-phenoxy)hexan-1-ol (1.25 g, 5.02 mmol, 1.5 eq.) and DMAP (0.08 g, 0.67 mmol, 0.2 eq.) were dissolved in anhydrous DCM (15 mL). At 0 °C, a solution of DCC (1.04 g, 5.02 mmol, 1.5 eq.) in anhydrous DCM (10 mL) was added. After 1 h the solution was warmed to ambient temperature, stirred overnight, filtered and concentrated under reduced pressure. The residual oil was purified via column chromatography on silica-gel with a 20:1 mixture that was changed gradually to 15:1 of *n*-hexane:ethyl acetate as eluent. The product-containing fractions were concentrated and the residue recrystallized from *n*-hexane:ethyl acetate. The product was obtained as orange crystals (1.10 g, 2.42 mmol, 72 %).

^{1}H-NMR (400 MHz, $CDCl_3$): [δ, ppm] = 1.31 (t, ^3J = 7.4 Hz, 3H, C***H***$_3$–CH_2), 1.38–1.56 (m, 4H, 2x C***H***$_2$–CH_2–CH_2–O), 1.57–1.75 (m, 10H, 2x C–C***H***$_3$; O=C–O–CH_2–C***H***$_2$), 1.81 (m, 2H, O–CH_2–C***H***$_2$), 3.27 (q, ^3J = 7.4 Hz, 2H, CH_3–C***H***$_2$), 4.04 (t, ^3J = 6.4 Hz, 2H, C***H***$_2$–O), 4.12 (t, ^3J = 6.4 Hz, 2H, C***H***$_2$–O–C=O), 7.00 (d, ^3J = 8.9 Hz, 2H, C***H***$_{arom.}$), 7.40–7.55 (m, 3H, C***H***$_{arom.}$), 7.82–7.97 (m, 4H, C***H***$_{arom.}$). **^{13}C-NMR** (100 MHz, $CDCl_3$): [δ, ppm] = 13.1 (CH_2–***C***H_3), 25.5 (2x ***C***H_3–C), 25.8 and 25.9 (2x ***C***H_2–CH_2–CH_2–O), 28.4 (O–CH_2–***C***H_2), 29.2 (O=C–O–CH_2–***C***H_2), 31.3 (***C***H_2–CH_3), 56.1 (***C***$(CH_3)2$), 66.1 (O=C–O–***C***H_2), 68.3 (O–***C***H_2), 114.8 (2x O–$CH_{arom.}$–***C***$H_{arom.}$), 122.7 (2x ***C***$H_{arom.}$), 124.9 (2x ***C***$H_{arom.}$), 129.2 (2x ***C***$H_{arom.}$), 130.4 (***C***$H_{arom.}$), 147.0 (***C***$_{arom.}$–N=N), 152.9 (***C***$_{arom.}$–N=N), 161.8 (O–***C***$_{arom.}$), 173.1 (***C***=O), 221.4 (***C***=S). **ESI-MS**: $[M + H^+]_{exp}$ = 505.25 m/z and $[M + H^+]_{calc}$ = 505.17 m/z.

7.4.1.1 Exemplary Synthesis of Endfunctionalized PDEAAm

1 (26.1 mg, 0.073 mmol, 1.0 eq.), DEAAm (311 mg, 2.49 mmol, 33.0 eq.), AIBN (2.4 mg, 0.015 mmol, 0.2 eq.), DMF (2.0 mL) and a stirring-bar were added into a Schlenk-tube. After three freeze-pump-thaw cycles the tube was backfilled with argon, sealed, placed in an oil bath at 60 °C and removed after 24 h. The tube was subsequently cooled with liquid nitrogen to stop the reaction. A NMR-sample was

withdrawn for the determination of the conversion, inhibited with a pinch of hydroquinone (approx. 5 mg) and $CDCl_3$ was added. A conversion of 99 % was calculated based on the NMR data (see Characterization Methods for details of the calculation). The residue was dialysed against deionized water with a SpectraPor3 membrane (MWCO = 1,000 Da) for 3 days at ambient temperature. The solvent was removed in vacuo to yield the polymer as a yellow solid (243 mg, 72 %, $M_{ntheo} = 4{,}500$ g mol^{-1}, **SEC(THF)**: $M_{nSEC} = 3{,}800$ g mol^{-1}, $Đ_m = 1.08$).

7.4.1.2 Exemplary Procedure for the Preparation of the Complexes for the Measurement of T_c

PDEAAm polymerized with **1** ($M_{nSEC} = 6{,}500$ g mol^{-1}; 3.0 mg, 0.46 μmol, 1.0 eq.) and Me-β-CD (1.2 mg, 0.96 μmol, 2.0 eq.) were added into a vial. Deionized H_2O (3 mL) was added and the solution stirred for 1 day at ambient temperature and kept in the fridge for 1 day. Subsequently, the T_c was measured according to the Characterization Methods Section.

7.4.1.3 Exemplary Procedure for the Shifting of the T_c via Addition of Competing Guests

PDEAAm polymerized with **1** ($M_{nSEC} = 3{,}800$ g mol^{-1}; 3.0 mg, 0.79 μmol, 1.0 eq.) and Me-β-CD (1.8 mg, 1.37 μmol, 1.7 eq.) were added into a vial. Deionized H_2O (3 mL) was added and the solution stirred for 1 day at ambient temperature and kept in the fridge for 1 day. Subsequently, 1-adamantyl amine hydrochloride (2.4 mg, 12.78 μmol, 16.0 eq.) was added and the solution stirred for 2 days at ambient temperature. Finally, the T_c was measured according to the Characterization Methods Section.

7.4.1.4 Exemplary Procedure for the Shifting of the T_c via Enzymatic Treatment

PDEAAm polymerized with **17** ($M_{nSEC} = 4{,}400$ g mol^{-1}; 3.0 mg, 0.69 μmol, 1.0 eq.) and β-CD (1.5 mg, 1.36 μmol, 2.0 eq.) were added into a vial. Deionized H_2O (3 mL) was added and the solution stirred for 1 day at ambient temperature and kept in the fridge for 1 day. Subsequently, Taka Diastase from *Aspergillus oryzae* (approx. 0.5 mg) was added and the solution was stirred for 2 days at 33 °C. Finally, the sample was cooled in the fridge, filtered and the T_c was measured according to the Characterization Methods Section.

References

1. Schmidt BVKJ, Hetzer M, Ritter H, Barner-Kowollik C (2013) Modulation of the thermoresponsive behavior of poly (N,N-diethylacrylamide) via cyclodextrin host/guest Interactions. Macromol Rapid Commun 34(16):1306–1311. doi:10.1002/marc.201300478
2. Alarcon CdlH, Pennadam S, Alexander C (2005) Stimuli responsive polymers for biomedical applications. Chem Soc Rev 34:276–285
3. Li Y, Lokitz BS, McCormick CL (2006) Thermally responsive vesicles and their structural locking through polyelectrolyte complex formation. Angew Chem Int Ed 45:5792–5795
4. Liu F, Urban MW (2010) Recent advances and challenges in designing stimuli-responsive polymers. Prog Polym Sci 35:3–23
5. Roy D, Brooks WLA, Sumerlin BS (2013) New directions in thermoresponsive polymers. Chem Soc Rev. 42:7214–7243
6. Schmaljohann D (2006) Thermo- and pH-responsive polymers in drug delivery. Adv Drug Deliv Rev 58:1655–1670
7. York AW, Kirkland SE, McCormick CL (2008) Advances in the synthesis of amphiphilic block copolymers via RAFT polymerization: stimuli-responsive drug and gene delivery. Adv Drug Deliv Rev 60:1018–1036
8. Hoogenboom R, Thijs HML, Jochems MJHC, van Lankvelt BM, Fijten MWM, Schubert US (2008) Tuning the LCST of poly(2-oxazoline)s by varying composition and molecular weight: alternatives to poly(N-isopropylacrylamide)?. Chem Commun 5758–5760
9. Lutz J-F (2011) Thermo-switchable materials prepared using the OEGMA-platform. Adv Mater 23:2237–2243
10. Smith AE, Xu X, Kirkland-York SE, Savin DA, McCormick CL (2010) "Schizophrenic" self-assembly of block copolymers synthesized via aqueous RAFT polymerization: from micelles to vesicles. Macromolecules 43:1210–1217
11. Hirokawa Y, Tanaka T (1984) Volume phase transition in a nonionic gel. J Chem Phys 81:6379–6380
12. Glatzel S, Laschewsky A, Lutz J-F (2010) Well-defined uncharged polymers with a sharp UCST in water and in physiological milieu. Macromolecules 44:413–415
13. Idziak I, Avoce D, Lessard D, Gravel D, Zhu XX (1999) Thermosensitivity of aqueous solutions of poly(N,N-diethylacrylamide). Macromolecules 32:1260–1263
14. Li H, Yu B, Matsushima H, Hoyle CE, Lowe AB (2009) The thiol/Isocyanate click reaction: facile and quantitative access to end-functional poly(N,N-diethylacrylamide) synthesized by RAFT radical polymerization. Macromolecules 42:6537–6542
15. Zhao Y, Tremblay L, Zhao Y (2011) Phototunable LCST of water-soluble polymers: exploring a topological effect. Macromolecules 44:4007–4011
16. Duan Q, Miura Y, Narumi A, Shen X, Sato S-I, Satoh T, Kakuchi TJ (2006) Synthesis and thermoresponsive property of end-functionalized poly(*N*-isopropylacrylamide) with pyrenyl group. Polym Sci Part A Polym Chem 44:1117–1124
17. Maatz G, Maciollek A, Ritter H (2012) Cyclodextrin-induced host/guest effects of classically prepared poly(NIPAM) bearing azo-dye end groups. Beilstein J Org Chem 8:1929–1935
18. Ritter H, Sadowski O, Tepper E (2003) Influence of cyclodextrin molecules on the synthesis and the thermoresponsive solution behavior of N-Isopropylacrylamide copolymers with adamantyl groups in the side-chains. Angew Chem Int Ed 42:3171–3173
19. Rauwald U, Barrio Jd, Loh XJ, Scherman OA (2011) "On-demand" control of thermoresponsive properties of poly(*N*-isopropylacrylamide) with cucurbit[8]uril host-guest complexes. Chem Commun 47:6000–6002
20. Summers MJ, Phillips DJ, Gibson MI (2013) "Isothermal" LCST transitions triggered by bioreduction of single polymer end-groups. Chem Commun 49:4223–4225
21. Jochum FD, zur Borg L, Roth PJ, Theato P (2009) Thermo- and light-responsive polymers containing photoswitchable azobenzene end groups. Macromolecules 42:7854–7862

22. Gan LH, Cai W, Tam KC (2001) Studies of phase transition of aqueous solution of poly(N,N-diethylacrylamide-co-acrylic acid) by differential scanning calorimetry and spectrophotometry. Eur Polym J 37:1773–1778

Chapter 8
Conclusions and Outlook

Supramolecular chemistry has emerged as an important tool in contemporary polymer science. The utilization of supramolecular motifs, e.g. hydrogen bonding, metal-complexes or inclusion complexes, has lead to a broad range of materials with novel properties and promising applications in the life and material sciences. The development of reversible-deactivation radical polymerization techniques had a very significant impact on polymer science as well, especially for the preparation of novel complex macromolecular architectures. The combination of both concepts to generate supramolecular driven complex macromolecular architectures is a highly important research topic from the view of fundamental science, yet with regard to applications as well.

One reasonable approach for the formation of complex macromolecular architectures governed by supramolecular interactions is the incorporation of supramolecular motifs into polymers via end functionalization, which can be conducted via click chemistry or the synthesis of the respective controlling agents. The control over polymer functionality is essential in such an approach and is certainly possible via RAFT polymerization. Such a functionality guided attempt facilitates the formation of complex macromolecular topologies and thus the combination of variable building blocks enables the formation of complex macromolecular architectures. Another key feature of the supramolecular approach is the possibility to combine the building blocks in a modular fashion. As different building blocks are combined to form complex architectures via specific supramolecular recognition motifs, it is easily possible to exchange the respective building blocks, e.g. with different polymer-types and thus to change the properties of the obtained materials easily.

In the current thesis, CDs were utilized as supramolecular motifs that are capable of forming inclusion complexes with hydrophobic molecules in aqueous solution. Their complexation ability was exploited in a new method to solubilize hydrophobic RAFT agents and subsequently perform RAFT polymerizations of several acrylamides, i.e. DMAAm, DEAAm and NIPAAm, in aqueous solution. Thus, hydrophilic polymers with hydrophobic endgroups were prepared in water in one step. In addition to the novel method for controlling chain endfunctionality, CDs

B. V. K. J. Schmidt, *Novel Macromolecular Architectures via a Combination of Cyclodextrin Host/Guest Complexation and RAFT Polymerization*, Springer Theses,
DOI: 10.1007/978-3-319-06077-4_8, © Springer International Publishing Switzerland 2014

were incorporated in polymers as endgroup. In combination with guest functionalized polymers, several complex macromolecular architectures were formed. Mono CD functionalized PHPMA was conjugated supramolecularly with doubly guest functionalized PDMAAm or PDEAAm to form supramolecular ABA block copolymers. In this case the stimuli responsive behavior of the supramolecular linkage was probed, i.e. via a temperature- and light-response. Thus, the formed triblock copolymers were disassembled upon external stimuli. Furthermore, the thermo-responsive PDEAAm block allowed the investigation of temperature-induced micellization. In the area of star architectures a three fold CD functional core was attached to guest endfunctionalized polymers to form three arm star polymers that showed disassembly of the stars at increased temperatures and re-formation of the supramolecular assemblies after cooling. An AB_2 miktoarm star polymer was prepared with CD-functionalized PDEAAm and a mid-chain guest functionalized PDMAAm. Again, the thermoresponsive nature of PDEAAm was utilized to form temperature-induced aggregates. Additionally, the thermoresponsive behavior of PDEAAm was modulated via complexation of hydrophobic endgroups with CD. This effect could be reversed via the addition of competing guest molecules or in a biocompatible way via enzymatic degradation of the CD molecules.

In conclusion, CD driven macromolecular architectures were put on a new level: From control over endgroups to complex architectures such as block copolymers or star polymers. Especially incorporation of stimuli-responsive linkages have proven to be a powerful property of the presented systems, especially if future applications are considered, e.g. drug-delivery or the formation of nano-objects. Furthermore, the utilization of thermoresponsive building blocks allows temperature-induced aggregation, which has again uses in drug-delivery. The next step with the materials presented in this thesis, is to put them to use in first application oriented studies, e.g. drug encapsulation and release or microphase separation of block copolymers.

CD-based macromolecular architectures are an interesting area of research that is at a turning point. Almost every conceivable architecture has been prepared so far and the focus of polymer scientists is turning from the fundamental level to more application oriented research. Biomedical science is the most promising area for applications in that regard, e.g. for drug-delivery. CDs are a viable choice in that case as native CDs are biocompatible and are already employed in food technology or drug-delivery. Furthermore, the association of CDs and guest molecules is performed in an aqueous environment, which is the solvent of choice for biological applications. From the point of view of biomedical applications, the frequently utilized CuAAc, which is certainly used so frequently due to the convenient preparation of mono azido functional CD, has to be exchanged with biocompatible click reactions, e.g. thiol-ene reactions or Diels-Alder processes. Branched structures and hydrogels have proven to be an important area of CD-based polymer science. This area will be important with regard to applications in the future as well, e.g. the formation of microgels, hydrogels for drug-delivery or self-healing materials. Another area of

rising importance in polymer science is the modification of surfaces and first steps of supramolecular surface modifications with CDs have been undertaken already in the Barner-Kowollik group and other research groups as well. Nevertheless, there are many opportunities left for different applications of supramolecularly attached molecules on surfaces.

Chapter 9
Experimental Part

Experiments employing anhydrous solvents were conducted with standard Schlenk-techniques under an atmosphere of argon. The glassware was dried with a heat-gun under high vacuum and the flasks were backfilled with argon prior to addition of reagents.

9.1 Materials

Acetic acid (Roth, 99 %), 1-adamantylamine hydrochloride (ABCR, 99 %), aluminium chloride (ABCR, 99 %), 2-amino-1-propanol (TCI, 98 %), 4,4′-azobis(4-cyanovaleric acid) (V-501; Sigma Aldrich, 98 %), β-cyclodextrin (β-CD; Wacker, pharmaceutical grade), 2,2-bis(hydroxymethyl)propionic acid (Sigma Aldrich, 98 %), 2-bromoisobutyric acid (Sigma Aldrich, 98 %), 3-bromopropionyl chloride (ABCR, 90 %), carbon disulfide (Acros, 99.9 %), 1-chloro-6-hydroxyhexane (Acros, 95 %), copper bromide (Sigma Aldrich, 99 %), deuterated acetone (acetone-D_6; Euriso-top, 99.8 %), deuterated chloroform ($CDCl_3$; Euriso-top, 99.9 %), deuterated dimethylsulfoxide (DMSO-D_6; Euriso-top, 99.8 %), deuterium oxide (D_2O; Euriso-top, 99.9 %), diisopropylazodicarboxylate (DIAD; ABCR, 94 %), N, N'-dicyclohexylcarbodiimide (DCC; ABCR, 99 %), *N*,*N*-dimethylaminopyridine (DMAP; Sigma Aldrich, 99 %), *N*,*N*-dimethylformamide (DMF; ABCR, 99 %), Dowex 50WX2-100 ion-exchange resin (Sigma Aldrich), ϵ-caprolactone (CL; Alfa Aesar, 99 %), ethanethiol (Acros, 99 %), ethylenediaminetetraacetic acid disodium salt (EDTA; ABCR, 99 %), hydroquinone (Fluka, 99 %), iodine (Acros, 99.5 %), 3-mercaptopropionic acid (Acros, 99 %), methacryloyl chloride (Sigma Aldrich, 97 %), 4-*tert*-butyl benzylbromide (Acros, 97 %), 4-*tert*-butyl phenol (Sigma Aldrich, 99 %), 4-*tert*-butyl aniline (Acros, 99 %), 4-*tert*-butylbenzyl mercaptan (Sigma Aldrich, 99 %), *p*-toluenesulfonic acid monohydrate (Sigma Aldrich, 99 %), *p*-toluenesulfonyl chloride (ABCR, 98 %), N,N,N',N'',N''-pentamethyldiethyltriamine (PMDETA; Merck, 99.9 %), 4-phenylazophenol

B. V. K. J. Schmidt, *Novel Macromolecular Architectures via a Combination of Cyclodextrin Host/Guest Complexation and RAFT Polymerization*, Springer Theses,
DOI: 10.1007/978-3-319-06077-4_9, © Springer International Publishing Switzerland 2014

(ABCR, 98 %), potassium carbonate (VWR, rectapur), potassium iodide (Sigma Aldrich, 99 %), potassium phosphate monohydrate (Sigma Aldrich, puriss.), propargylalcohol (Alfa Aesar, 99 %), randomly methylated β-cyclodextrin (Me-β-CD, average methylation grade 1.8 per glucose unit, pharmaceutical grade, was a gift from Wacker), silica gel (Merck, Geduran SI60 0.063–0.200 mm), sodium acetate (Roth, 99 %), sodium azide (Acros, 99 %), sodium hydroxide (Roth, 99 %), Taka-Diastase from *aspergillus oryzae* (Sigma Aldrich, 126 u mg^{-1}), tetrabutyl ammonium hydrogen sulfate (Sigma Aldrich, 97 %), triethylamine (Acros, 99 %), trifluoroacetic acid (TFA; ABCR, 99 %), triphenylphosphine (Merck, 99 %), tripropargylamine (Sigma Aldrich, 98 %) were used as received. Anhydrous dichloromethane (DCM), *N*,*N*-dimethylformamide (DMF) and tetrahydrofuran (THF) were purchased from Acros (extra dry over molecular sieves) and used as received. Diethyl ether (VWR Analpur) was dried over CaH_2 and distilled before use. 1,4-Dioxane (VWR, HPLC-grade) was passed over a short column of basic alumina prior to use. All other solvents were of analytical grade and used as received. 2,2′-Azobis[2-(2-imidazolin-2-yl)propane]dihydrochloride (VA-044; Wako, 99 %) and 2,2′-azobis (2-methylpropionitrile) (AIBN; Fluka, 99 %) were recrystallized twice from methanol. *N*,*N*-Diethylacrylamide (DEAAm; TCI, 98 %) and *N*,*N*-dimethylacrylamide (DMAAm; TCI, 99 %) were passed over a short column of basic alumina prior to use. *N*-Isopropylacrylamide (NIPAAm, Acros, 99 %) was recrystallized twice from *n*-hexane. Milli-Q water was obtained from a Milli-Q Advantage A10 Ultrapure Water Purification System (Millipore, USA). Acetic acid/acetate buffer had a pH of 5.2 with an acetic acid concentration of 0.27 mol L^{-1} and a sodium acetate concentration of 0.73 mol L^{-1}. 4-(Dimethylamino)-pyridinium *p*-toluenesulfonate (DPTS) [1] and isopropylidene-2,2-bis(methoxy)propionic acid (**13**) [2] were prepared according to the literature.

9.2 Additional Experimental Procedures

In the following, procedures are described that were utilized for the preparation of starting materials in the previous chapters.

9.2.1 Synthesis of Mono-(6-O-(p-toluenesulfonyl))-β-CD (18)

According to the literature, [3] β-CD (50.0 g, 44.05 mmol, 1.0 eq.) was dissolved in sodium hydroxide solution (500 mL, 0.4 M) and cooled to 5 °C in an ice-bath. The solution was stirred vigorously and *p*-toluenesulfonyl chloride (35.0 g, 183.53 mmol, 4.2 eq.) was added in small portions, over a period of 5 min. The mixture was stirred at 5 °C for 30 min and filtered subsequently. The filtrate was neutralized with conc. HCl and stirred for 1 h. A white precipitate formed, was filtered off and washed

three times with deionized H_2O. The white precipitate was freeze dried to yield the product as white solid (14.1 g, 10.91 mmol, 25 %).

^{1}H-NMR (400 MHz, DMSO-D_6): [δ, ppm] = 2.43 (s, 3H, CH_3), 3.14–3.76 (m, 42H, $\boldsymbol{H}_{2,3,4,5,6}$), 4.07–4.60 (m, 6H, O$\boldsymbol{H}_6$), 4.70–4.87 (m, 7H, ^3J = 3.2 Hz, $\boldsymbol{H}_1$), 5.57–5.94 (br s, 14H, O$\boldsymbol{H}_{2,3}$), 7.43 (s, 2H, ^3J = 8.2 Hz, $\boldsymbol{H}_{\text{arom}}$), 7.75 (s, 2H, ^3J = 8.2 Hz, $\boldsymbol{H}_{\text{arom}}$).

9.2.2 Synthesis of Mono-(6-azido-6-desoxy)-β-CD (β-CD-N_3)

Based on a literature procedure, [3] mono-(6-*O*-(*p*-toluene sulfonyl))-*β*-CD (**18**) (10.0 g, 7.76 mmol, 1.0 eq.) was suspended in deionized H_2O (100 mL) and heated to 80 °C. Sodium azide (2.2 g, 33.85 mmol, 4.4 eq.) was added and the mixture was stirred at 80 °C over night, the solution was filtered and the product precipitated in cold acetone (600 mL). The white precipitate was filtered off and dried under high vacuum. The white solid was recrystallized from deionized H_2O to give the product as white crystals (3.9 g, 3.41 mmol, 44 %).

^{1}H-NMR (400 MHz, DMSO-D_6): [δ, ppm] = 3.22–3.46 (m, 14H, $\boldsymbol{H}_{2,4}$), 3.48–3.81 (br m, 28H, $\boldsymbol{H}_{3,5,6}$), 4.39–4.58 (m, 6H, O$\boldsymbol{H}_6$), 4.83 (d, 6H,^3J = 3.2 Hz, $\boldsymbol{H}_1$), 4.87 (d, 1H, ^3J = 3.4 Hz, $\boldsymbol{H}_1$), 5.73 (br s, 14H, O$\boldsymbol{H}_{2,3}$). **ESI-MS**: $[M + Na^+]_{exp}$ = 1182.50 m/z and $[M + Na^+]_{calc}$ = 1182.37 m/z.

9.2.3 Synthesis of 2-(((Ethylthio)carbonothioyl)thio)-2-methylpropanoic Acid (EMP)

Based on a literature procedure, [4] in a 100 mL round-bottom-flask ethanethiol (1.4 mL, 18.91 mmol, 1.2 eq.) was dissolved in a suspension of $K_3PO_4 \cdot H_2O$ (4.27 g, 18.57 mmol, 1.1 eq.) in acetone (60 mL) at ambient temperature. After stirring for 20 min carbon disulfide (3.0 mL, 49.69 mmol, 3.0 eq.) was added and the solution turned yellow. 2-Bromoisobutyric acid (2.74 g, 16.41 mmol, 1.0 eq.) was added after 20 min and the mixture stirred at ambient temperature overnight. 1M HCl (200 mL) was added and the aqueous phase was extracted with DCM (2 × 150 mL). The combined organic extracts were washed with deionized H_2O (75 mL), brine (75 mL), dried over Na_2SO_4 and filtered. After evaporation of the solvent the yellow oily residue was purified via column chromatography on silica-gel with *n*-hexane:ethyl acetate 2:1 as eluent. The yellow fractions were combined, evaporated and the residue recrystallized from *n*-hexane at 40 °C to give the product as yellow crystals (2.71 g, 12.09 mmol, 74 %).

^{1}H-NMR (400 MHz, $CDCl_3$): [δ, ppm] = 1.27 (t, 3H, ^3J = 7.4 Hz, C$\boldsymbol{H}_3$), 1.66 (s, 6H, C–(C$\boldsymbol{H}_3$)$_2$), 3.23 (q, 2H, ^3J = 7.4 Hz, C$\boldsymbol{H}_2$). **^{13}C-NMR** (100 MHz, $CDCl_3$): [δ, ppm] = 11.9 (***C***H_3), 24.2 (C–(***C***H_3)$_2$), 30.3 (***C***H_2), 54.6 (***C***–$(CH_3)_2$), 177.9 (***C***=O), 219.6 (***C***=S). **ESI-MS**: $[M + Na^+]_{exp}$ = 247.09 m/z and $[M + Na^+]_{calc}$ = 246.99 m/z.

9.2.4 Synthesis of 2-((((2-Carboxyethyl)thio)carbonothioyl)thio)-2-methylpropanoic Acid (CEMP)

Based on a literature procedure, [4] in a 250 mL round-bottom-flask 3-mercaptopropionic acid (1.2 mL, 13.77 mmol, 1.1 eq.) was dissolved in a suspension of $K_3PO_4 \cdot H_2O$ (3.19 g, 13.86 mmol, 1.1 eq.) in acetone (80 mL) at ambient temperature. After stirring for 20 min at ambient temperature carbon disulfide (2.5 mL, 41.40 mmol, 3.3 eq.) was added and the solution turned yellow. 2-Bromoisobutyric acid (2.09 g, 12.53 mmol, 1.0 eq.) was added after 20 min and the mixture was stirred at ambient temperature overnight. 1M HCl (200 mL) was added and the aqueous phase was extracted with DCM (2 × 150 mL). The combined organic extracts were washed with deionized H_2O (150 mL), brine (150 mL), dried over Na_2SO_4 and filtered. After evaporation of the solvent the yellow solid was recrystallized from acetone to give the product as yellow crystals in two fractions (1.92 g, 6.48 mmol, 52 %).

^{1}H-NMR (400 MHz, DMSO-D_6): [δ, ppm] = 1.62 (s, 6H, C–(C***H***$_3$)$_2$), 2.64 (t, 2H, ^3J = 6.9Hz, O=C–C***H***$_2$), 3.45 (t, 2H, ^3J = 6.9 Hz, S–C***H***$_2$), 12.73 (br s, 2H, 2x COO***H***). **^{13}C-NMR** (100 MHz, DMSO-D_6): [δ, ppm] = 25.0 (C–(***C***H$_3$)$_2$), 31.4 (O=C–***C***H$_2$), 32.3 (S–***C***H$_2$), 56.3 (***C***–(CH$_3$)$_2$), 172.4 and 173.1 (***C***=O), 221.5 (***C***=S). **ESI-MS**: [M + Na^+]$_{exp}$ = 291.08 m/z and [M + Na^+]$_{calc}$ = 290.98 m/z.

9.2.5 Synthesis of 2-(1-Carboxy-1-methylethylsulfanylthio--carbonylsulfanyl)-2-methylpropionic Acid (CMP)

In modification of the literature, [5] carbon disulfide (9.2 mL, 152.37 mmol, 1.0 eq.), chloroform (30.5 mL, 378.12 mmol, 2.5 eq.), acetone (27.9 mL, 379.49 mmol, 2.5 eq.) and tetrabutylammonium hydrogen sulfate (1.02 g, 3.00 mmol, 0.02 eq.) were mixed in petrolether (51 mL). At 0 °C sodium hydroxide solution (50 wt% in deionized water; 85 g, 1,063 mmol, 7.0 eq.) were added dropwise over 90 min. The mixture was stirred overnight and deionized water (380 mL) was added. Finally conc. HCl (51 mL) was added cautiously as gas was formed during the addition. The mixture was stirred for 30 min with argon purge. The residue was extracted twice with diethyl ether (300 mL). The organic phase was washed with 1N HCl (300 mL), brine (300 mL), dried over Na_2SO_4 and the solvent was subsequently removed in vacuo. The crude product was recrystallized from acetone to give the product as a yellow crystalline solid in two fractions (8.71 g, 30.84 mmol, 20 %).

^{1}H-NMR (400 MHz, DMSO-D_6): [δ, ppm] = 1.60 (s, 12H, C–(C***H***$_3$)$_2$), 12.91 (br s, 2H, COO***H***). **^{13}C-NMR** (100 MHz, DMSO-D_6): [δ, ppm] = 24.9 (C–(***C***H$_3$)$_2$), 56.2 (O=C–***C***H$_3$), 173.1 (***C***=O), 219.0 (***C***=S). **ESI-MS**: [M + Na^+]$_{exp}$ = 305.08 m/z and [M + Na^+]$_{calc}$ = 305.00 m/z.

9.2.6 Synthesis of 4-Cyano-4-(((ethylthio)carbonothioyl)thio) pentanoate (CEP)

According to the literature procedure, [6] in a 250 mL Schlenk-flask ethanethiol (2.8 mL, 37.85 mmol, 1.0 eq.) was added dropwise to a suspension of sodium hydride (60 wt% in mineral oil, 1.64 g, 41.00 mmol, 1.1 eq.) in anhydrous diethyl ether (75 mL). Subsequently carbon disulfide (2.4 mL, 39.75 mmol, 1.05 eq.) was added dropwise resulting in a yellow precipitate. The precipitate was filtered off and washed with *n*-hexane. Furthermore the resulting filtrate was treated with *n*-hexane leading to further precipitation that was filtered off as well. The two fractions were combined to yield ethyl sodium carbonotrithioate as a yellow solid (5.84 g, 36.53 mmol, 97 %). Subsequently the product was suspended in diethyl ether (70 mL) and iodine (4.30 g, 16.94 mmol, 0.5 eq.) was added in portions. After stirring for 1 h at ambient temperature a white precipitate was filtered off. The filtrate was washed with saturated $Na_2S_2O_3$ solution (100 mL), dried over Na_2SO_4 and filtered. Evaporation of the solvent yielded diethyl carbonotrithioate disulfide as yellow oil (3.99 g, 14.55 mmol, 80 %) that was used subsequently in the next step. The disulfide was dissolved in ethyl acetate (150 mL) and V-501 (6.11 g, 21.91 mmol, 1.5 eq.) was added. The mixture was degassed via two freeze-pump-thaw cycles and heated to reflux under argon for 18 h. After cooling to ambient temperature the solvent was evaporated in vacuo and the residual oil was subjected to a filtration on a silica pad with *n*-hexane:ethyl acetate as eluent that was gradually changed from 1:1 to 1:20. The product was obtained after evaporation of the solvent as a yellow solid (7.05 g, 26.91 mmol, 92 %).

^{1}H-NMR (400 MHz, DMSO-D_6): [δ, ppm] = 1.36 (t, 3H, ^3J = 7.3 Hz, CH_2–C***H***$_3$), 1.88 (s, 3H, C–C***H***$_3$), 2.29–2.60 (m, 2H, O=C–C***H***$_2$), 3.35 (q, 2H, ^3J = 7.3 Hz, C***H***$_2$–CH_3), 11.00 (br s, 1H, COO***H***). **^{13}C-NMR** (100 MHz, DMSO-D_6): [δ, ppm] = 12.9 (CH_2–***C***H_3), 25.0 (C–***C***H_3), 29.7 (O=C–***C***H_2), 31.5 (O=C–CH_2–***C***H_2), 33.6 (S–***C***H_2), 46.3 (***C***–CN), 119.0 (***C***–N), 177.5 (***C***=O), 216.8 (***C***=S). **ESI-MS**: $[M + Na^+]_{exp}$ = 286.08 m/z and $[M + Na^+]_{calc}$ = 286.00 m/z.

9.2.7 Synthesis of N-(Adamantan-1-yl)-6-hydroxyhexanamide (8)

According to the literature procedure, [7] aluminium chloride (11.8 g, 88.50 mmol, 2.2 eq.) were suspended in anhydrous DCM (100 mL). At 0 °C triethylamine (17.2 mL, 124.08 mmol, 3.1 eq.) were added dropwise via a syringe. After stirring for 15 min at 0 °C, the mixture was warmed to ambient temperature. Subsequently, a solution of ϵ-caprolactone (4.2 mL, 39.74 mmol, 1.0 eq.), triethylamine (6.1 mL, 46.89 mmol, 1.2 eq.) and adamantylamine hydrochloride (8.25 g, 43.95 mmol, 1.1 eq.) in anhydrous DCM (100 mL) was added dropwise. The mixture was stirred over night and subsequently poured into an ice cold solution of sodium carbonate (30 g) in ice water (300 mL). The organic phase was separated and the aqueous

phase extracted three times with DCM (200 mL). The combined organic extracts were washed with deionized water (500 mL), brine (500 mL), dried over Na_2SO_4, filtered and concentrated in vacuo. The resulting solid was recrystallized from an acetonitrile/methanol mixture to give 7.09 g (26.72 mmol, 67 %) of the product as off-white crystals.

^{1}H-NMR (400 MHz, $CDCl_3$): [δ, ppm] = 1.31–1.43 (m, 2H, C***H***$_2$–CH_2–CH_2–O), 1.51–1.73 (m, 10H, C***H***$_2$–CH_2–O; C***H***$_2$–CH_2–C=O; 3x C***H***$_{2,adamantyl}$), 1.92–2.00 (m, 6H, 3x NH–C–C***H***$_{2,adamantyl}$), 2.01–2.12 (m, 5H, 3x C***H***$_{adamantyl}$; C***H***$_2$–C=O–NH), 3.63 (t, 2H, ^3J = 6.5 Hz, C***H***$_2$–OH), 5.17 (br s, 1H, N***H***). **^{13}C-NMR** (100 MHz, $CDCl_3$): [δ, ppm] = 25.4 (***C***H_2–CH_2–C=O; ***C***H_2–CH_2–CH_2–C=O), 29.6 (3x ***C***$H_{adamantyl}$), 32.4 (***C***H_2–CH_2–OH), 36.5 (3x ***C***$H_{2,adamantyl}$), 37.7 (***C***H_2–C=O), 41.8 (3x ***C***$H_{2,adamantyl}$–C–NH), 51.9 (***C***–NH), 62.6 (***C***H_2–OH), 172.3 (***C***=O). **ESI-MS**: $[M + Na^+]_{exp}$ = 288.36 m/z and $[M + Na^+]_{calc}$ = 288.19 m/z.

9.2.8 Synthesis of N-(2-Hydroxypropyl)methacrylamide (HPMA)

According to the literature, [8] in a 250 mL Schlenk-flask 1-amino-2-propanol (48.6 mL, 621.17 mmol, 2.0 eq.) was dissolved in anhydrous DCM (20 mL). At 0 °C methacryloyl chloride (30.0 mL, 307.09 mmol, 1.0 eq.) in anhydrous DCM (20 mL) was added dropwise over 1 h. After 1 h the ice bath was removed and the mixture was stirred for further 30 min at ambient temperature. The mixture was cooled to −20 °C in a freezer. The formed precipitate was treated with DCM at 40 °C. Any remaining insoluble salt was removed by filtration and the product crystallized at −20 °C. This procedure was repeated three times to obtain *N*-(2-hydroxypropyl)methacrylamide as a white crystalline solid (22.91 g, 162.45 mmol, 53 %).

^{1}H-NMR (400 MHz, D_2O+DSS): [δ, ppm] = 1.17 (d, 3H, ^3J = 6.4 Hz, CH–C***H***$_3$), 1.93 (s, 3H, O=C–C–C***H***$_3$), 3.20–3.38 (m, 2H, C***H***$_2$), 3.86–4.05 (m, 1H, C***H***–CH_3), 5.46 (s, 1H, C***H***$_{trans}$), 5.71 (s, 1H, C***H***$_{cis}$). **^{13}C-NMR** (100 MHz, D_2O+DSS): [δ, ppm] = 20.4 (O=C–C–***C***H_3), 22.1 (CH–***C***H_3), 48.9 (***C***H_2–NH), 68.9 (***C***H–OH), 123.7 (C–***C***H_2), 141.7 (O=C–***C***–CH_3), 174.8 (***C***=O).

9.2.9 Synthesis of 6-(4-(Phenyldiazenyl)phenoxy)hexan-1-ol (9)

According to the literature, [9] 1-chloro-6-hydroxyhexane (8.1 mL, 60.72 mmol, 1.5 eq.), 4-phenylazophenol (8.00 g, 40.34 mmol, 1.0 eq.), K_2CO_3 (8.40 g, 60.78 mmol, 1.5 eq.) and potassium iodide (0.20 g, 1.21 mmol, 0.03 eq.) were suspended in anhydrous DMF (24 mL). The mixture was heated to 120 °C for 24 h. After cooling to ambient temperature the mixture was added to deionized water (400 mL) under stirring. The resulting orange precipitate was filtered off, dried and dissolved in ethyl acetate (400 mL). The organic phase was washed with deionized water (400 mL), brine (400 mL) and subsequently dried over Na_2SO_4. After filtration and removal of

the solvent in vacuo the crude product was recrystallized from methanol to give the product as orange solid (8.90 g, 29.78 mmol, 74 %).

^{1}H-NMR (400 MHz, $CDCl_3$): [δ, ppm] = 1.35–1.55 (m, 4H, C***H***$_2$–CH_2–CH_2–O; C***H***$_2$–CH_2–CH_2–CH_2–O), 1.56–1.66 (m, 2H, HO–CH_2–C***H***$_2$), 1.78–1.89 (m, 2H, CH_{arom}–O–CH_2–C***H***$_2$), 3.67 (t, 2H, ^{3}J = 6.5 Hz, C***H***$_2$–OH), 4.04 (t, 2H, ^{3}J = 6.5 Hz, C***H***$_2$–O–CH_{arom}), 7.00 (d, 2H, ^{3}J = 9.0 Hz, C***H***$_{arom}$), 7.40–7.46 (m, 2H, C***H***$_{arom}$), 7.47–7.53 (m, 2H, C***H***$_{arom}$), 7.82–7.95 (m, 4H, 2x C***H***$_{arom}$). **^{13}C-NMR** (100 MHz, $CDCl_3$): [δ, ppm] = 25.7 and 26.0 (2x ***C***H_2–CH_2–CH_2–O), 29.3 (CH_{arom}–O–CH_2–***C***H_2), 32.8 (HO–CH_2–***C***H_2), 63.0 (HO–***C***H_2), 68.3 (O–***C***H_2), 114.8 (O–***C***$_{arom}$–CH_{arom}), 122.7 (***C***H_{arom}), 124.9 (2x ***C***H_{arom}), 129.2 (2x ***C***H_{arom}), 130.4 (2x ***C***H_{arom}), 147.0 (***C***$_{arom}$–N=N), 152.9 (***C***$_{arom}$–N=N), 161.8 (O–***C***$_{arom}$). **ESI-MS**: [M + H^+]$_{exp}$ = 299.33 m/z and [M + H^+]$_{calc}$ = 299.18 m/z.

9.3 Characterization and Methods

Nuclear magnetic resonance (NMR) measurements were conducted on a Bruker AM250 spectrometer at 250 MHz for hydrogen nuclei for kinetic measurements, a Bruker Avance III 300 spectrometer at 300 MHz for hydrogen nuclei for kinetic measurements and a Bruker AM400 spectrometer at 400 MHz for hydrogen-nuclei and at 100 MHz for carbon-nuclei for structure verification. ROESY (rotating frame nuclear Overhauser effect spectroscopy) and NOESY (nuclear Overhauser effect spectroscopy) NMR-spectra were measured on a Bruker Avance III 300 spectrometer at 300 MHz or a Bruker Avance III 600 spectrometer at 600 MHz. For the determination of the conversion of DMAAm the integrals of one vinylic proton (5.78–5.89 ppm) and the methyl sidechain protons (2.87–3.28 ppm) were employed. The conversion of DEAAm was determined with the integral of one vinylic proton (5.57–5.73 ppm) and with the integral of the sidechain methyl groups and backbone protons (0.81–1.97 ppm). The calculation of the NIPAAm conversion was carried out with the integrals of one vinylic proton (5.47–5.59 ppm) and the integral of the sidechain methyl groups and the backbone protons (0.92–1.95 ppm). The conversion of HPMA was calculated with the integral of one vinylic proton (5.48–5.58 ppm) and with the integral of one side-chain proton (3.86–4.14 ppm).

Size exclusion chromatography (SEC) employing *N*,*N*-dimethylacetamide (DMAc) as eluent containing 0.03 wt% LiBr was performed for PDMAAm and PHPMA on a Polymer Laboratories PL-GPC 50 Plus Integrated System, comprising an autosampler, a PLgel 5 µm bead-size guard column (50 × 7.5 mm) followed by three PLgel 5 µm MixedC columns (300 × 7.5 mm) and a differential refractive index detector at 50 °C with a flow rate of 1.0 mL min^{-1}. The SEC system was calibrated against linear PSty standards standards with molecular weights ranging from 160 to 6 × 10^{6} g mol^{-1} or PMMA standards with molecular weights ranging from 700 to 2 × 10^{6} g mol^{-1}. All SEC calculations for PDMAAm and PNIPAAm were carried out relative to a PSty calibration. The SEC calculations for PHPMA were carried out relative to a PMMA calibration.

SEC employing tetrahydrofuran (THF) as eluent containing 200 ppm 2,6-di-*tert*-butyl-4-methylphenol for PDEAAm was performed on a Polymer Laboratories PL-GPC 50 Plus Integrated System, comprising an autosampler, a PLgel 5 µm bead-size guard column (50 × 7.5 mm) followed by three PLgel 5 µm MixedC columns (300 × 7.5 mm), a PLgel 5 µm MixedE column (300 × 7.5 mm) and a differential refractive index detector at 35 °C with a flow rate of 1.0 mL min^{-1}. The SEC system was calibrated against linear PSty standards with molecular weights ranging from 160 to 6 × 10^6 g mol^{-1}. All SEC calculations for PDEAAm were carried out relative to PSty. The molecular-weight dispersity is abbreviated as $Đ_m$.

Electrospray ionization mass spectrometry (ESI-MS) was performed on a LXQmass spectrometer (ThermoFisher Scientific, San Jose, CA) equipped with an atmospheric pressure ionization source operating in the nebulizer-assisted electrospray mode. The instrument was calibrated in the m/z range 195–1822 Da using a standard containing caffeine, Met-Arg-Phe-Ala acetate (MRFA), and a mixture of fluorinated phosphazenes (Ultramark 1621) (all from Aldrich). A constant spray voltage of 4.5 kV was used, and nitrogen at a dimensionless sweep gas flow rate of 2 (~3 L min^{-1}) and a dimensionless sheath gas flow rate of 12 (~1 L min^{-1}) were applied. The capillary voltage, the tube lens offset voltage, and the capillary temperature were set to 60 V, 110 V, and 300 °C respectively.

Turbidity measurements (Chaps. 4 and 6) were performed on a Cary 300 Bio UV/VIS spectrophotometer (Varian) at 600 nm. The heating rate was set to 0.32 °C min^{-1} and the concentration was 1 mg mL^{-1}. For the determination of the LCST the point of inflection of the transmittance versus temperature plot was used.

Turbidity measurements (Chap. 5) were performed in a temperature range from 5 to 100 °C with a heating and cooling ramp of 1 °C min^{-1} under stirring (700 rpm). During these controlled heating/cooling cycles, the transmission was monitored in a Crystal 16 TM (Avantium Technologies) instrument.

Dynamic light scattering (DLS) (Chap. 4) was performed on a 380 DLS spectrometer (Particle Sizing Systems, Santa Barbara, USA) with a 90 mW laser diode operating at 658 nm equipped with an avalanche photo diode detector. Every measurement was performed four times at 10 °C for samples containing PDEAAm and at 25 °C for samples containing PDMAAm. The data was evaluated with an inverse Laplace algorithm. The scattered light was recorded at an angle of 90° to the incident beam. For the temperature sequenced measurements the sample was equilibrated at the specific temperature for 5 min, then the DLS measurement was performed three times for 3 min and the temperature changed again. The entire procedure was performed three times and the data points were finally averaged. All hydrodynamic diameters (D_h) in the text are the averages of the number weighted distributions. The samples were prepared in Milli-Q water and filtered with a 0.2 µm regenerated cellulose syringe filter (Roth, Rotilabo).

DLS (Chap. 5) was performed at a scattering angle of 90° on an ALV CGS-3 instrument and a He–Ne laser operating at a wavelength of $\lambda = 633$ nm at 25 °C. The CONTIN algorithm was applied to analyze the obtained correlation functions. For temperature dependent measurements the DLS is equipped with a Lauda thermostat.

Apparent hydrodynamic radii were calculated according to the Stokes-Einstein equation. All CONTIN plots are number-weighted distributions.

DLS (Chap. 6) was performed on a 380 DLS spectrometer (Particle Sizing Systems, Santa Barbara, USA) with a 90 mW laser diode operating at 658 nm equipped with an avalanche photo diode detector. Every measurement was performed 4 times at 25, 44 °C or 50 °C and the data was evaluated with an inverse Laplace algorithm. The scattered light was recorded at an angle of 90° to the incident beam. For the temperature sequenced measurements the sample was equilibrated at the specific temperature for 3 min, then the DLS measurement was performed 2 times for 5 min and the temperature changed again. The entire procedure was performed 3 times and the data points were finally averaged. All hydrodynamic diameters (D_h) in the text are the averages of the number weighted distributions. The samples were prepared in Milli-Q water and filtered with a 0.2 µm regenerated cellulose syringe filter (Roth, Rotilabo).

UV/VIS spectra were measured on a Cary 300 Bio UV/VIS spectrophotometer (Varian) at a temperature of 25 or 10 °C depending on the sample.

UV irradiation for investigation of photoresponse was applied via a BLB-8 UV lamp (8 W, Camag) with an emission maximum at 350 nm for the DLS samples and via a UVASPOT 2000RF2 (2000 W, Hönle technology) with its main irradiation between 315–420 nm for NMR samples.

Theoretical molecular weights (M_{ntheo}) were calculated according to Eqs. 2.8 and 9.1 with the following equation, with m_M as the molar mass of the monomer, m_{CTA} as the molar mass of the CTA and $[M]_0$ or $[CTA]_0$ as the initial concentration of the respective compounds:

$$M_{ntheo} = conversion \cdot m_M \cdot \frac{[M]_0}{[CTA]_0} + m_{CTA} \tag{9.1}$$

References

1. Moore JS, Stupp SI (1990) Room temperature polyesterification. Macromolecules 23:65–70
2. Ihre H, Hult A, Fréchet JMJ, Gitsov I (1998) Double-stage convergent approach for the synthesis of functionalized dendritic aliphatic polyesters based on 2,2-bis(hydroxymethyl)propionic acid. Macromolecules 31:4061–4068
3. Amajjahe S, Choi S, Munteanu M, Ritter H (2008) Pseudopolyanions based on poly(NIPAAM-co-beta-cyclodextrin methacrylate) and ionic liquids. Angew Chem Int Ed 47:3435–3437
4. Skey J, O'Reilly, R. K. (2008) Facile one pot synthesis of a range of reversible addition-fragmentation chain transfer (RAFT) agents. Chem Commun 4183–4185
5. Lai JT, Filla D, Shea R (2002) Functional polymers from novel carboxyl-terminated trithiocarbonates as highly efficient RAFT agents. Macromolecules 35:6754–6756
6. Moad G, Chong YK, Postma A, Rizzardo E, Thang SH (2005) Advances in RAFT polymerization: the synthesis of polymers with defined end-groups. Polymer 46:8458–8468
7. Yu Z, Sawkar AR, Whalen LJ, Wong C-H, Kelly JW (2006) Isofagomine- and 2,5-Anhydro-2,5-imino-d-glucitol-based glucocerebrosidase pharmacological chaperones for gaucher disease intervention. J Med Chem 50:94–100

8. Apostolovic B, Deacon SPE, Duncan R, Klok H-A (2010) Hybrid polymer therapeutics incorporating bioresponsive, coiled coil peptide linkers. Biomacromolecules 11:1187–1195
9. Li C, Lo C-W, Zhu D, Li C, Liu Y, Jiang H (2009) Synthesis of a photoresponsive liquid-crystalline polymer containing azobenzene. Macromol Rapid Commun 30:1928–1935

Appendix A
CD-Complexed RAFT Agents (Appendix to Chapter 3)

See Figs. A.1, A.2, A.3, A.4, A.5, A.6, A.7, A.8, A.9 and Tables A.1, A.2, A.3.

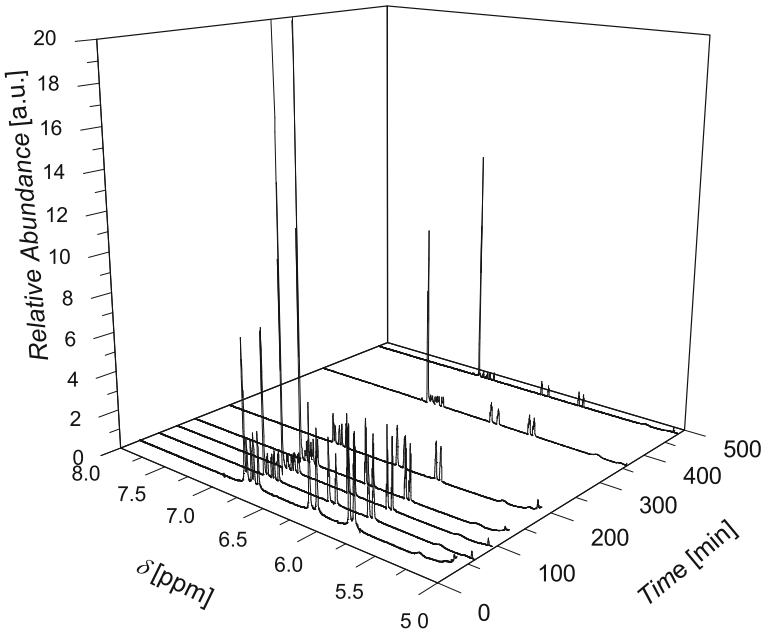

Fig. A.1 3D plot of the vinyl region of the kinetic ^{1}H-NMR-data for the polymerization of DMAAm at 25 °C with DMAAm/**1**/I: 298/1/0.2

B. V. K. J. Schmidt, *Novel Macromolecular Architectures via a Combination of Cyclodextrin Host/Guest Complexation and RAFT Polymerization*, Springer Theses,
DOI: 10.1007/978-3-319-06077-4, © Springer International Publishing Switzerland 2014

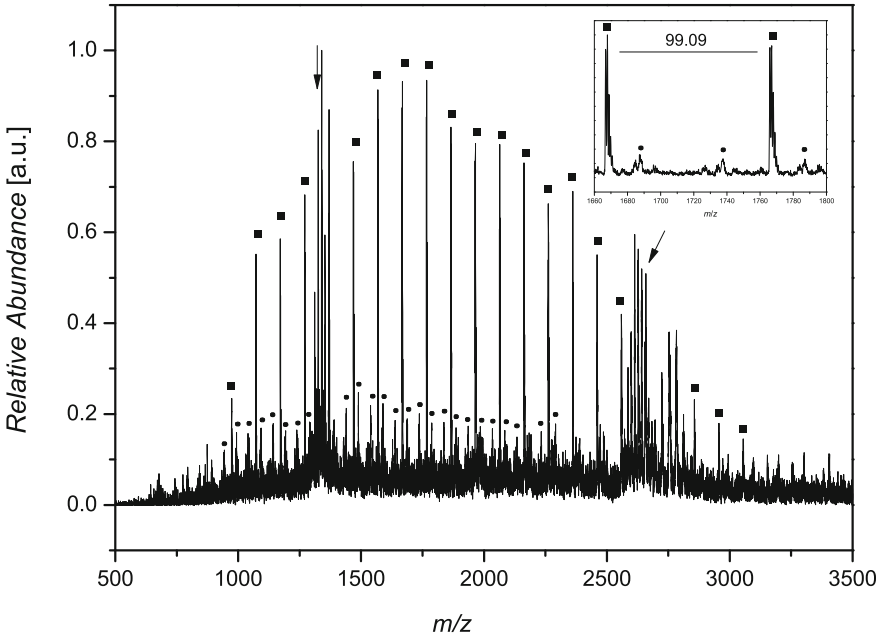

Fig. A.2 ESI-MS-spectrum of PDMAAm (M_{nSEC} = 3,000 g mol^{-1}, $Đ_m$ = 1.18) polymerized with **1** (the arrow marks residual Me-β-CD)

Table A.1 Theoretical and experimental m/z of PDMAAm polymerized with **1**

Species	m/z_{theo}	m/z_{exp}	Δ m/z
■ $[\mathbf{2} + (DMAAm)_{13} + Na]^+$	1,666.97	1,666.82	0.15
• $[\mathbf{2} + (DMAAm)_{30} + 2Na]^{2+}$	1,687.57	1,687.27	0.30

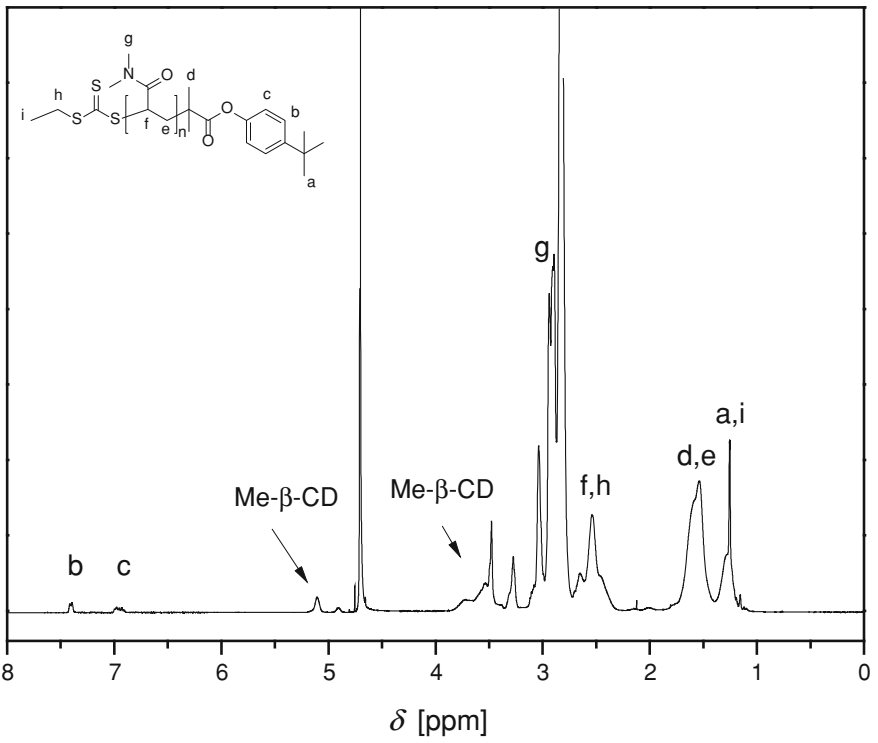

Fig. A.3 ^{1}H-NMR spectrum (400 MHz, D_2O) of PDMAAm polymerized with **1** ($M_{nSEC} = 10{,}000$ g mol^{-1}, $Đ_m = 1.17$)

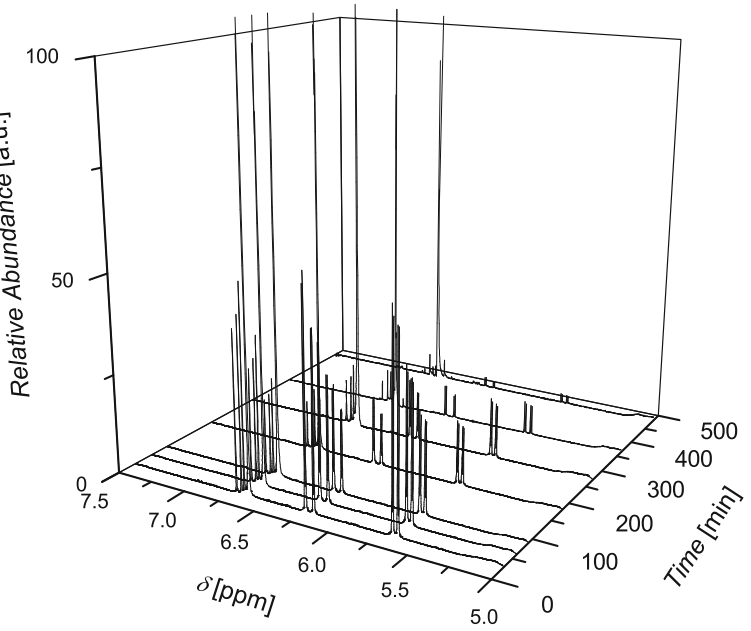

Fig. A.4 3D plot of the vinyl region of the kinetic ^{1}H-NMR-data for the polymerization of DEAAm at 25 °C with DEAAm/**1**/I: 242/1/0.2

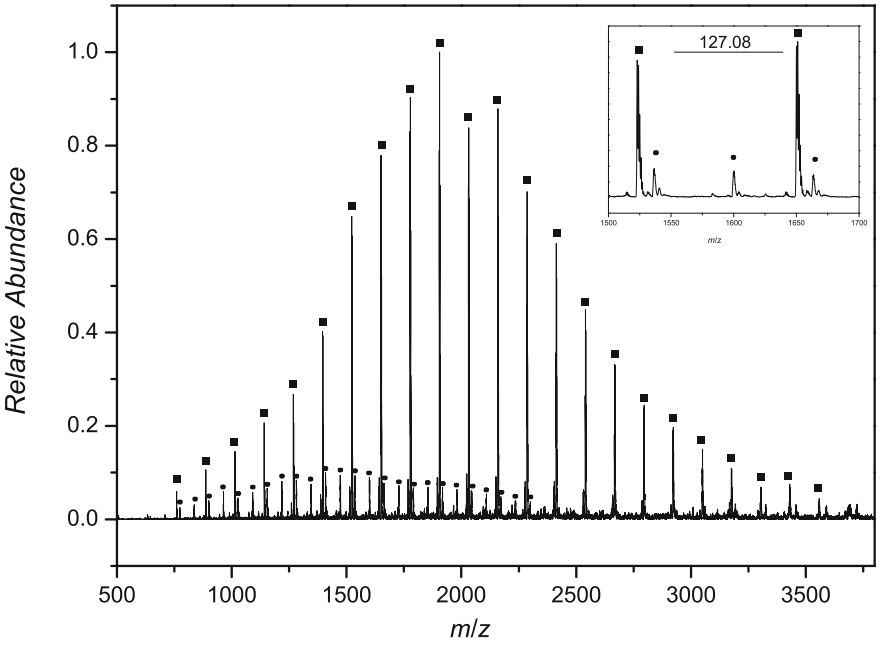

Fig. A.5 ESI-MS-spectrum of PDEAAm (M_{nSEC} = 4,000 g mol^{-1}, $Đ_m$ = 1.15) polymerized with **1**

Table A.2 Theoretical and experimental m/z of PDEAAm polymerized with **1**

Species	m/z_{theo}	m/z_{exp}	Δ m/z
■ [**1** + $(DEAAm)_9$ + Na]$^+$	1,522.98	1,523.00	0.02
• [**1** + $(DEAAm)_{22}$ + 2Na]$^{2+}$	1,599.75	1,600.25	0.50

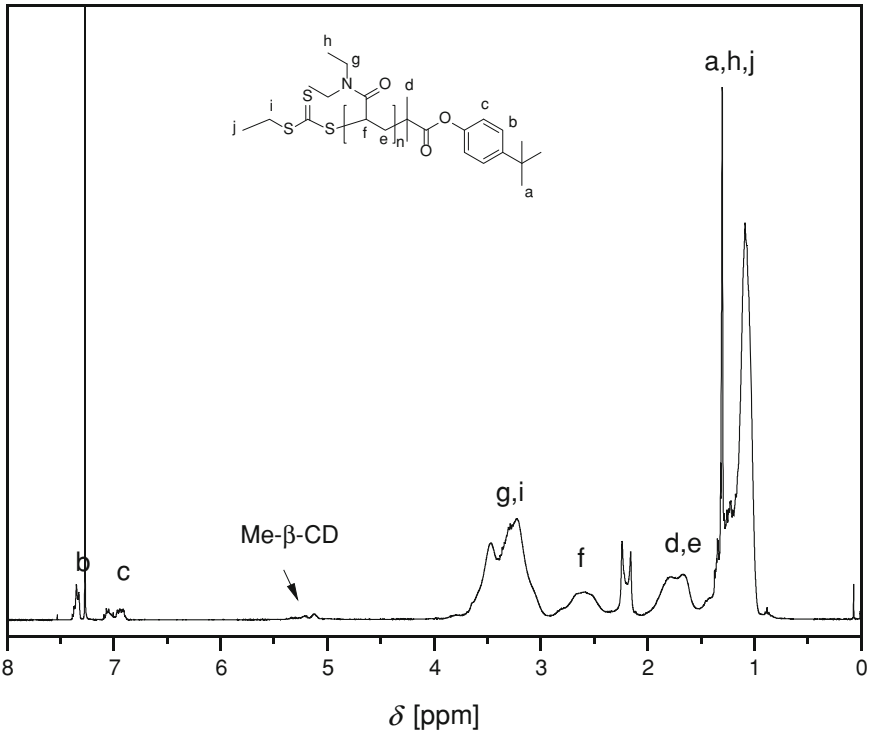

Fig. A.6 ^{1}H-NMR spectrum (400 MHz, $CDCl_3$) of PDEAAm polymerized with **1** ($M_{nSEC} = 4{,}000$ g mol^{-1}, $Đ_m = 1.15$)

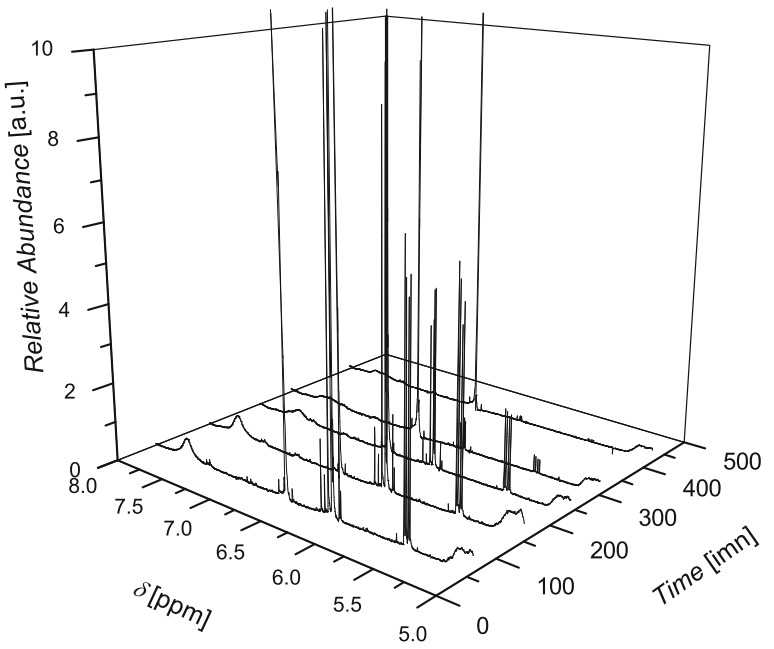

Fig. A.7 3D plot of the vinyl region of the kinetic ^{1}H-NMR-data for the polymerization of NIPAAm at 25 °C with NIPAAm/**1**/I:48/1/0.2

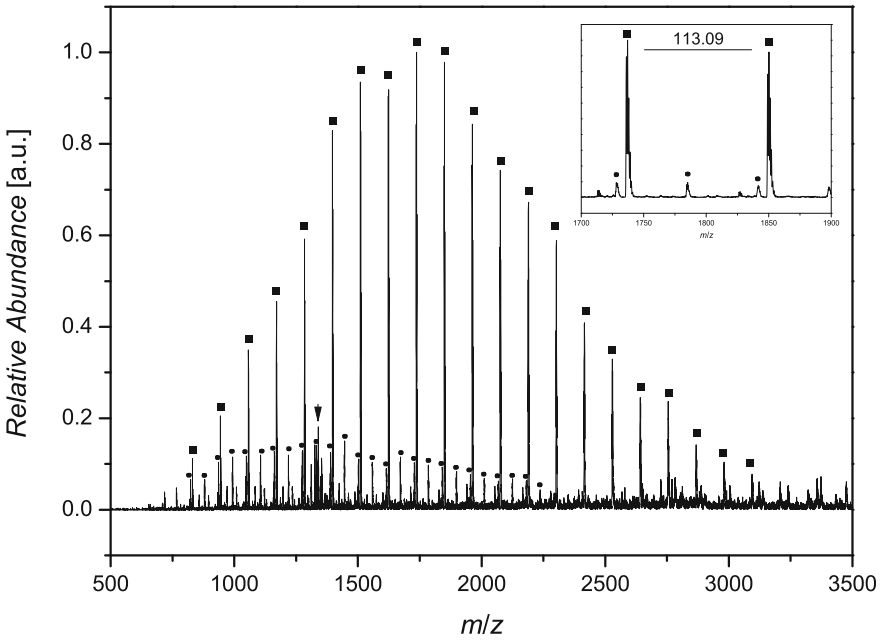

Fig. A.8 ESI-MS-spectrum of PNIPAAm (M_{nSEC} = 4,000 g mol^{-1}, $Đ_m$ = 1.15) polymerized with **1**

Table A.3 Theoretical and experimental m/z of PNIPAAm polymerized with **1**

Species	m/z_{theo}	m/z_{exp}	Δ m/z
■ [**1** + $(NIPAAm)_{12}$ + Na]$^+$	1,736.09	1,736.18	0.09
• [**1** + $(NIPAAm)_{27}$ + 2Na]$^{2+}$	1,728.18	1,728.09	0.09

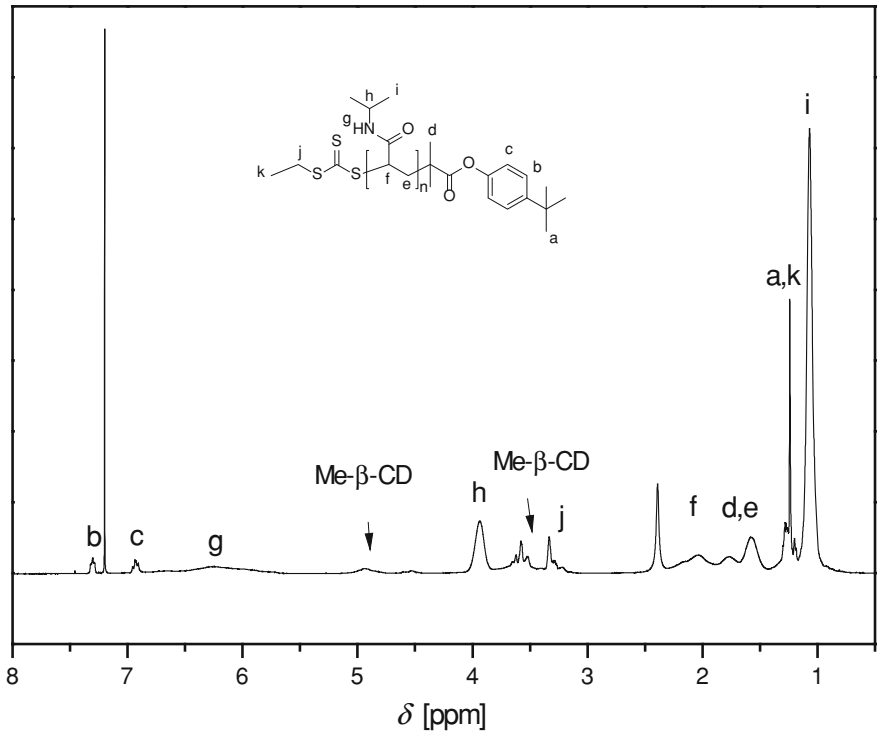

Fig. A.9 ^{1}H-NMR spectrum (400 MHz, $CDCl_3$) of PNIPAAm polymerized with **1** (M_{nSEC} = 4,000 g mol^{-1}, $Đ_m$ = 1.15)

Appendix B
Supramolecular ABA Triblock Copolymers (Appendix to Chapter 4)

See Figs. B.1, B.2, B.3, B.4, B.5, B.6, B.7, B.8, B.9, B.10, B.11, B.12, B.13, B.14 and Tables B.1, B.2, B.3, B.4, B.5.

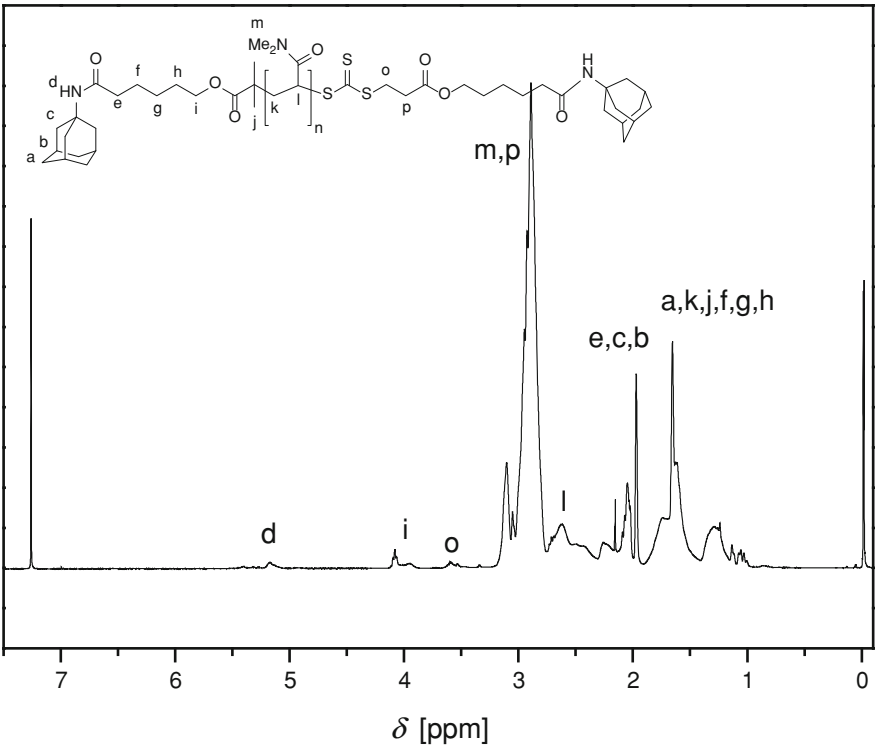

Fig. B.1 ^{1}H-NMR spectrum (400 MHz, $CDCl_3$) of doubly adamantyl-functionalized PDMAAm (M_{nSEC} = 6,400 g mol^{-1}, $Đ_m$ = 1.06) polymerized with **5** at 25 °C

B. V. K. J. Schmidt, *Novel Macromolecular Architectures via a Combination of Cyclodextrin Host/Guest Complexation and RAFT Polymerization*, Springer Theses, DOI: 10.1007/978-3-319-06077-4, © Springer International Publishing Switzerland 2014

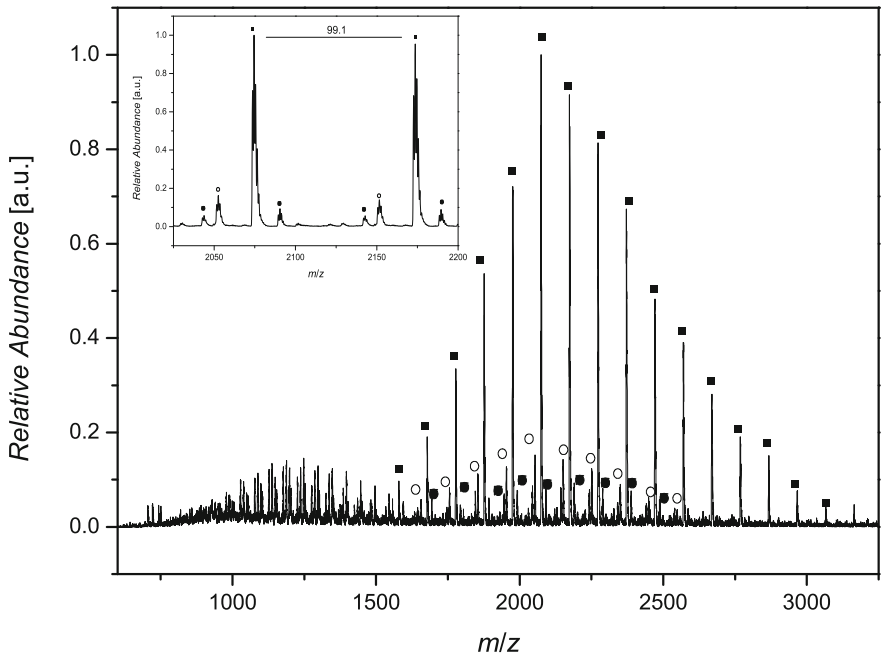

Fig. B.2 ESI-MS spectrum of doubly adamantyl-functionalized PDMAAm (M_{nSEC} = 3,300 g mol^{-1}, $Đ_m$ = 1.06) polymerized with **5**

Table B.1 Theoretical and experimental m/z of PDMAAm polymerized with **5**

Species	m/z_{theo}	m/z_{exp}	Δ m/z
■ $[\mathbf{5} + (DMAAm)_{13} + Na]^+$	2,074.26	2,074.45	0.19
○ $[\mathbf{5} + (DMAAm)_{14} + H]^+$	2,151.35	2,151.45	0.10
• $[\mathbf{5} + (DMAAm)_{34} + 2Na]^{2+}$	2,089.34	2,090.18	0.84

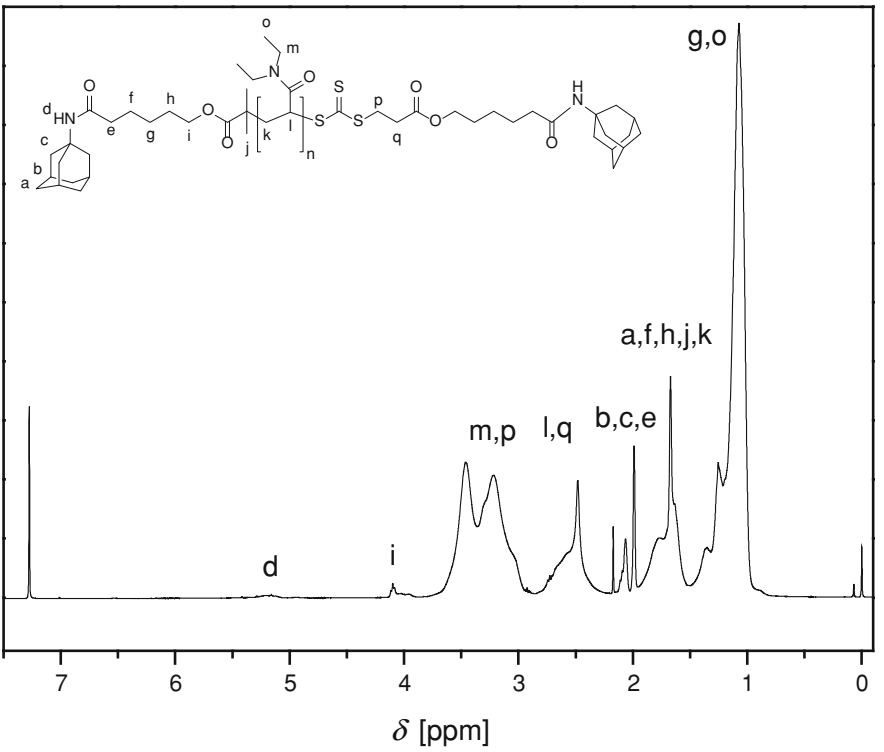

Fig. B.3 ^{1}H-NMR spectrum (400 MHz, $CDCl_3$) of doubly adamantyl-functionalized PDEAAm ($M_{nSEC} = 5{,}100$ g mol^{-1}, $Đ_m = 1.05$) polymerized with **5** at 25 °C

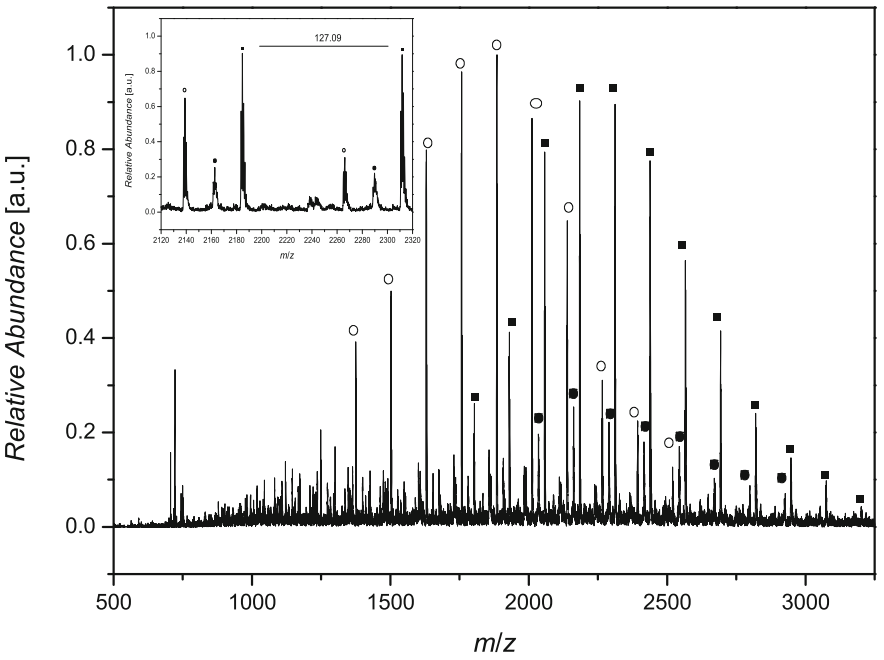

Fig. B.4 ESI-MS spectrum of doubly adamantyl-functionalized PDEAAm (M_{nSEC} =1,800 g mol^{-1}, $Đ_m = 1.06$) polymerized with **5**

Table B.2 Theoretical and experimental m/z of PDEAAm polymerized with **5**

Species	m/z_{theo}	m/z_{exp}	Δ m/z
■ $[\mathbf{5} + (DEAAm)_{11} + Na]^+$	2,074.26	2,074.45	0.19
○ $[\mathbf{5} + (DEAAm)_{10} - C_{20}H_{30}NO_3S_3 + Na]^+$	2,151.35	2,151.45	0.10
• $[\mathbf{5} + (DEAAm)_{11} + H]^+$	2,089.34	2,090.18	0.84

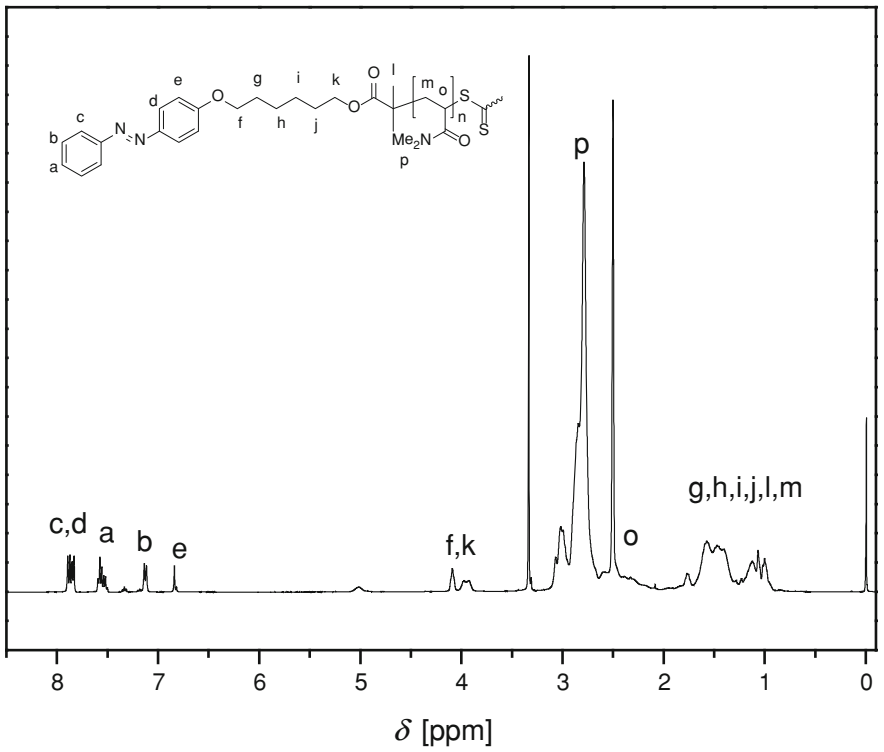

Fig. B.5 ^{1}H-NMR spectrum (400 MHz, DMSO-D_6) of doubly azobenzene-functionalized PDMAAm ($M_{nSEC} = 5{,}400$ g mol^{-1}, $Đ_m = 1.10$) polymerized with **6** at 25 °C

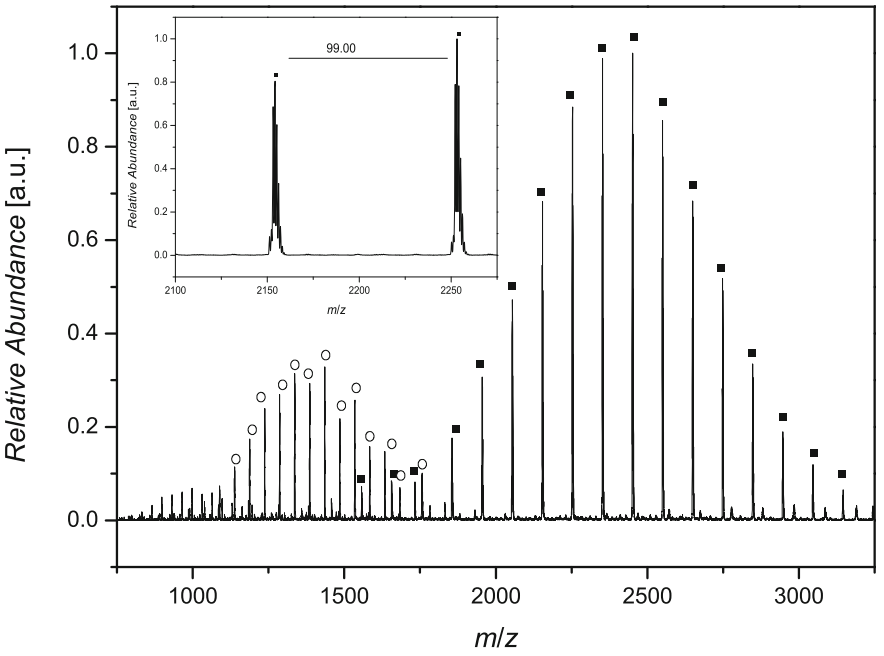

Fig. B.6 ESI-MS spectrum of doubly azobenzene-functionalized PDMAAm (M_{nSEC} = 4,000 g mol^{-1}, $Đ_m$ = 1.06) polymerized with **6**

Table B.3 Theoretical and experimental m/z of PDMAAm polymerized with **6**

Species	m/z_{theo}	m/z_{exp}	Δ m/z
■ [**6** + $(DMAAm)_{15}$ + Na]$^+$	2,352.34	2,352.27	0.07
○ [**6** + $(DMAAm)_{20}$ + 2Na]$^{2+}$	1,435.34	1,435.82	0.48

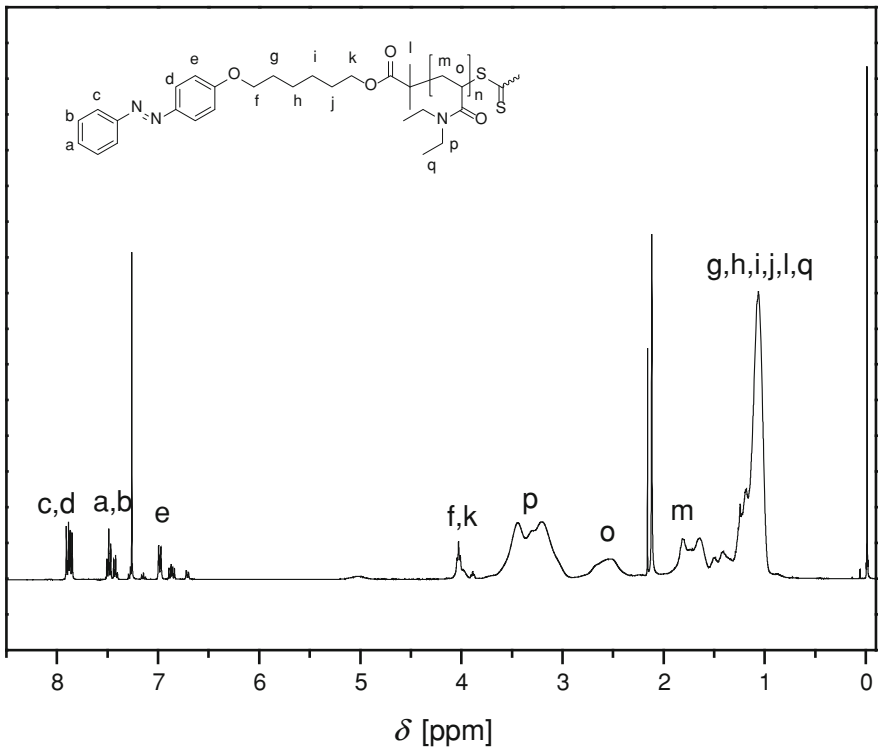

Fig. B.7 ^{1}H-NMR spectrum (400 MHz, $CDCl_3$) of doubly azobenzene-functionalized PDEAAm ($M_{nSEC} = 4{,}000$ g mol^{-1}, $Đ_m = 1.10$) polymerized with **6** at 25 °C

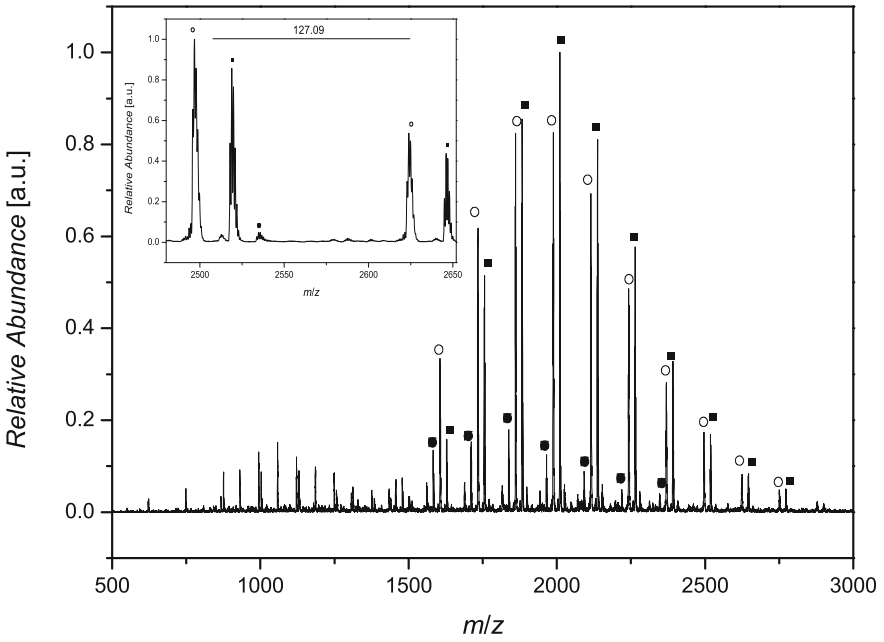

Fig. B.8 ESI-MS spectrum of doubly azobenzene-functionalized PDEAAm ($M_{\mathrm{nSEC}} = 1{,}900$ g mol^{-1}, $Đ_{\mathrm{m}} = 1.05$) polymerized with **6**

Table B.4 Theoretical and experimental m/z of PDEAAm polymerized with **6**

Species	m/z_{theo}	m/z_{exp}	Δ m/z
■ $[\mathbf{6} + (\mathrm{DEAAm})_{13} + \mathrm{Na}]^+$	2,518.6100	2,518.55	0.06
○ $[\mathbf{6} + (\mathrm{DEAAm})_{13} + \mathrm{H}]^+$	2,496.6820	2,496.45	0.23
• $[\mathbf{6} + (\mathrm{DEAAm})_8 - \mathrm{C_{18}H_{21}N_2O_2} + \mathrm{Na}]^+$	1,584.9477	1,584.09	0.86

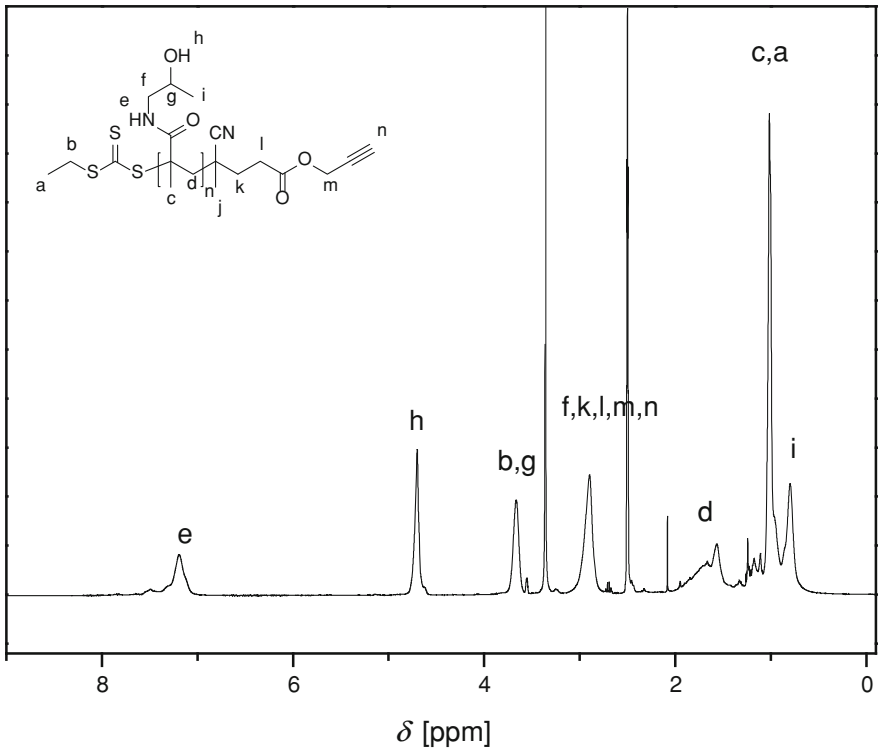

Fig. B.9 ^{1}H-NMR spectrum (400 MHz, DMSO-D_6) of an alkyne-functionalized PHPMA ($M_{nSEC} = 4{,}300$ g mol^{-1}, $Đ_m = 1.15$) polymerized with **7** at 25 °C

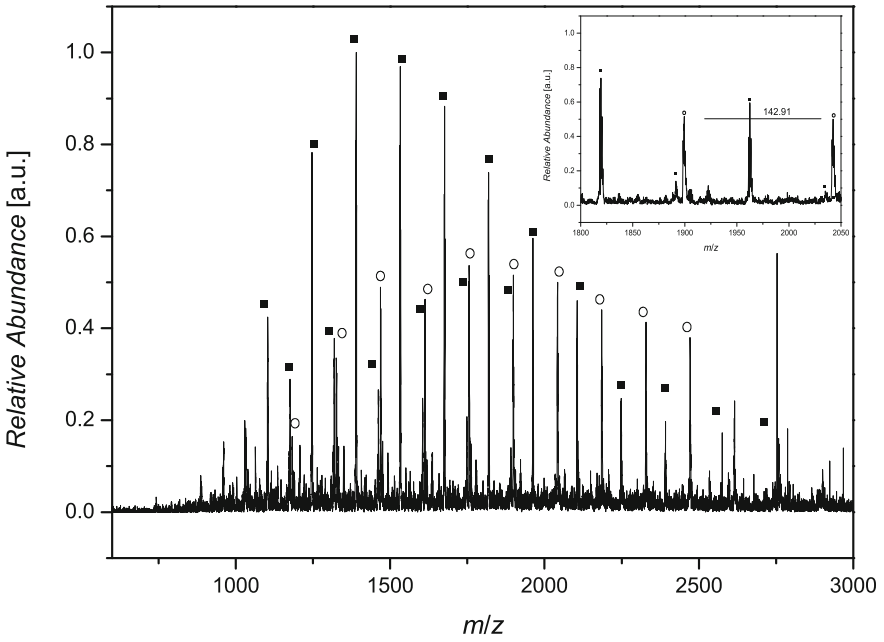

Fig. B.10 ESI-MS spectrum of an alkyne-functionalized PHPMA ($M_{\mathrm{nSEC}} = 3,900$ g mol^{-1}, $Đ_{\mathrm{m}} = 1.17$) polymerized with **7**

Table B.5 Theoretical and experimental m/z of PHPMA polymerized with **7**

Species	m/z_{theo}	m/z_{exp}	Δ m/z
■ $[\mathbf{7} + (\mathrm{HPMA})_{17} + 2\mathrm{Na}]^{2+}$	1,390.31	1,390.18	0.13
∘ $[\mathbf{7} + (\mathrm{HPMA})_{10} + \mathrm{Na}]^{+}$	1,754.96	1,755.27	0.31

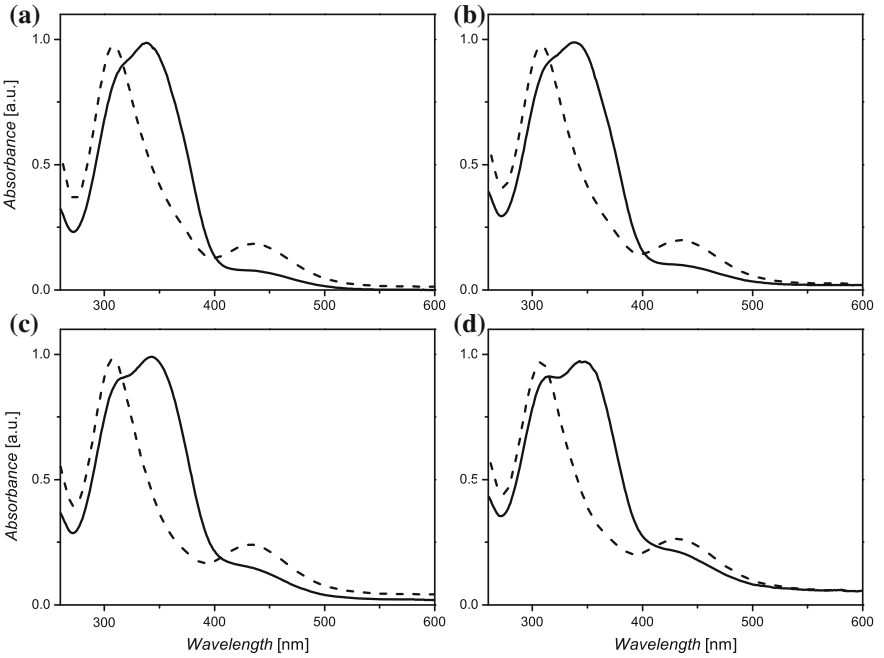

Fig. B.11 Overlay of the UV spectra before irradiation (*solid curve*) and after irradiation at 350 nm for 30 min (*dashed curve*) at 25 °C: **a** $PDMAAm_{46}Azo_2$; **b** $PDMAAm_{46}Azo_2$-*b*-$(PHPMA_{26}$-β-$CD)_2$; **c** $PDMAAm_{103}Azo_2$; **d** $PDMAAm_{103}Azo_2$-*b*-$(PHPMA_{26}$-β-$CD)_2$

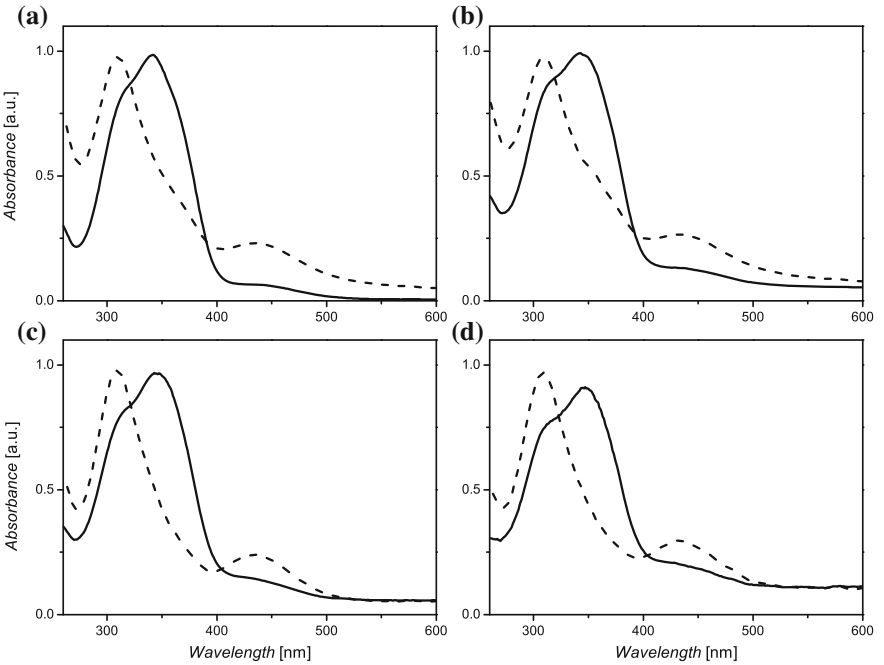

Fig. B.12 Overlay of the UV spectra before irradiation (*solid curve*) and after irradiation at 350 nm for 30 min (*dashed curve*) at 10 °C: **a** $PDEAAm_{36}Azo_2$; **b** $PDEAAm_{36}Azo_2$-*b*-$(PHPMA_{28}$-β-$CD)_2$; **c** $PDEAAm_{80}Azo_2$; **d** $PDEAAm_{80}Azo_2$-*b*-$(PHPMA_{28}$-β-$CD)_2$

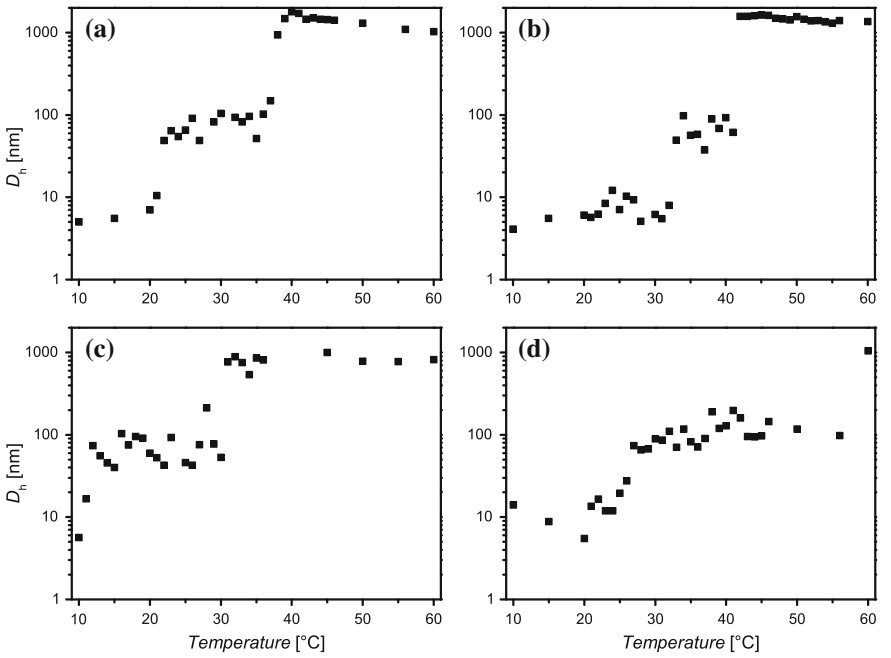

Fig. B.13 **a** Temperature sequenced DLS measurement of $PDEAAm_{45}Ad_2$-*b*-$(PHPMA_{28}$-β-$CD)_2$ at a heating rate of 0.2 °C min^{-1} and a concentration of 1 mg mL^{-1}; **b** temperature sequenced DLS measurement of $PDEAAm_{89}Ad_2$-*b*-$(PHPMA_{28}$-β-$CD)_2$ at a heating rate of 0.2 °C min^{-1} and a concentration of 1 mg mL^{-1}; **c** temperature sequenced DLS measurement of $PDEAAm_{36}Azo_2$-*b*-$(PHPMA_{28}$-β-$CD)_2$ at a heating rate of 0.2 °C min^{-1} and a concentration of 1 mg mL^{-1}; **d** temperature sequenced DLS measurement of $PDEAAm_{80}Azo_2$-*b*-$(PHPMA_{28}$-β-$CD)_2$ at a heating rate of 0.2 °C min^{-1} and a concentration of 1 mg mL^{-1}

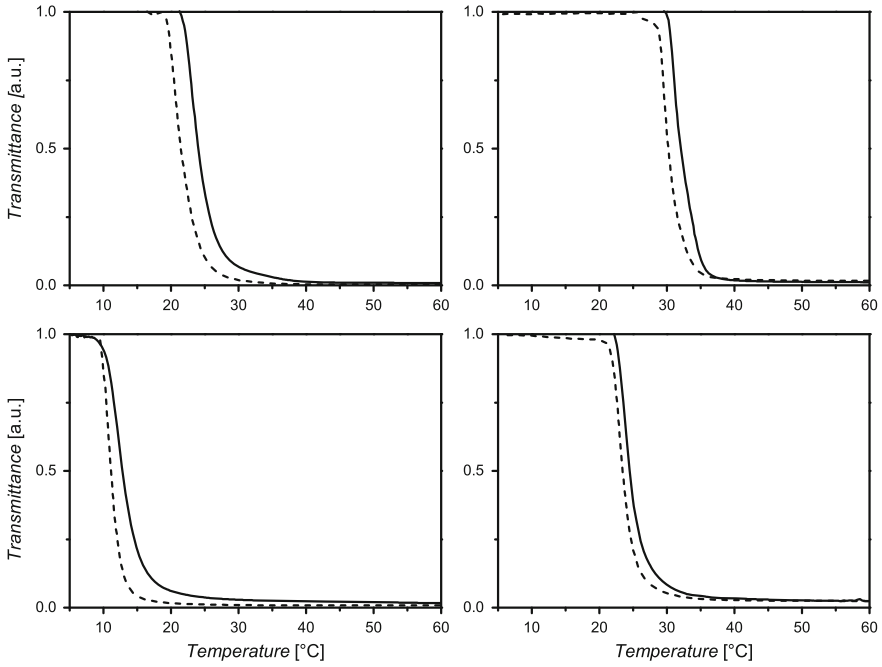

Fig. B.14 Turbidity measurements (cooling ramp) with a heating/cooling rate of 0.32 °C min^{-1} and at a concentration of 1 mg mL^{-1} for **a** $PDEAAm_{45}Ad_2$ (*dashed line*) and the supramolecular triblock copolymer $PDEAAm_{45}Ad_2$-*b*-$(PHPMA_{28}$-β-$CD)_2$ (*solid line*); **b** $PDEAAm_{89}Ad_2$ (*dashed line*) and the supramolecular triblock copolymer $PDEAAm_{89}Ad_2$-*b*-$(PHPMA_{28}$-β-$CD)_2$ (*solid line*); **c** $PDEAAm_{36}Azo_2$ (*dashed line*) and the supramolecular triblock copolymer $PDEAAm_{36}Azo_2$-*b*-$(PHPMA_{28}$-β-$CD)_2$ (*solid line*); **d**) $PDEAAm_{80}Azo_2$ (*dashed line*) and the supramolecular triblock copolymer $PDEAAm_{80}Azo_2$-*b*-$(PHPMA_{28}$-β-$CD)_2$ (*solid line*)

Appendix C
Supramolecular Three Armed Star Polymers (Appendix to Chapter 5)

See Figs. C.1, C.2, C.3, C.4, C.5, C.6, and Tables C.1, C.2, C.3.

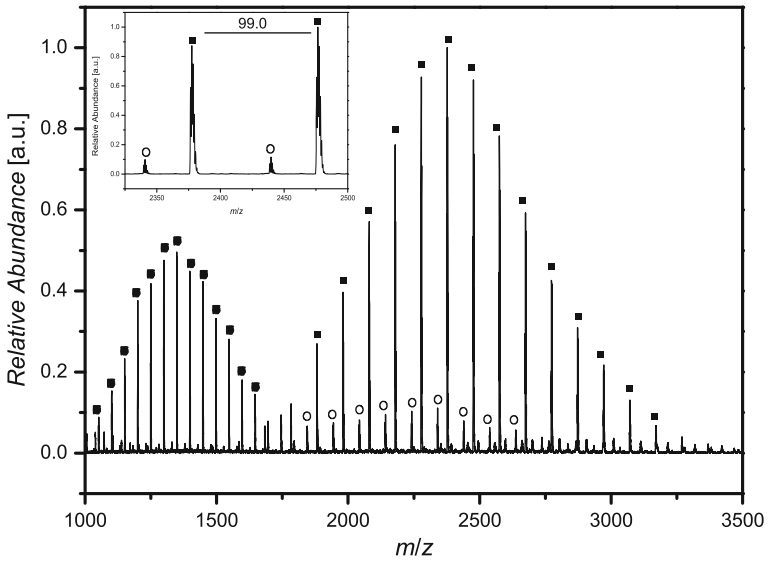

Fig. C.1 ESI-MS-spectrum of an adamantyl-functionalized PDMAAm (M_{nSEC} = 3,900 g mol^{-1}, $Đ_m$ = 1.07) polymerized with **10**

Table C.1 Theoretical and experimental m/z of PDMAAm polymerized with **10**

Species	m/z_{theo}	m/z_{exp}	Δ m/z
■ [**10** + $(DMAAm)_{20}$ + Na]$^+$	2,476.56	2,476.55	0.01
• [**10** + $(DMAAm)_{23}$ + 2Na]$^{2+}$	1,348.84	1,348.82	0.02
○ [**10** + $(DMAAm)_{25}$ − Adamantyl + Na]$^+$	2,440.516	2,439.82	0.69

B. V. K. J. Schmidt, *Novel Macromolecular Architectures via a Combination of Cyclodextrin Host/Guest Complexation and RAFT Polymerization*, Springer Theses, DOI: 10.1007/978-3-319-06077-4, © Springer International Publishing Switzerland 2014

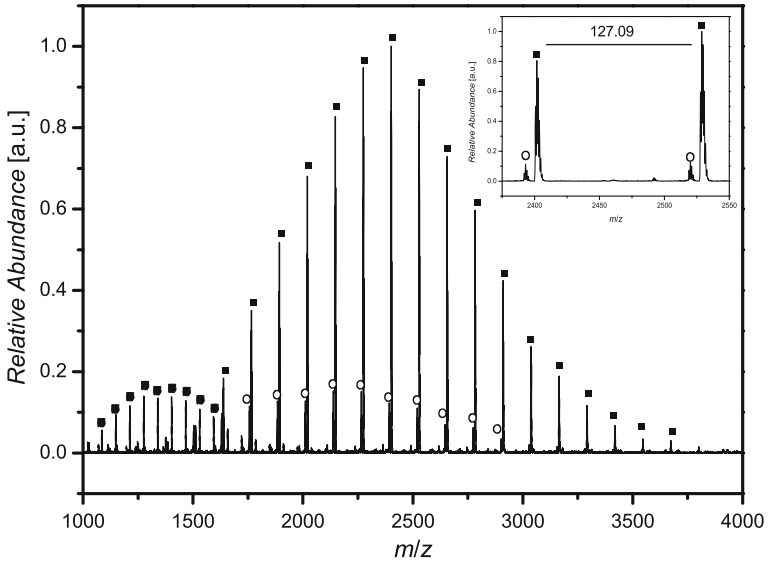

Fig. C.2 ESI-MS-spectrum of an adamantyl-functionalized PDEAAm ($M_{\mathrm{nSEC}} = 2{,}700$ g mol^{-1}, $Đ_{\mathrm{m}} = 1.08$) polymerized with **10**

Table C.2 Theoretical and experimental m/z of PDEAAm polymerized with **10**

Species	m/z_{theo}	m/z_{exp}	Δ m/z
■ [**10** + $(\mathrm{DEAAm})_{16}$ + $\mathrm{Na}]^+$	2,528.78	2,528.82	0.04
• [**10** + $(\mathrm{DEAAm})_{17}$ + $2\mathrm{Na}]^{2+}$	1,339.44	1,339.45	0.01
○ [**10** + $(\mathrm{DEAAm})_{17}$ − Adamantyl + $\mathrm{Na}]^+$	2,520.76	2,500.00	0.76

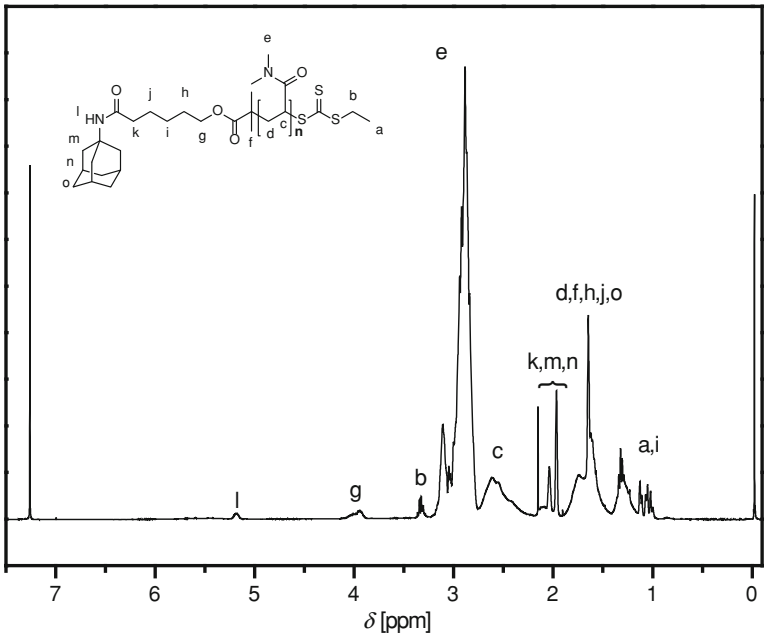

Fig. C.3 ^{1}H-NMR spectrum (400 MHz, $CDCl_3$) of an adamantyl-functionalized PDMAAm ($M_{nSEC} = 3{,}900$ g mol^{-1}, $Đ_m = 1.07$) at 25 °C polymerized with **10**

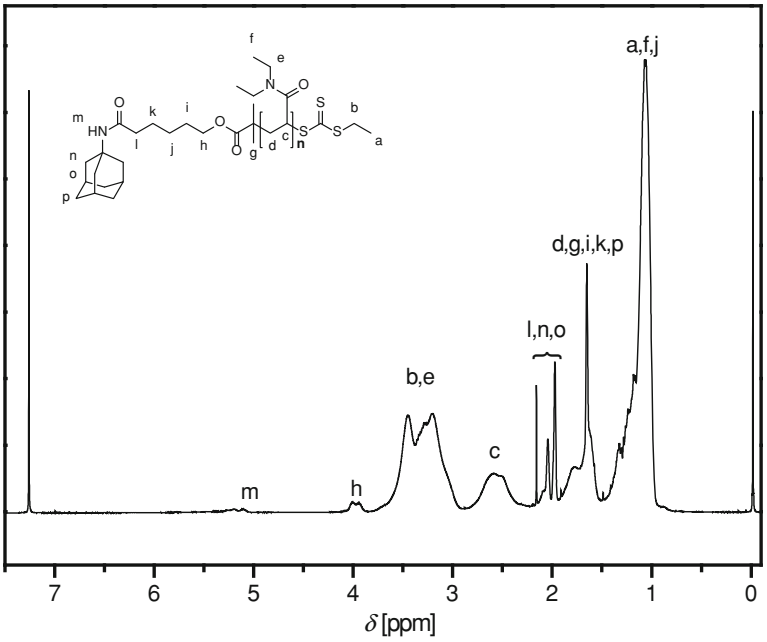

Fig. C.4 ^{1}H-NMR spectrum (400 MHz, $CDCl_3$) of an adamantyl-functionalized PDEAAm ($M_{nSEC} = 2{,}700$ g mol^{-1}, $Đ_m = 1.08$) at 25 °C polymerized with **10**

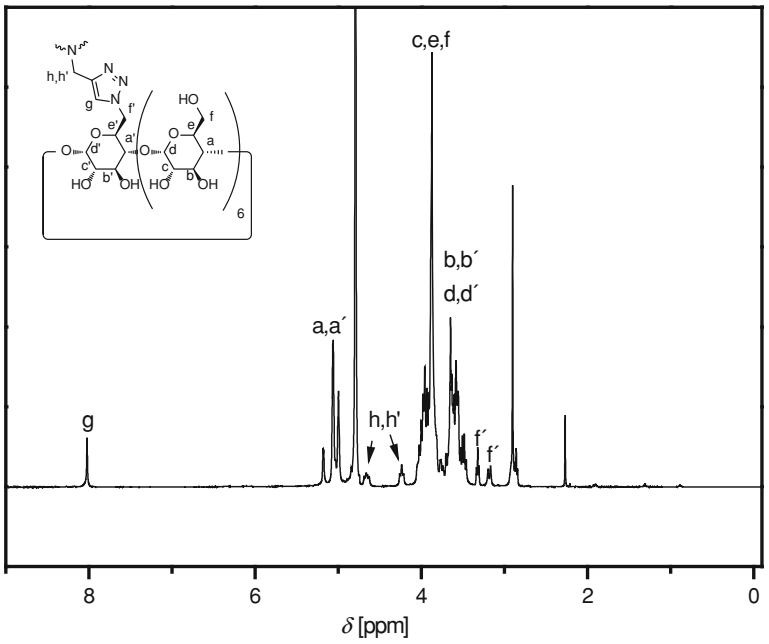

Fig. C.5 ^{1}H-NMR spectrum of the three-pronged β-CD core (β-CD_3) recorded in D_2O at 25 °C

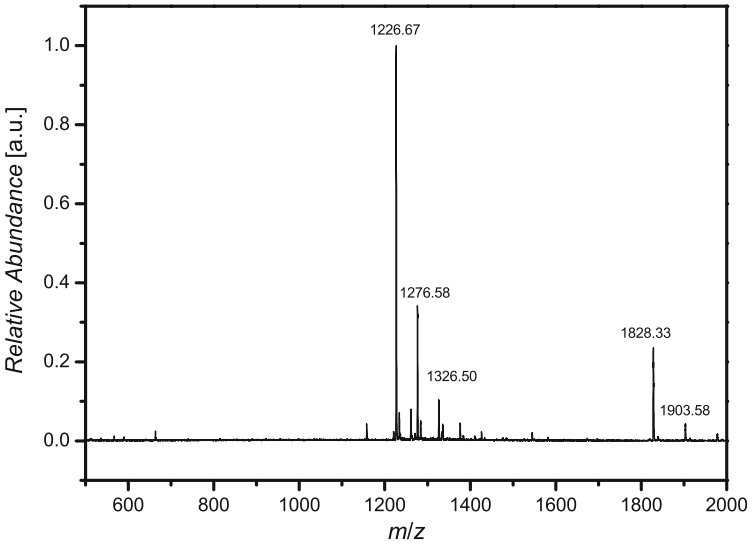

Fig. C.6 ESI-MS-spectrum of the three-pronged β-CD core (β-CD_3) (ionized with NaI)

Table C.3 Theoretical and experimental m/z of β-CD_3 (ionized with NaI)

Species	m/z_{theo}	m/z_{exp}	Δ m/z
$[\beta - CD_3 + 2Na]^{2+}$	1,828.09	1,828.33	0.24
$[\beta - CD_3 + I^- + 3Na]^{2+}$	1,903.04	1,903.58	0.54
$[\beta - CD_3 + 3Na]^{3+}$	1,226.396	1,226.67	0.28
$[\beta - CD_3 + I^- + 4Na]^{3+}$	1,276.66	1,276.58	0.22
$[\beta - CD_3 + 2I^- + 5Na]^{3+}$	1,326.32	1,326.50	0.18

Appendix D
AB_2 Miktoarm Star Polymers (Appendix to Chapter 6)

See Figs. D.1, D.2, D.3, D.4, D.5 and Tables D.1, D.2.

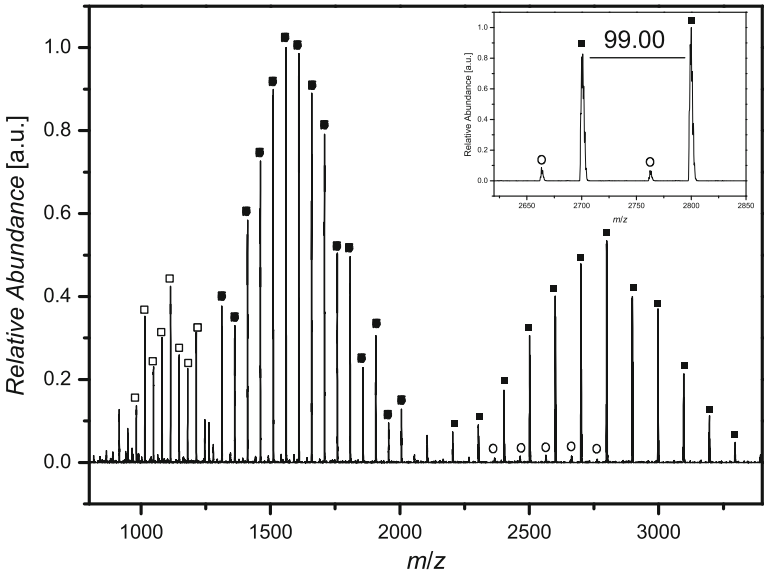

Fig. D.1 ESI-MS-spectrum of a mid-chain adamantyl-functionalized PDMAAm (M_{nSEC} = 4,000 g mol^{-1}, $Đ_m$ = 1.09) polymerized with **11**

Table D.1 Theoretical and experimental m/z of PDMAAm polymerized with **11**

Species	m/z_{theo}	m/z_{exp}	Δ m/z
■ [**11** + $(DMAAm)_{20}$ + Na]$^+$	2,798.59	2,799.09	0.50
• [**11** + $(DMAAm)_{21}$ + 2Na]$^{2+}$	1,559.39	1,559.73	0.34
○ [**11** + $(DMAAm)_{25}$ + 3Na]$^{3+}$	1,113.30	1,113.91	0.61
□ [**11** + $(DMAAm)_{20}$ − Adamantyl + Na]$^+$	2,663.47	2,663.27	0.20

B. V. K. J. Schmidt, *Novel Macromolecular Architectures via a Combination of Cyclodextrin Host/Guest Complexation and RAFT Polymerization*, Springer Theses, DOI: 10.1007/978-3-319-06077-4, © Springer International Publishing Switzerland 2014

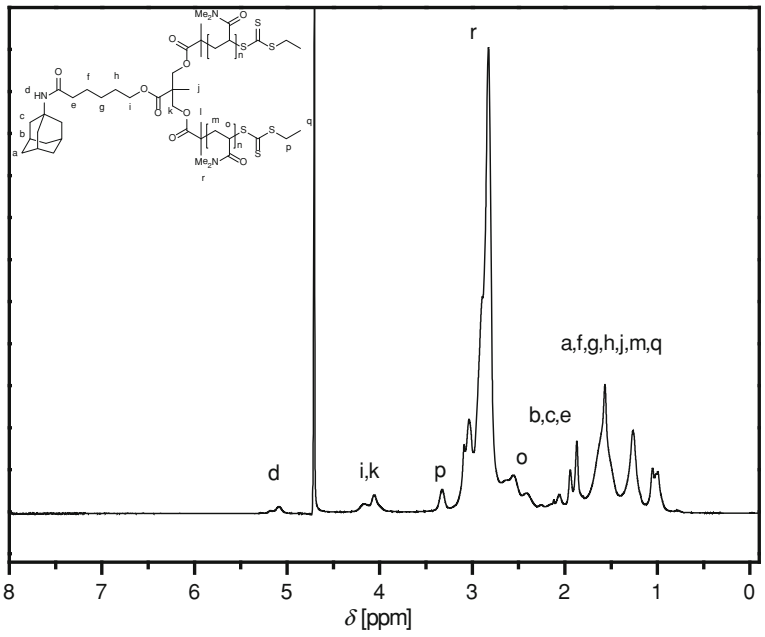

Fig. D.2 ^{1}H-NMR spectrum (400 MHz, D_2O) of a mid-chain adamantyl-functionalized PDMAAm polymerized with **11** ($M_{nSEC} = 4{,}000$ g mol^{-1}, $Đ_m = 1.09$) at 25 °C

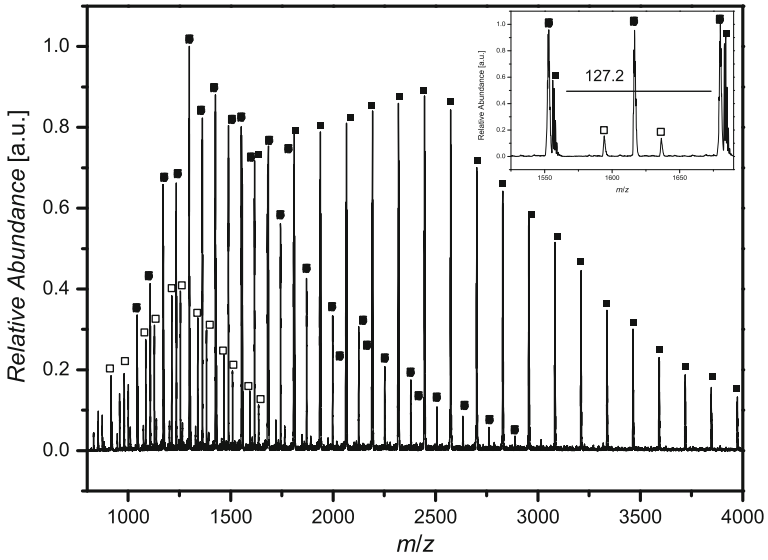

Fig. D.3 ESI-MS-spectrum of the alkyne-functionalized PDEAAm (M_{nSEC} = 2,400 g mol^{-1}, $Đ_m$ = 1.14) polymerized with **12**

Table D.2 Theoretical and experimental m/z of PDEAAm polymerized with **12**

Species	m/z_{theo}	m/z_{exp}	Δ m/z
■ [**12** + $(DEAAm)_{11}$ + Na]$^+$	1,683.10	1,683.18	0.08
• [**12** + $(DEAAm)_{22}$ + 2Na]$^{2+}$	1,552.60	1,552.55	0.05
□ [**12** + $(DEAAm)_{35\text{-Adamantyl}}$ + 3Na]3+	1,593.83	1,594.09	0.26

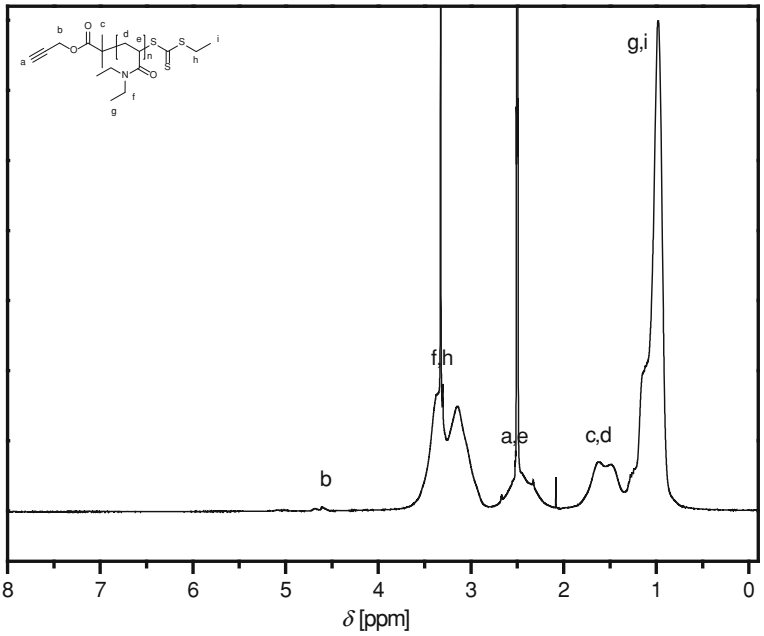

Fig. D.4 ^{1}H-NMR spectrum (400 MHz, DMSO-D_6) of the alkyne-functionalized PDEAAm polymerized with **12** ($M_{nSEC} = 6{,}800$ g mol^{-1}, $Đ_m = 1.13$) at 25 °C

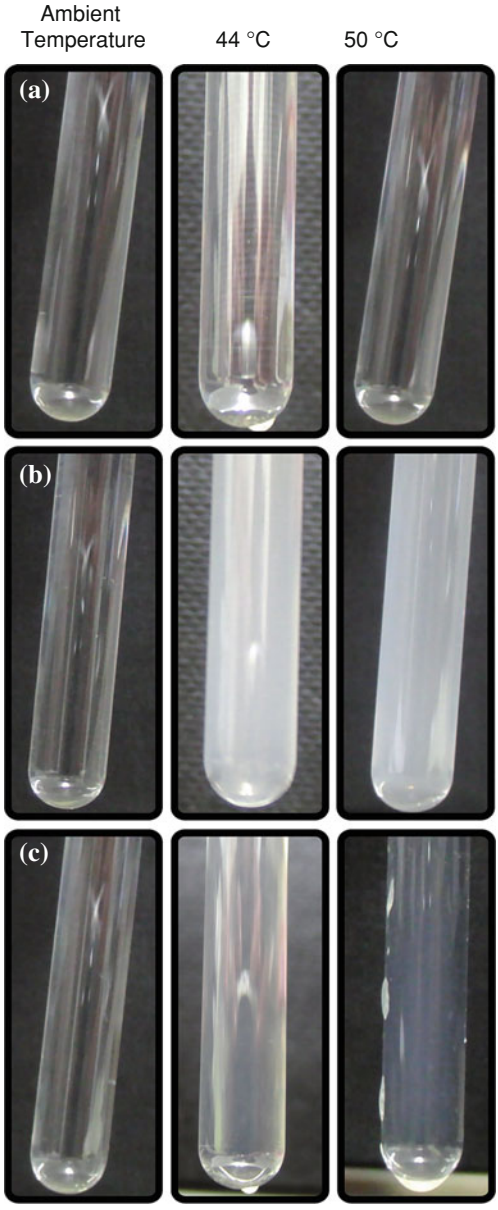

Fig. D.5 Pictures of the polymer solutions at different temperatures at a concentration of 1 mg mL^{-1}: **a** Mid-chain adamantyl-functionalized $PDMAAm_{155}$-Ad, **b** β-CD-functionalized $PDEAAm_{57}$-β-CD and **c** the supramolecular miktoarm star polymer

Appendix E
Modulation of the Thermoresponsitivity of PDEAAm via CD Addition (Appendix to Chapter 7)

See Fig. E.1, and Tables E.1, E.2, E.3, E.4, E.5, E.6, E.7, E.8, E.9, E.10, E.11, E.12.

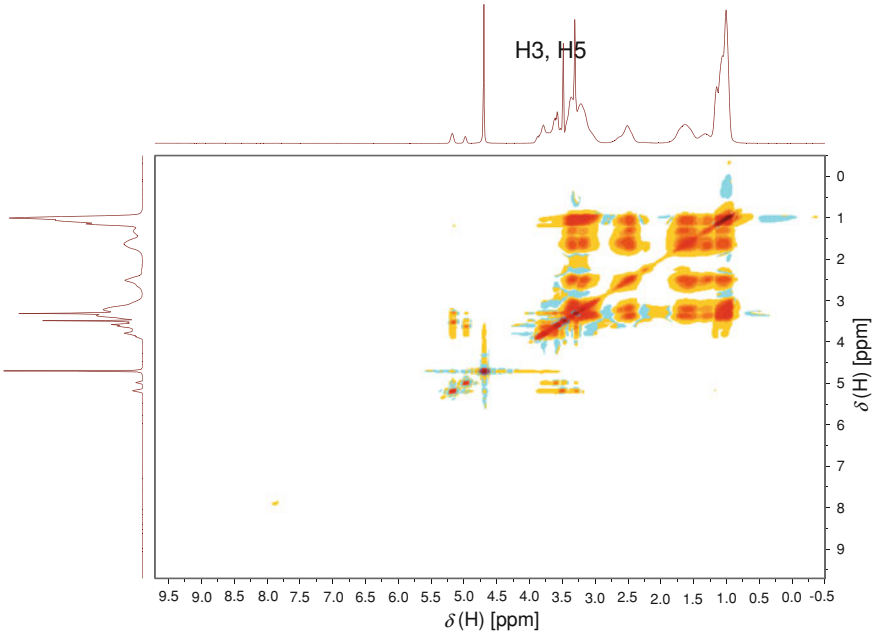

Fig. E.1 NOESY spectrum in D_2O at 25 °C of a mixture of carboxylic acid functionalized PDEAAm ($M_n = 6{,}600$ g mol^{-1}) and 2 eq. of Me-β-CD

B. V. K. J. Schmidt, *Novel Macromolecular Architectures via a Combination of Cyclodextrin Host/Guest Complexation and RAFT Polymerization*, Springer Theses,
DOI: 10.1007/978-3-319-06077-4, © Springer International Publishing Switzerland 2014

Table E.1 SEC-data of the utilized polymers (polymerized with **EMP** in DMF at 60 °C for 24 h with AIBN as initiator) and the corresponding T_cs before and after addition of Me-β-CD [a]

DEAAm/CTA/I	*Conv.*	M_{ntheo} (g mol^{-1})	M_{nSEC} (g mol^{-1})	$Đ_m$	T_c (°C)	$T_{cMe\text{-}\beta\text{-}CD}$ (°C)
17/1/0.2	quant. (%)	2,400	1,600	1.08	32.3/31.2	39.5/39.4
34/1/0.2	99	4,500	3,500	1.07	41.1/39.9	40.9/41.0
48/1/0.2	97	6,100	5,000	1.10	39.9/38.1	38.8/37.4
65/1/0.2	98	8,300	6,600	1.09	37.4/35.5	41.6/40.1
82/1/0.2	98	10,400	7,200	1.10	37.5/35.8	40.0/38.4
160/1/0.2	90	18,500	10,800	1.18	37.7/35.6	37.7/36.7

[a] First T_c from the heating ramp/second T_c from the cooling ramp

Table E.2 SEC-data of the utilized polymers (polymerized with **1** in DMF at 60 °C for 24 h with AIBN as initiator) and the corresponding T_cs before and after addition of Me-β-CD [a]

DEAAm/CTA/I	*Conv.* (%)	M_{ntheo} (g mol^{-1})	M_{nSEC} (g mol^{-1})	$Đ_m$	T_c (°C)	$T_{cMe\text{-}\beta\text{-}CD}$ (°C)
16/1/0.2	99	2,400	1,800	1.06	< 4	22.9/37.3
33/1/0.2	99	4,500	3,800	1.08	26.5/25.9	32.9/38.1
49/1/0.2	99	6,600	5,300	1.07	28.4/27.7	32.6/31.7
65/1/0.2	99	8,600	6,500	1.09	30.3/28.3	33.5/32.0
79/1/0.2	99	10,400	7,700	1.1	31.6/30.1	34.2/32.8
159/1/0.2	99	20,600	11,200	1.2	33.0/31.5	34.5/32.6

[a] First T_c from the heating ramp/second T_c from the cooling ramp

Table E.3 SEC-data of the utilized polymers (polymerized with **17** in DMF at 60 °C for 24 h with AIBN as initiator) and the corresponding T_cs before and after addition of Me-β-CD [a]

DEAAm/CTA/I	*Conv.* (%)	M_{ntheo} (g mol^{-1})	M_{nSEC} (g mol^{-1})	$Đ_m$	T_c (°C)	$T_{cMe\text{-}\beta\text{-}CD}$ (°C)
16/1/0.2	98	2,400	1,800	1.18	< 4	33.5/38.9
31/1/0.2	99	4,300	3,000	1.19	< 4	35.6/38.7
42/1/0.2	99	5,700	3,700	1.21	7.7/12.7	35.3/35.2
64/1/0.2	99	8,500	4,400	1.28	26.1/24.2	38.0/36.8
81/1/0.2	99	10,600	5,600	1.28	26.8/26.8	36.1/34.4
155/1/0.2	99	19,900	7,400	1.28	30.7/28.2	36.7/34.9

[a] First T_c from the heating ramp/second T_c from the cooling ramp

Table E.4 SEC-data of the utilized polymers (polymerized with **10** in DMF at 60 °C for 24 h with AIBN as initiator) and the corresponding T_cs before and after addition of Me-β-CD [a]

DEAAm/CTA/I	*Conv.* (%)	M_{ntheo} (g mol^{-1})	M_{nSEC} (g mol^{-1})	$Đ_m$	T_c (°C)	$T_{cMe\text{-}\beta\text{-}CD}$ (°C)
33/1/0.2	98	4,600	3,200	1.07	27.3/27.8	33.4/33.3
59/1/0.2	99	7,900	4,900	1.11	29.8/31.7	35.1/34.1
157/1/0.2	99	20,200	8,300	1.21	33.7/31.7	35.6/34.2

[a] First T_c from the heating ramp/second T_c from the cooling ramp

Table E.5 SEC-data of the utilized polymers (polymerized with **5** in DMF at 60 °C for 24 h with AIBN as initiator) and the corresponding T_cs before and after addition of Me-β-CD.[a]

DEAAm/CTA/I	*Conv.* (%)	M_{ntheo} (g mol^{-1})	M_{nSEC} (g mol^{-1})	$Đ_m$	T_c (°C)	$T_{cMe\text{-}\beta\text{-}CD}$ (°C)
34/1/0.2	99	5,000	5,100	1.05	< 4	27.8/28.3
65/1/0.2	99	8,900	7,700	1.10	< 4	33.9/32.2
154/1/0.2	99	20,100	12,700	1.24	33.0/31.5	36.1/35.2

[a] First T_c from the heating ramp/second T_c from the cooling ramp

Table E.6 SEC-data of the utilized polymers (polymerized with **19** in DMF at 60 °C for 24 h with AIBN as initiator) and the corresponding T_cs before and after addition of Me-β-CD [a]

DEAAm/CTA/I	*Conv.* (%)	M_{ntheo} (g mol^{-1})	M_{nSEC} (g mol^{-1})	$Đ_m$	T_c (°C)	$T_{cMe\text{-}\beta\text{-}CD}$ (°C)
32/1/0.2	92	4,200	3,600	1.09	15.1/16.0	17.4/15.7
65/1/0.2	92	8,100	5,000	1.13	25.3/24.0	25.9/24.0
158/1/0.2	97	20,000	7,700	1.23	29.0/27.0	30.2/30.7

[a] First T_c from the heating ramp/second T_c from the cooling ramp

Table E.7 SEC-data of the utilized polymers (polymerized with **6** in DMF at 60 °C for 24 h with AIBN as initiator) and the corresponding T_cs before and after addition of Me-β-CD [a]

DEAAm/CTA/I	*Conv.* (%)	M_{ntheo} (g mol^{-1})	M_{nSEC} (g mol^{-1})	$Đ_m$	T_c (°C)	$T_{cMe\text{-}\beta\text{-}CD}$ (°C)
32/1/0.2	81	4,100	4,000	1.1	< 4	< 4
66/1/0.2	78	7,400	5,300	1.19	15.6/17.3	14.8/–
160/1/0.2	89	18,800	11,500	1.33	25.5/30.2	25.1/29.3

[a] First T_c from the heating ramp/second T_c from the cooling ramp

Table E.8 SEC-data of the utilized polymers (polymerized with **19** in DMF at 60 °C for 24 h with AIBN as initiator) and the corresponding T_cs before and after addition of α-CD [a]

DEAAm/CTA/I	*Conv.* (%)	M_{ntheo} (g mol^{-1})	M_{nSEC} (g mol^{-1})	$Đ_m$	T_c (°C)	$T_{c\alpha-CD}$ (°C)
32/1/0.2	92	4,200	3,600	1.09	15.1/16.0	15.1/13.9
65/1/0.2	92	8,100	5,000	1.13	25.3/24.0	24.7/23.8
158/1/0.2	97	20,000	7,700	1.23	29.0/27.0	28.7/27.7

[a] First T_c from the heating ramp/second T_c from the cooling ramp

Table E.9 SEC-data of the utilized polymers (polymerized with **6** in DMF at 60 °C for 24 h with AIBN as initiator) and the corresponding T_cs before and after addition of α-CD [a]

DEAAm/CTA/I	*Conv.* (%)	M_{ntheo} (g mol^{-1})	M_{nSEC} (g mol^{-1})	$Đ_m$	T_c (°C)	$T_{c\alpha-CD}$ (°C)
32/1/0.2	81	4,100	4,000	1.1	< 4	< 4
66/1/0.2	78	7,400	5,300	1.19	15.6/17.3	13.7/16.8
160/1/0.2	89	18,800	11,500	1.33	25.5/30.2	24.8/23.8

[a]: First T_c from the heating ramp/second T_c from the cooling ramp

Table E.10 T_cs in dependence of the Me-β-CD equivalents for a sample polymer polymerized with **1** or **EMP**[a]

Equiv. CD/**1**: $M_{nSEC} = 3,800$ g mol^{-1}	**1**: $M_{nSEC} = 6,500$ g mol^{-1}	**EMP**: $M_{nSEC} = 3,500$ g mol^{-1}
Polymer $T_{cMe\text{-}\beta\text{-}CD}$ (°C)	$T_{cMe\text{-}\beta\text{-}CD}$ (°C)	$T_{cMe\text{-}\beta\text{-}CD}$ (°C)
0.5	28.5/29.6	30.5/28.8	38.9/40.0
1.0	32.5/37.3	31.8/31.0	39.5/38.9
1.5	30.7/33.0	33.1/33.1	40.1/39.8
2.0	32.9/38.1	33.5/32.0	40.9/41.0
3.0	34.4/36.5	33.4/32.1	41.6/41.4
5.0	36.6/36.5	34.9/34.6	40.9/40.2

[a]: First T_c from the heating ramp/second T_c from the cooling ramp

Table E.11 T_cs of polymers polymerized with **1** or **17** after addition of 16 eq. 1-adamantylamine hydrochloride[a]

Polymer	T_c (°C)	$T_{cMe\text{-}\beta\text{-}CD}$ (°C)	$T_{cMe\text{-}\beta\text{-}CD\,Ad}$ (°C)
1: $M_{nSEC} = 3,800$ g mol^{-1}	26.5/25.9	32.9/38.1	27.9/–
17: $M_{nSEC} = 5,600$ g mol^{-1}	26.8/26.8	36.1/34.4	30.9/–

[a] First T_c from the heating ramp/second T_c from the cooling ramp

Table E.12 T_cs after enzymatic treatment of polymers polymerized with **17** or **EMP** and complexed with β-CD [a]

Polymer	$T_{cMe\text{-}\beta\text{-}CD\,Enzyme}$ (°C)	$T_{cMe\text{-}\beta\text{-}CD}$ (°C)	T_c (°C)
1: $M_{nSEC} = 4,400$ g mol^{-1}	26.5/24.9	30.4/28.9	26.1/24.2
EMP: $M_{nSEC} = 5,000$ g mol^{-1}	40.8/39.0	40.6/39.6	39.9/38.1

[a] First T_c from the heating ramp/second T_c from the cooling ramp

Curriculum Vitae

Date of Birth:	January the 22nd, 1984
Place of Birth:	Hanau, Germany
Nationality:	German

Education

06/2010–07/2013	**Doctoral Studies in Chemistry** Under the supervision of Prof. Dr. Christopher Barner-Kowollik Karlsruhe Institute of Technology, Germany Topic: "Novel Macromolecular Architectures via Combination of Cyclodextrin Host/Guest Complexation and RAFT Polymerization"
09/2009	**Diploma in Chemistry: Diplom Ingenieur** Diploma thesis under supervision of Prof. M. Rehahn: "Synthese endfunktionalisierter Poly(*N*-Vinylcarbazole) durch kontrollierte radikalische Polymerisation" Technical University Darmstadt, Germany
10/2004–09/2009	**Studies of Chemistry** Technical University Darmstadt, Germany
08/1994–06/2003	**High School Certificate (Abitur)** Grimmelshausen Gymnasium Gelnhausen, Germany

B. V. K. J. Schmidt, *Novel Macromolecular Architectures via a Combination of Cyclodextrin Host/Guest Complexation and RAFT Polymerization*, Springer Theses,
DOI: 10.1007/978-3-319-06077-4, © Springer International Publishing Switzerland 2014

Professional Experience

11/2013–to date	**Materials Research Laboratory** in the group of Prof. C. J. Hawker University of California, Santa Barbara, USA Postdoctoral Researcher
06/2010–09/2013	**Institut für Technische Chemie und Polymer Chemie** in the group of Prof. C. Barner-Kowollik Karlsruhe Institute of Technology, Karlsruhe, Germany Scientific Co-worker
01/2010–03/2010	**Fraunhofer Institute for Applied Polymer Science** in the group of Dr. habil. J.-F. Lutz Potsdam/Golm, Germany Complementary Scientist
10/2009–12/2009	**Fraunhofer Institute for Applied Polymer Science** in the group of Dr. habil. J.-F. Lutz Potsdam/Golm, Germany Internship
08/2004	**Degussa** Industriepark Wolfgang, Germany Internship
10/2003–07/2004	**Community Service** Kath. Kirchengemeinde St. Peter, Behindertenwerk Main-Kinzig Care for the elderly and disabled

Publications and Conference Contributions

Peer Reviewed Publications[1]

1. Defined Poly[styrene-*block*-(ferrocenylmethyl methacrylate)] Diblock Copolymers via Living Anionic Polymerization
   Gallei, M.; Schmidt, B. V. K. J.; Klein, R.; Rehahn, M. *Macromol. Rapid Commun.* **2009**, *30* (13), 1463–1469.
2. Controlled folding of synthetic polymer chains through the formation of positionable covalent bridges
   Schmidt, B. V. K. J.; Fechler, N.; Falkenhagen, J.; Lutz, J.-F. *Nat. Chem.* **2011**, *3* (3), 234–238.
3. Tailored Polymer Microstructures Prepared by Atom Transfer Radical Copolymerization of Styrene and N-substituted Maleimides
   Lutz, J.-F.; Schmidt, B. V. K. J.; Pfeifer, S. *Macromol. Rapid Commun.* **2011**, *32* (2), 127–135.
4. Low Temperature Aqueous Living/Controlled (RAFT) Polymerization of Carboxybetaine Methacrylamide up to High Molecular Weights
   Rodriguez-Emmenegger, C.; Schmidt, B. V. K. J.; Sedlákova, Z.; Šubr, V.; Bologna Alles, A.; Brynda, E.; Barner-Kowollik, C. *Macromol. Rapid Commun.* **2011**, *32*, 958–965.
5. *Cyclodextrin-Complexed RAFT Agents for the Ambient Temperature Aqueous Living/Controlled Radical Polymerization of Acrylamido-Monomers
   Schmidt, B. V. K. J.; Hetzer, M.; Ritter, H.; Barner-Kowollik, C. *Macromolecules* **2011**, *44* (18), 7220–7232.
6. *Miktoarm Star Polymers via Cyclodextrin-Driven Supramolecular Self-Assembly
   Schmidt, B. V. K. J.; Hetzer, M.; Ritter, H.; Barner-Kowollik, C. *Polym. Chem.* **2012**, *3*, 3064–3067.

[1] The with * marked publications or conference contributions were accomplished in the course of this thesis

B. V. K. J. Schmidt, *Novel Macromolecular Architectures via a Combination of Cyclodextrin Host/Guest Complexation and RAFT Polymerization*, Springer Theses,
DOI: 10.1007/978-3-319-06077-4, © Springer International Publishing Switzerland 2014

7. *Supramolecular Three-Armed Star Polymers via Cyclodextrin Host/Guest Self-Assembly
   Schmidt, B. V. K. J.; Rudolph, T.; Hetzer, M.; Ritter, H.; Schacher, F. H.; Barner-Kowollik, C. *Polym. Chem.* **2012**, *3*, 3139–3154.
8. Limitations of Cyclodextrin Mediated Amphiphilic Block Copolymer Formation
   Hetzer, M.; Schmidt, B. V. K. J.; Barner-Kowollik, C.; Ritter, H. *J. Polym. Sci. A: Polym. Chem.* **2013**, *51* (11), 2504–2517.
9. *UV-Light and Temperature Supramolecular ABA Triblock Copolymers via Reversible Cyclodextrin Complexation
   Schmidt, B. V. K. J.; Hetzer, M.; Ritter, H.; Barner-Kowollik, C. *Macromolecules* **2013**, *46* (3), 1054–1065.
10. Photochemical Generation of Light Responsive Surfaces
    Blasco, E.; Piñol, M.; Oriol, L.; Schmidt, B. V. K. J.; Welle, A.; Trouillet, V.; Barner-Kowollik, C. *Adv. Funct. Mater.* **2013**, *23* (32), 4011–4019.
11. *Complex Macromolecular Architecture Design via Cyclodextrin Host/Guest Complexes
    Schmidt, B. V. K. J.; Hetzer, M.; Ritter, H.; Barner-Kowollik, C. *Prog. Polym. Sci* **2013**, *39* (1), 235–249.
12. Dual Thermo- and Photo-Responsive Micelles Based on Miktoarm Star Polymers
    Blasco, E.; Schmidt, B. V. K. J.; Barner-Kowollik, C.; Piñol, M.; Oriol, L. *Polym. Chem.* **2013**, *4*, 4506–4514.
13. *Modulation of the Thermoresponsive Behavior of Poly(*N*,*N*-diethylacrylamide) via Cyclodextrin Host/Guest Interactions
    Schmidt, B. V. K. J.; Hetzer, M.; Ritter, H.; Barner-Kowollik, C. *Macromol. Rapid Commun.* **2013**, *34* (16), 1306–1311.
14. Visual Recognition of Supramolecular Graft Polymer Formation via Phenolphthalein-Cyclodextrin Association
    Hetzer, M.; Fleischmann, C.; Schmidt, B. V. K. J.; Barner-Kowollik, C.; Ritter, H. *Polymer* **2013**, *54* (19), 5141–5147.
15. Supramolecular Polymer Networks of Building Blocks Prepared via RAFT Polymerization
    Hetzer, M.; Schmidt, B. V. K. J.; Barner-Kowollik, C.; Ritter, H. *Polym. Chem.* **2014**, *5*, 2142–2152.
16. Supramolecular X- and H-Shape Star Block Copolymers via Cyclodextrin-Driven Supramolecular Self-Assembly
    Schmidt, B. V. K. J.; Barner-Kowollik, C. *Polym. Chem.* **2014**, *5*, 2461–2472.
17. Individually Addressable Thermo- and Redox-Responsive Block Copolymers by Combining Anionic Polymerization and RAFT Protocols
    Schmidt, B. V. K. J.; Elbert, J.; Barner-Kowollik, C.; Gallei, M. *Macromol. Rapid Commun.* **2014**, *35* (7), 708–714.

18. A Novel Photo-Responsive Azobenzene-Containing Miktoarm Star Polymer: Self-Assembly and Photoresponse Properties
    Blasco, E.; Schmidt, B. V. K. J.; Barner-Kowollik, C.; Piñol, M.; Oriol, L. *submitted*.
19. Reversible Single-Chain Self-Folding via Cyclodextrin Driven Host/Guest Chemistry in Water
    Willenbacher, J.; Schmidt, B. V. K. J.; Schulze-Sünnighausen, D.; Altintas, O.; Luy, B.; Delaittre, G.; Barner-Kowollik, C. *submitted*.
20. Redox-Switchable Supramolecular Graft Polymer Formation via Ferrocene-Cyclodextrin Assembly
    Szillat, F.; Schmidt, B. V. K. J.; Hubert, A.; Barner-Kowollik, C.; Ritter, H. *Macromol. Rapid Commun., accepted*.

Non-peer Reviewed Publications

1. Defined Poly(Styrene-*b*-Ferrocenylmethyl methacrylate) Diblock Copolymers via Living Anionic Polymerization
   Gallei, M.; Schmidt, B. V. K. J.; Klein, R.; Rehahn, M. *Polym. Preprints* **2009**, *50* (2), 456–457.
2. Polymer Chemistry: Macromolecules made to order
   Schmidt, B. V. K. J.; Barner-Kowollik, C. *Nat. Chem.* **2013**, *5* (12), 990–992.

Conference Contributions (the presenter is underlined)

1. Novel poly(carboxybetaine methacrylamides) Synthesized via Living/Controlled Aqueous RAFT Polymerization
   Rodriguez-Emmenegger, C.; Schmidt, B. V. K. J.; Sedlákova, Z.; Šubr, V.; Bologna Alles, A.; Brynda, E.; Barner-Kowollik, C.
   European Polymer Congress, Granada **2011**.
2. *Cyclodextrin-Complexed RAFT Agents for the Ambient Temperature Aqueous Living/Controlled Radical Polymerization of Acrylamido-Monomers
   Schmidt, B. V. K. J.; Hetzer, M.; Ritter, H.; Barner-Kowollik, C.
   Bayreuth Polymer Symposium, Bayreuth **2011**.
3. *Miktoarm Starpolymers via Cyclodextrin-Driven Supramolecular Self-Assembly
   Schmidt, B. V. K. J., Hetzer, M.; Ritter, H.; Barner-Kowollik, C.
   Macrogroup UK International Conference on Polymer Synthesis & UKPCF International Conference on Polymer Colloids, Warwick **2012**.
4. *Supramolecular Three-Armed Star Polymers via Cyclodextrin Host/Guest Self-Assembly
   Schmidt, B. V. K. J.; Rudolph, T.; Hetzer, M.; Ritter, H.; Schacher, F. H.; Barner-Kowollik, C.
   Smart Polymers: Biennial Meeting of the GDCh-Division of Macromolecular Chemistry, Mainz **2012**.

5. Photochemical Generation of Light Responsive Surfaces
   Blasco, E.; Schmidt, B. V. K. J.; Welle, A.; Bruns, M.; Barner-Kowollik, C.; Piñol, M.; Oriol, L.
   5ª Jornada de Jóvenes Investigadores en Aragón, Zaragoza **2012**.
6. Limitations of Cyclodextrin Mediated Amphiphilic Block Copolymer Formation
   Hetzer, M.; Schmidt, B. V. K. J.; Barner-Kowollik, C.; Ritter, H.
   Belgian-German (Macro)Molecular Meeting: Advanced Materials by Modular Strategies: From Synthesis to Industrial Applications, Houffalize **2012**.